NEUROTRANSMITTERS AND THE DEVELOPMENT OF THE EMBRYONIC CHICK RETINA

SUZETTE ALLCORN

A thesis submitted for the degree of
Doctor of Philosophy
in the
University of London

Department of Physiology
University College London

November 1995

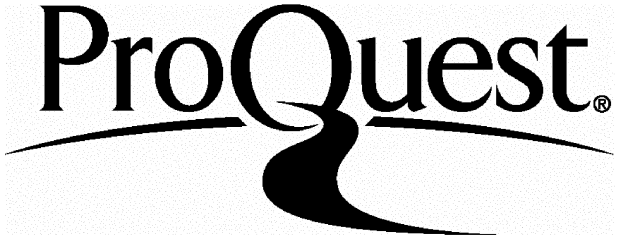

Für Ilse

Eine bewundernswerte, starke Frau, deren Mut eine grosse Quelle der Inspiration für mich ist. Ich werde sie immer in meinem Herzen tragen.

Abstract

Neurotransmitters exert important influences on a variety of processes during the development of the central nervous system, including neurite outgrowth, cell migration and cell survival (Pearce et al., 1987, Kumoro and Rakic, 1993, Choi, 1988). In this thesis the embryonic chick retina has been used to investigate the temporal sequence in which neurotransmitter receptors develop, their influence on intracellular calcium concentration ($[Ca^{2+}]_i$) and their possible functions during development. Electrophysiological and Ca^{2+} imaging techniques show that receptors for the excitatory neurotransmitters glutamate and acetylcholine and for the inhibitory neurotransmitter GABA appear prior to synaptogenesis, suggesting possible developmental roles for these transmitters. Many of the developmental effects of glutamate and other transmitters are attributed to their ability to alter $[Ca^{2+}]_i$ and recently it has been shown that AMPA/kainate receptors that exclude the GLUR2 subunit are Ca^{2+}-permeable (Hollmann et al., 1991). Here the presence of Ca^{2+}-permeable AMPA/kainate receptors in the embryonic chick retina is demonstrated both *in vivo* and *in vitro*. Retinal explants and cultures of dissociated retinal cells were treated with glutamate analogues to investigate the role of non-NMDA (AMPA/kainate) receptors during the development of the chick retina. Activation of AMPA/kainate receptors with kainate late in retinal development leads to excitotoxic cell death, however exposure to this neurotoxin early on has no affect on cell survival in both dissociated cultures and explant cultures. Cell survival in kainate is correlated with a decrease in the Ca^{2+}-permeability of the AMPA/kainate receptor, suggesting it may play a role in cell survival during development. Activation of this receptor early in development produces a significant reduction in the number of processes extended by the cells, showing glutamate may influence neurite growth in the developing retina via activation of non-NMDA receptors.

Contents

Chapter 1

Introduction

Chapter 2

Methods

Chapter 3

Early *in vitro* development of neurotransmitter- and voltage-gated channels in dissociated retinal neurons

Chapter 4

The consequences of non-NMDA receptor activation in the chick retina during development

Chapter 5

The effects of glutamate analogues on neurite extension in embryonic chick retinal cells

Chapter 6

Imaging of Ca^{2+} signals evoked by neurotransmitters in the developing chick retina

List of figures

List of tables

Acknowledgments

I am indebted to my supervisor, Peter Mobbs, for his guidance, enthusiasm and encouragement, and for teaching me so much throughout the three years of my Ph.D. I am also grateful to David Attwell who was available on many occasions for help, advice and chocolate.

I was very fortunate to work in such a friendly and fun environment and a big thank you must go to everyone associated with the lab past and present, in particular Marina Catsicas for her endless help, support and patience and to Brian Billups for rescuing me so often with his computer expertise. To Monique Sarantis, Muriel Bouvier, Alessandra Amato, Barbara Miller, Michiko Takahashi, Martine Harmann, David Rossi and Viola Bonneß - many thanks for your moral support and for making work so much fun.

My thanks go to Ollie Quain and James Walsh, who played a large part in maintaining my sanity (just) with unconditional friendship and a multitude of outrageous nights out.

Finally I would like to say a special thank you to my parents for their inexhaustible support, encouragement and love, without which I would not have been able to do this.

This work was supported by the Medical Research Council of Great Britain and by the Wellcome Trust.

Chapter 1

Introduction

Neurotransmitters, in addition to their function in synaptic information coding, play an important role in the development and maintenance of neurons in the central nervous system (CNS). They can act as guidance cues in the formation of the appropriate connections between neurons, are important in the maintenance of these connections once formed, and can trigger neuronal degeneration (Mattson, 1988). The concentration of a neurotransmitter can be crucial in determining its effects; at low levels neuronal outgrowth may be stimulated while higher concentrations may lead to dendritic pruning or even neuronal death. In order for a neuron to respond to a neurotransmitter it is necessary that the appropriate cell surface receptor be expressed. Thus, as a prerequisite to studying the effects of neurotransmitters on neuronal development, it is important to establish when and where transmitter receptors are expressed. The majority of the developmental changes produced by neurotransmitters are mediated through second messengers such as calcium, inositol phosphates and cyclic nucleotides (Mattson, 1988). Calcium (Ca^{2+}) appears to be responsible for executing many neurotransmitter-initiated developmental signals, thus it is of particular interest to establish how some transmitters influence intracellular Ca^{2+} concentrations ($[Ca^{2+}]_i$). The embryonic chick retina provides an excellent model for studying the early development of the CNS because the spatial and temporal order in the generation and differentiation of its cell types are well-defined (Kahn, 1974). In addition, the retina is readily accessible for investigation using a variety of techniques that include electrophysiology, Ca^{2+} imaging and immunocytochemical methods.

This thesis describes experiments that show the presence of a variety of neurotransmitter receptors in the embryonic chick retina, both in dissociated cultures and in the isolated retina. Whole-cell patch-clamping has been employed to characterize the electrophysiological properties of these receptors and Ca^{2+} imaging techniques show the effects of receptor activation on $[Ca^{2+}]_i$ and enable the temporal sequence of receptor expression to be determined. The effects of transmitter receptor stimulation on developmental processes such as neurite outgrowth, cell survival and receptor expression is also investigated. A brief review follows of the basic physiology of the retina and the current state of knowledge of the role of neurotransmitters during development. The introduction is organized under the following headings: 1. Organization and development of the retina, 2. Classification and localization of neurotransmitter receptors, 3. Uptake of neurotransmitters, 4. The role of neurotransmitters during development, 5. Mechanisms by which neurotransmitters affect neuronal development, 6. Neurotransmitters and cell death, 7. Aims of the current study.

1.1 Organization and development of the retina

1.1.1 General structure of the retina

All vertebrate retinae consist of two synaptic layers termed the inner and outer plexiform layers (IPL, OPL), between which three cellular layers are intercalated. The cellular layers are termed the inner and outer nuclear layers (INL, ONL) and the ganglion cell layer (GCL) (figure 1.1). Photoreceptors are the most distal cells of the retina and their cell bodies lie in the ONL. The other main classes of retinal neuron are the horizontal, bipolar, amacrine, ganglion and interplexiform cells. The perikarya of the horizontal cells lie in the outer part of the INL, those of the bipolar cells are located mainly in the

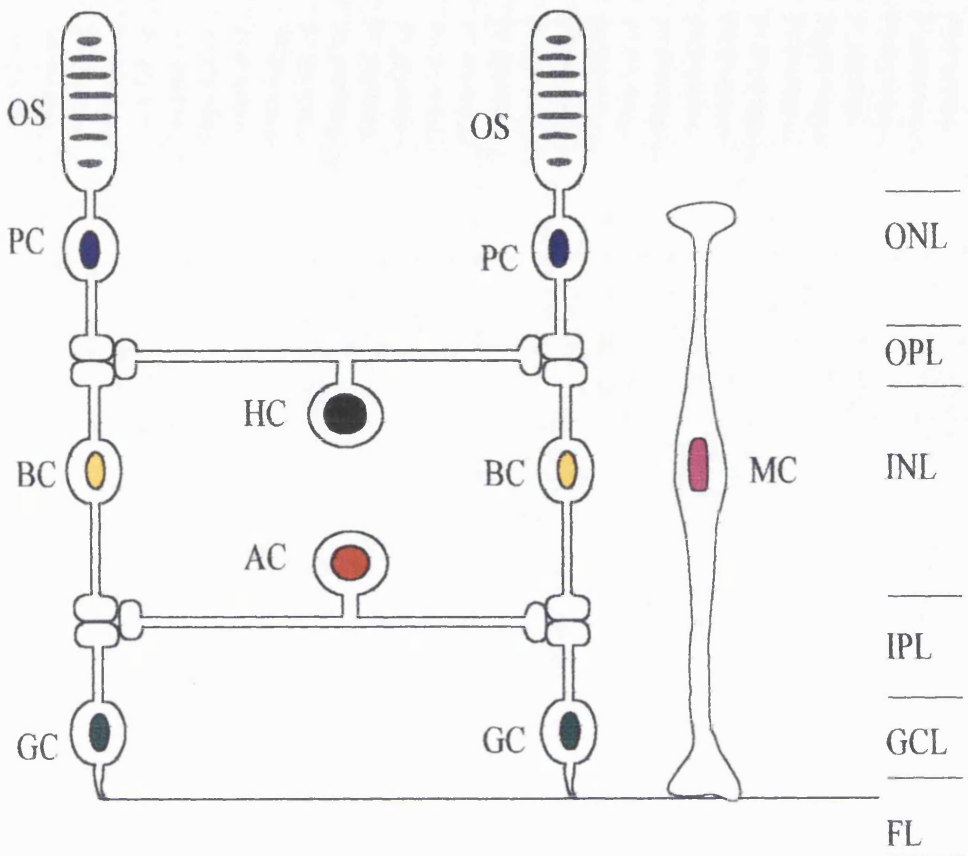

Figure 1.1

Schematic diagram of the vertebrate retina.

The diagram shows the main cell types of the retina and their positioning within the retinal layers. Light is captured by rhodopsin (the visual pigment) located in the outer segment (OS) of photoreceptor cells (PC) and converted into an electrical signal. The visual signal passes vertically through the retina in bipolar cells (BC) and ganglion cells (GC) and is modulated via the lateral connections made with horizontal cells (HC) and amacrine cells (AC). The signal passes to the brain in the form of action potentials in ganglion cell axons that form the fiber layer (FL). Müller cells (MC) extend throughout the neural retina. Abbreviations: ONL, outer nuclear layer, OPL, outer plexiform layer, INL, inner nuclear layer, IPL, inner plexiform layer, GCL, ganglion cell layer.

middle part of this layer and the amacrine and interplexiform cell bodies are positioned at the proximal border of the INL. The cell bodies of ganglion cells form the most proximal layer of the retina, the GCL. Sometimes horizontal and bipolar cells are found in the ONL, ganglion cells in the INL and most commonly amacrine cells in the GCL. These are called displaced cells. The glial cells of the retina are the Müller cells which extend vertically from the distal margin of the ONL (the outer limiting membrane) to the inner margin of the retina (the inner limiting membrane).

1.1.2 Retinal processing

Visual pigments, located in the outer segments of rods and cones (the photoreceptors), capture light. The receptor cells convert light into an electrical signal and provide the input to the OPL that contains the processes of the bipolar, horizontal and interplexiform cells. Bipolar cells carry the visual information from the OPL to the IPL which contains the processes of the amacrine, bipolar and ganglion cells. Horizontal cells and amacrine cells mediate lateral interactions within the retina. Interplexiform cells extend processes in the OPL and the IPL and carry information between them. Ganglion cells are the output neurons of the retina and they carry signals out of the IPL. Their axons collect at the optic fissure to form the optic nerve which takes information from the eye to higher visual centers.

1.1.3 Development of the retina

Although some differences in the genesis of the retina occurs between species, there are some features that are common to most mammalian and avian species. The primordium of the brain and spinal cord is the neural tube which is derived from the neural plate (figure 1.2A). Embryonic tissue that is

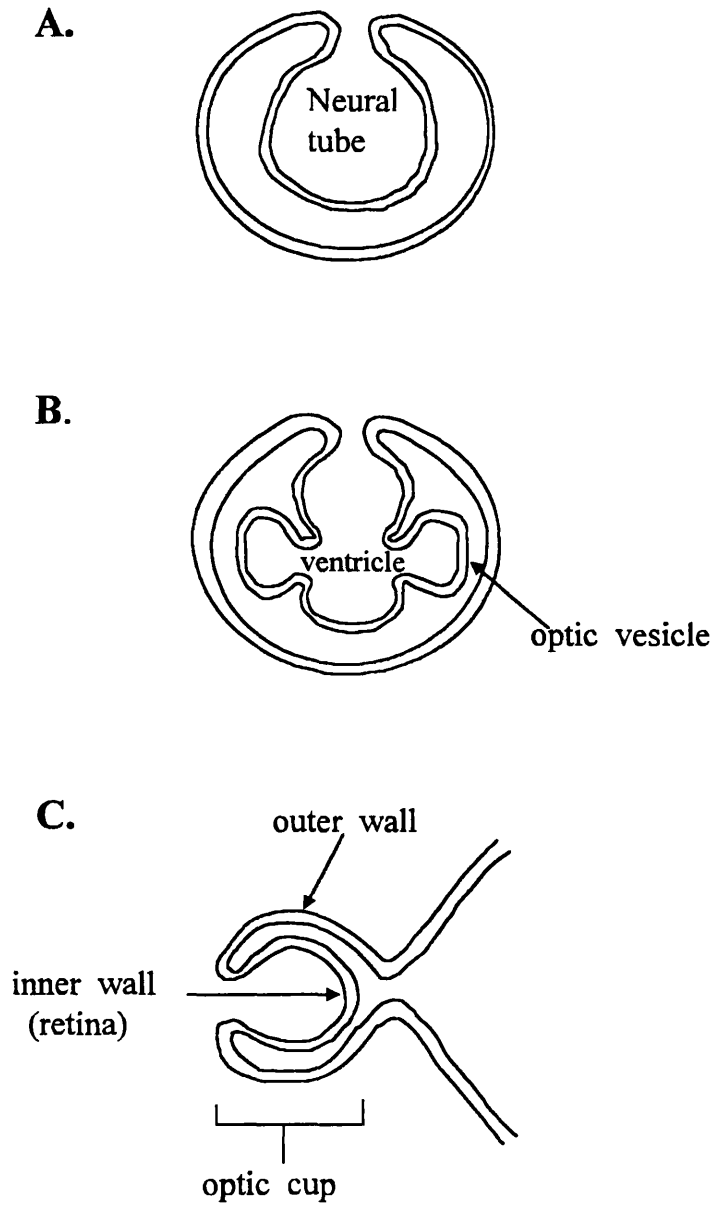

Figure 1.2

Schematic diagram showing the formation of the optic cup.

A. The neural tube evaginates to form two optic vesicles. **B.** The neural epithelium of an optic vesicles subsequently invaginates to produce an optic cup. **C.** The cells in the inner wall of the optic cup develop into layers of the retina.

destined to become the retina evaginates from the neural tube to form two primary optic vesicles in the head region of the embryo (Duke-Elder, 1963, Mann, 1964) (figure 1.2B). The neural epithelium of each optic vesicle subsequently invaginates to form an optic cup (figure 1.2C). The interior of the optic cup is confluent with the ventricles of the brain and is termed the optic ventricle. Initially both walls of the optic cup are one cell thick. The external wall remains one cell thick and the cells differentiate into the pigment epithelium that lines the back of the eye. Cells of the inner wall divide repeatedly to form the neuroepithelial layer. These newly formed cells, termed neuroblasts, accumulate near the center of the optic cup and differentiate into retinal cells. Some neuroblasts migrate vitread to the neuroepithelium and form a second nuclear layer, resulting in a inner and outer neuroblastic layer and two anuclear layers.

Cells in the inner neuroblastic layer develop into ganglion, amacrine and Müller cells and those in the outer layer form the bipolar, horizontal and photoreceptor cells. The nuclei of the Müller and amacrine cells separate from the ganglion cells and the IPL forms between them. Similarly, the bipolar and horizontal nuclei split from the photoreceptors and the OPL develops in-between. Thus a single nuclear layer forms that contains the nuclei of amacrine, Müller, bipolar and horizontal cells. Müller cells extend processes that span the retina filling most of the extracellular space and differentiation of retinal neurons then proceeds.

Retinal neurons are born in two phases. In the first phase ganglion cells, amacrine cells, cones and type A horizontal cells appear. Ganglion cells are usually born first, however there is a lot of overlap in the times of generation of the other classes of cells. In the second phase, bipolar cells, type B horizontal cells and rods appear. Ciliated ependymal cells on the

ventricular surface of the neural tube develop into the outer segments of the photoreceptors. During development the photoreceptors and pigment epithelial cells interdigitate. However, tight cell adhesion rarely occurs between them and so in most species the intact retina is easily lifted from the back of the eye. Unlike some other brain regions, the last born cells of the retina do not accumulate at either one surface of the retina but are found in both the INL and ONL.

1.2 Classification and localization of neurotransmitter receptors

In the past 25 years a large number of amino acid, monoamine, peptide and purine neurotransmitter receptors have been characterized. Nearly all of the receptors found in the CNS are found in the retina. The discussion below considers the localization and characteristics of the neurotransmitter receptors studied in this thesis.

1.2.1 Ionotropic glutamate receptors

Glutamate is the most abundant amino acid in the mammalian CNS (Fonnum, 1984). It mediates excitatory neurotransmission and acts as a regulatory signal in CNS development via activation of a number of different ionotropic and metabotropic receptors (for reviews see Collingridge and Lester, 1989, Nicoll et al., 1990). Ionotropic glutamate receptors are ligand-gated ion channels and are commonly classified as N-methyl-D-aspartate (NMDA) and non-NMDA receptor types based on their preferential responses to synthetic receptor agonists (Watkins and Olverman, 1987). Non-NMDA receptors are further classified pharmacologically into kainate and α-amino-3-hydroxy-5-methyl-4-isoxazole propionate (AMPA)/kainate receptors (Monaghan et al., 1989). Electrophysiological techniques suggest that

different glutamate receptor channel types can co-exist in many cells (Stern et al., 1992a). These channels differ in their ionic permeabilities, conductance properties and kinetics.

AMPA/kainate receptors are thought to mediate most fast excitatory neurotransmission in the CNS. Their fast channel kinetics, rapid desensitization and low Ca^{2+}-permeability make them ideally suited for this purpose. However, the recent discovery that some AMPA/kainate receptors are highly Ca^{2+}-permeable (see section 1.2.1b) has raised the possibility that these receptors trigger processes previously thought to result exclusively from NMDA receptor activation. NMDA receptors are highly Ca^{2+}-permeable and can trigger different processes ranging from trophic developmental processes (Kumoro and Rakic, 1993) to the plastic changes in synapses that underlie some forms of learning and memory (Collingridge and Singer, 1990). Excessive activation of NMDA receptors can lead to neuronal death via the influx of Ca^{2+} through the receptor (Choi, 1988). The function of kainate receptors is not well understood, though the presence of functional kainate receptors has been established in sensory ganglia (Huettner, 1990) and some glial cell lines (Gallo et al., 1994).

a) NMDA receptors

The NMDA receptor is linked to a cation channel that has a large single-channel conductance (Nowak et al, 1984) and is highly permeable to Ca^{2+} as well as sodium (Na^{+}) and potassium (K^{+}) (Ascher and Nowak, 1988). The channel is blocked by magnesium (Mg^{2+}) in a voltage-dependent manner and at negative potentials the presence of Mg^{2+} in the pore prevents the passage of ions through the channel (Mayer et al., 1984, Nowak et al., 1984). Hence the current-voltage (IV) relationship shows a region of negative slope

conductance between -60 and -30mV. NMDA receptors have a high affinity for glutamate (K_D: 0.5-1μM), activate relatively slowly compared to non-NMDA receptors and display much slower desensitization and deactivation rates (Lester et al., 1990, Lester and Jahr, 1992, Lester et al., 1993). The receptor/channel complex has several regulatory sites. Glycine is a co-agonist that is required for receptor activation by binding to a site that is allosterically coupled to the NMDA binding site (Kleckner and Dingledine, 1988, Benveniste et al., 1990). At nanomolar concentrations glycine greatly potentiates activation of NMDA receptors (Johnson and Ascher, 1987). A phencyclidine (PCP) binding site in the receptor channel produces sensitivity to dissociative anesthetics such as PCP, ketamine and MK-801 (Kemp et al., 1988). Zinc (Zn^{2+}) and polyamines also regulate receptor activity at distinct sites (Peters et al., 1987, Ransom and Stec, 1988, Westbrook and Mayer, 1987). NMDA, glutamate, ibotenate, L-aspartate and homocysteate are all effective agonists at the NMDA receptor and antagonists include D(-)-2-amino-5-phosphonopentanoic acid (D-AP5), 3-((D)-2-carboxypiperazin-4-yl)-propyl-1-phosphonic acid (D-CPP), CGS-19775, MK-801 and Zn^{2+}.

Hydrophobicity plots predict that the polypeptide chain of all glutamate receptor subunits spans the membrane four times (TM I-IV) with the amino and carboxy terminal end in the extracellular and intracellular space respectively (Seeburg, 1993). Expression cloning in *Xenopus* oocytes has enabled the molecular characterization of the main NMDA receptor subunit, NR1 (Kress et al., 1992). NR1 can form functional homomeric receptor channels that display all of the characteristics of the endogenous channels described above. However, four NR2 subunits exist (NR2A-D) (Monyer et al., 1992, Kutsuwada et al., 1992, Meguro et al., 1992, Ikeda et al., 1992, Ishii et al., 1993) and when NR1 is co-expressed with an NR2 subunit membrane currents activated by glutamate or NMDA increase several fold in magnitude.

NR2 subunits do not form homomeric receptor channels nor heteromeric channels when combined with each other. Functional NMDA receptors are believed to be formed *in vivo* by heteromeric expression of NR1 with any one of the NR2 subunits, with the NR2 subunit imparting subunit-specific properties to the channel gating kinetics and conductance (Monyer et al., 1992, Meguro et al., 1992, Stern et al., 1992, Ishii et al., 1993). NR1 and NR2 subunits share only an 18% sequence homology and NR2 subunits differ in their structural properties compared to all other glutamate receptor subunits in that their carboxy terminal is extended by 50 amino acids (Seeburg, 1993). However both NR1 and NR2 subunits contain an asparagine (N) residue in the putative channel-forming region, TM II, responsible for their high Ca^{2+}-permeability and the voltage-dependent Mg^{2+} block of the channel (Mori et al., 1992, Sakurada et al., 1993).

b) AMPA/kainate receptors

AMPA is a selective and potent agonist at the AMPA/kainate receptor. The AMPA/kainate receptor binds glutamate with high affinity (K_D in the low nanomolar range). Both AMPA and glutamate evoke a rapidly activating current at this receptor that nearly completely desensitizes in the presence of the agonist (Trussell and Fischbach, 1989, Jonas and Sakmann, 1992, Colquhoun et al., 1992). In contrast, kainate induces long-lasting currents at the AMPA/kainate receptor that persist in the presence of the drug (Patneau and Mayer, 1991, Keinänen et al., 1990). The AMPA/kainate receptor channel is permeable to Na^+ and K^+ and in most neurons is characterized by a low Ca^{2+}-permeability (Iino et al., 1990). Until recently it was believed that Ca^{2+}-entry resulting from AMPA/kainate receptor activation was indirect, for example via voltage-gated Ca^{2+} channels activated by depolarization. However, several studies have since shown that AMPA/kainate receptors in

some neurons are highly permeable to Ca^{2+} (Gilbertson et al., 1991, Burnashev et al., 1992a). The AMPA/kainate receptor is antagonized by a group of quinoxalinediones that include CNQX (6-cyano-7-nitroquinoxaline-2,3-dione) and DNQX (6,7-dinitro-quinoxaline-2,3-dione (Honoré et al., 1988).

Molecular cloning studies have identified four AMPA/kainate receptor subunits, GLUR1-4 (Hollmann et al., 1989, Boulter et al., 1990, Keinänen et al, 1990, Nakanishi et al., 1990). All these subunits are capable of forming homomeric or heteromeric channels. They are approximately 900 amino acids in length and form four transmembrane domains with a similar topology to NMDA receptor subunits (Seeburg, 1993). However subunits GLUR1-4 occur in two major forms termed flip and flop, which differ slightly in a sequence of 38 amino acids preceding the last transmembrane region (TM IV) (Sommer et al., 1990). These two forms have different expression profiles in the mature and developing mammalian brain, with the flop form not appearing until early postnatal stages (Sommer et al, 1990, Monyer et al., 1991). Each combination of the four AMPA/kainate receptor subunits has different properties. GLUR2 is particularly important in determining the channel characteristics; its inclusion in the receptor complex gives rise to a linear IV-relationship and a low Ca^{2+}-permeability (Boulter et al., 1990, Verdoorn et al., 1991, Hollmann et al., 1991). Channels that exclude the GLUR2 subunit display a doubly rectifying IV-relationship and a high Ca^{2+}-permeability (Hollmann et al., 1991, Verdoorn et al., 1991, Dingledine et al., 1992). The permeability to Ca^{2+} is determined by a single amino acid residue in TM II of the GLUR subunits (Hume et al., 1991, Burnashev et al., 1992b). In GLUR2 this amino acid is an arginine (R), conferring low Ca^{2+}-permeability, while in GLUR1, 3 and 4 a glutamine (Q) is found at this site, termed the Q/R site, facilitating high Ca^{2+}-permeability. Curiously, the GLUR2 gene does not

normally carry the arginine codon at the Q/R site and it is only present after modification by RNA editing (Sommer et al., 1991).

c) Kainate receptors

Kainate is a potent agonist at kainate receptors at which it activates a transient response in the continued presence of kainate (Huettner, 1990). Kainate also evokes large currents at AMPA/kainate receptors (see section 1.2.1b). However kainate has a much lower potency at these receptors and elicits currents that persist in the presence of the agonist (Egebjerg et al., 1991, Patneau and Mayer, 1991, Keinänen et al., 1990). AMPA can evoke currents at some kainate receptors, however concentrations in the region of 500μM or more (compared to low μM concentrations for kainate) are required to produce half-maximal effects (Sommer et al., 1992). Recently, non-NMDA receptor classification has been made easier by the finding that lectins such as concanavalin-A greatly potentiate kainate receptor responses (Werner et al., 1991). Lectins are far less effective at potentiating AMPA/kainate receptor responses (Partin et al., 1993, Wong and Mayer, 1993). Kainate receptors gate a cation channel that is highly permeable to Na^+ and K^+, and in some cases Ca^{2+} (see below). As with AMPA/kainate receptors, kainate receptors are antagonized by CNQX and related compounds.

The five cloned kainate receptor subunits have been subdivided into two groups: GLUR5-7, and KA1 and KA2 (Bettler et al., 1990, Werner et al., 1991, Bettler et al., 1992, Egebjerg et al., 1991, Herb et al., 1992, Lomeli et al., 1992, Morita et al., 1992, Sakimura et al., 1992, Sommer et al., 1992). Homomeric receptors formed from the subunits GLUR5-7 have lower affinities for kainate (K_D:35-95nm) than either KA1 or KA2 (K_D:5-15nm) (Bettler et al., 1992, Lomeli et al., 1992, Sommer et al., 1992). KA1 and KA2

exhibit appropriate binding affinities when recombinantly expressed, however they do not alone, or in combination with each other, form functional channels (Werner et al., 1991, Herb et al., 1992). Thus it is thought that KA1 and KA2 act as modulatory subunits in the native protein. Like GLUR2, the Ca^{2+}-permeability of the kainate receptor is determined by the amino acid residue at the Q/R site of TM II. GLUR5 and GLUR6 undergo RNA editing at this site (Sommer et al, 1992), however the effects of this on Ca^{2+}-permeability also depends on RNA editing in the TM I domain (Köhler et al., 1993). While the GLUR2 subunit is only found in the edited form *in vivo*, GLUR5 and GLUR6 are found both in the edited and unedited forms (Hollmann and Heinemann, 1994).

1.2.2 Metabotropic glutamate receptors

Metabotropic glutamate receptors are not linked directly to ion channels but are coupled via G proteins to second messenger systems (reviewed by Monaghan et al., 1989). Activation of some metabotropic receptors leads to increased levels of cellular phopholipase C and thus production of inositol triphosphate (IP_3) and diacylglycerol (DAG) (Sladeczec et al., 1985, Nicoletti et al., 1986, Novelli et al., 1987). This leads to mobilization of Ca^{2+} from internal stores (Berridge and Irvine, 1984). However, recently it has been shown that some metabotropic receptors are linked to an inhibitory cascade of cyclic adenosine monophosphate (cAMP) formation (see below). Agonists at the metabotropic receptor include L-glutamate, ibotenate and quisqualate. The glutamate analogue *trans*-1-amino-cyclopentyl-1, 3-dicarboxylic acid (*trans*-ACPD) is a selective agonist for metabotropic receptors (Palmer et al., 1989), though its potency varies for the different receptor subtypes (for review see Nakanishi, 1994). L-2-amino-3-phosphonoproprionic acid (L-AP3) is an antagonist at all metabotropic

receptors excluding some L-AP4-sensitive subtypes of the receptor (see below).

Molecular cloning studies have shown that metabotropic glutamate receptor subunits form a family consisting of at least eight subtypes termed mGLUR1-8 (for review see Nakanishi, 1994). The subunits possess seven putative transmembrane segments with an unusually large extracellular domain and share a 40% sequence homology (Nakanishi, 1992). The receptor subunits mGLUR1 and mGLUR5 are coupled to IP_3/Ca^{2+} signal transduction (Aramori and Nakanishi, 1992, Abe et al., 1992) and mGLUR1 has also been shown to increase arachidonic acid and cAMP production (Aramori and Nakanishi, 1992). The other six receptor subunits inhibit cAMP formation. The subunits mGLUR2, 3 and 8 are strongly activated by *trans*-ACPD (Tanabe et al., 1992, 1993) whereas mGLUR4, 5 and 7 are strongly activated by L-2-amino-4-phosponobutyrate (L-AP4) (Tanabe et al., 1993, Nakajima et al., 1993, Okamoto et al., 1994, Saugstad et al., 1994).

1.2.3 Localization of glutamate receptors in the retina

Nearly all neurons in the CNS can be excited by glutamate (Curtis and Johnston, 1974). The mRNA for the NMDA receptor subunit NR1 is expressed ubiquitously in almost all neuronal cells throughout the brain (Moriyoshi et al., 1991). *In situ* hybridization studies in the rat retina have shown that mRNAs for NR1 and NR2A-C are expressed in the GCL of the retina and NR1 mRNA is expressed homogeneously in the INL (Brandstatter et al., 1994).

The mRNA distribution for the AMPA/kainate receptor subunits GLUR1-GLUR7 has been investigated by Hamassaki-Britto et al. (1993) in

the rat and cat retina using *in situ* hybridization. The mRNAs for these glutamate receptor subunits were shown to be present in the adult retina of both species. Probes for GLUR1 and GLUR2 mRNAs produced labelling over the whole of the INL and GCL, with GLUR3-7 having more localized distribution in the INL and GCL. GLUR5 produced only scattered labelling in the GCL, though it produced strong labelling in the outer region of the INL. GLUR6 and GLUR7 had a restricted pattern of labelling in the rat retina, but in the cat retina they were widely distributed similarly to GLUR1.

The mRNAs for kainate receptor subunits can be found throughout the CNS in the adult rat (Wisden and Seeburg, 1993), with KA2 and GLUR6 mRNAs being particularly widespread. GLUR6, GLUR7 and KA2 mRNAs are expressed in the rat retina, with KA2 being homogeneously expressed in the INL (Brandstatter et al., 1994). However, there is little evidence for the presence of functional kainate receptors in the CNS except in sensory dorsal root ganglion cells (Huettner, 1990) and some primary glial cell lines (Gallo, 1994).

The mRNA distribution for the metabotropic receptor subtypes in the CNS has not been so widely investigated, however mGLUR4, 6 and 7 are present in the rat retina (Akazawa et al., 1994) and mGLUR2 and 3 in the rat brain (Ohishi et al., 1993a, 1993b).

1.2.4 Acetylcholine receptors

Acetylcholine (ACh) is a major excitatory neurotransmitter in the CNS that influences many aspects of development through activation of two classes of ACh receptors. ACh stimulates ionotropic receptors at which nicotine is a selective agonist and thus these receptors are termed nicotinic ACh receptors

(nAChR). Muscarinic ACh (mAChR) receptors, activated specifically by muscarine, are linked to G-proteins rather than directly to ion channels and can trigger a variety of intracellular signalling pathways.

a) Nicotinic receptors

Nicotinic receptors are linked to a cation channel that is permeable to Na^+, K^+ and sometimes Ca^{2+} (Vernino et al., 1992). Antagonists include *d*-tubocurarine, hexamethonium and α-bungarotoxin (the classical neuromuscular blocker). However, it is now known that some combinations of nAChR subunits are insensitive to α-bungarotoxin (for review see Clarke, 1992).

Molecular cloning studies have classified nAChR into two groups, the ligand-binding α subunits and the structural β subunits. The polypeptide chain of each subunit spans the membrane four times, like glutamate receptor subunits. The α1 subunit is found in muscle and α2-α9 are found only in the CNS. The β group of subunits currently has three members, β2, β3 and β4. It is believed that the complete receptor is composed of five subunits formed by expression of α/β subunit pairs or by α subunits alone (for review see McGehee and Role, 1995).

b) Muscarinic receptors

Muscarinic receptors belong to a family of G-protein coupled receptors that modulate many different signal transduction pathways. They are single subunit receptors and five subtypes of mAChRs termed m1-m5 have been identified, all of which are expressed in mammalian brain (Peralta et al., 1987,

Bonner et al., 1987, 1988, Liao et al., 1989). The receptors are predicted to have seven transmembrane domains and a large cytoplasmic loop between TM V and TM VI (Peralta et al., 1987). The subtypes m1, m3 and m5 are linked to phosphoinositide (PI) hydrolysis and release Ca^{2+} from IP_3-sensitive stores. In contrast subtypes m2 and m4 are linked to adenylyl cyclase and reduce cAMP levels, and are only weakly linked to PI hydrolysis (for review see Hosey, 1992). All mAChRs are activated by muscarine and carbachol and antagonized by atropine at low concentrations. Pirenzipine and gallamine are selective antagonists at m1 and m2 receptors respectively. Selective antagonists for mAChR3-5 are not yet available.

1.2.5 Localization of ACh receptors in the retina

In situ hybridization studies have revealed a widespread pattern of nAChRs in the CNS (Wada et al., 1989, Heinemann et al., 1990, Morris et al., 1990, Dineley-Miller and Patrick, 1992). Genes for nAChRs are expressed widely by cells in the INL and GCL of the rat and goldfish retina (Wada et al., 1989, Cauley et al., 1990, Hoover and Goldman, 1992). Localization of nAChR subunits in the chick retina has been particularly well studied. Amacrine and ganglion cells contain α3, α7 and α8 and β2 subunits (Keyser et al., 1988, Hamassaki-Britto et al., 1991) and the α8 subunit is expressed in bipolar cells and in the OPL (Keyser et al., 1993, Hamassaki-Britto et al., 1994a).

Until recently cholinergic receptor studies focused mainly on nicotinic receptors, however the presence of muscarinic receptors has now been demonstrated in several regions of the brain. The subtypes m1, m2 and m4 have been found in rat striatal neurons (Bernard et al., 1992), m1 in rat visual cortex (Wang et al., 1994) and m1-m4 in rat hippocampus (Levey et al.,

1995). Ligand-binding studies have demonstrated the presence of mAChRs in the IPL of ferret and human retina (Hutchins, 1994, Hutchins and Hollyfield, 1985), however the subtypes of receptor expressed in the retina has yet to be established.

1.2.6 GABA receptors

GABA (γ-aminobutyric acid) acts as inhibitory neurotransmitter in the mammalian CNS (Krnjevic and Schwartz, 1967), although during development its actions are often depolarizing in immature neurons (Segal and Barker, 1984, Muëller et al., 1984, Zhang et al., 1991, Cherubini et al., 1991). There are three distinct types of GABA receptors termed $GABA_A$, $GABA_B$ and $GABA_C$ receptors (Johnston, 1986, Silvlotti and Nistri, 1991). $GABA_A$ receptor activation leads to the opening of a chloride (Cl^-)-permeable channel that leads to the classical hyperpolarizing action of GABA (Bormann, 1988, Feigenspan et al., 1993). $GABA_A$ channels thus have a reversal potential that shows a Nernstian dependence on the Cl^- concentration. Muscimol is a selective $GABA_A$ receptor agonist and bicuculline and picrotoxin are selective antagonists at this receptor. $GABA_B$ receptors are linked indirectly via G-proteins to Ca^{2+} and K^+ channels (reviewed by Bormann, 1988). These receptors are insensitive to bicuculline and are selectively activated by baclofen. The third class of GABA receptor, $GABA_C$, is linked to a Cl^- channel like the $GABA_A$ receptor. However it is insensitive to both bicuculline and baclofen and is activated by the GABA analogue *cis*-4-aminocrotonic acid. $GABA_C$ receptors further differ from $GABA_A$ receptors in that they are not modulated by benzodiazepines and barbiturates (Cutting et al., 1991, Shimada et al., 1992).

The molecular biology of GABA receptors is complex. Recent cloning

studies have revealed at least 15 different GABA receptor subunits that include 6 α, 3 β, 3 γ, 3 δ and 2 ρ subunits (reviewed by Burt and Kamatchi, 1991). Combinations of all of these subunits form $GABA_A$ receptors except the δ subunits that appear to form $GABA_C$ receptors (Cutting et al., 1991, 1992). The metabotropic $GABA_B$ receptor is coupled to GTP-binding proteins however the structure of the receptor is as yet unknown.

1.2.7 Localization of GABA receptors in the retina

Using immunocytochemical and biochemical techniques Lin and Yazulla (1994) have shown that $GABA_A$ receptors are present in the IPL and OPL of the goldfish retina. Greferath et al. (1994) have also shown that mRNAs for the $GABA_A$ receptor subunits α1, β2, β3 and γ2 are expressed in sub-populations of amacrine, bipolar and ganglion cells in the rabbit retina. The mRNAs encoding the δ subunit that produces $GABA_C$ receptor pharmacology is expressed widely and possibly exclusively in the retina (Cutting et al., 1991, O'Hara et al., 1995). Binding studies have shown the presence of $GABA_B$ receptors in the rat cerebellum (Turgeon and Albin, 1993) and the rabbit retina (Friedman and Redburn, 1990).

1.3 Uptake of neurotransmitters

After neurotransmitters have been released they must be removed from the synaptic cleft in order to terminate synaptic transmission. This can be done by diffusion out of the cleft, metabolism by extracellular enzymes or uptake back into the nerve terminal or adjacent glial cells. ACh is broken down by cholinesterases, however there are no extracellular enzymes to break down glutamate or GABA. These transmitters are transported into glial cells where they are metabolized by glutamine synthase and GABA transaminase

respectively or into neurons where they are taken up into vesicles for re-release. In the retina glutamate is transported preferentially into Müller cells (White and Neal, 1976, Ehinger, 1977) via an electrogenic carrier that transports a net positive charge into the cell with each cycle of the carrier (Brew and Attwell, 1987). The co-transport of Na^+ ions provides the energy required to carry glutamate in this way. GABA is accumulated by glia and neurons by a similar Na^+-dependent manner to glutamate.

Recently three Na^+-dependent glutamate transporters have been cloned and termed GLT-1, EAAC1 and GLAST (Pines et al., 1992, Kanai and Hediger, 1992, Storck et al., 1992). Subsequent localization studies in rat brain have demonstrated that GLT-1 is localized to glial cells, EAAC1 is neuronal and GLAST is found in subsets of neurons and glia (Rothstein et al., 1994, Torp et al., 1994).

Molecular cloning has revealed four GABA transporters, GAT1-4 (Guastella et al., 1990, Lopéz-Corcuera et al., 1992, Liu et al., 1993). GAT1 has been localized in the rat and mouse retina using *in situ* hybridization and is present mainly in amacrine, interplexiform and some ganglion cells and at lower levels in Müller cells (Brecha and Weigman, 1994, Ruiz et al., 1994). GAT1, to date, is the only GABA transporter that has been found in glial cells (Jursky et al., 1994). Under certain physiological and pathological conditions transport mechanisms, such as those for glutamate and GABA, can run backwards transporting the transmitter out of the cell (for review see Adam-Vizi, 1992). The mechanism of GABA release from horizontal cells in the retina is thought to occur via a transporter rather than by Ca^{2+}-dependent exocytosis (Schwartz, 1987).

1.4 The role of neurotransmitters during development

Neurotransmitter receptors are expressed in the developing CNS before the onset of synaptogenesis (reviewed by Lipton and Kater, 1989, Lauder, 1993), making them ideal candidates for modulating neuronal growth and development in the early embryo. The cellular site at which neurotransmitters mediate their effects on neuronal outgrowth seems to be the growth cone, the elongating tip of neurites. Growth cones are capable of releasing transmitters and contain transmitter receptors (Hume et al., 1983, Lockerbie and Gordon-Weeks, 1986, Young, 1986).

Several *in vitro* experiments on preparations as diverse as snail ganglion, mammalian retina and hippocampus provide direct evidence that neurotransmitters influence neuronal architecture. In the buccal ganglion of the snail *Helisoma* the neurotransmitter serotonin produces rapid withdrawal of the filopodia of growth cones and prevents further neurite elongation (Haydon et al., 1984). In contrast, glutamate enhances the sprouting of neurites from axotomized buccal neurons (Jones et al., 1986), demonstrating that different transmitters can have diverse effects in the same preparation. When growth cones are physically isolated from neurites of *Helisoma* buccal ganglion they continue to elongate and remain sensitive to the effects of serotonin and glutamate on outgrowth (Haydon et al., 1984, Mattson and Kater, 1987).

In the mammalian retina cells from both the intact tissue and those in culture spontaneously release ACh. Inhibition of nicotinic ACh receptors with antagonists such as tubocurarine leads to increased neuronal process outgrowth from retinal cells in culture (Lipton et al., 1988). This suggests that endogenous levels of ACh may inhibit neuronal growth. Similarly, Mattson et

al. (1988b) have demonstrated that glutamate inhibits dendritic outgrowth in the hippocampus. These authors showed that glutamate, spontaneously released from cortical explants, blocks dendritic outgrowth in explants of young hippocampal pyramidal neurons and promotes synaptogenesis. The effects of glutamate were blocked by glutamate receptor antagonists and prevented by the addition of TTX and the reduction of extracellular Ca^{2+}, manoeuvers which reduce glutamate release. Glutamate appeared to mediate its actions via non-NMDA receptors since NMDA had no effect on dendrite outgrowth, an observation consistent with previous findings by Mattson et al. (1988a) using dissociated cultures of young hippocampal pyramidal neurons. Application of glutamate suppressed the rate of dendritic elongation at low levels and led to process regression at higher levels. These effects were mimicked by quisqualate and kainate, but not by NMDA, and could not be blocked by AP5, a specific NMDA receptor antagonist. Conversely, glutamate acting at NMDA receptors in rat cerebellar granule cells *in vitro* stimulates outgrowth, demonstrating that the same transmitter can have different effects that depend on the system studied (Pearce et al., 1987, Rashid and Cambray-Deakin, 1992). The inhibitory transmitter GABA, like glutamate, suppresses neurite extension in cultured hippocampal pyramidal neurons (Mattson et al., 1987) suggesting that excess excitation or inhibition can reduce outgrowth. This notion is supported by further experiments in this system that show outgrowth continues when both GABA and glutamate are applied together at levels that normally produce dendritic regression when they are applied alone (Mattson and Kater, 1989).

The effects of neurotransmitters on neuronal architecture has also been demonstrated *in vivo*. In one study using amphibian an additional eye primordium was implanted into the optic tectum of *Rana pipiens*, resulting in it being innervated by two eyes. The inputs from the two eyes segregated and

produced a striped organization on the surface of the tectum (Reh and Constantine-Paton, 1985). Application of the NMDA antagonist AP5 disrupted this organization (Cline et al., 1987), indicating that the action of glutamate at the NMDA receptor was necessary to maintain the ordered structure of the tectum. In another *in vivo* study levels of serotonin were reduced pharmacologically in the early *Helisoma* embryo (Goldberg and Kater, 1989). This severely altered the morphology and connectivity of identified neurons and in particular produced excessive outgrowth of buccal neurons. This is consistent with results obtained from *in vitro* experiments described above.

Neurotransmitters have also been implicated in the regulation of neuronal migration, cell survival and more recently growth cone pathfinding. Zheng et al. (1994) showed that ACh is a chemoattractant during the neuronal development of embryonic *Xenopus* spinal neurons *in vitro*. ACh induced the turning of growth cones, such that a gradient of ACh produced a positive chemotropic effect on neuronal growth. The effects were blocked by nicotinic receptor antagonists and required the presence of extracellular Ca^{2+}. This is the only direct evidence to date of a chemotropic role for transmitters in neurite outgrowth. Kumoro and Rakic (1993) demonstrated the involvement of glutamate in the migration of cerebellar granule cells in the developing mouse. They showed that activating NMDA receptors or blocking the uptake of endogenous glutamate increased the rate of granule cell migration, while blocking NMDA receptors greatly decreased the rate of cell movement. NMDA receptor activation also promotes the survival of cultured cerebellar granule cells (Balázs et al., 1988). Granule cell growth in culture reaches a critical period in which cell death is activated. However activation of NMDA receptors during this period prevents cell death. The effects of non-NMDA receptor activation on granule cell survival is more complex. Addition of

kainate to these cultures at low levels promotes cell survival, whereas at higher levels it results in cell death (Balázs et al., 1990). The diverse effects of kainate are believed to depend on $[Ca^{2+}]_i$, with slightly raised levels promoting cell growth and higher levels producing excitotoxic death.

1.5 Mechanisms by which neurotransmitters affect neuronal development

Neuronal development can be affected by electrical activity (Marsh and Beams, 1946, Jaffe and Poo, 1979, Hinkle et al., 1981, Shatz and Stryker) and second messengers such as cAMP (Mattson et al., 1988c), PKC (Spinelli and Ishii, 1984) and Ca^{2+} (reviewed by Mattson, 1988, Kater et al., 1988). In particular, Ca^{2+} is known to play a major role in the regulation of neuronal outgrowth by neurotransmitters. The fluorescent Ca^{2+} indicators developed by Tsien (1989) have enabled the measurement and localization of Ca^{2+} in living growth cones. In *Helisoma* buccal neurons the inhibition of outgrowth by serotonin is associated with a dramatic rise in cytoplasmic Ca^{2+} of over 500nM in the growth cone (Cohan et al., 1987). In addition Ca^{2+} channel blockers prevent the reductions in dendrite length normally seen in responses to glutamate in hippocampal neurons while Ca^{2+} ionophores mimic the effects of glutamate (Mattson et al., 1988a). Decreases in $[Ca^{2+}]_i$ can also inhibit outgrowth. For example when high concentrations of Ca^{2+} channel blockers are applied to *Helisoma* neurons growing normally the growth cone ceases to be motile (Mattson and Kater, 1987). Al-Mohanna et al (1992) varied extracellular Ca^{2+} levels and measured its effects of neurite outgrowth in rat sensory neurons. They demonstrated that process extension is inhibited by both low and high levels of $Ca^{2+}{}_i$ and that it shows a bell-shaped dependence on $[Ca^{2+}]_i$, a model first proposed by Kater et al. (1988). Thus, the ability of many neurotransmitters to alter $[Ca^{2+}]_i$ is the likely mechanism by which transmitters affect neuronal outgrowth.

The influence of transmitters on neuronal migration and cell survival is also thought to be mediated via Ca^{2+}_i. The increase in the rate of granule cell migration produced by glutamate, as described in section 1.4, is significantly reduced in low extracellular Ca^{2+} concentrations ($[Ca^{2+}]_e$) (Kumoro and Rakic, 1993), suggesting glutamate mediates its effects on migration via its influence on Ca^{2+}. Balázs et al. (1988) showed that granule cell survival is promoted by NMDA receptor activation (section 1.4). Application of the Ca^{2+} ionophore ionomycin, at a concentration that raises $[Ca^{2+}]_i$ to the same level as NMDA, also promotes cell survival (Pearson et al., 1992). This indicates that glutamate may be exerting its effects on cell survival by altering $[Ca^{2+}]_i$.

Further evidence for the importance of Ca^{2+} during CNS development comes from the presence of spontaneous Ca^{2+} transients in several regions of the embryonic nervous system. Retinal neurons of the ferret show transient increases in $[Ca^{2+}]_i$ that last 10-15 seconds and that sometimes move from cell to cell in a wave across the retina (Wong et al., 1995). These Ca^{2+} waves are present when waves of electrical activity are known to occur in the ferret retina and they spread at similar rates and over similar areas to the electrical waves commonly seen during retinal development. Meister et al. (1991) used electrode arrays to record action potentials generated amongst ganglion cells of the ferret and cat retina at a time when mature photoreceptors are absent. The waves spread across the retina and lasted several seconds followed by one or two minutes silence. The axons of ganglion cells grow into the lateral geniculate nucleus (LGN) and the spatial distribution of ganglion cell terminals is dependent on their electrical activity (Shatz and Stryker, 1988). The correlated firing of action potentials by adjacent ganglion cells strengthens their connections in the LGN and is necessary for the withdrawal of supernumerary branches in inappropriate layers.

Spitzer (1994) has suggested that Ca^{2+} transients may stimulate Ca^{2+}-dependent transcription. In *Xenopus* spinal cord neurons Ca^{2+} transients influence ion channel phenotype and control GABA expression in interneurons (Desarmenjen and Spitzer, 1991, Spitzer et al., 1993). However, the involvement of neurotransmitters in the triggering and propagation of Ca^{2+} waves is as yet unclear (for review see Catsicas and Mobbs, 1995).

1.6 Neurotransmitters and cell death

The work of Lucas and Newhouse in 1957 was the first to show that glutamate can have lethal effects on neurons in the CNS. They found that systemic injection of high concentrations of glutamate into mice caused widespread cell death in the retina. It is now well-established that excessive activation of excitatory amino acid (EAA) receptors can trigger a cascade of intracellular biochemical events that lead to cell death (Olney et al., 1973, Choi, 1988). Consistent with this, excitotoxic neuronal death in the immature brain can be blocked by selective antagonists of EAA receptors (for review see McDonald and Johnston, 1990). The neurotoxic effects of many transmitters involves an increase in $[Ca^{2+}]_i$ (for review see Frandsen and Schousboe, 1993). That this is so has been particularly well demonstrated by the experiments of Tymianski et al. (1993) who showed that neuronal death triggered by over-activation of NMDA receptors can be reduced by the addition of cell-permeant Ca^{2+}-chelators such as BAPTA-AM. Neurotransmitters can increase levels of cytoplasmic Ca^{2+} via several mechanisms: Ca^{2+} may enter directly through the receptor channel itself, through depolarization-evoked opening of voltage-gated Ca^{2+} channels or through second messenger systems that lead to the release of Ca^{2+} from internal stores. Sensitivity to EAA neurotoxicity changes profoundly during development with different brain regions exhibiting different developmental profiles of susceptibility. For example, in the

immature brain NMDA is a potent neurotoxin (McDonald et al., 1988, Ikonomidou et al., 1989) while sensitivity to kainate is low (Campochiaro and Coyle, 1978). In contrast, there is a high sensitivity to kainate in the adult rat brain and NMDA produces little neurotoxicity (Olney, 1978). Similarly, in the chick retina kainate is potently neurotoxic only in the adult and late in embryonic development (Schwarcz and Coyle, 1977, Ehrlich and Morgan, 1980, Ingham and Morgan, 1983, Catsicas and Clarke, 1987).

It has long been recognized that cell death is an important and normal part of CNS development (Glücksmann, 1951). This phenomenon is often termed naturally-occurring cell death and is widespread throughout a variety of tissues and organs (reviewed by Oppenheim, 1991, Ellis et al., 1991). In the chick retina most synapse formation takes place between embryonic day (E) 12 and 16. This coincides with the period of naturally-occurring cell death that takes place in the chick retina, in particular in the GCL (Hughes and LaVelle, 1974, Hughes and McLoon, 1979, Rager, 1980). However, the involvement of neurotransmitters and their receptors in naturally occurring cell death is as yet unknown.

1.7 Aims of the current study

The aim of this thesis was first to identify which and at what time different neurotransmitter receptors are present in chick retina during embryonic development. This information was used in an investigation of the developmental effects of these transmitters in the retina. Many of the experiments in this thesis were performed on primary cultures of embryonic chick retina in which the receptors could be electrophysiologically characterized and their developmental effects quantified.

Chapter 2 describes the methods employed in this thesis. **Chapter 3** describes the identification of cells in embryonic chick retinal cultures and experiments in which the whole-cell patch clamp technique was used to characterize the neurotransmitter receptors and voltage-gated channels found in these cells. **Chapter 4** describes consequences of non-NMDA receptor activation at different times in development. **Chapter 5** reports the effects of glutamate and its analogues on neurite extension in cultured embryonic retinal cells. Finally **Chapter 6** describes the effects of neurotransmitters on $[Ca^{2+}]_i$ in isolated embryonic chick retina and developmental profiles of receptor expression are made based on the ability of transmitters to influence $[Ca^{2+}]_i$.

Chapter 2

Methods

2.1 Preparation of primary retinal cultures

Many of the experiments described in this thesis used primary cultures of embryonic chick retina. They were prepared as follows: Large forceps were used to open an eight day old egg and the embryo was lifted out. After decapitation the eyes were scooped out using small curved forceps and placed in a petri dish containing Ca^{2+}- and Mg^{2+}-free modified Hanks Balanced Salt Solution (MHBSS) at pH 7.4 (Sigma). The front of the eye and the schlera were removed to leave the retina supported on the vitreous humour. The retina was peeled away and placed in a small petri dish containing MHBSS. Retinae from four embryos were collected and all adherent pigment epithelium was removed. The retinae were broken into small fragments using two pairs of fine forceps and transferred to a culture flask containing 2mls MHBSS and incubated for 10 minutes at 37°C in order to reduce Ca^{2+} and Mg^{2+} in the extracellular environment as much as possible. The retinal pieces were transferred to a centrifuge tube and spun for three minutes at 200xg. The supernatant was discarded and the cell pellet was resuspended in 7mls of 0.1% trypsin (Sigma T8918) in MHBSS and incubated for 25 minutes at 37°C. The cells were repelleted by centrifugation at 300xg for 5 minutes and resuspended in 10mls of Dulbecco's Modified Eagles Medium (DMEM) (Sigma). The DMEM was supplemented with 10% fetal calf serum, 4mM L-glutamine and 0.2 units/ml penicillin/streptomycin (all Gibco). The tip of a Pasteur pipette was used to add a small amount of DNAase I (Sigma) to the cell suspension and the cells were then triturated using a fire-polished Pasteur pipette. Cells

were plated in 35x10mm diameter culture dishes (Falcon 3001) at a density of $1x10^6$ cells/ml.

The cell cultures were maintained at 37°C in an atmosphere containing 5% carbon dioxide and the culture medium was replaced with fresh DMEM every 2 days.

2.2 Preparation of retinal explant cultures

Embryos were killed at E6 by decapitation and the eyecups were dissected out and placed in modified Hank's Balanced Salt solution (HBSS) with Ca^{2+} and Mg^{2+}. The retinae were removed as described in section 2.1. 2-4mm^2 pieces of retina were cut out from the centre of the retina and transferred onto the membrane of a Millicell culture plate insert (Millipore) placed in a petri dish containing DMEM supplemented as in section 2.1. The retinal pieces were flattened using fine forceps and the HBSS was removed from the central well to leave the tissue exposed at an air-liquid interface. This step was crucial in obtaining subsequent "organotypic" growth of the explants. The explants were maintained as in section 2.1.

2.3 Immunocytochemistry

2.3.1 Identification of neuronal cell types

Primary retinal cultures were washed twice in phosphate buffered saline (PBS) (Gibco) and fixed for 30 minutes in 4% formaldehyde in PBS. Non-specific binding sites were blocked by a 30 minute treatment with PBS containing 1.5% horse serum (Vectastain ABC kit, Vector). Excess serum was removed and the cells incubated for an hour in a buffer solution (PBS,

0.1% bovine serum albumin (Sigma) and 0.3% Triton-X-100 (BDH)) containing a 1 in 200 dilution of anti-syntaxin protein antibodies (HPC-1) raised in mouse (Sigma). After 3 washes in PBS the cells were bathed for 45 minutes in a 0.5% solution of biotinylated goat anti-mouse antibodies in PBS and 1.5% horse serum (Vector). The avidin:biotinylated horseradish peroxidase complex (Vector) was prepared in PBS and bound to the secondary antibody to provide amplified staining (figure 2.1). The cells were rinsed 3 times in PBS and 3-amino-9-ethylcarbazole (AEC) (Sigma) was used to visualise immunostained cells.

The above procedure was repeated with the following modifications. Anti-syntaxin was replaced with anti-THY-1 protein antibodies (gift from Peter Jeffrey, CMRI, Camperdown, Australia) at a dilution of 1 in 750. Triton-X-100 was excluded from the primary antibody buffer solution and the cells were fixed prior to treatment with AEC. For identification of GABAergic neurons the procedure for anti-syntaxin labelling was altered to include the following changes. The cells were fixed in 4% glutaraldehyde and the primary antibody was anti-GABA raised in rabbit (Sera-lab, AES 131). Cells were incubated in the antibody overnight at a dilution of 1 in 500. Biotinylated anti-rabbit antibodies at a dilution of 1 in 200 were used as the secondary antibody. The peroxidase substrate DAB (3,3'-diaminobenzidine tetrahydrochloride) (Sigma) was used to visualise the cells in place of AEC.

2.3.2 Cobalt-staining of cells expressing Ca^{2+}-permeable kainate receptors

The technique established by Pruss et al. (1991) was used to detect the entry of cobalt (Co^{2+}) via cation-permeable non-NMDA (AMPA/kainate) glutamate-gated receptors. Retinal explants from E6 chicks were prepared as described in section 2.2. After several days in culture the explants were

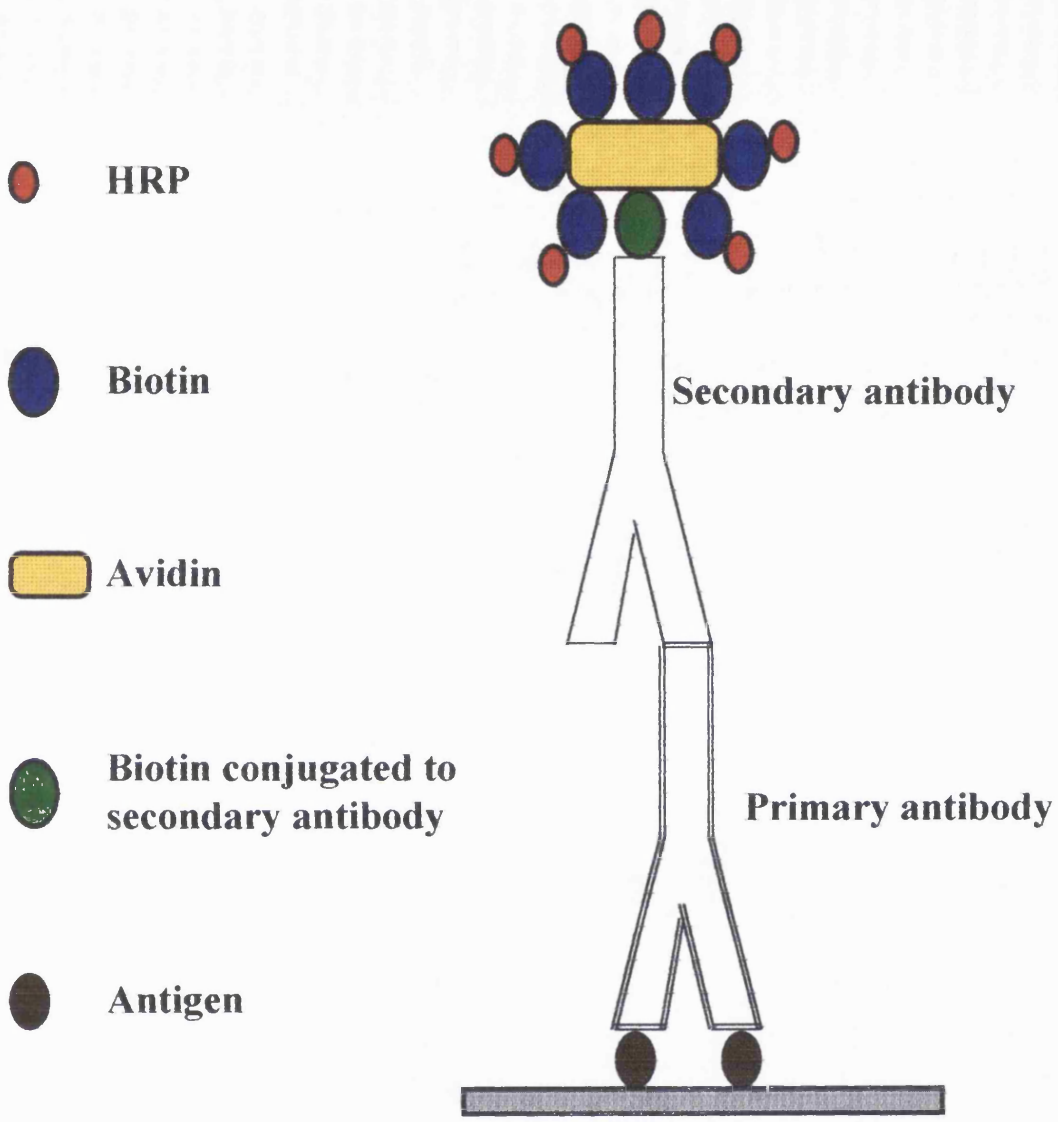

Figure 2.1

Schematic diagram of the biotin/avidin technique. The secondary antibody is conjugated to biotin and an avidin/biotin complex labelled with horseradish peroxidase is used for detection. Aminoethylcarbazole (AEC), which yields a red reaction product, was used as the substrate for HRP.

washed in solution D and stimulated at room temperature for 15 minutes in solution D (table 2.1) containing 5mM $CoCl_2$ and 100μM kainate (Sigma). To remove non-specifically bound Co^{2+} the explants were rinsed twice in solution D containing 2mM EDTA. The Co^{2+} was precipitated by a 5 minute treatment with solution D containing 0.75% $(NH_4)_2S$. The explants were then washed 3 times in solution D and fixed for 15 minutes in 95% ethanol and 5% acetic acid. The tissue was prepared for paraffin embedding by a 60 minute wash in 95% ethanol followed by dehydration in 100% ethanol, again for 60 minutes. The explants were soaked in Cedar wood oil overnight and embedded in paraffin at 60°C for an hour. 10μm sections were cut and transferred to gelatinised slides (0.5% gelatine and 0.1% thymol to prevent bacterial growth). The sections were rehydrated through Histoclear (National Diagnostics) and a series of ethanol solutions and CoS precipitation was enhanced by a 15 minute exposure to a silver intensification solution which consisted of 5.9mM $AgNO_3$ in 22mM sodium acetate, 15mM sodium tungstate, 1.3mM ascorbic acid, 0.8% Triton-X-100 and 6% glacial acetic acid. The intensification solution was washed off with solution D and the sections dehydrated before mounting in Canada balsam. A similar procedure that excluded paraffin embedding was applied to dissociated retinal cultures and following silver intensification the cells were mounted in a permanent aqueous mountant (Serotec).

To check for the possibility that Co^{2+} might enter cells via voltage-gated Ca^{2+} or NMDA channels the following controls were carried out. Dissociated cultures were Co^{2+} stained after 6 DIV as described above with some modifications. Kainate was excluded from solution D, Na^+ was replaced with K^+ and 50μM CNQX (an AMPA/kainate receptor antagonist) was added to the solution. Under these conditions the cells should be strongly depolarized. In another control kainate was replaced with 100μM NMDA,

5μM glycine and 20μM CNQX (all tocris), and Mg^{2+} was excluded from the solution. No Co^{2+}-staining of cells was observed in either control demonstrating the specificity of the technique for the labelling of cells that express AMPA/kainate receptors.

2.3.3 Nissl-staining of retinal explant cultures

For clearer visualisation of structure, retinal explants were paraffin embedded and sectioned as described in section 2.3.2. The sections were rehydrated through Histoclear and a graded series of ethanol solutions (100%, 95%, 70% to H_2O) and stained with cresyl violet for about 20 seconds. After dehydration the sections were mounted in Canada balsam and cover-slipped.

2.3.4 Double labelling with cobalt-staining and antibodies

The cobalt-staining technique was carried out as described in section 2.3.2 for dissociated cultures with the following modifications. The cells were fixed with 4% formaldehyde in PBS and prior to CoS precipitation the cells were immunostained as described in section 2.3.1 using anti-syntaxin as the primary antibody. To determine the proportion of syntaxin-positive cells that were Co^{2+}-positive, immunostained cells were photographed and the same fields were then re-photographed after development of the Co^{2+}-stain.

2.3.5 Labelling dead cells with propidium iodide

The DNA labelling fluorescent dye propidium iodide (Sigma) was used to detect cells in retinal cell cultures that had lost their membrane integrity. The culture medium was removed and replaced with HBSS containing 20μM propidium iodide. The cells were incubated at 37°C for 20 minutes in the

propidium iodide solution and then washed in HBSS and viewed by UV light under a fluorescence microscope equipped with fluorescein filters.

2.3.6 Data analysis

In some experiments the number of cells, their processes or the fraction of immunostained cells in retinal cultures were counted using a hand tally counter. In order to do this Petri dishes were examined by phase contrast using a Zeiss Achrostigmat x35 lens and x10 eyepieces. For counts of Co^{2+}-stained cells the cultures were examined by bright field illumination and for propidium iodide under fluorescent illumination. The counts were normalised to the number of cells stained or the number of processes per 100 cells and the data were statistically analysed using the two-tailed Student's T-test. This test allows a comparison to be made between the means of two small samples as follows:

$$t = \frac{\bar{x}_1 + \bar{x}_2}{s\sqrt{\frac{1}{n_1} + \frac{1}{n_2}}}$$

where the first sample has n_1 observations and a mean $\bar{x}_1$, while in the second the corresponding quantities are n_2 and $\bar{x}_2$.
S is an estimate of the standard deviation based on both samples jointly and can be calculated as follows:

$$s^2 = \frac{(n_1 - 1)s_1^2 + (n_2 - 1)s_2^2}{n_1 + n_2 - 2}$$

where s_1 and s_2 are the standard deviation of the first and second sample respectively.

The resultant value of t can be used to find the probability, p, of observing this t value for a particular sample size.

2.4 Superfusion

The same gravity fed perfusion system was used to change the extracellular solution bathing dissociated embryonic chick retinal cells during patch-clamp recordings and pieces of embryonic chick retina during imaging experiments. Extracellular solutions were contained in syringe barrels and led through polythene tubes to a common inlet at the side of the bath. Superfusion was continuous and stopcocks in the solution line enabled the selection of one of several different solutions during experiments. The solution level in the bath was kept constant by a suction pump connected to an outlet on the side of the bath opposite to the inlet. The inlet could be moved and was positioned near to the cell or piece of tissue under study to enable a rapid change of the bathing medium. Solution exchanges were typically complete within 1-2s. When pieces of embryonic chick retina were used they were held down by a "harp" made from a platinum wire with nylon strings. In imaging experiments the perfusion chamber (volume 500μl) consisted of a petri dish in which part of the bottom was replaced with a thin glass coverslip. In patch-clamp experiments 35x10mm diameter culture dishes were used as the recording chamber, providing a 1ml bath volume

2.5 External solutions

Table 2.1 gives the composition of solutions used to superfuse retinal cells during patch-clamp and imaging experiments. The pH of all external solutions was 7.4. The external solutions used HEPES as a pH buffer and were bubbled with O_2 throughout the course of the experiments.

Most drug stock solutions were made up in distilled water and then diluted in the extracellular solution. However stocks of CNQX (Tocris), diltiazem and nifedipine were made up in DMSO (Sigma). Where significant quantities of DMSO were incorporated in drug containing solutions then DMSO was also added to the solutions employed in the controls.

2.6 Internal solutions

Table 2.2 gives solutions used to fill patch-pipettes during whole-cell patch-clamp experiments. The standard internal solution was solution A. The pH of all internal solutions was titrated to 7.0 using KOH and occasionally NMDG. In some experiments patch-pipettes also contained Lucifer Yellow CH (Sigma). The dye was added at a concentration of 1.0 mg/ml of internal solution and the cells were visualised by illumination with UV light.

2.7 Ionophoresis

In some patch-clamp experiments the distribution of neurotransmitter receptors within the cell membrane was mapped. In these experiments ionophoresis was used for rapid, local application of the drug. Ionophoretic electrodes were pulled on a Livingstone-type microelectrode puller (Narashige model PG-1, No.8101) from thin-walled borosilicate glass with a microfilament insertion (Clark Electromedical GC150TF10). Electrodes were connected via a silver/silver chloride (Ag/AgCl) wire to a constant current device providing currents appropriate to retain or eject the drug.

2.8 Recording from isolated cells

The whole-cell patch-clamp technique (Hamill et al., 1981) was employed to study the voltage- and transmitter-gated currents in cultured chick retinal cells. In some experiments this method was used to examine the electrogenic uptake of glutamate into retinal glial cells. Patch-pipettes were pulled on a BBCH puller (Mecanex, Geneva) from thick-walled borosilicate glass with an internal filament (Clark Electromedical Instruments No. Gc150F10). The resistance of the pipettes before sealing onto a cell was usually between 5 and 10MΩ.

Recordings were made from cells grown in 35x10mm diameter culture dishes, which provided a bath volume of approximately 1ml. The tissue culture dish was mounted directly on the stage of an upright Zeiss microscope and the cells observed under Hoffman contrast optics. The patch-pipette was inserted in a perspex electrode holder (Clark Electromedical) and moved up to the cell of interest using a micromanipulator (Narishige). Gentle suction aided the formation of a high resistance seal between the glass and the cell membrane. Further suction, combined with membrane hyperpolarization, led to the rupture of the underlying membrane required for whole-cell patch-clamping. Typically the cell could then be held in voltage clamp for up to 30 minutes. During a voltage clamp experiment the membrane voltage was controlled and the transmembrane current required to maintain the voltage was measured as the voltage drop across a 500MΩ resistance of a current to voltage converter (Axopatch 1-C, Axon Instruments, Foster City, CA, USA). Pulses of 10mV amplitude were applied to the cell on entry into the whole-cell mode and capacity transients were stored for later analysis. A Ag/AgCl pellet placed in the bath solution was the earth electrode and all measurements were made relative to this ground.

2.8.1 Cell capacitance and series resistance

In an ideal experiment the resistance of the patch pipette would be zero, in which case only the speed of the electronics would limit the time resolution for measuring membrane currents. However, in reality the resistance of the pipette may be such that if the current flowing is large, then the series resistance of the tip of the pipette will not be negligible. This means that the actual voltage seen by the cell membrane can be significantly different from the command voltage. It is therefore important to calculate the series resistance (R_p) in the pathway from the patch-pipette to the cell as this enables a measurement of the voltage error to be made. Both the series resistance and the cell membrane capacitance were measured from the current response to a 10mV voltage step from a holding potential near to the zero current potential. The cell membrane can be treated as a combination of a resistor (R_m) and a capacitor (C_m) placed in parallel (figure 2.2). R_{seal} is the resistance of the seal between the pipette tip and the cell membrane. The capacity transient resulting from the 10mV pulse (figure 2.3) was fitted by a single exponential using a curve fitting computer program (Clampfit, Axon Instruments) and is predicted to produce a current change with the following time course:

$$I(t) = V (1+R_m e^{-t/\tau} / R_p) / (R_m+R_p)$$

Where V = magnitude of the voltage step

R_m = membrane resistance

R_p = pipette series resistance

τ = time constant of the capacity current decay

$t = 0$ at the onset of the voltage step

The program allowed, by positioning of cursors, measurements of the initial

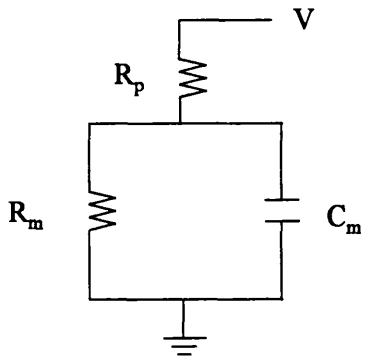

Figure 2.2

Circuit diagram of a whole-cell patch-clamped cell. V is the input voltage, R_p the series resistence, R_m the membrane resistance and C_m the cell membrane capactitance.

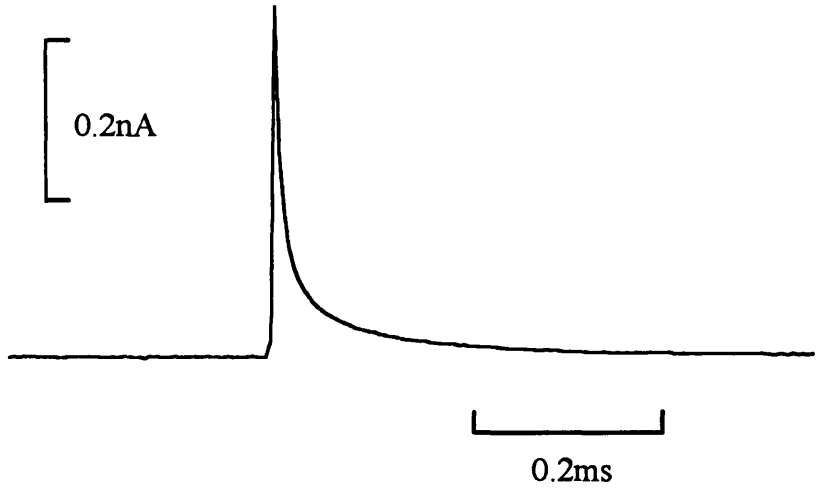

Figure 2.3

Current flow in a whole-cell patch-clamped retinal neuron in response to a 10mV depolarizing pulse from a holding potential of -62mV. For this cell the series resistance was 20.8MΩ, the cell capacitance was 5.3pF and the membrane resistance was 320MΩ. The time constant of the current decay (τ) was 0.11ms.

pipette current ($I_p(0)$), the steady state pipette current at the end of the pulse ($I_p(\infty)$) and the time constant (τ).
The series resistance can then be calculated from the ratio between the voltage step and the current at time zero:

$$R_p = V / I_p(0)$$

The steady-state current (at time $t = \infty$) is:

$$I_p(\infty) = V / (R_m+R_p)$$

The membrane resistance can thus be deduced from:

$$R_m = (V/ I_p(\infty)) - R_p$$

and finally the cell membrane capacitance can be calculated:

$$C_m = \tau (R_m+R_p) / R_mR_p$$

which reduces to $C_m= \tau / R_p$ when the membrane resistance is much larger than the pipette series resistance (Marty and Neher, 1983). This was the case in all cells studied.

The series resistances were typically between 10 and 30MΩ, and although these resistances are relatively high, the error voltages were minimal because the cells have a low surface area and capacitance (1-5pF for retinal neurons and up to 20pF for glial cells) and because the series resistances were always much smaller than the membrane resistance. The maximum current (I)

seen in these experiments was around 200pA, for which with a series resistance of 30MΩ (a worst case example) the voltage error (V) is:

$V = IR_p$

V = 200 x 10-12 x 30 x 106 = 6mV

Thus in the worst case the voltage drop was 6mV. Data from cells where the series resistance voltage drop was greater than 5mV are not included in this thesis.

2.8.2 Correction for junction potentials

Junction potentials occur whenever dissimilar conductors are in contact. The patch-pipette and the bath solution are of different ionic composition. This means that when the pipette is placed in the bath solution a diffusion potential will develop across the liquid-liquid interface at the pipette tip. The magnitude of the junction potential depends on the concentration, charge and mobility of the ions in both the internal and external solutions. In the solutions used in this thesis Cl^- ions are the most important in determining the liquid junction potential because Na^+ ions in the external and K^+ ions in the internal solution have the same charge and similar mobilities to one another and their contributions to this potential thus cancel out. When the patch-pipette is lowered into the bath solution the experimenter sets the zero current potential using the junction null control on the patch-clamp amplifier. Thus the zero-current potential is set with an error voltage equal to the liquid junction potential. This error exists because the true zero current potential can only be set with patch-pipette solution in the bath and the pipette.

The magnitude of junction potentials was measured as described by Fenwick et al. (1982). The zero current potential of a filled pipette in bath solution was recorded by switching the patch-clamp amplifier to current

clamp, allowing changes in voltage to be monitored. A 4M NaCl agar bridge was used to connect the reference electrode to the bath to prevent changes in the reference electrode potential. The junction potential was then observed by changing the bath solution from the external solution to the internal pipette solution. The potentials obtained were specific for pairs of solutions and are listed in table 2.2.

2.8.3 Data acquisition

During patch-clamp experiments data were recorded onto a video tape using a pulse code modulator (Sony PCM 701ES) and in most experiments were also simultaneously stored on digital magnetic media using a computer equipped with a Labmaster laboratory interface (TL-1, Axon Instruments).

2.8.4 Data analysis

Currents recorded from retinal neurons and glial cells were analysed using "PCLAMP" software (Axon Instruments) and the Borland Quatro Pro spreadsheet programme. Graphs were plotted in Sigma Plot for Windows 6.0 (Jandel Scientific).

2.8.5 Noise analysis

The presence of noise in cell membrane currents is due to the random opening and closing of ion channels in the membrane. The open probability of ligand-gated channels increases when neurotransmitters are applied at non-saturating doses and this is seen as an increase in the noise in the evoked current. Such noise increases indicate that the current is a result of the opening of ion channels and not the operation of an electrogenic carrier.

When carriers such as those transporting glutamate operate, the noise increases produced are usually too small to resolve (Brew and Attwell, 1987). To examine noise changes in membrane current noise, data were digitized from tape recordings using a computer (PDP11/73) equipped with an analogue to digital converter (12 bit). The data was low pass filtered at 1000Hz (8 pole Butterworth, Bar and Stroud EF5-01 filter), to ensure that there were no components of the signal at frequencies higher than half the sampling frequency (2048Hz), and high pass filtered at 10Hz to remove frequencies associated with the gross change in the current produced by the drug. The variance of the current noise about the mean was measured before, during and after drug application.

2.9 Measurements of $[Ca^{2+}]_i$ using fluorescent probes

Changes in $[Ca^{2+}]_i$ evoked by activation of neurotransmitter- or voltage-gated channels were measured using Ca^{2+}-sensitive fluorescent dyes. Fluorescence measurements of intracellular ion concentrations use a dye molecule coupled to an ion chelator in such a way that the dye changes its properties when the chelator binds the ion of interest. A range of fluorescent dyes have been produced that have high selectivity and sensitivity for physiological concentrations of intracellular ions and messengers such as Ca^{2+}, K^+, H^+ and cAMP (Tsien, 1989). Ion sensitive dyes allow measurements of ion concentrations both within the cytoplasm of single cells and in tissues comprised of large numbers and several types of cells such as the retina.

Ca^{2+}-sensitive dye molecules such as fura-2, indo-1 and Calcium Green utilise the Ca^{2+}-selective binding site of a derivative of the non-fluorescent Ca^{2+} chelator molecule BAPTA. The chelator is conjugated to a fluorophore such as fluorescein or rhodamine. The Ca^{2+} binding site has a high selectivity

for Ca^{2+} and when Ca^{2+} is bound a lone pair of electrons from an amino nitrogen, located on the Ca^{2+} binding site, moves away from the fluorophore causing a change in its fluorescence. Ca^{2+}-sensitive fluorescent dyes fall into two general categories: single-wavelength (SW) and ratiometric dyes. SW indicators, e.g. Calcium Green or fluo-3, change the intensity of their fluorescence and the spectrum of the light they emit in response to changes of $[Ca^{2+}]_i$, without any significant change in their spectral maxima. Ratiometric dyes, e.g. fura-2 or indo-1, not only show changes in intensity with changing Ca^{2+} levels, but the Ca^{2+}-free and Ca^{2+}- bound forms of the dye have distinct spectra and their spectral maxima lie at different wavelengths.

The SW indicator Calcium Green-1 (Molecular Probes) was used to monitor changes in $[Ca^{2+}]_i$ in primary cultures of embryonic retinal cells and in isolated embryonic retina in response to application of neurotransmitters. Calcium Green-1 is a visible light-excitable probe derived from fluorescein and is excited at long wavelengths. It has an excitation maximum of 506nm and exhibits an increase in fluorescence emission intensity with little shift in wavelength (Fig 2.4). Calcium Green-1 is structurally similar to fluo-3 but is considerably brighter at low Ca^{2+} levels and bleaches at a significantly slower rate. It increases its fluorescence fourteen times on binding Ca^{2+} and has a K_D for Ca^{2+} of 189nM.

Using ratiometric dyes like fura-2 obviates the problems associated with variations in dye loading, bleaching, dye leakage and differences in cell thickness and allows an estimation of the Ca^{2+} concentration in the cell or cells of interest to be made. However ratiometric measurements were not possible because the necessary equipment was not available. Of the SW dyes Calcium Green has advantages in that it is slow to bleach, its emission is in regions of the spectrum where cellular autofluorescence and scattering is

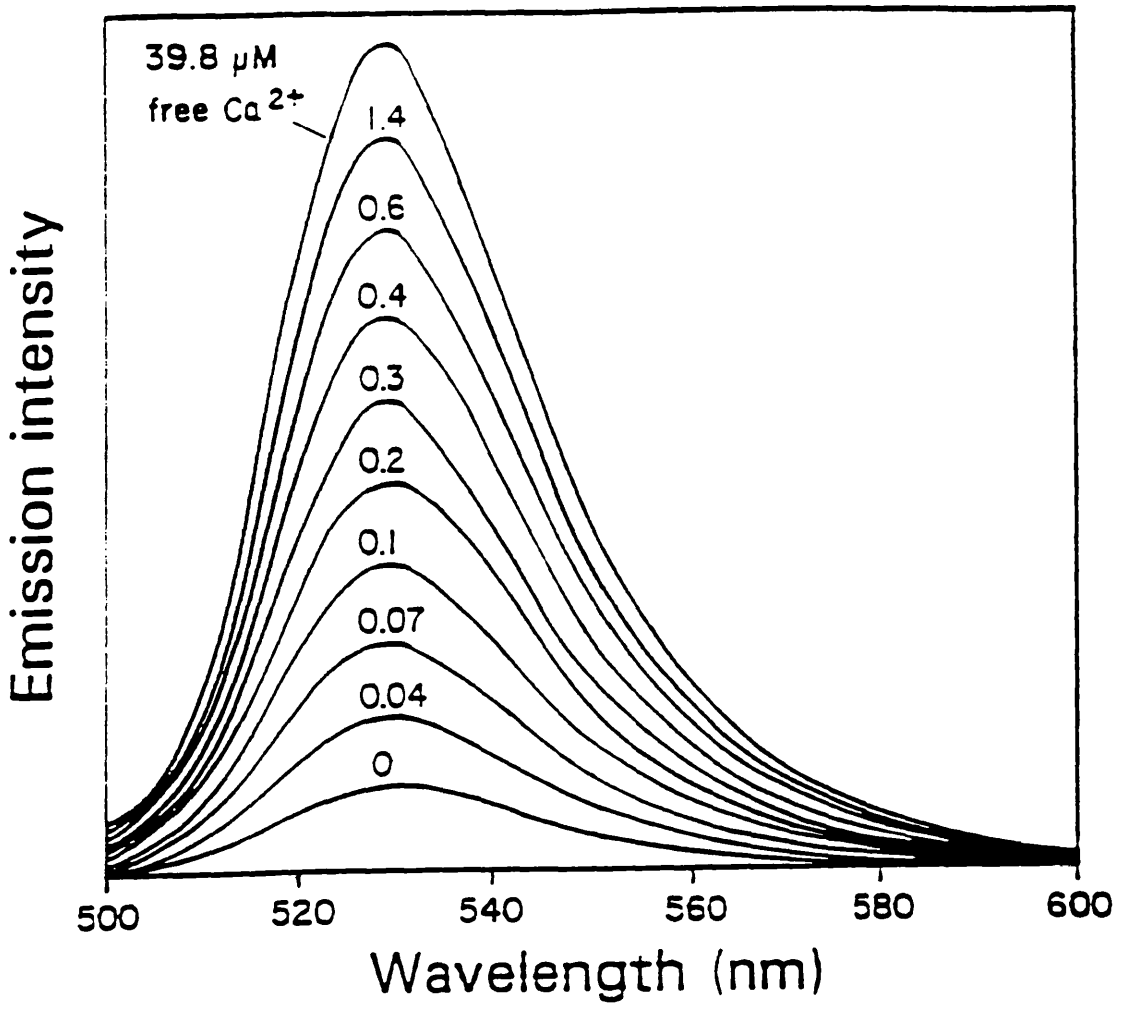

Figure 2.4

The emission spectra of Calcium Green-1 (reproduced from Molecular Probes catalogue, 1995). The fluorescence emission intensity is plotted as a function of wavelength in increasing concentrations of free Ca^{2+} (indicated above each trace). Calcium Green-1 has an excitation wavelength of around 505nm and increases its emission intensity on Ca^{2+} binding without any shift in wavelength. The maximum emission wavelength occurs at around 530nm.

minimal, and the low energy of excitation light needed reduces the risk of cellular photodamage.

2.9.1 Dye loading

Calcium Green-1 is available in a membrane-permeable form in which the carboxylic groups are masked with acetoxymethyl (AM) ester groups. This molecule is uncharged and readily permeates the cell membrane. Once inside the cell the lipophilic groups are cleaved by non-specific esterase activity leaving the charged free acid form of the dye inside the cell. This form of the dye leaks out of the cell far more slowly than the AM ester.

Whole retinae, dissected as described in section 2.2, were loaded with Calcium Green-1 AM (Molecular Probes C3011) by maintaining them for 1 hour at 37°C in the dye solution bubbled with O_2. The dye solution was prepared as follows; 1.25μl of 20% pluronic acid (in DMSO) was added to a 10μl aliquot of 2mM Calcium Green-1 AM (in anhydrous DMSO) just before use. 10μl of this mixture was added to 2mls of solution A (table 2.1) to give a final concentration of 10μM Calcium Green and 0.01% pluronic acid. After loading, retinae were washed thoroughly for 1 hour in oxygenated solution A (table 2.1) to remove excess dye and any uncleaved AM ester that leaked from the cells.

2.9.2 The fluorescence set-up

The imaging set-up is shown in figure 2.5. Cells were examined under an Axioscope 100 fluorescence microscope equipped with a fluorescein epi-illumination filter set (Omega Optical Company) and a Zeiss Fluar 100x lens (NA 1.4). Cells were illuminated by a Xenon arc lamp directed through a

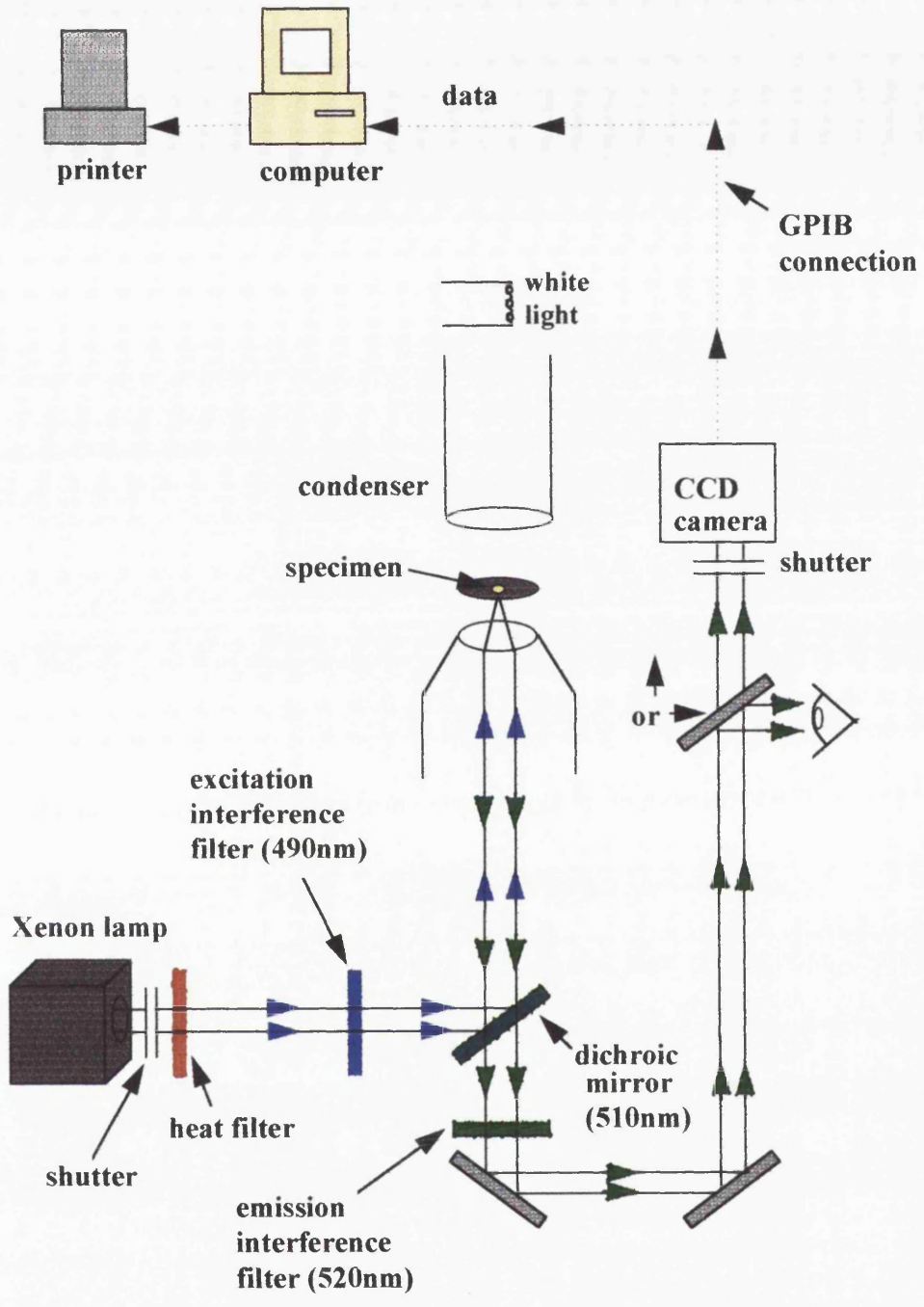

Figure 2.5

Schematic diagram of the fluorescent imaging set-up.

Cells were illuminated by a Xenon arc lamp directed through a 490nm excitation filter (blue) and emitted fluorescence was collected at 520nm (green) by a cooled CCD camera. Images were transferred to computer for storage. Mirrors are represented by grey rectangles.

490nm excitation filter and neutral density filters to reduce the lamps intensity. Emitted fluorescence was collected at 520nm by a slow-scan cooled CCD camera (Digital Pixel model 2000). Synchronized electronic shutters in front of the lamp and the camera were used to control exposure of the CCD to the emitted light and to prevent bleaching of the specimen. Images were transferred to a computer and stored on its hard disk. The mean intensity within the central part of the image was calculated using Lucida 2.0 software (Kinetic Imaging Ltd, Liverpool, England).

Drugs were bath applied as described in section 2.4 and the solutions continuously bubbled with O_2.

2.9.3 Image analysis

Calcium Green is not a ratiometric dye, however estimates of Ca^{2+} concentration can be made using the single-wavelength equation (reviewed by Thomas and Delaville, 1991). However, in the experiments described in this thesis Ca^{2+} concentrations were not calculated since light was collected from areas of retina in which some cells underwent $[Ca^{2+}]_i$ increases and others did not. Instead changes in Calcium Green fluorescence were normalised to the initial baseline fluorescence intensity. For some experiments responses were normalised with respect to the largest fluorescence change produced by application of a drug. Intensity data were analysed using the Borland Quatro Pro spreadsheet programme and graphs were plotted in Sigma Plot for Windows 6.0. Images were background subtracted. This was done by taking an image that did not include retinal tissue and subtracting this from the images obtained during an experiment using Lucida 2.0 software.

2.9.4 Confocal imaging

A Leica confocal scanning laser microscope (Heidelberg, Germany) was used to visualise sections in the ZX plane of flat-mounted embryonic chick retinae before, during and after application of a drug. This enabled identification and localization of the population of responsive cells.

Table 2.1: External solutions

	A	B	C	D
NaCl	136.9	136.9	116.9	57.5
KCl	5.3	5.3	5.3	5
$MgCl_2$	0.41		0.41	2
$CaCl_2$	3	3	3	2
$BaCl_2$			10	
HEPES	3	3	3	10
glucose	5.6	5.6	5.6	12
sucrose				139
TEACl			5	
TTX			100nM	
pH	7.4	7.4	7.4	7.6
pH with	NaOH	NaOH	NaOH	NaOH

All concentrations are in mM unless otherwise stated

Table 2.2: Internal solutions

	A	B
K-acetate	150	
KCl	10.0	
$MgCl_2$	2	2.0
$CaCl_2$	0.1	0.1
HEPES	10	10
$K_{2.5}$ EGTA	1.1	
Na_2EGTA	1.0	5.6
NMDG*-gluconate		160
EGTA-NMDG*		1.1
ATP-Mg_2		1.0
pH	7.0	7.0
pH with	KOH	NMDG*
tip potential	3mV	4mV

* NMDG is N-methyl-D-glucamine

All concentrations are in mM

Chapter 3

Early *in vitro* development of neurotransmitter- and voltage-gated channels in dissociated retinal neurons

3.1 Introduction

Little is known of the temporal sequence in which neurotransmitter receptors, uptake and release mechanisms develop in the vertebrate retina. The purpose of this chapter is to describe a culture system of E8 chick retinal cells of which extensive use has been made in the remainder of this thesis. In particular, the identity of cells in these cultures and the variety and sequence of appearance of ligand-gated channels they express were established as an essential prerequisite to studying the effects of neurotransmitters on their development. In this system embryonic chick retinal cells differentiate, extend processes and develop functional synapses with one another. Dissociated cultures of E8 chick retinal cells provide a model in which retinal neurons and glial cells are readily accessible for study using electrophysiological, histological and immunocytochemical techniques, which are difficult or impossible to apply to their counterparts *in vivo*. Identification of cells in this culture system was achieved using immunocytochemical techniques that show the majority of neurons in the culture to be GABAergic amacrine cells. Electrophysiological recordings show that these cells express functional glutamate-, GABA- and glycine-gated channels early in development and prior to the presence of spontaneous synaptic activity that indicates synapse formation. Voltage-gated Ca^{2+} channels that are important for transmitter release are also expressed in these neurons. Glial (Müller) cells are present in this culture system and patch-clamp experiments show that they express glutamate uptake carriers from early times.

3.2 Methods

Primary cultures of embryonic day 8 chick retinal cells were used for all experiments in this chapter (see section 2.1). Immunocytochemical staining with antibodies directed against syntaxin, THY-1 and GABA were employed to identify amacrine, ganglion and GABAergic neurons respectively (see section 2.3.1). Currents evoked by glutamate (sodium-L-glutamic acid), AMPA ((s)-α-amino-3-hydroxy-5-methyl-4-isoxazolepropionic acid), kainate (kainic acid) GABA (λ-aminobutyric acid) and glycine were measured using the whole-cell patch-clamp technique (see section 2.8). Recordings were made from retinal neurons and Müller cells which can be identified on the basis of their morphology. No recordings were made from photoreceptors. In all figures inward membrane currents are shown as downward deflections. Patch-pipettes contained internal solution A (table 2.2) unless otherwise stated. In some experiments Lucifer Yellow CH (Sigma) was included in the pipette solution for clearer visualisation of cells and their processes (see section 2.6). GABA, glycine, AMPA and kainate were bath applied. In some experiments glutamate was applied to cells by ionophoresis using a constant current device. Ionophoretic electrodes were filled with 1M glutamate at pH 8.0. At this pH glutamate is mainly negatively charged and so positive current was used to retain the drug (~ +25nA) while negative current was used to eject it (~ -35nA). The external solution was usually solution A (table 2.1). However for some experiments in which glutamate-evoked currents were investigated Mg^{2+} was removed and glycine (1μM) added (solution B, table 2.1) to enhance responses at NMDA receptors. Voltage-gated Ca^{2+} channels were investigated using voltage step protocols generated by CLAMPEX software. CLAMPAN and CLAMPFIT were used for data analysis (CLAMPEX, CLAMPAN and CLAMPFIT are commercial programs supplied by Axon Instruments, Foster City, U.S.A.) and graphs plotted using Sigma

Plot for Windows (Jandel Scientific). The internal solution for experiments examining Ca^{2+} currents contained NMDG (solution B, table 2.2), and TEA and TTX were added to the external solution (solution C, table 2.1) in order to obtain records free from contamination by K^+ and Na^+ currents. Capacitance compensation was used to null the capacitative current components that result from the charging of the pipette and cell capacitances. Cell membrane resistances and membrane capacitances were calculated from analysis of the current transients resulting from a 10mV voltage step (see section 2.8.1).

3.3 Results

3.3.1 The morphology of dissociated chick retinal cells held in culture

Recently dissociated chick retinal cells are initially spherical and without processes. After 24 hours in culture some cells extend short processes (figure 3.1A). Over a period of days the cells differentiate and several cell types can be distinguished on the basis of their morphology (figure 3.1B). Large flat glial cells form a sheet covering the bottom of the culture dish. These are thought to be Müller cells, since the chick retina is avascular and astrocytes are found only in retinae with blood vessels (Schnitzer, 1987). Other studies have shown that these flat cells found in culture are derived from the same cells that give rise to Müller cells in the intact retina (Moyer et al, 1990). Cone photoreceptors also develop in this culture system and can be identified by the oil droplet characteristic of avian cones *in vivo*, and a large population of cells form retinal neurons that are of several types (see below). After a period of days *in vitro* the glial cells have grown to form extensive sheets and some of the neurons that grow on the surface of the glial sheet extend processes that connect neighbouring cell clumps. One such cell is shown in figure 3.2 filled with Lucifer Yellow by whole-cell patch clamping.

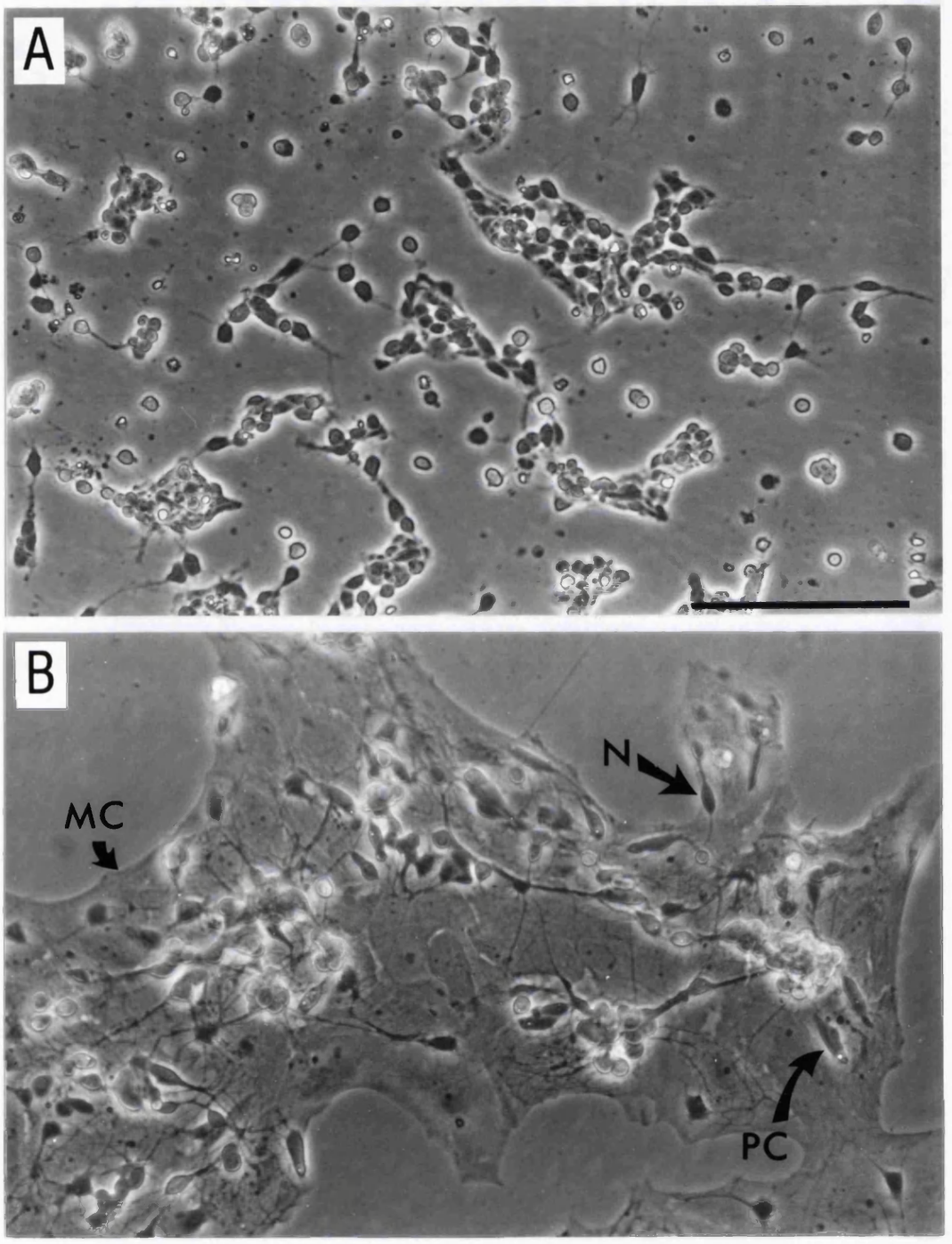

Figure 3.1

The morphology of dissociated E8 chick retinal cells in culture.

A. 1 DIV. Retinal cells are clumped and some extend short processes.

B. 6 DIV. Neurons (N), Müller cells (MC) and photoreceptor cells (PC) can be identified on the basis of their morphology (see text). Some cells remain spherical without processes. Bar represents 100μm.

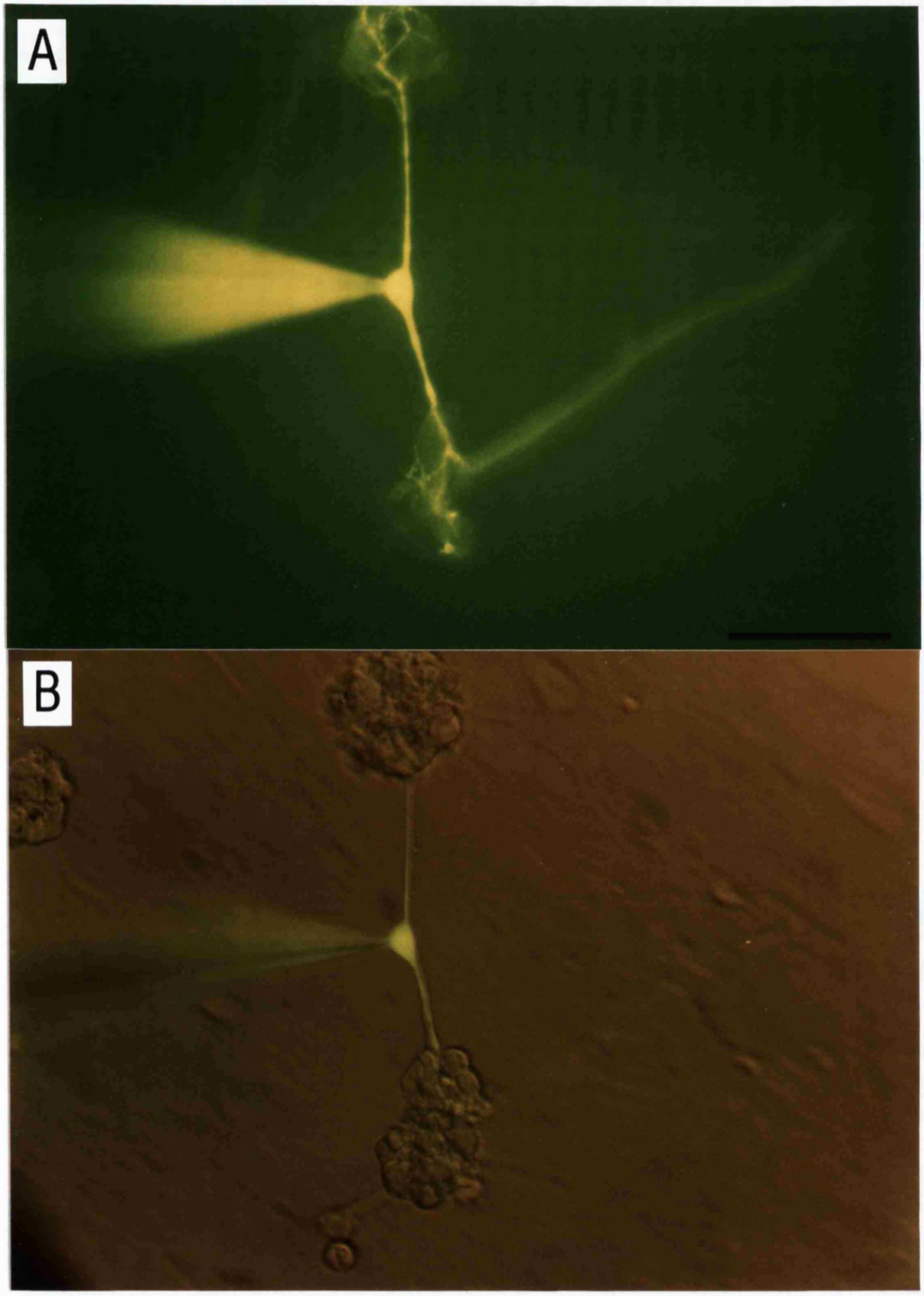

Figure 3.2

Lucifer Yellow filled neuron (12 DIV) with processes connecting two groups of cells.

A. Under UV illumination. **B.** Illuminated with both UV and white light. Bar represents 50μm.

Other cells were clearly of a different morphology and extended many processes intrinsic to the clump of neurons to which they were a member. An example of such a neuron is shown in figure 3.3 filled with Lucifer Yellow.

3.3.2 Neuronal identification using immunochemical techniques

Retinal neurons were identified using antibodies as described in section 2.3.1. Staining with the ganglion cell marker anti-THY-1 (Barnstable and Dräger, 1984, Sheppard et al., 1991) showed only background levels of staining, suggesting that these neurons or the THY-1 antigen are not present in culture (figure 3.4A). This was probably due to the absence of growth factors that are normally required to maintain ganglion cells *in vitro* (see section 3.4.1). The same technique applied to slices of embryonic retina strongly labels cells in the GCL (M. Catsicas, unpublished observations). In contrast, the amacrine marker anti-syntaxin (HPC-1) (Barnstable et al., 1985) produced clear labelling of about 31% of cells in the culture (figure 3.4B). Counts included all retinal neurons and photoreceptors, but excluded Müller cells. The population of neurons that did not label with anti-syntaxin or anti-THY-1 can not all be identified with certainty, but many were photoreceptors (mean=38±2%) identified by virtue of their oil drop, and the remainder were probably bipolar and horizontal cells.

GABA is a major inhibitory neurotransmitter in the mature nervous system, however during early development it is believed to depolarize neurons (Segal and Barker, 1984, Wu et al., 1992, Yamashita and Fukada, 1993a and see chapter 4). Other studies using primary cultures of embryonic chick retina have described the neurons present in this culture system as GABAergic (Huba et al., 1990, Gleason et al., 1993). The availability of antibodies directed against GABA provides a useful tool for identification of large

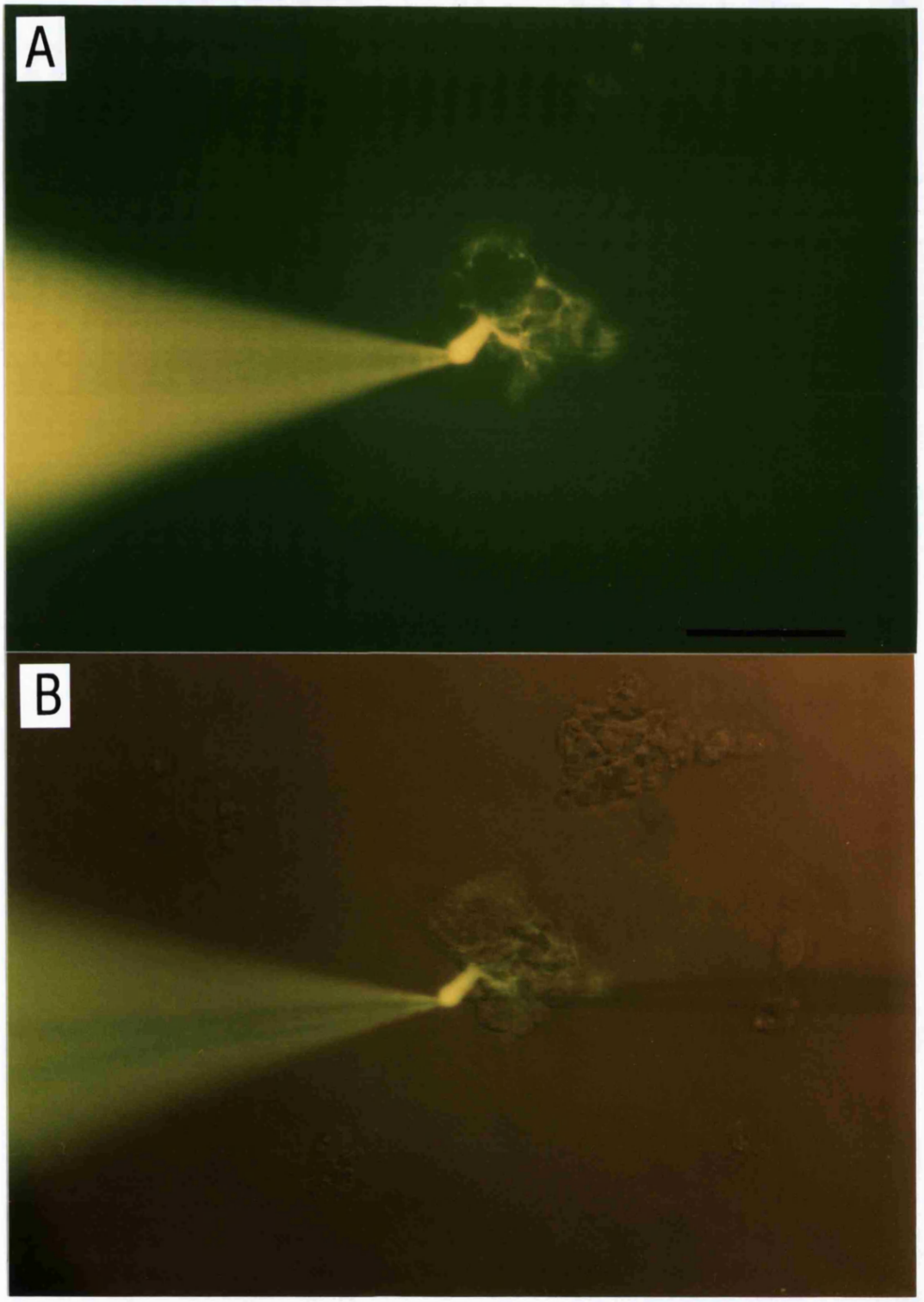

Figure 3.3

Lucifer Yellow filled neuron (5 DIV) with processes intrinsic to the group of cells to which it is a member.

A. Under UV illumination. **B.** Illuminated with both UV and white light. Bar represents 50μm.

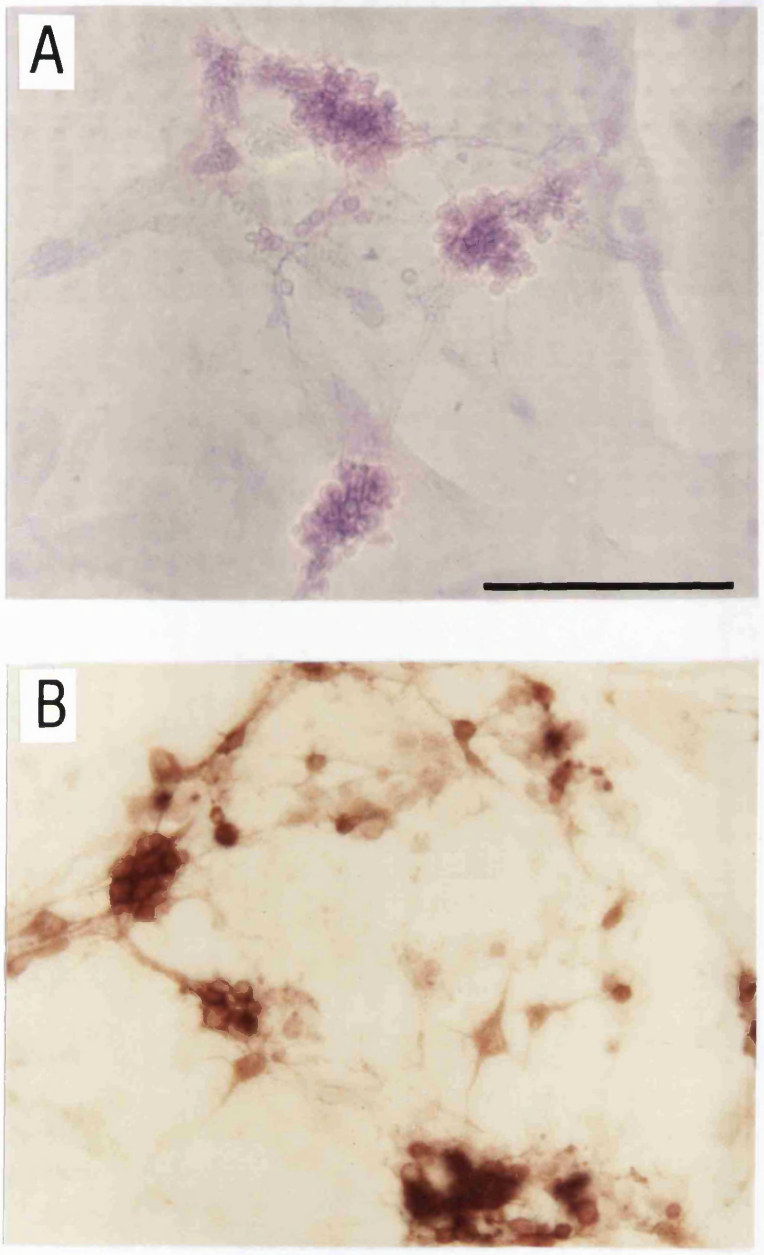

Figure 3.4

Determination of the neuronal composition of dissociated cultures using antibodies. **A.** Staining with the ganglion cell marker anti-THY-1 at 6 DIV shows only background levels of staining. Bar represents 100μM **B.** In the same cultures the amacrine marker HPC-1 labels about 31% of retinal cells.

numbers of GABAergic cells. Immunostaining of cells (7 DIV) with anti-GABA (Sera-lab) showed the majority of neurons to be GABA-immunoreactive (figure 3.5), confirming that many retinal neurons in these cultures are GABAergic.

3.3.3 Passive membrane properties of chick retinal neurons

In total over 200 retinal neurons were recorded. Cell membrane resistances and membrane capacitances were determined from analysis of the current transients resulting from a 10mV voltage step (see section 2.8.1). The decay of the current transients following the voltage step were fitted by a single exponential, suggesting that the processes of the cells do not contribute a significant internal resistance and that the cells were adequately space-clamped. The mean membrane resistance and capacitance were 2.88±0.7GΩ and 7.5±1pF respectively (n=9). Resting potentials were between -30 and -90mV. The mean of the time constant of decay (τ) was 0.23±0.1ms.

3.3.4 Glutamate-gated channels in chick retinal neurons

For experiments involving study of glutamate-evoked currents the external solution was solution B (table 2.1) and the pipette solution was solution A (table 2.2). Application of glutamate evoked inward membrane currents at negative holding potentials in 93% of retinal neurons whole-cell patch-clamped after 3 DIV (n=42). It evoked currents in 55% of neurons patched at 3 DIV (n=20) but it did not produce membrane currents in neurons patched before 3 days in culture (n=17). Figure 3.6 shows an example of the responses of a retinal neuron (14 DIV) to bath application of 100μM glutamate in the presence of 1μM glycine and the absence of Mg^{2+} (to enhance the NMDA component of the current) at various holding potentials. The

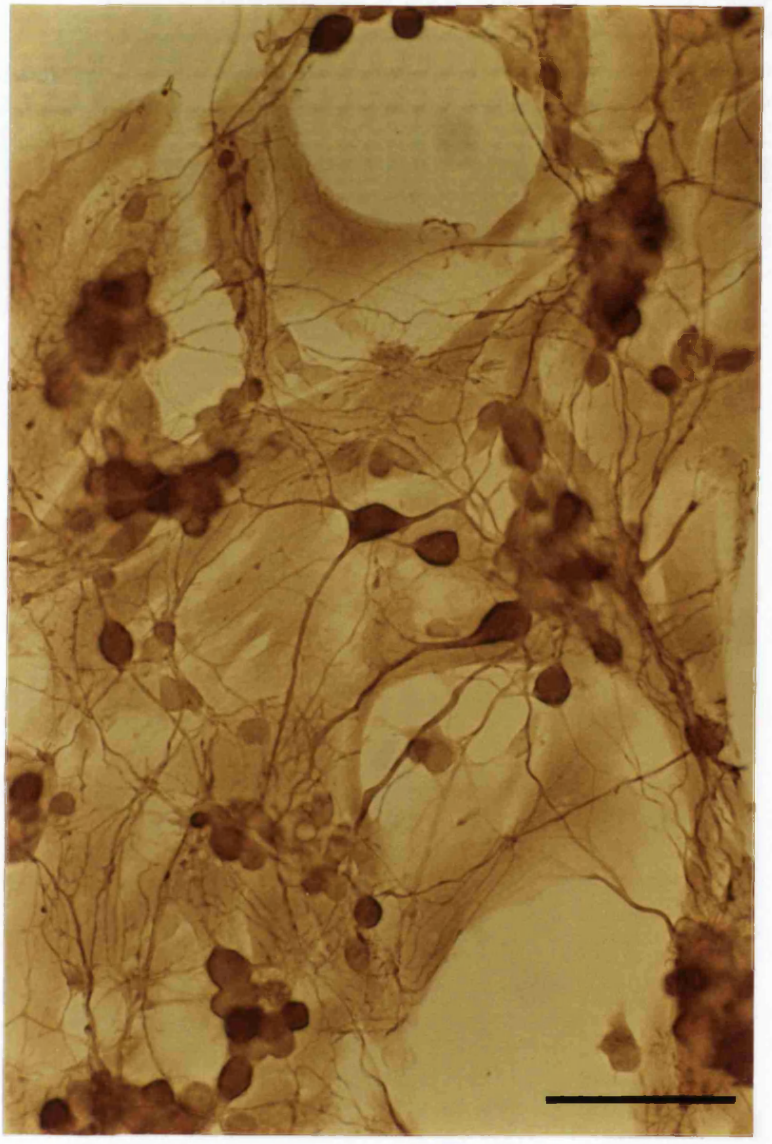

Figure 3.5

Immunostaining of cells with anti-GABA.

Staining of chick retinal cultures (7 DIV) with anti-GABA shows the majority of neurons in culture to be positive for GABA. Bar represents 50μM.

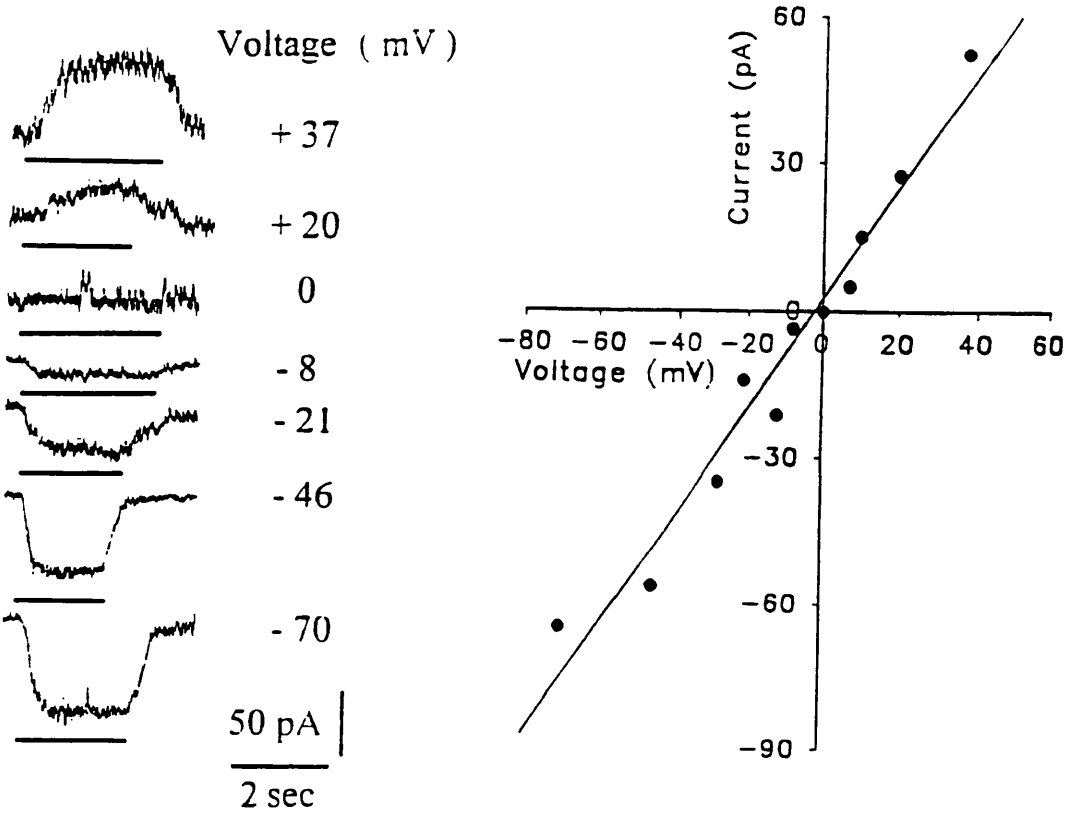

Figure 3.6

Voltage-dependence of the glutamate-induced current in retinal neurons. Left-hand panel: Changes in membrane current evoked by application of 100μM glutamate to a retinal neuron at 14 DIV. The holding potential was varied and is indicated alongside each trace. Timing of glutamate applications is shown by the solid bar below the current traces. Right-hand panel: The peak glutamate current is plotted as a function of membrane potential for same cell as above. The current reverses at -2mV and the IV relationship is linear. The line is a least squares fit to the data.

current-voltage relation for the glutamate-evoked current is plotted as a least squares fit in the right-hand panel of figure 3.6. At negative potentials the current produced was inward and at positive potentials it was outward. The IV relationship was linear and the reversal potential for the current was 3±3.14mV (n=6).

3.3.5 Glutamate responses are mediated via NMDA and non-NMDA receptors

All glutamate evoked currents could be reduced by application of the NMDA receptor antagonist AP5 (20μM) (Tocris). The mean reduction was 66±5% in 5 cells recorded. The residual current that was not blocked by AP5 could be further reduced by co-application of the non-NMDA receptor antagonist CNQX (20μM) (Tocris) with AP5 (n=39). The mean reduction in AP5 and CNQX was 84±4.4% (n=5). Figure 3.7 shows an example of the inhibition of the glutamate-evoked current by AP5 and AP5 with CNQX in a neuron (14 DIV) at a holding potential of -59mV. The external solution had glycine (5μM) added and Mg^{2+} was absent (solution B, table 2.1). These data show that many cultured retinal neurons express both NMDA and non-NMDA receptors.

The presence of non-NMDA receptors was confirmed using the glutamate analogues kainate and AMPA which act as agonists at non-NMDA receptors. Bath application of either 100μM kainate or 100μM AMPA produced inward membrane currents at negative holding potentials in all neurons patched after 3 DIV (n=57 and 11 respectively) (figure 3.8). The steady-state current response to bath application of glutamate and kainate was maintained during application of the drug. Receptor desensitization was only occasionally apparent during AMPA application. However, the changes in drug concentration achieved by the gravity fed superfusion system were

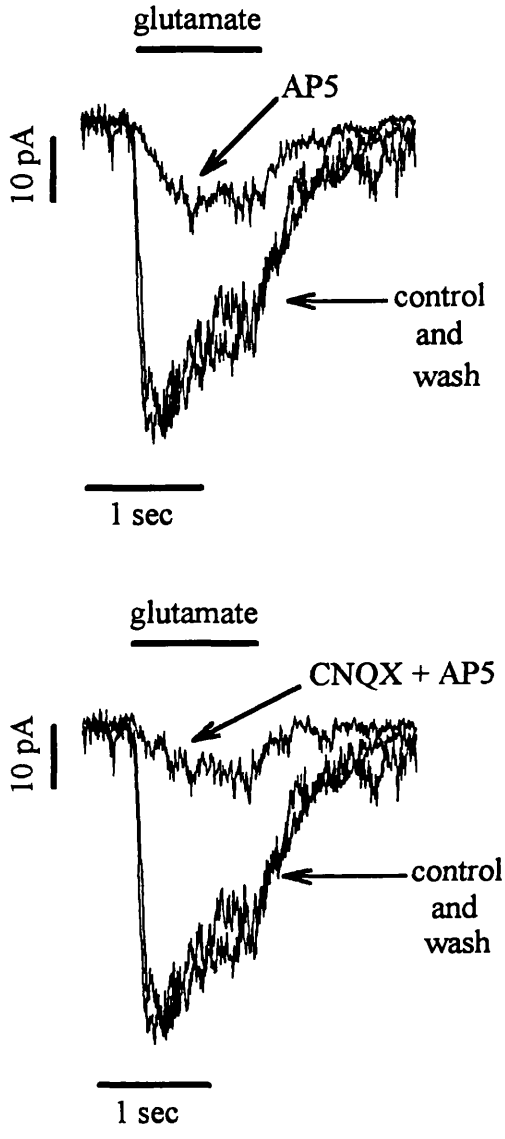

Figure 3.7

Both NMDA and non-NMDA responses contribute to the glutamate-evoked current present in dissociated retinal neurons.

Top panel: An inward current recorded from a neuron (14 DIV) during application of 100μM glutamate at a holding potential of -59mV. The response was partially blocked by the NMDA receptor antagonist AP5 (n=39).

Bottom panel: Addition of the non-NMDA receptor antagonist CNQX with AP5 further reduced the glutamate-evoked current (n=39).

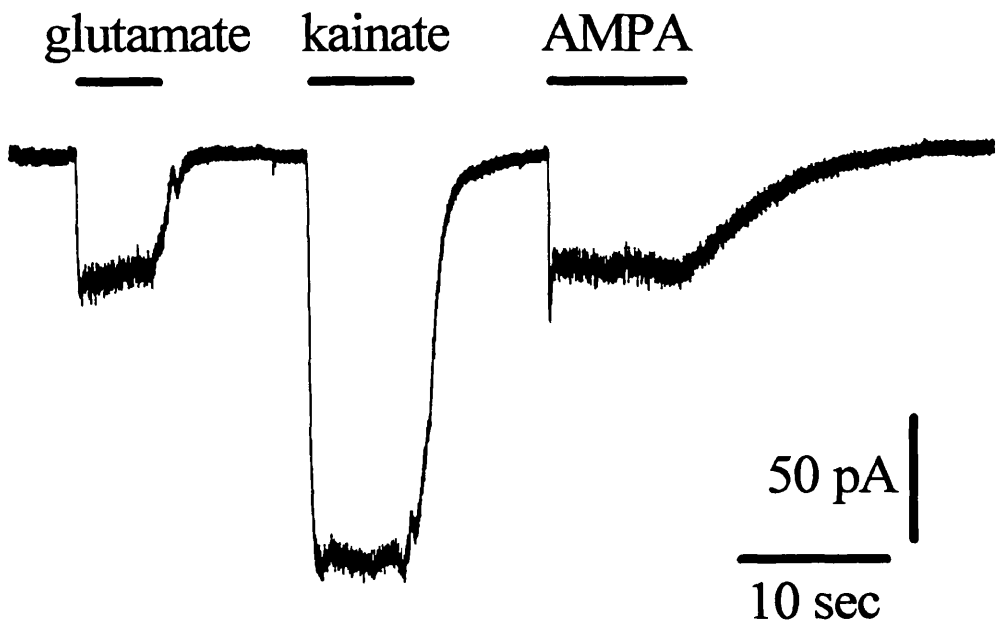

Figure 3.8

Non-NMDA receptor agonists evoke membrane currents in retinal neurons. The membrane currents evoked by bath application of glutamate, kainate and AMPA (all 100μM). This neuron (5 DIV) was voltage-clamped at -40mV. The timing of drug applications is shown by the solid bars.

probably too slow to reveal the fast transients seen in the AMPA current elsewhere when concentration-clamp steps are applied (Hamill et al., 1981).

3.3.6 Changes in noise variance associated with glutamate application

The responses to glutamate shown in figure 3.6 and 3.7 are associated with an increase in membrane current noise, as would be expected to result from the opening and closing of ligand-gated ion channels. Figure 3.9 shows the response of a retinal neuron (7 DIV) to application of 100μM glutamate at a holding potential of -23mV. The bottom trace is the glutamate-evoked current low pass filtered at 500Hz (8 pole) and shows an increase in noise as the current increases. This is presumably due to a glutamate-induced increase in the opening and closing of ion channels. In order to better show the noise increase produced by glutamate application the same data is shown in the top trace but with the addition of high pass filtering at 10Hz (8 pole). The filtered data was used to calculate the variance of the current noise fluctuations about the mean current. The data segments over which the variance was calculated are shown by solid bars. It is clear that the variance is greatest at the time of glutamate application, indicating an increase in the opening and closing of ion channels.

3.3.7 Localization of glutamate receptors

Glutamate receptors may be localized on the cell body of retinal neurons in culture and/or at the synaptic region where the process of one cell contacts another. To investigate this glutamate was applied using an ionophoretic pipette to allow focal application of the drug. Figure 3.10 shows the response of a neuron (4 DIV) to glutamate at a holding potential of -50mV. The ionophoretic pipette was positioned either over a region where a

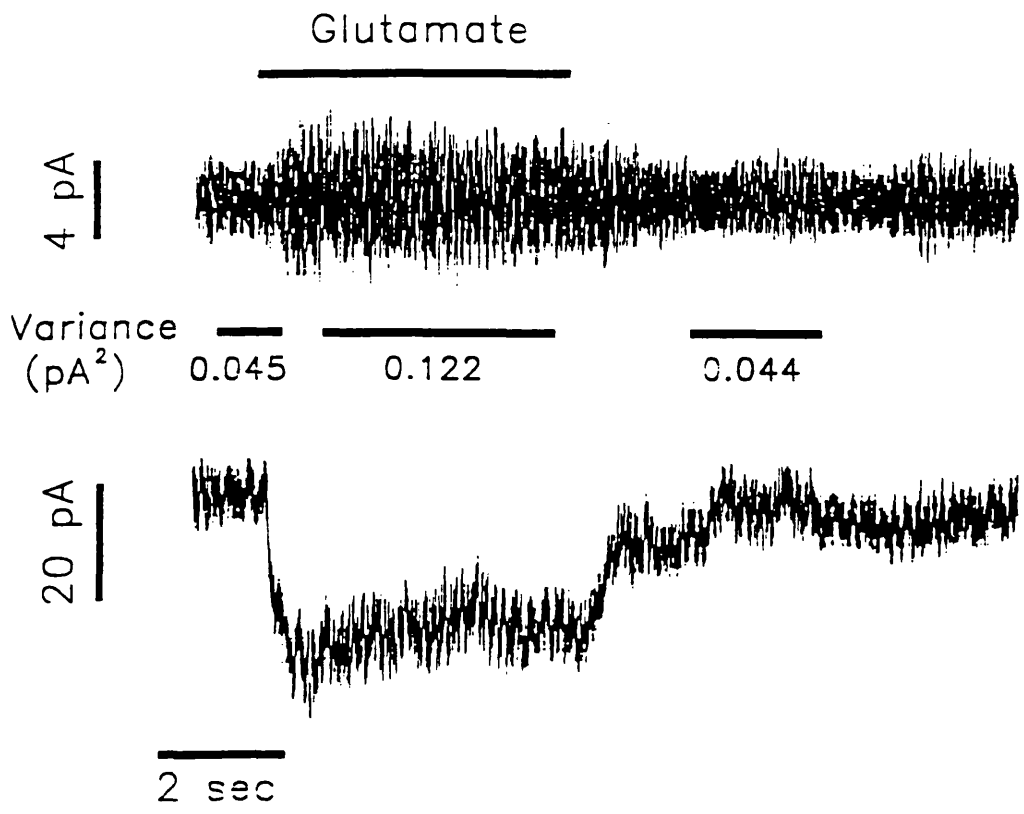

Figure 3.9

Noise analysis of a glutamate-induced noise increase in a retinal neuron. The current evoked by bath application of 100μM glutamate in a retinal neuron (7 DIV) voltage-clamped at -23mV. Top trace: The change in noise evoked by glutamate is shown by low and high pass filtering the current (500Hz and 10Hz respectively). The variance was calculated for 3 periods: before, during and after drug application. These are shown by the solid bars below the current trace. Bottom trace: The same glutamate-evoked current after only low pass filtering at 500Hz.

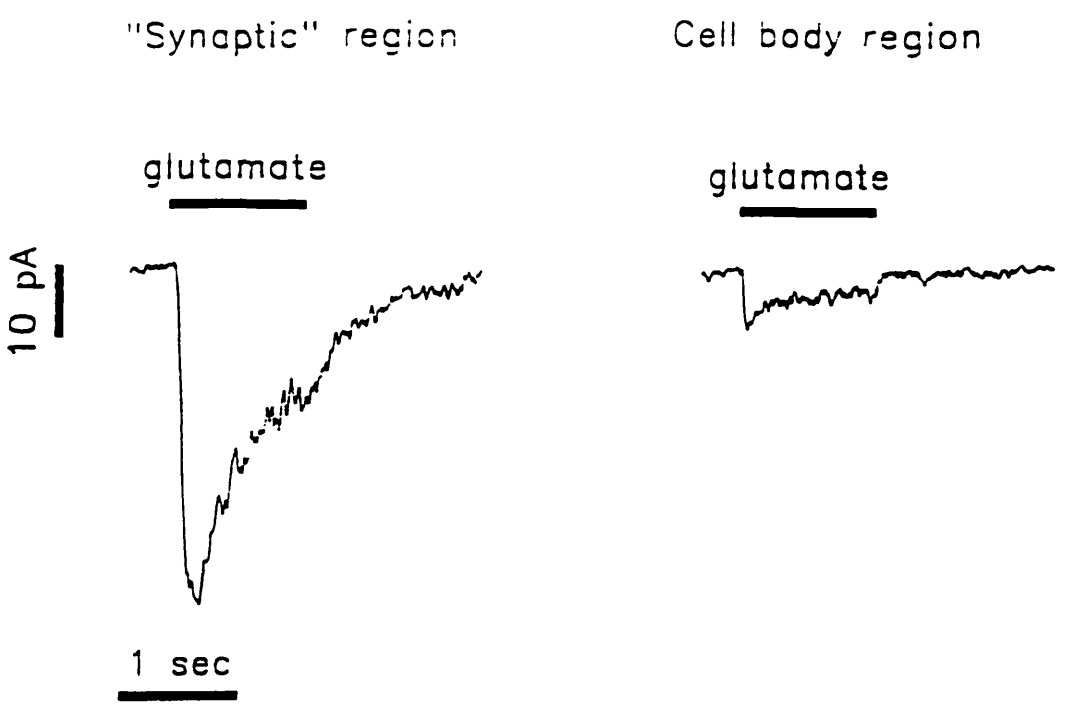

Figure 3.10

Localization of the glutamate-evoked current in retinal neurons.
Response of a neuron (4 DIV) to glutamate applied by ionophoresis using constant current pulses at a holding potential of -50mV. The left-hand trace shows the current evoked by glutamate when the ionophoretic pipette was positioned over the point of contact between the process of the patch-clamped cell and a neighbouring cell clump. The right-hand panel shows the response of the same cell when the ionophoretic pipette was moved to the cell body.

process clearly made contact with a group of cells or over the cell body located some distance away from any possible point of contact with another cell. The response to glutamate was much larger at the region of contact and the mean current at the cell body was only 22±3% of the current at the region of contact (n=5). This indicates that by this time receptors are aggregated at potential synaptic sites (n=5).

3.3.8 Glutamate-mediated spontaneous synaptic activity

By 12 DIV spontaneous synaptic activity was apparent in many of the neurons in the culture. The spontaneous activity took the form of both large and small inward deflections in membrane current at negative holding potentials and were not seen before 10 DIV. Figure 3.11 shows an example of the spontaneous events recorded from a retinal neuron at 12 DIV, from a holding potential of -65mV and in the absence of Mg^{2+} and presence of 1μM glycine (n=8). These spontaneous events appeared approximately every 10 seconds and could be abolished by co-application of the glutamate receptor antagonists AP5 and CNQX (both 20μM) (figure 3.11, centre trace). The spontaneous events returned on reperfusion with normal Ringer's (bottom trace, figure 3.11). The GABA and glycine receptor antagonists bicuculline and strychnine respectively had no effect (data not shown). Thus these currents probably reflect the formation of networks of neurons connected by excitatory glutamatergic synapses, although it is impossible to rule out the participation of circuits involving other transmitters.

3.3.9 Passive membrane properties of Müller cells

Müller cells found in retinal cultures form thin sheets which makes them difficult to record. In total 22 Müller cells were whole-cell patch-

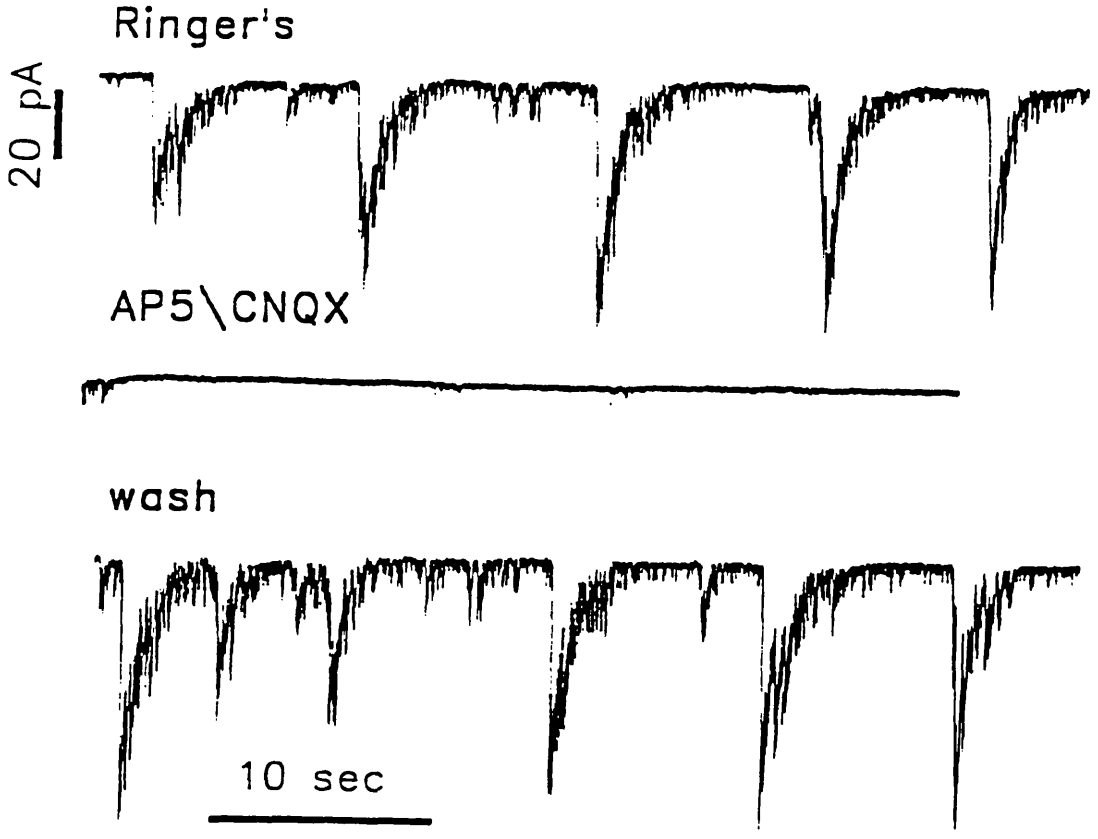

Figure 3.11

Glutamate-mediated spontaneous synaptic activity.

The spontaneous changes in membrane current recorded from a retinal neuron (12 DIV) voltage-clamped at -65mV. Top trace: In Mg^{2+}-free Ringer's with 1μM glycine. Center trace: The spontaneous events are abolished in the presence of the glutamate receptor antagonists AP5 and CNQX (both 20μM). Bottom trace: The spontaneous activity returns after reapplying Ringer's.

clamped. Analysis of the current transients produced by a 10mV voltage step allowed the membrane resistances and membrane capacitances of the cells to be calculated (see section 2.8.1). Decay of the current transients were well fitted by a single exponential suggesting these cells were adequately space-clamped. The mean membrane resistance was 0.59±0.1GΩ and the mean membrane capacitance was 20.5±5.7pF from a sample of 6 cells. Resting potentials were between -30 and -90mV. The mean of the time constant of the current decay (τ) was 1±0.2ms.

3.3.10 Glutamate uptake in retinal glial cells

Müller glial cells were whole-cell patch-clamped with solution A (table 2.1) as the external solution and solution A (table 2.2) as the internal solution. Bath application of 100μM glutamate evoked inward membrane currents in 73% of the cells that had been held in culture for 3 days or more (n=22). Figure 3.12 (left-hand panel) shows an example of the responses of a Müller cell (8 DIV) to 100μM glutamate at various holding potentials. The current-voltage relationship is plotted in the right-hand panel of figure 3.12 and shows that the glutamate-evoked current did not reverse and was inward between -80 and +40mV. The current was largest at more negative potentials This suggests that the current produced by glutamate in Müller cells is not due to the presence of glutamate-gated ion channels, but rather results from the uptake of glutamate via a carrier (Brew and Attwell, 1987).

3.3.11 Glutamate uptake is inhibited by PDC

The presence of glutamate uptake carriers in retinal Müller cells was confirmed using the glutamate uptake blocker L-*trans*-Pyrrolidine-2,4-dicarboxylic acid (PDC) (Tocris). PDC is a competitive blocker of glutamate

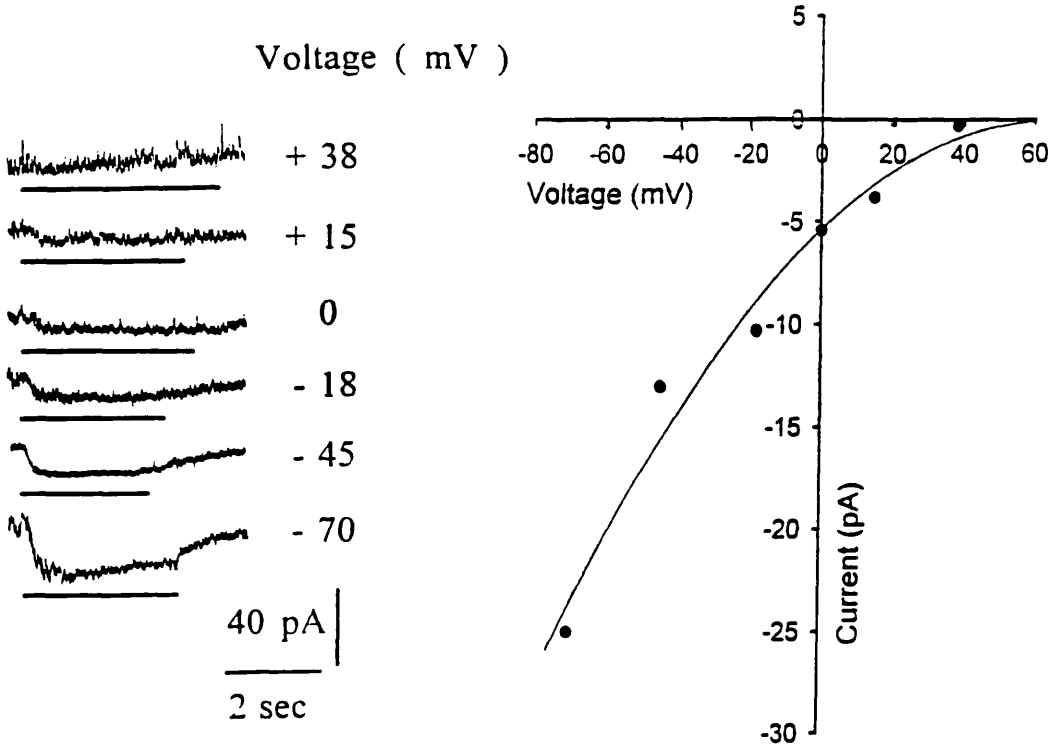

Figure 3.12

The voltage-dependence of the glutamate-evoked current in Müller cells.
Left-hand panel: Changes in membrane current produced by application of 100μM glutamate to a Müller cell (8 DIV) at various holding potentials (indicated alongside each trace). The duration of each glutamate application is shown by a solid bar below each trace. Right-hand trace: The current-voltage relationship is shown as a plot of the peak glutamate current as a function of the membrane potential. The current is inward at all membrane potentials. Under the conditions used the current evoked by glutamate at ionotropic receptors reverses at 0mV.

uptake and is itself carried by the transporter causing an inward current (Bridges et al., 1991). In the presence of PDC the glutamate-evoked current is reduced because although PDC is carried it is transported more slowly than glutamate, so reducing the rate of transport. Figure 3.13 shows an example of the current evoked by application of 100μM PDC in a Müller cell (7 DIV) at a holding potential of -39mV (n=10). The current response to application of 100μM glutamate is reduced in the presence of PDC (n=10), which is consistent with the current in these cells being generated by glutamate uptake.

3.3.12 Glutamate uptake is not associated with any change in noise variance

The responses to glutamate shown in figure 3.12 and 3.13 are not associated with any apparent increase in membrane current noise. This would be expected if the currents evoked by glutamate were produced by the operation of an uptake carrier (Brew and Attwell, 1987). Figure 3.14 shows the response of a Müller cell (7 DIV) to application of 100μM glutamate at a holding potential of -39mV. The bottom trace is the glutamate-evoked current low pass filtered at 500Hz (8 pole) and shows no change in noise as the current increases. In order to better show the membrane current noise the same data is shown in the top trace but with the addition of high pass filtering at 10Hz (8 pole). The filtered data was used to calculate the variance of the current noise fluctuations about the mean current. The data segments over which the variance was calculated are shown by solid bars. There was no significant change in noise variance during glutamate application, as expected if the membrane current was produced by the operation of a glutamate transporter.

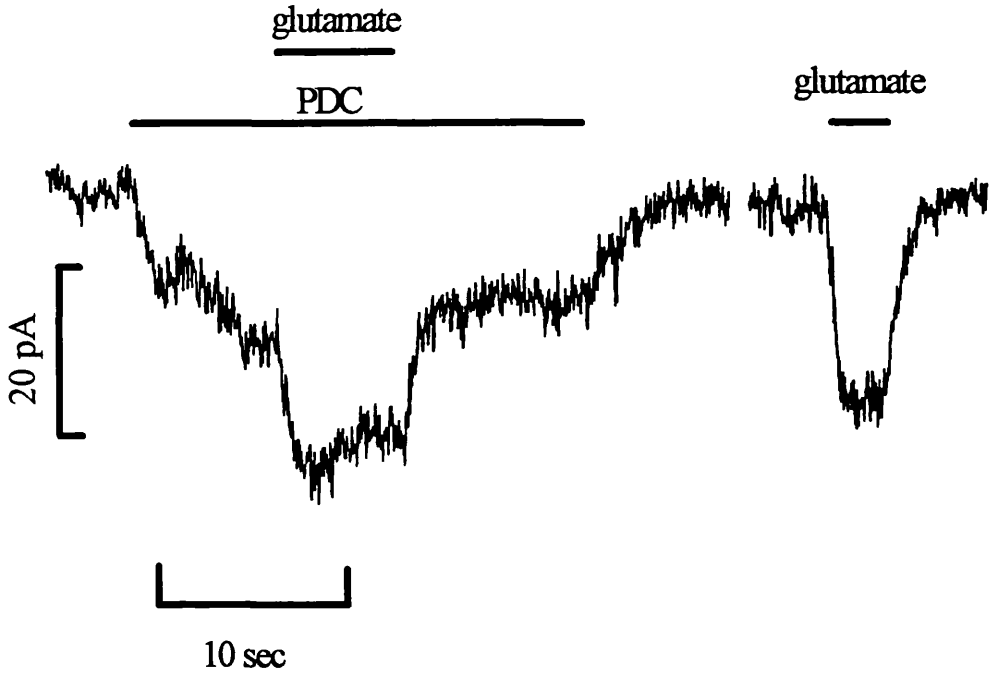

Figure 3.13

PDC reduces the glutamate uptake current in Müller cells.

Application of the glutamate uptake blocker and competitive agonist PDC (100μM) produced an inward current in a glial cell (7 DIV) at a holding potential of –39mV. In addition, PDC reduced the response to application of glutamate (100μM, n=10).

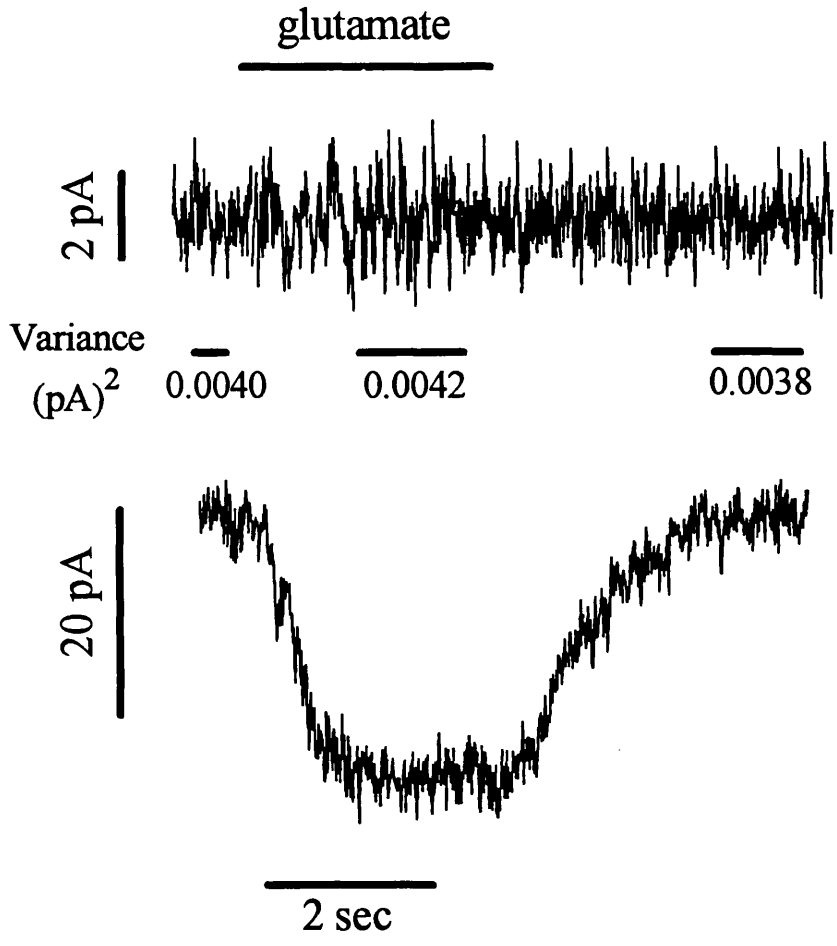

Figure 3.14

Glutamate responses in Müller cells are not associated with any change in noise.

The current evoked by bath application of 100μM glutamate in a Müller cell (7 DIV) at a holding potential of -39mV. Top trace: The current noise produced by glutamate is shown after low and high pass filtering the current (500Hz and 10Hz respectively). The variance was calculated for 3 periods; before, during and after drug application and these are shown by the solid bars below the current trace. Bottom trace: The same glutamate-evoked current after only low pass filtering at 500Hz.

3.3.13 GABA-gated channels in retinal neurons

Application of GABA evoked membrane currents in all retinal neurons tested at 3 DIV (n=12). Figure 3.15 shows the responses of a retinal neuron to bath application of 20μM GABA at different holding potentials. The right-hand panel in this figure is a plot of the current-voltage relation for the steady-state current evoked by 20μM GABA. The IV-relationship was linear and the line shown is least squares fit to the data. With 14.2mM Cl^- in the patch-pipette (solution A, table 2.2) and 149.02mM Cl^- in the external solution (solution A, table 2.1), GABA evoked inward currents at potentials negative to -53.1±2.5mV (n=4) and outward currents at more positive voltages. The Cl^- reversal potential (E_{Cl}) with the internal and external solutions used is -59mV. This was calculated using the Nernst equation shown below:

$$E_{Cl} = \frac{RT}{zF} \ln \frac{Cl_i}{Cl_o}$$

R, gas constant = 8.315 J K^{-1} mol^{-1}

T, absolute temperature = 298K

z, valency = -1

F, Faraday's constant = 9.648 x 10^4 C mol^{-1}

This value for E_{Cl} is close to the reversal potential (E_{rev}) calculated for the GABA-evoked current in retinal neurons and this suggests that the current produced by GABA results largely from the opening of Cl^--specific channels. The difference between the values for E_{Cl} and E_{rev} may be explained by the permeability of the GABA-gated Cl^- channel to acetate which was used in the internal solution (Bormann et al., 1987). The permeability of the channel to acetate can be calculated as the permeability ratio of acetate to Cl^- (P_A/P_{Cl})

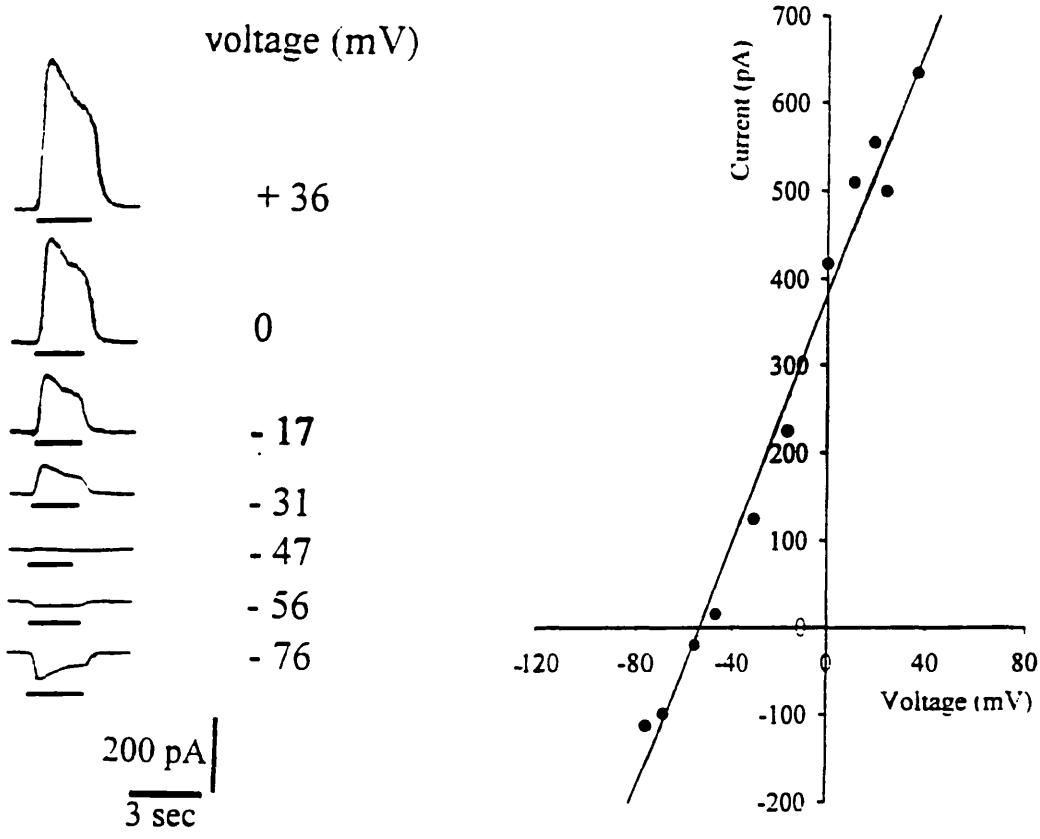

Figure 3.15

Voltage-dependence of the GABA-evoked current in a retinal neuron.
Left-hand panel: Membrane currents of a retinal neuron (3 DIV) evoked by 20μM GABA at different membrane potentials (indicated next to each trace). The timing of GABA applications is shown by the solid bar below each trace. Right-hand panel: The peak GABA current is shown plotted as a function of the membrane potential. The current reverses at -53mV and the IV relationship is linear. The line is a least squares fit to the data.

using the Goldman-Hodgkin-Katz equation (Goldman, 1943, Hodgkin and Katz, 1949) as follows:

$$E_{rev} = -\frac{RT}{F}\ln\frac{[Cl^-]_o + P_A / P_{Cl}[A^-]_o}{[Cl^-]_i + P_A / P_{Cl}[A^-]_i}$$

The P_A/P_{Cl} ratio was 0.095

3.3.14 Bicuculline blocks the GABA-evoked current in retinal neurons

Bicuculline is a potent antagonist of the $GABA_A$ channel. Figure 3.16 shows the effects of 50μM bicuculline (Tocris) on the current evoked by bath application of 20μM GABA to a neuron (4 DIV) at a holding potential of -48mV. Bicuculline completely abolished the GABA-evoked current and the response returned on reperfusion with normal Ringer's (n=3).

The pharmacology of the response, its dependence on the Cl^- concentration and the noise produced by the drug application show the response produced by GABA results from the operation of a $GABA_A$ channel.

3.3.15 Glycine-gated channels in retinal neurons

At 3 DIV all retinal neurons tested responded to glycine (n=6). Figure 3.17 (left-hand panel) shows an example of the responses of a retinal neuron (3 DIV) to bath application of 20μM glycine from different holding potentials. The right-hand panel is a plot of the current-voltage relation of the steady-state current response. The line is a least squares fit. The internal solution contained 14.2mM chloride (solution A, table 2.2) and the external solution 149.02mM chloride (solution A , table 2.1). Under these conditions glycine

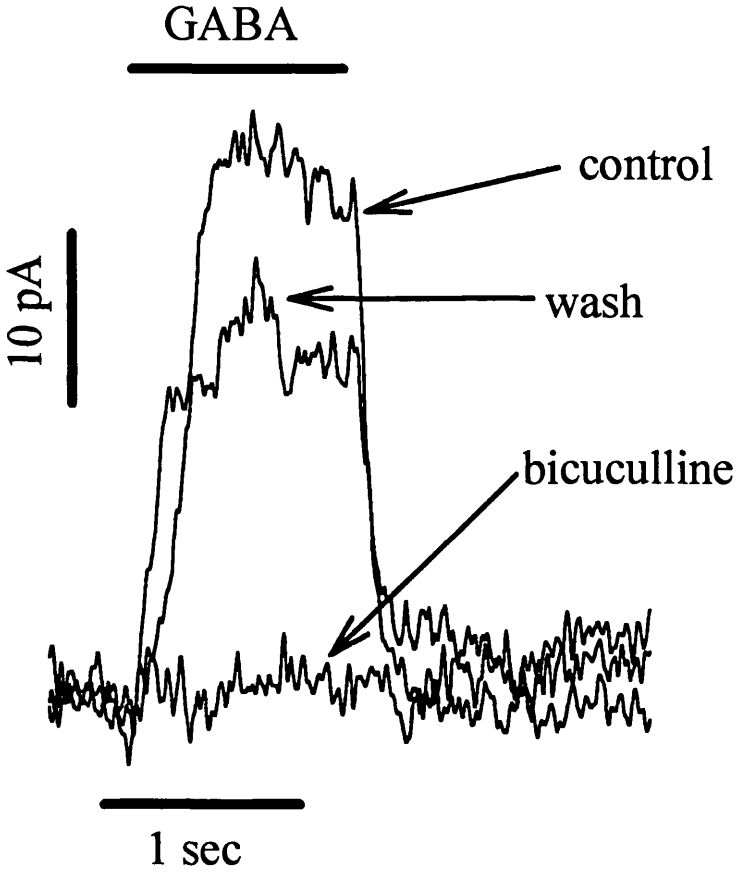

Figure 3.16

Bicuculline blocks the GABA-evoked current in retinal neurons.

Application of 20μM GABA evokes an outward current in a retinal neuron (4 DIV) at a holding potential of -48mV. Co-application of the $GABA_A$ receptor antagonists bicuculline (50μM) blocks the GABA-evoked current (n=3).

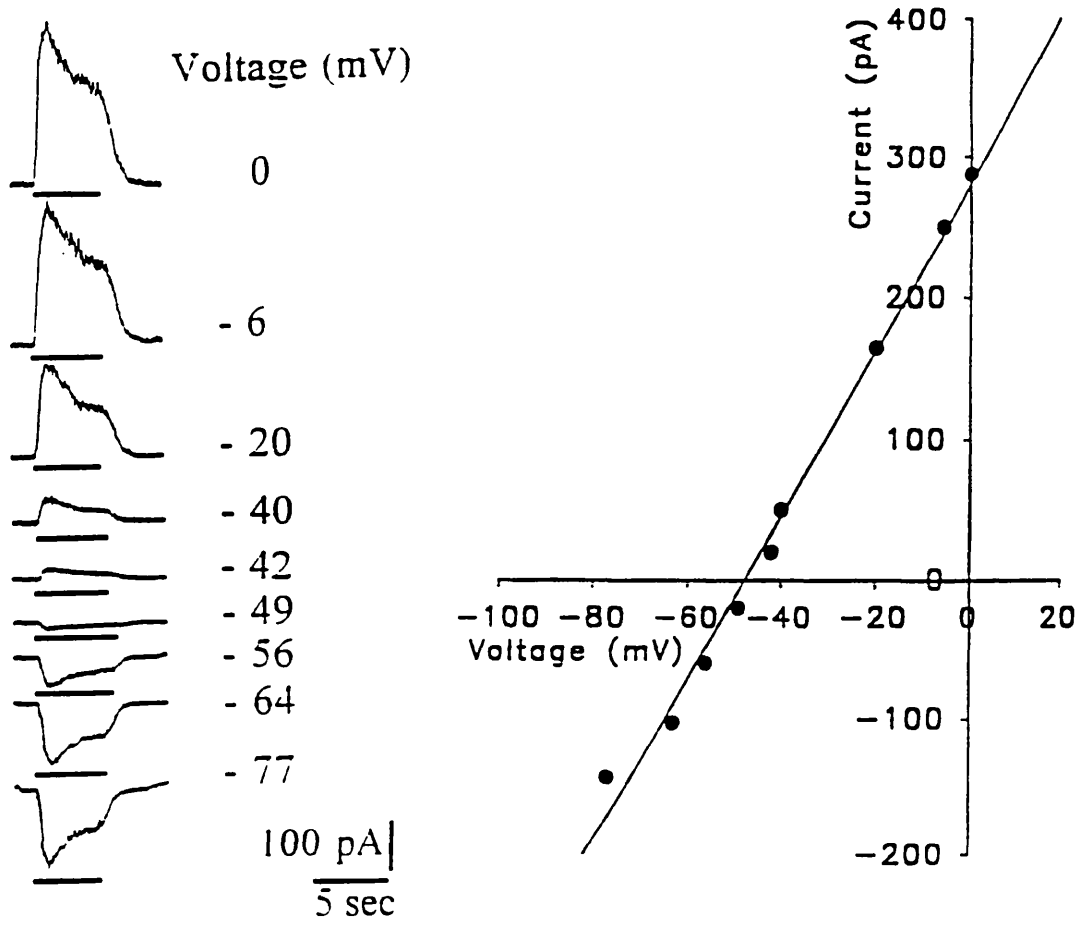

Figure 3.17

Voltage-dependence of the glycine-evoked current in a retinal neuron.
Left-hand panel: Membrane current responses of a retinal neuron (3 DIV) to application of 20μM glycine at various holding potentials (indicated next to each trace). The duration of glycine applications is shown by the solid bar below each trace. Right-hand panel: The peak glycine current is plotted as a function of the membrane potential for the same cell. The current reverses at -47mV and the IV relationship is linear. The line is a least squares fit to the data.

evoked inward membrane currents negative to -46±0.8mV and outward currents positive to this reversal potential (n=4). The E_{Cl} at these chloride concentrations is -59mV (as calculated in section 3.3.12). As for the GABA channel, the glycine-gated chloride channel is permeable to acetate which was used in the internal solution. Using the Goldman-Hodgkin-Katz equation as described in section 3.3.12 the P_A/P_{Cl} ratio was 0.095, as for GABA. The permeability to acetate may explain the deviation from Nernstian behaviour.

3.3.16 Strychnine blocks the glycine-evoked current

Strychnine is a potent glycine receptor antagonist. Figure 3.18 shows the effects of 50μM strychnine (Sigma) on the current evoked by bath application of 100μM glycine to a neuron (4 DIV) at a holding potential of -75mV. At this potential glycine produces an inward current (figure 3.18A). Strychnine completely abolished the glycine-evoked current (figure 3.18B) and the response returned on reperfusion with normal Ringer's (n=2).

3.3.17 Voltage-gated Ca^{2+} channels in retinal neurons

Experiments were carried out to investigate whether Ca^{2+} currents were present in cultured retinal neurons and if so how these currents could be blocked. This was essential for experiments in the remainder of this thesis where the effects of the activation of ligand-gated channels were studied. One of the actions of the transmitters used in this thesis is to depolarize cells thereby opening voltage-gated Ca^{2+} channels. In order to eliminate Ca^{2+}-entry through these channels as a mechanism by which the transmitters exert their actions, it was necessary to determine how voltage-gated Ca^{2+} channels could be blocked. Barium (Ba^{2+}) was included in the external solution during whole-cell patch-clamp experiments (solution C, table 2.1). This ion has a

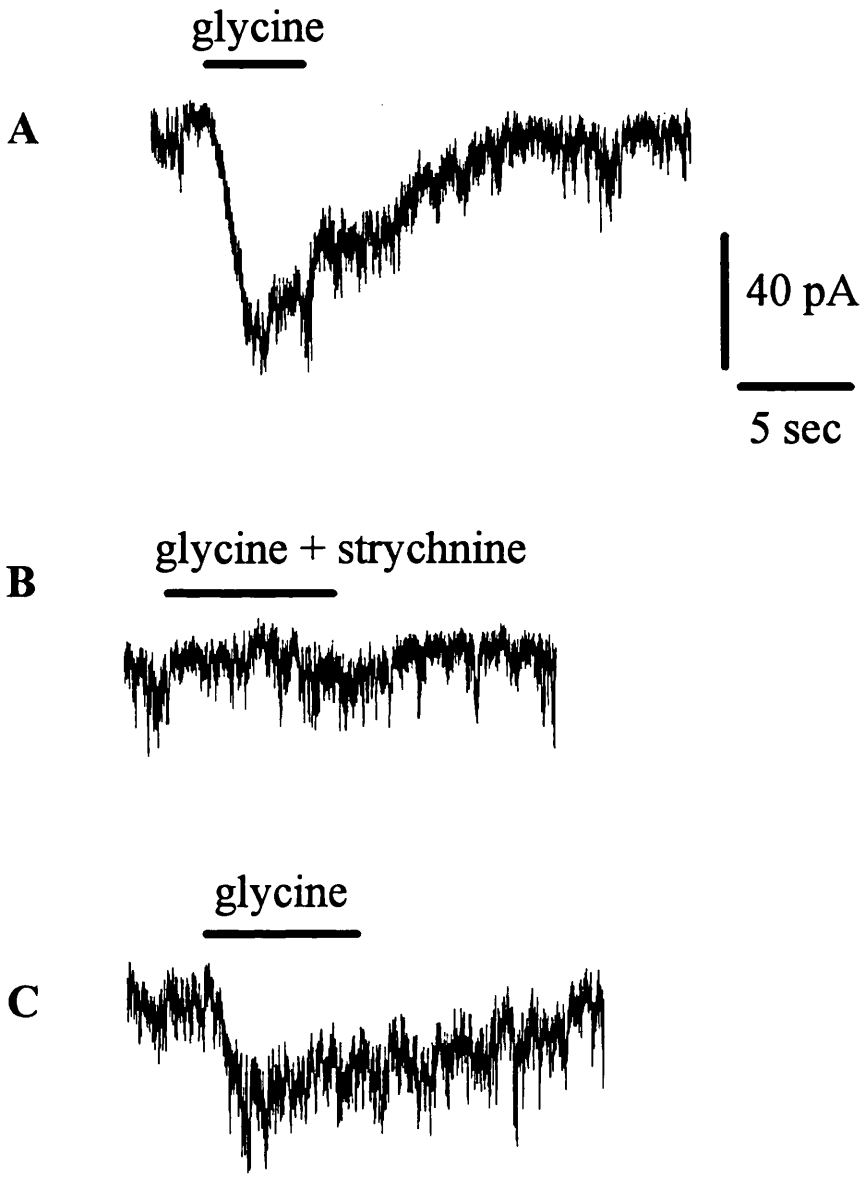

Figure 3.18

Strychnine blocks the glycine-evoked current in retinal neurons.

A. Bath application of glycine (100μM) evokes an inward current at a holding potential of -75mV in a retinal neuron (4 DIV). **B.** Co-application of the glycine receptor antagonist strychnine (50μM) blocks the glycine-evoked current (n=2). **C.** The glycine-evoked current returned after strychnine was washed off for 5 minutes.

permeability equal or greater than Ca^{2+} through most Ca^{2+} channels, so it accentuates any Ca^{2+} conductance present. Ca^{2+} currents were examined using a voltage protocol where 225ms voltage steps, in 10mV increments, were made from a holding potential of -95mV and the resulting currents recorded. TTX (100nM) (Sigma) was added to the external solution to block any Na^{+} current in the cells. Whole-cell recordings of retinal neuron membrane currents in response to positive voltage steps are usually dominated by outward K^{+} current. The Ba^{2+} in the external solution blocks a large part of the current but to further reduce any contamination of the inward Ca^{2+} current by the K^{+} current TEA (5mM) (Sigma) was added to the external solution and the K^{+} in the internal solution was replaced with NMDG (solution B, table 2.1).

Under the conditions described above a Ca^{2+} current was apparent in 81% of cells tested (n=88), with some cells exhibiting Ca^{2+} currents as early as 2 DIV. Figure 3.19 shows a typical whole-cell current response to a series of voltage steps made from a holding potential of -95mV (with K^{+} and Na^{+} currents blocked). The first 2 voltage steps were negative from the holding potential (-95mV) to -115 and -105mV and were followed by a series of positive steps, in 10mV increments, to +35mV. The protocol was repeated 16 times before the current responses were averaged. The resulting Ca^{2+} currents did not decay during the voltage-step and required strong depolarization to activate them. These characteristics resemble those described by Nowycky et al. (1985) for L-type Ca^{2+} channels. Some outward current remained under the conditions used and can be seen during the smaller voltage steps before much Ca^{2+} current was activated. This probably represents K^{+} current that remained unsuppressed by the TEA and the Ba^{2+} in the external solution.

Figure 3.20 (top trace) shows the inward current resulting from a single

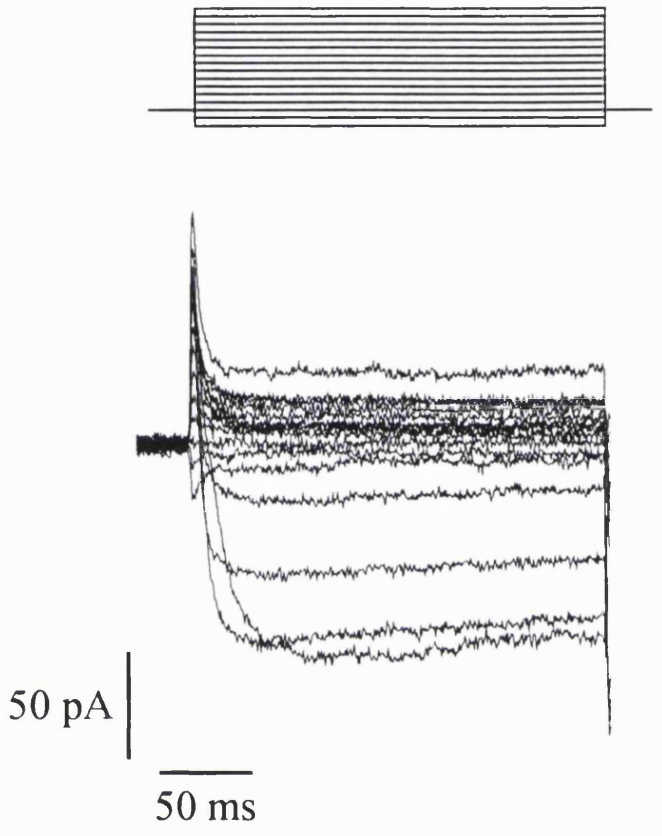

Figure 3.19

Ca^{2+} currents reminiscent of L-type currents are present in retinal neurons. The whole-cell current response of a retinal neuron (5 DIV) to a series of negative and positive 10mV voltage steps from a holding potential of -95mV. The external medium contained TEA, TTX and Ba^{2+} and the internal NMDG to replace K^{+}. The Ca^{2+} currents evoked required strong depolarization for activation and did not decay during the voltage-step.

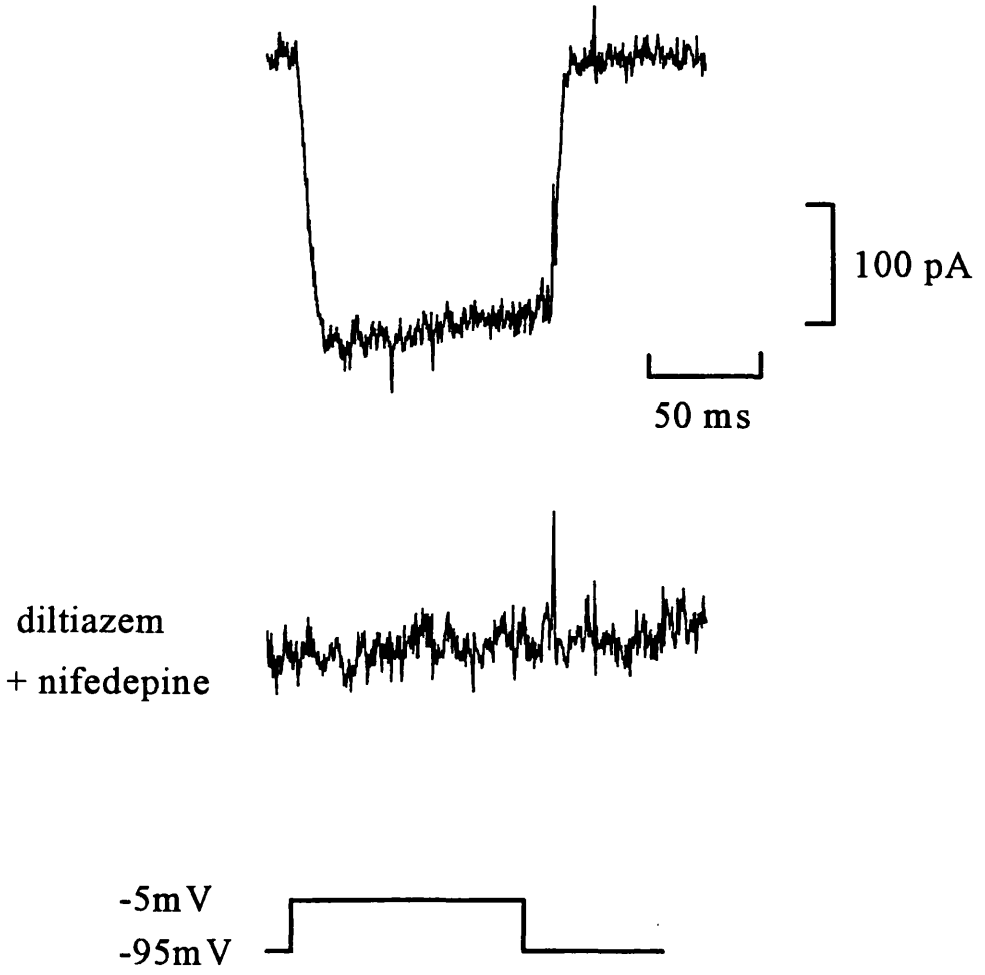

Figure 3.20

The Ca^{2+} current in retinal neurons is blocked by diltiazem and nifedipine. Top trace: An example of the Ca^{2+} current evoked by a single voltage step to -5mV from a holding potential of -95mV (the timing of the voltage step is shown in the bottom trace). The external solution contained TTX and TEA and the data has been leak subtracted to better show the current. Center trace: In the presence of diltiazem and nifedipine (both 20μM) the current is abolished.

voltage step to -5mV from a holding potential of -95mV. The data has been leak subtracted to better show the inward current. This was done by using a voltage step protocol that included a positive 10mV step in advance of the large voltage step used to activate the Ca^{2+} current. The steps were made alternately 16 times before they were averaged. The current response to the small voltage step was then scaled by 9 and subtracted from the average of the currents produced by the 90mV step. The current produced was long-lasting and the large depolarizing step required for its activation is again reminiscent of an L-type Ca^{2+} current. This was confirmed by use of the L-type Ca^{2+} channel blockers nifedipine and diltiazem. To avoid run-down of the Ca^{2+} current that may occur if some intracellular component is "washed-out" by the patch-pipette solution, the voltage steps were applied first in the presence and then in the absence of diltiazem and nifedipine. In the presence of nifedipine and diltiazem (both 20μM, Sigma) the inward currents evoked by large voltage steps were absent (bottom trace, figure 3.20). The blockers reduced the current produced by the 90mV step by about 90% in 17 cells tested, reducing the current from26.9±1.9pA/pF to2.5± 1 pA/pF. This confirmed that the Ca^{2+} channels present in the dissociated retinal neurons recorded were of the L-type.

3.4 Discussion

3.4.1 Dissociated retinal cultures as an experimental model for studying aspects of retinal development in vitro

Dissociated cultures were prepared from chick retina taken from day 8 embryos. The retinae of chick embryos lack blood vessels and connective tissue and can be isolated cleanly from other ocular tissues including the pigment epithelium. Thus dissociated cultures can be obtained that are free of

contamination from non-neuronal cells such as fibroblasts or endothelial cells. Neurons of the chick retina appear to be born in 2 phases during development. In the early phase ganglion cells, amacrine cells, cones and type A horizontal cells are born and in the later phase bipolar cells, type B horizontal cells and rod photoreceptors appear (Kahn, 1974). The generation times for different cell types in the chick retina overlap considerably, but the trend in both the mammalian and avian retina is for ganglion cells to be born first and bipolar cells last (Sidman, 1961, Webster, 1985). By E8, the time when retinae are used to prepare dissociated cultures, the proliferation of amacrine cell precursors is just finishing (Prada et al., 1991) and ganglion cells are most advanced in their differentiation. At the start of the *in vitro* period the cells in E8 cultures are round and indistinguishable from one another. At the time the cultures are made synaptogenesis has not yet begun in the chick retina (around E12 *in vivo*, Sheffield and Fischman, 1970, Hughes and LaVelle, 1974). Over a period of days cells in the cultures differentiate to form a heterogeneous population within which several cell types can be distinguished.

Large, flat cells appear within 48 hours of plating and these are thought to be Müller cells since this is the only type of glial cell found in chick retina (Schnitzer, 1987). Müller cells are the radial glial cells of the retina and are important in regulating extracellular levels of K^+ and glutamate (Newman, 1984, Newman et al., 1984, Brew and Attwell, 1987, Barbour et al., 1988, Mobbs et al., 1988, Sarantis and Attwell, 1990). Over a period of days these cells form a sheet on the bottom of the culture dish, and other cells grow on their surface. The large, flat glial cells seen in culture are very different from Müller cells in the retina which are long and thin and extend from the inner to outer retina. However, Müller cells in culture express several antigens found in their counterparts *in vivo* (Hyndman and Lemmon, 1987, Linser and Perkins, 1987, Lewis et al., 1988). For example, in the intact chick retina

Müller cells are the only cells that label for vimentin (Lemmon and Reiser, 1983), as are the glial cells in E8 chick retinal cultures (Moyer et al., 1990), suggesting that they are indeed Müller cells.

Cone photoreceptors are present in the culture and can be identified with ease by virtue of the oil droplet (Araki, 1984, Alder and Lindsey, 1985, Alder, 1986) that is characteristic of avian cones *in vivo* (Cohen, 1963). Young cones in culture are small and round and contain a very small oil droplet. After a few days they become polarized and the cells elongate, extending a single pedicle-like process from one pole and flat membranous processes from the other that may represent a reduced form of the outer segment.

A large population of cells in culture are of neuronal appearance and usually extend several neurites. After several days *in vitro* the neurons in culture often extended long processes that connected two neighbouring cell clumps. Some cells in these clumps were round without processes and remained so throughout the culture period. Many neurons elongated several branching processes that connected clumps of cells, whilst others extended neurites intrinsic to a cell clump. Ganglion cells, or at least the THY-1 antigen (Barnstable and Dräger, 1984, Sheppard et al., 1991), appeared to be absent under the culture conditions used here. This was not unexpected as it is well known that ganglion cells require special culture conditions for survival *in vitro* or the presence of their target tissue. To maintain embryonic mammalian ganglion cells *in vitro* they must either be grown on a substrate like laminin, their media supplemented with the required growth factors or their neural targets (the lateral geniculate nucleus) included in the culture dish (McLoon and Lund, 1984, Cohen et al., 1987, Rodriguez-Tebar et al., 1989, Raju et al., 1994). Many neurons under the culture conditions used were

amacrine cells since they label with the cell marker HPC-1 (Barnstable et al., 1985). Amacrine cells in the retina do not usually have axons, however many within the culture extended long axon-like processes. Gleason and Wilson (1989) used electron microscopy to identify synapses in E8 chick retinal cultures and found that the anatomy of synapses present were characteristic of those made by amacrine cells, as well as some made by bipolar and possibly horizontal cells. *In situ* amacrine cells form synaptic contacts with bipolar cells, ganglion cells and each other. The remaining population of neurons in culture may represent bipolar or horizontal cells, but in the absence of markers for these cells they could not be identified with certainty.

3.4.2 Retinal neurons in vitro express glutamate-gated receptors early in development

Ionotropic glutamate receptors have many important roles in the developing nervous system (Pearce et al., 1987, Komuro and Rakic, 1993, Choi, 1988). In cultures of E8 chick retinal cells about half of the cells tested responded to glutamate by 3 DIV. Before this time no responses were found and after 3 DIV all the neurons recorded showed glutamate-evoked currents. Glutamate may produce membrane currents either through operation of an electrogenic uptake carrier or by opening ion channels. The current associated with Na^+-dependent glutamate uptake shows strong inward rectification and does not reverse under normal conditions even at very positive potentials (Barbour et al., 1991). The IV-relationship for the current produced by glutamate was linear with a reversal potential around 0mV. Glutamate-evoked currents were accompanied by an increase in membrane current noise and blocked by AP5 and CNQX, and thus must result from the presence of glutamate-gated ion channels.

The responses of retinal neurons to glutamate were partially blocked by the NMDA receptor antagonist AP5 and further blocked by the non-NMDA receptor antagonist CNQX, suggesting that these cells express both NMDA and non-NMDA receptors. This was confirmed using the non-NMDA receptor agonists kainate and AMPA. Both these glutamate analogues evoked currents that did not desensitize fully in all retinal neurons patch-clamped from 3 DIV. These results are interesting because they suggest that both kainate and AMPA can be used to activate the glutamate receptors of dissociated retinal neurons in the longer term. This is unexpected because in most systems responses desensitize almost completely in the presence of AMPA (see below). Yamashita et al. (1994a) observed non-NMDA responses at 2 DIV in amacrine cells in these cultures, with NMDA responses only apparent from 3 DIV. However this discrepancy may simply arise from differences in culture technique (they grew cells on a polyornithine substrate).

Non-NMDA receptors fall into 2 main categories, namely AMPA/kainate receptors and kainate-preferring receptors. Kainate-preferring receptors are characterized electrophysiologically by a transient response to kainate followed by almost complete desensitization in the continued presence of the drug (Herb et al., 1992, Sommer et al., 1992). In contrast kainate evokes long-lasting, non-desensitizing responses at AMPA/kainate receptors (Patneau and Mayer, 1991, Keinänen et al., 1990). Kainate produced a long-lasting response when applied to dissociated retinal neurons that persisted in the presence of the agonist (see chapter 4), thus indicating that kainate was acting at AMPA/kainate receptors. However, kainate was bath applied to the cells and solution changes were in the range of 1-2 seconds, so rapidly desensitizing responses may not be seen. The kainate-evoked response did not desensitize fully though, as would be expected if kainate were acting at solely at kainate receptors. Further evidence that neurons in these cultures express

AMPA/kainate receptors comes from the ability of AMPA to evoke currents in these cells. AMPA can only activate some subtypes of kainate-preferring receptors, and then only at very high concentrations (Herb et al., 1992, Bettler et al., 1992). Together these data show that chick retinal neurons express the AMPA/kainate type of non-NMDA receptors in culture from 3 DIV.

Another major excitatory neurotransmitter in the CNS is acetylcholine (ACh). The presence of ACh receptors in retinal cultures was not investigated using whole-cell patch-clamp experiments in this thesis. However Yamashita et al. (1994b) have shown that muscarinic ACh receptors are expressed as early as E3 in the embryonic chick retina and Ca^{2+}-imaging studies in chapter 6 confirm the presence of these receptors in the chick retina.

3.4.3 Localization of glutamate receptors occurs prior to spontaneous synaptic activity

A crude attempt was made to map the distribution of glutamate receptors using ionophoretic application of glutamate. These experiments showed that by 4 DIV glutamate receptors were aggregated at potential synaptic sites. Glutamate-evoked currents were much larger in regions where the process of one neuron made contact with another, compared to responses evoked at the cell body or along the length of the processes. If the assumption is made that the size of the evoked response reflects the receptor channel density, the data suggests that a higher density of receptors was present at sites of contact. This clustering may be an essential step in preparation for the formation of functional synapses. A similar aggregation of receptors at potential synaptic sites is seen at the neuromuscular junction during development. ACh receptors and release mechanisms are present in solitary muscle cells before innervation (Cohen et al., 1979, Frank and Fischbach,

1979, Young and Poo, 1983, Hume et al., 1983). On contact with other motoneurons postsynaptic ACh receptors redistribute so that they are positioned to optimally detect transmitter release in the synaptic cleft (reviewed by Hall and Sanes, 1993).

Later on in the culture period (10 DIV), several days after the clustering of glutamate receptors, spontaneous synaptic activity was apparent in retinal neurons. These mainly took the form of large inward deflections in membrane current at negative potentials, however smaller events were often apparent. The spontaneous events were inhibited by the glutamate receptor antagonists AP5 and CNQX. It seems likely that these currents reflect the spontaneous release of glutamate from synaptic regions, indicating the formation of functional glutamatergic synapses. Gleason and Wilson (1989) used electron microscopy techniques to study the formation of synapses in E8 chick retinal cultures. Consistent with the observations described above they found that conventional synapses were not abundant until cells had been held in culture for 8 days or more.

3.4.4 Cultured Müller cells express glutamate uptake carriers

Glutamate uptake carriers derive energy for the transport of glutamate from the co-transport of Na^+ ions into cells with each cycle of the carrier (Brew and Attwell, 1987). This allows glutamate uptake to be measured as a current using electrophysiological techniques. Müller cells in culture exhibit glutamate uptake currents that can be detected from 3 DIV onwards. Glutamate has been shown previously to operate an electrogenic uptake carrier in salamander retinal Müller cells (Barbour et al., 1991). The following lines of evidence show that glutamate evokes a current in chick Müller cells by activating uptake rather than by opening ion channels. Firstly, the IV-

relationship was inwardly rectifying and did not reverse even at positive potentials. If the current resulted from glutamate opening ion channels it would be expected to reverse around 0mV using solutions of the ionic composition employed in these experiments. Secondly, the application of glutamate was not associated with any change in membrane current noise and finally, the glutamate uptake blocker PDC inhibited the glutamate-evoked response and itself produced a current. PDC is carried by the glutamate uptake carrier but it is transported more slowly than glutamate so reducing the rate of glutamate transport. Glutamate uptake carriers are expressed in cultured retinal Müller cells from the earliest times at which they can be morphologically distinguished (3 DIV). The presence of glutamate uptake carriers provides a mechanism for removing glutamate from the synaptic cleft to terminate synaptic transmission (Hertz, 1979) and to prevent glutamate concentrations reaching neurotoxic levels (Nicholls and Attwell, 1990). The presence of these uptake carriers prior to the formation of functional synapses (as reflected by spontaneous activity) may be important in setting the concentration of glutamate in the extracellular space of the developing retina. These results are important because they show that glutamate cannot be used in experiments to determine the effects of long-term activation of glutamate receptors of cultured retinal neurons. Uptake of glutamate by glial cells will rapidly reduce its concentration in the culture medium and for this reason kainate was used in Chapters 4 and 5 to activate glutamate receptors because it is not taken up on glutamate uptake carriers (Brew and Attwell, 1987).

3.4.5 Retinal neurons express GABA- and glycine-gated channels early in development

GABA is a major inhibitory neurotransmitter in the CNS. Yamashita and Fukada (1993a) have shown that GABA receptors appear very early on in

chick retinal development (by E3) suggesting GABA may have an important developmental role. Staining with the anti-GABA antibody labelled the majority of neurons in the cultures. Müller cells and cones did not stain with anti-GABA and since the remaining cells in culture are mostly amacrine it seems likely that most of these cells are GABAergic. GABA is the transmitter for a large fraction of amacrine cells in the adult chicken retina (Brecha, 1983).

GABA evoked membrane currents in all retinal neurons tested at 3 DIV, as did glycine, another important inhibitory neurotransmitter in the CNS. The currents produced by GABA and glycine could not result from the operation of electrogenic carriers since the IV-relationships were linear and the currents reversed near the Cl^- equilibrium potential. This suggests that these receptors are linked to Cl^--specific channels. The GABA- and glycine-evoked responses were inhibited by the $GABA_A$ receptor antagonist bicuculline and the glycine receptor antagonist strychnine respectively. Responses to GABA did not desensitize so in Chapters 4 and 5 it could be used to activate GABA receptors of dissociated retinal cells in the longer term. The presence of $GABA_A$ and glycine receptors linked to Cl^- channels has previously been demonstrated in amacrine cells in these cultures (Gleason et al., 1993, Huba and Hoffman, 1991, Yamashita et al., 1994a). It can be concluded that cultured chick retinal neurons express both $GABA_A$ and glycine receptors early on in the culture period.

There is a discrepancy between the time of appearance of responses to transmitters in dissociated retinal cultures and those in the intact embryonic chick retina, as demonstrated in Chapter 6 by Ca^{2+} imaging experiments. Responses to glutamate and GABA appear prior to E8 in the intact retina, which is several days before responses to these transmitters are seen in

cultured cells. This may be because the dissociation procedure appears to set retinal cells back a few days in their development.

3.4.6 Voltage-gated Ca^{2+} channels are expressed prior to transmitter receptors in retinal neurons

Voltage-gated Ca^{2+} channels were present in cultured retinal neurons as early as 2 DIV and prior to the appearance of functional transmitter receptors. The Ca^{2+} currents evoked persisted throughout the voltage step, required strong depolarizing steps for activation and were blocked by nifedipine and diltiazem. These properties are characteristic of L-type channels (Nowycky et al., 1985). Huba et al. (1992) demonstrated the presence of Ca^{2+} currents in cultured chick retinal neurons and Gleason et al. (1992) observed L-type Ca^{2+} currents in cultured E8 chick cones after 3 DIV. Ca^{2+} imaging techniques show L-type Ca^{2+} channels to be present in the chick retina at E3 at which time GABA depolarizes cells sufficiently to activate them (Yamashita and Fukada, 1993a). Ca^{2+}-entry is required for vesicular release of transmitters and while there is as yet no evidence, the presence of voltage-gated Ca^{2+} channels and a variety of transmitter-gated receptors at very early times in development opens the possibility that such release may play some physiological role prior to synapse formation.

Chapter 4

The consequences of non-NMDA receptor activation in the chick retina during development

4.1 Introduction

The excitatory neurotransmitter glutamate plays a crucial role in the development of the central nervous system. It controls processes as varied as neurite outgrowth (see chapter 5), cell migration (Komuro and Rakic, 1993), and differentiation (Aruffo et al., 1987). Glutamate has also been strongly implicated in cell survival (Choi, 1988) and excitotoxicity (Olney, 1969, Olney, 1978). During ischemia and hypoxia an increase in glutamate release and the subsequent excessive activation of glutamate receptors is a major factor leading to neuronal cell death (for review see Szatkowski and Attwell, 1994). The likely mechanism by which glutamate mediates many of these diverse effects is through its influence on $[Ca^{2+}]_i$ (Pearce et al., 1987, Rashid and Cambray-Deakin, 1992, Komuro and Rakic, 1993, Hartley et al., 1993, Choi, 1985). Glutamate may alter $[Ca^{2+}]_i$ via activation of ionotropic receptors (NMDA or non-NMDA), metabotropic receptors, or indirectly via membrane depolarization leading to the opening of voltage-gated channels. Whilst metabotropic receptor activation can lead to the release of Ca^{2+} from internal stores, some ionotropic glutamate receptors are themselves permeable to Ca^{2+}. NMDA receptors are well established as Ca^{2+}-permeable ligand-gated channels (MacDermott et al., 1986, Mayer and Westbrook, 1987, Ascher and Nowak, 1988), however more recently it has been shown that AMPA/kainate receptors can also be Ca^{2+}-permeable (Murphy and Miller, 1989, Iino et al., 1990, Gilbertson et al., 1991, Burnashev et al., 1992a). The Ca^{2+}-permeability of AMPA/kainate receptors depends on their subunit composition. So far four

AMPA/kainate receptor subunits (GLUR1-4) have been cloned. GLUR1 ,3 and 4 form channels with high Ca^{2+}-permeability while GLUR2, alone or in combination with other subunits, forms receptors that are Ca^{2+}-impermeable (Hollmann et al., 1991, Burnashev et al., 1992b; for review, Seeburg, 1993).

The excitotoxic effects of glutamate and its analogues are often attributed to NMDA receptor activation (Choi, 1987, Andine et al., 1988, Silver and Erecinska, 1990), however more recently it has been shown in some cells to result from the Ca^{2+}-influx through AMPA/kainate receptors (Yin et al., 1994, Brorson et al., 1994). In the adult brain and retina as well as during late embryonic development the non-NMDA receptor agonist kainate produces excitotoxic cell death (Schwarcz and Coyle, 1977, Ehrlich and Morgan, 1980, Ingham and Morgan, 1983, Catsicas and Clarke, 1987). Studies in the rat brain demonstrate that the ratio of the mRNAs for the Ca^{2+}-permeable to Ca^{2+}-impermeable AMPA/kainate subunits decreases with age (Pellegrini-Giampietro et al., 1991, 1992). If this is reflected at the protein level, their observation suggests that the expression of Ca^{2+}-permeable AMPA/kainate receptors may exert an important influence on cell survival during development. Using kainate as a tool to stimulate AMPA/kainate receptors and the cobalt (Co^{2+})-technique of Pruss et al. (1991) the results in this chapter show:

1. When and where Ca^{2+}-permeable AMPA/kainate receptors are present in the developing chick retina.
2. Activation of these receptors with kainate at late times in development causes cell death.
3. Retinal cells survive chronic activation of AMPA/kainate receptors during their early development and this survival correlates with the down-regulation of Ca^{2+}-entry into cells that normally express Ca^{2+}-permeable AMPA/kainate

receptors.

4. The effects of chronic AMPA/kainate receptor activation with kainate can be mimicked by glutamate.

5. The effects of prolonged activation of AMPA/kainate receptors can be prevented by the non-NMDA receptor antagonist CNQX.

6. These effects do not involve the NMDA receptor, the metabotropic glutamate receptor or activation of voltage-gated Ca^{2+} channels.

5. The inhibitory neurotransmitter GABA has no effect on the expression of the Ca^{2+}-permeable form of the AMPA/kainate receptor.

4.2 Methods

Embryonic retinal explants and dissociated retinal cells were cultured as described in section 2.1. Nissl-staining with cresyl violet was used to better visualise explant cultures as described in section 2.3.3. The Co^{2+}-staining technique of Pruss et al. (1991) was used to identify cells expressing a Ca^{2+}-permeable form of the AMPA/kainate receptor (section 2.3.2). Dissociated retinal cells were identified using markers for ganglion cells (THY-1) and amacrine cells (HPC-1) as detailed in section 2.3.1. A combination of Co^{2+}-staining and immunostaining (see section 2.3.4) in these cultures enabled the identification of cells that express Ca^{2+}-permeable AMPA/kainate receptors. In some experiments retinal explants and dissociated retinal cells were Co^{2+}-stained after prolonged treatment with a drug or combination of drugs. Drugs were added to the culture medium of dissociated cultures after 1 DIV and to that of retinal explants at the time of plating. In dissociated cultures the fraction of cells expressing a Ca^{2+}-permeable AMPA/kainate receptor was counted using a hand-operated tally counter and cell counts were normalised to the number stained per 100 cells. The Student's two-tailed t-test was used to determine the significance of these data (see section 2.3.6). Cell viability

was monitored using the fluorescent label propidium iodide (see section 2.3.5) which stains the DNA of cells that have lost their membrane integrity and counts were made as described above.

The whole-cell patch clamp technique (Hamill et al., 1981) was used to study the kainate-evoked current in dissociated retinal cultures (detailed in section 2.8). The external solution used was solution A (table 2.1) and the internal solution was solution A (table 2.2). Bath solution changes were achieved using a gravity fed perfusion system. Stock solutions of some drugs (CNQX, diltiazem and nifedipine) have to be dissolved in DMSO. In experiments using these agents DMSO was added to control solutions at the same concentration that was present in the solution containing drugs.

4.2.1 Controls to determine the specificity of the Co^{2+}-staining technique for cells expressing AMPA/kainate receptors

The Co^{2+}-staining technique was established by Pruss et al. (1991) and is widely believed to only label cells that express the Ca^{2+}-permeable form of the AMPA/kainate receptor (those that exclude the GLUR2 subunit). However, AMPA/kainate receptors that include the GLUR2 subunit also have some permeability to Ca^{2+} (Leinders-Zufall et al., 1994, Burnashev et al., 1995). Thus it is possible that cells that express receptors that include the GLUR2 subunit may also stain if these are present at sufficiently high density. Here Co^{2+}-staining is taken to be a reflection of total Ca^{2+}-entry through all forms of the AMPA/kainate receptor channel regardless of their subunit composition.

The basis of the specificity of the Co^{2+} technique is that Co^{2+} ions block voltage-gated Ca^{2+} channels and NMDA receptor channels, but pass

through AMPA/kainate receptor channels (Tsien et al., 1987, Mayer and Westbrook, 1987, Ascher and Nowak, 1988, Winegar et al. 1991, Pruss et al., 1991). While the Co^{2+}-labelling technique has been applied to many CNS tissues it has not been used with chick retina. To check its specificity in embryonic retina the following controls were carried out. Dissociated cultures (6 DIV) were stained using the Co^{2+} technique with the following modifications. Kainate was excluded from solution D (table 2.1), the AMPA/kainate receptor antagonist CNQX (50μM) included and Na^{+} was replaced with K^{+}. This provided a high K^{+} solution in which the cells should be strongly depolarized and voltage-gated channels activated. Addition of CNQX prevented any glutamate released from activating AMPA/kainate receptors. Cells treated with Co^{2+} in this way were unstained, indicating that Co^{2+} did not permeate voltage-gated Ca^{2+} channels. To determine whether NMDA channels were permeable to Co^{2+} the cells were treated with Co^{2+} in solution D (table 2.1) but with the omission of Mg^{2+} and the inclusion of 100μM NMDA, 5μM glycine and 20μM CNQX. Under these conditions NMDA receptors will be strongly activated. However, none of the cells labelled with Co^{2+}, confirming previous studies that show NMDA channels to be impermeant to Co^{2+} ions. Similar results were obtained with intact retina from E15 embryos.

4.3 Results

4.3.1 Co^{2+}-staining of embryonic retinal explant cultures

Retinal explants were placed in culture at E6 and held *in vitro* for 6 days. The explants appear relatively undifferentiated at that time but over a period of days they develop a laminated morphology similar to that seen *in vivo* (shown by Nissl-staining in figure 4.1A). Application of the Co^{2+}

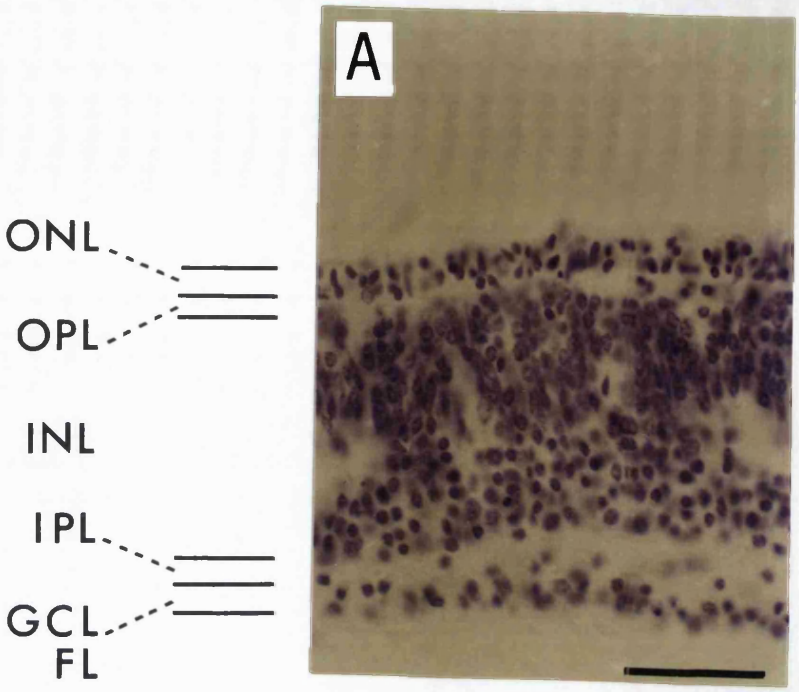

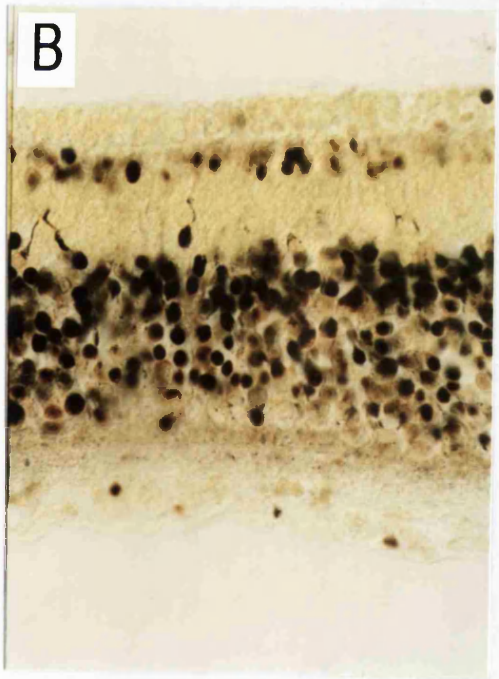

Figure 4.1

Control E6 retinal explants after 6 DIV. **A.** Nissl stained transverse section. The explant has developed a laminated morphology but few cells survive in the ganglion cell layer (GCL). FL: fiber layer; INL: inner nuclear layer; IPL: inner plexiform layer; ONL: outer nuclear layer, OPL: outer plexiform layer. Scale bar represents 50μm. **B.** Transverse section of a Co^{2+}-stained retina. Cells in the GCL and the inner and outer part of the INL are labelled.

technique at 6 DIV reveals a population of neurons that express AMPA/kainate receptors with a significant permeability to Ca^{2+} (figure 4.1B). Many Co^{2+}-labelled cells were present in the inner part of the INL. One population of the neurons that stain with Co^{2+} in this region have large cell bodies and may represent amacrine cells. Another population have smaller cell bodies and are probably bipolar cells. A band of unlabelled INL neurons separates these cells from a row of densely labelled neurons in the outermost part of the INL, the position of which suggests they may be horizontal cells. Occasional staining was seen in the GCL.

4.3.2 Retinal explants survive prolonged activation of AMPA/kainate receptors early in development

In order to study the effects of AMPA/kainate receptor activation on retinal development, E6 retinal explants were maintained for 6 days in 100μM kainate from the time of plating and then Nissl-stained. Explants treated with kainate at this early stage of development laminate normally with no obvious loss of cells and appear similar to control explants (figure 4.2A).

In contrast, when E6 retinal explants that had been held in culture for 6 days were treated with 100μM kainate for 24 hours they showed extensive damage with clear loss of cells from the INL (figure 4.2C). This result is consistent with previous reports that show that activation of AMPA/kainate receptors leads to excitotoxic death in the adult and late embryonic retina.

4.3.3 Co^{2+}-staining in explants is reduced by prolonged activation of AMPA/kainate receptors early in development

The effects of kainate on the Ca^{2+}-permeablity of AMPA/kainate

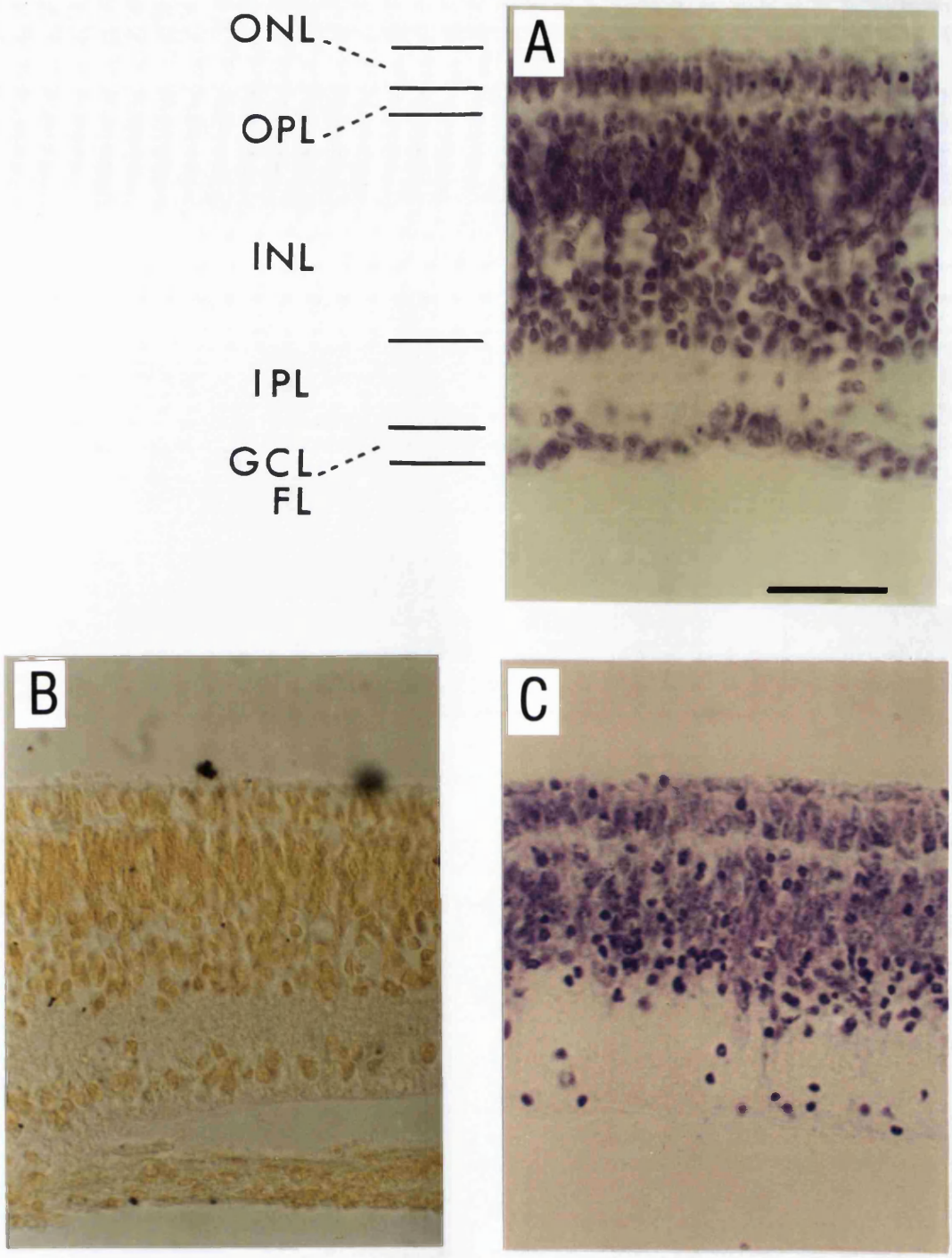

Figure 4.2

Chronic and acute effects of kainate on retinal explants. **A.** Nissl- and **B.** Co^{2+}-stained section through an E6 retinal explant grown for 6 days in 100μM kainate. The explant develops normally, but no cells stain with Co^{2+} (c.f. figure 4.1B). Bar represents 50μm. **C.** Nissl-stained section of an explant treated with 100μM kainate for 24 hours at 6 DIV. Cell death is apparent in the INL and GCL.

receptors was investigated using the Co^{2+} technique. E6 retinal explants were treated with 100μM kainate after plating and maintained in this concentration of the drug for 6 days before they were Co^{2+}-stained. This prolonged treatment with 100μM kainate completely abolished the staining normally seen in retinal explants at this time (figure 4.2B) (n=12 in 3 independent experiments). The absence of staining seen following kainate treatment was not accompanied by any obvious changes in the structure of the retina or loss of cells.

It proved difficult to quantify these effects in retinal explants because their development in culture is dependent on the region of the embryonic retina from which they are drawn and cell counts are difficult to make in histological sections. In order to quantify the effects of activating AMPA/kainate receptors during retinal development dissociated cell cultures were used for the remainder of the experiments in this chapter.

4.3.4 Co^{2+}-staining of dissociated retinal cells

Application of the Co^{2+}-staining technique to dissociated embryonic retinal cells suggests that many of them express AMPA/kainate receptors that permit significant Ca^{2+}-entry (figure 4.3A), with as many as 35-50% of the cells staining with Co^{2+} by 5 DIV (see section 4.3.11).

4.3.5 Identification of Co^{2+}-labelled cells in retinal cultures

Müller cells and photoreceptors in dissociated retinal cultures can be identified on the basis of their morphology (see chapter 3). These cells did not label with Co^{2+}. Antibodies were used to label ganglion (THY-1) and amacrine cells (HPC-1). Immunostaining of cultures with THY-1 showed that

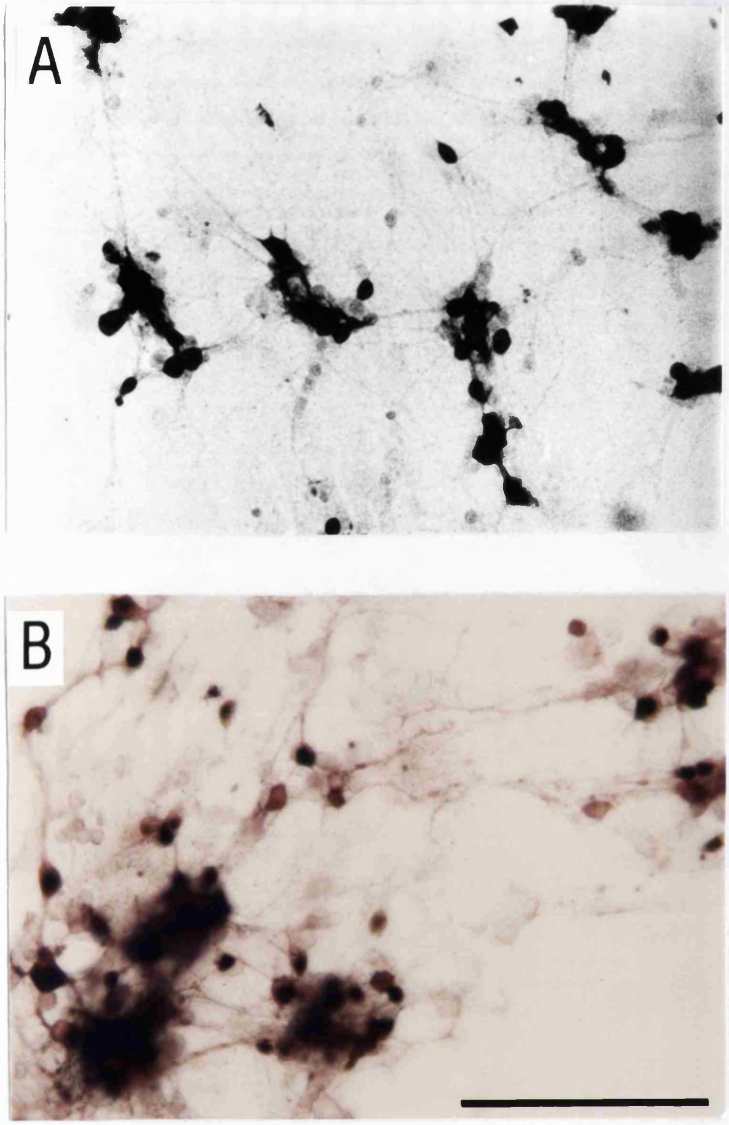

Figure 4.3

A. Co^{2+}-staining of cultured retinal cells (6 DIV) reveals cells that express AMPA/kainate receptors that permit significant Ca^{2+}-influx. **B.** Double-labelling of retinal cells (5 DIV) using the Co^{2+} technique and HPC-1 labelling shows cells that are HPC-1-positive, HPC-1- and Co^{2+}-positive and Co^{2+}-positive alone. Bar represents 100μm.

ganglion cells were absent under the culture conditions used (see figure 3.4A chapter 3). Immuno-labelling with HPC-1 stained approximately 33% of the cells in culture suggesting that they were amacrines (figure 3.4B, chapter 3). Combined staining using the Co^{2+} technique and HPC-1 labelling showed that HPC1-positive cells consist of 2 distinct populations of which 48% were HPC-1 positive alone and 52% labelled with both HPC-1 and Co^{2+} (figure 4.3B). Another 30% of the cells were labelled by Co^{2+} alone and could not be identified with certainty. However it is possible that they represent the population of bipolar cells and/or horizontal cells seen in Co^{2+}-staining of explant cultures.

4.3.6 Isolated retinal cells also survive activation of AMPA/kainate receptors early in development

In order to quantify the effects of activating AMPA/kainate receptors on cell survival, dissociated E8 retinal cells were exposed to 10, 100 and 500μM kainate after 1 DIV and maintained in these concentrations of the drug for 5 days. This treatment had no apparent effect on cell viability and the cells appeared healthy and similar to those in control cultures of the same age (figure 4.4A and B), although the number of neurites they extended was reduced (see chapter 5). Cell counts showed that chronic activation of AMPA/kainate receptors with kainate had no effect on total cell number (figure 4.5). All cultures were plated at the same density and the density remained unchanged over the period in culture (447.6±19.5 cells/field at 2 DIV, 441±10 cells/field at 5 DIV, n=5). In contrast, when 6 day old cells that had not previously been exposed to kainate were treated with 100μM of the drug for just 12 hours, cell numbers were reduced by 59.6±0.3% (figure 4.5). The effects on these older cultures was rapid and the cells appeared swollen with many retracting their processes after a few hours in kainate (figure 4.4C).

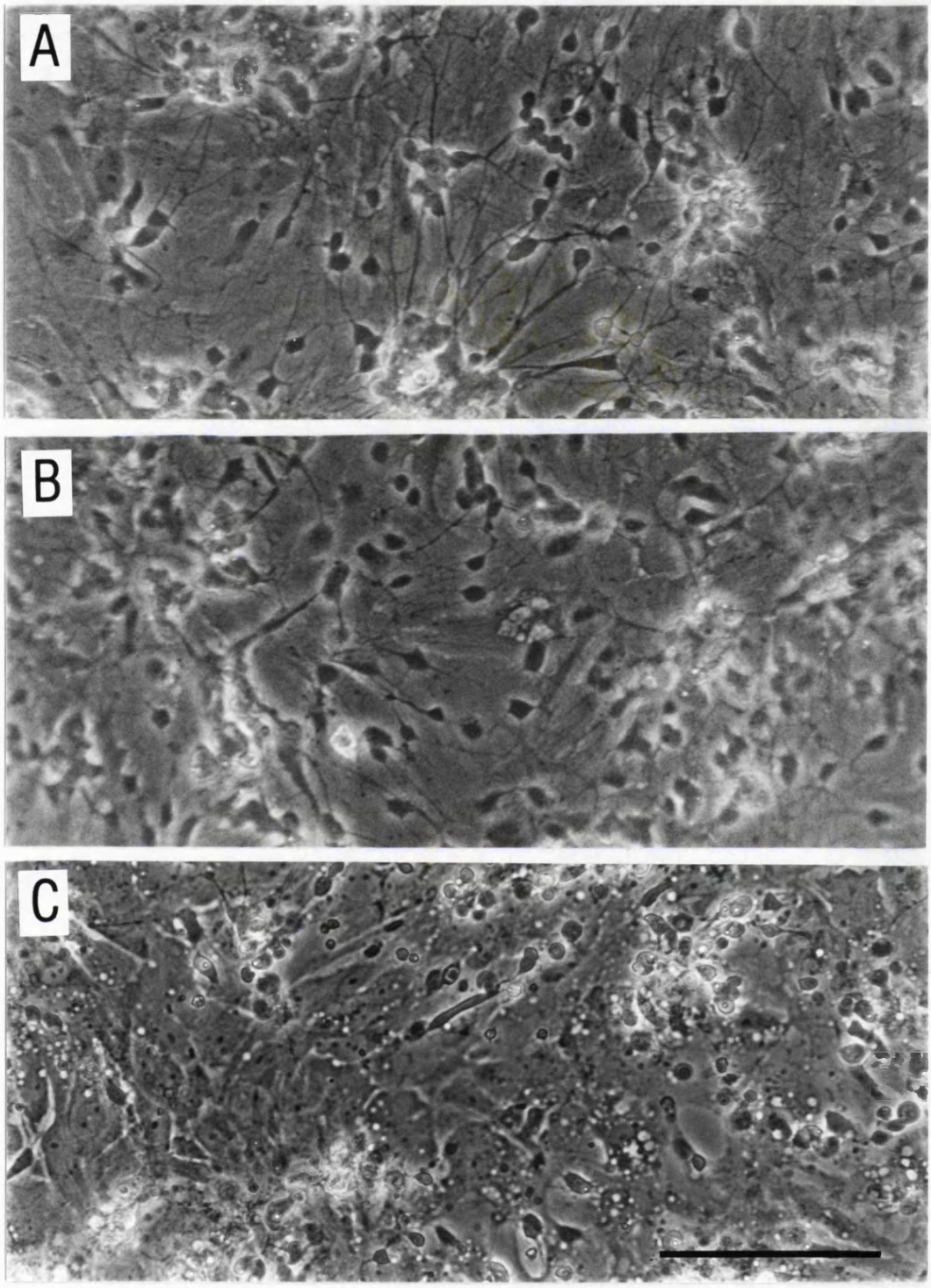

Figure 4.4

Dissociated retinal cells can survive in high concentrations of kainate.

A. Control culture of embryonic retinal cells (6 DIV). **B.** Retinal cells (6 DIV) grown in 500μM kainate from 1 DIV. **C.** Retinal cells after acute exposure to 100μM kainate for 12 hours at 6 DIV. Bar represents 100μm.

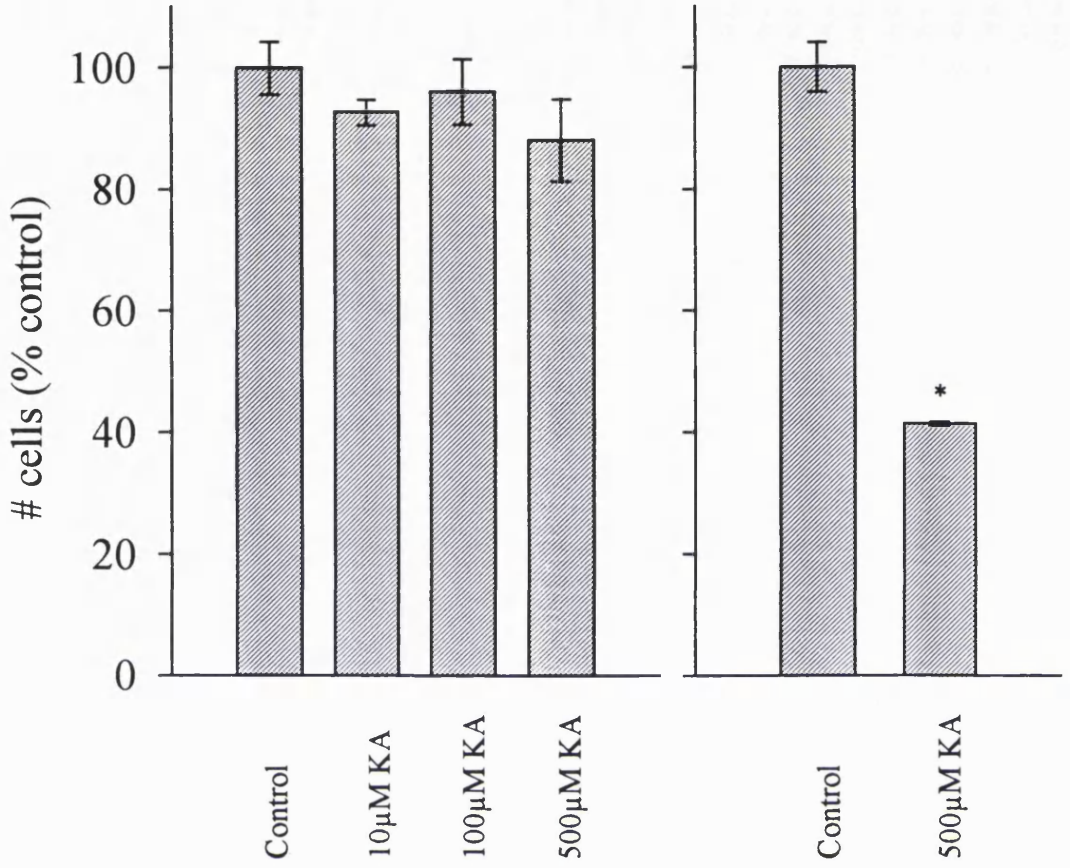

Figure 4.5

The effects of chronic and acute kainate treatment on cell number.

Left-hand panel: Dissociated retinal cells were exposed to 10, 100 and 500μM kainate from 1 DIV and counts of cell number were made after 5 days in kainate. Cell numbers were not affected by chronic kainate treatment and were similar to controls in all 3 kainate concentrations. Counts were made from 7 fields in 2 dishes with a mean of 1037.7±42.6 cells per field.

Right-hand panel: Cells were exposed to 100μM kainate at 6 DIV for 12 hours. Acute kainate treatment produced a significant reduction in cell number ($p \leq 0.001$). Counts were made from 6 fields from 2 dishes with a mean of 1235±50.3 cells per field before kainate application.

The fluorescent dye propidium iodide was used to identify dead cells. The number of cells that labelled in control cultures at 6 DIV was low (1.1±0.3%) showing that the majority were alive (figure 4.6A). In cultures that were chronically exposed to 500μM kainate after 1 DIV and maintained in the drug for 5 days, the number of cells that labelled with propidium iodide was not significantly different to controls (0.6±0.2%) (figure 4.6B). This again shows that most of the cells in these cultures survive treatment with kainate. However, in cultures exposed to 100μM kainate for 12 hours after 6 DIV 26.7±2.4% of the cells labelled with the dye indicating that many of the cells were dead or dying (figure 4.6C). The cells affected by kainate treatment were neurons; cone photoreceptors and glial Müller cells were unaffected.

Together these data show that late in their development embryonic retinal cells are killed by acute activation of AMPA/kainate receptors with 100μM kainate (12 hours). However, the same E8 retinal cells can be maintained in concentrations of up to 500μM kainate when it is added to the culture medium early in development (from 1 DIV).

4.3.7 Cell survival in kainate is accompanied by a reduction in the fraction of cells stained by Co^{2+} in cultures of dissociated retinal cells

To study the effects of AMPA/kainate receptor activation on the Ca^{2+}-influx through these receptors dissociated retinal cells were grown in the presence of 10, 100 and 500μM kainate from 1 DIV. The cells were then Co^{2+}-stained after 7 DIV and counts made as described in section 4.2. The fraction of Co^{2+}-positive cells was significantly reduced in all 3 kainate concentrations compared to controls (figure 4.7). The decrease was greater with increasing concentrations of kainate, with 500μM kainate reducing the fraction of Co^{2+}-stained cells by 90%. The reduction in staining was

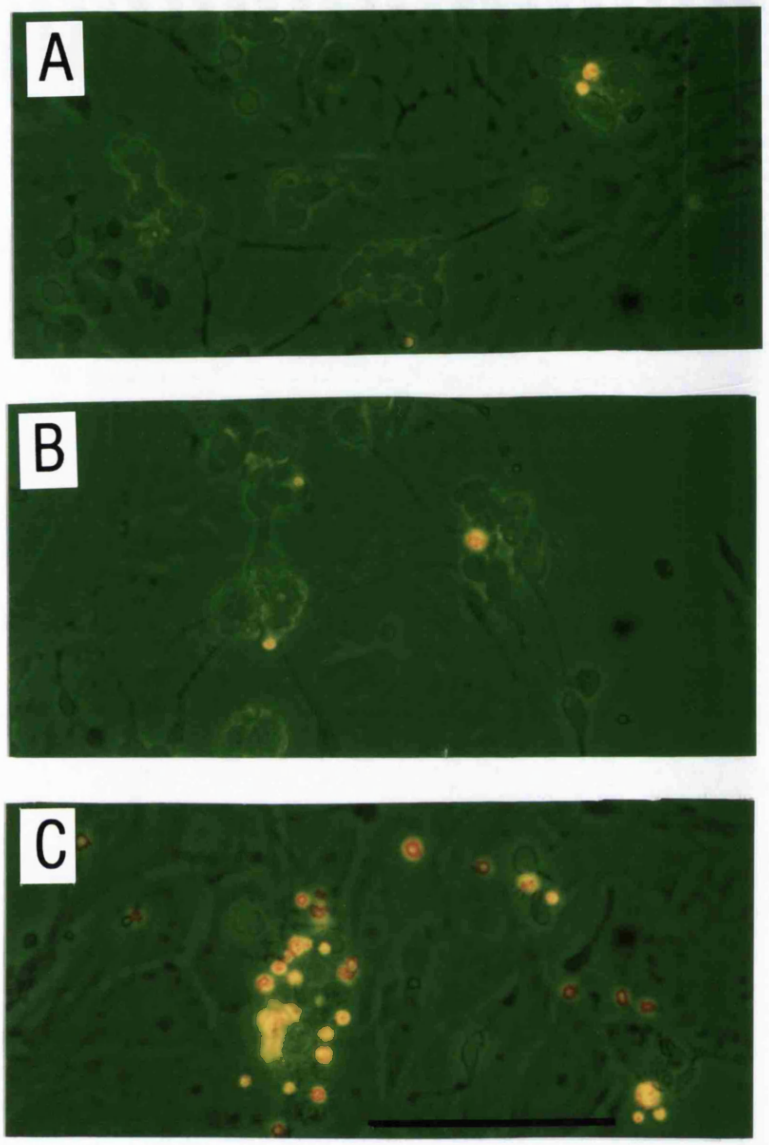

Figure 4.6

Propidium iodide (PI) labelling of retinal cultures after chronic and acute exposure to kainate.

A. Control culture (6 DIV). **B.** Retinal cells (6 DIV) after chronic exposure to 500μM kainate. As in control cultures, few cells label with PI. **C.** Retinal cells after acute exposure to 100μM kainate at 6 DIV. The membranes of many cells are permeant to PI. Bar represents 100μm.

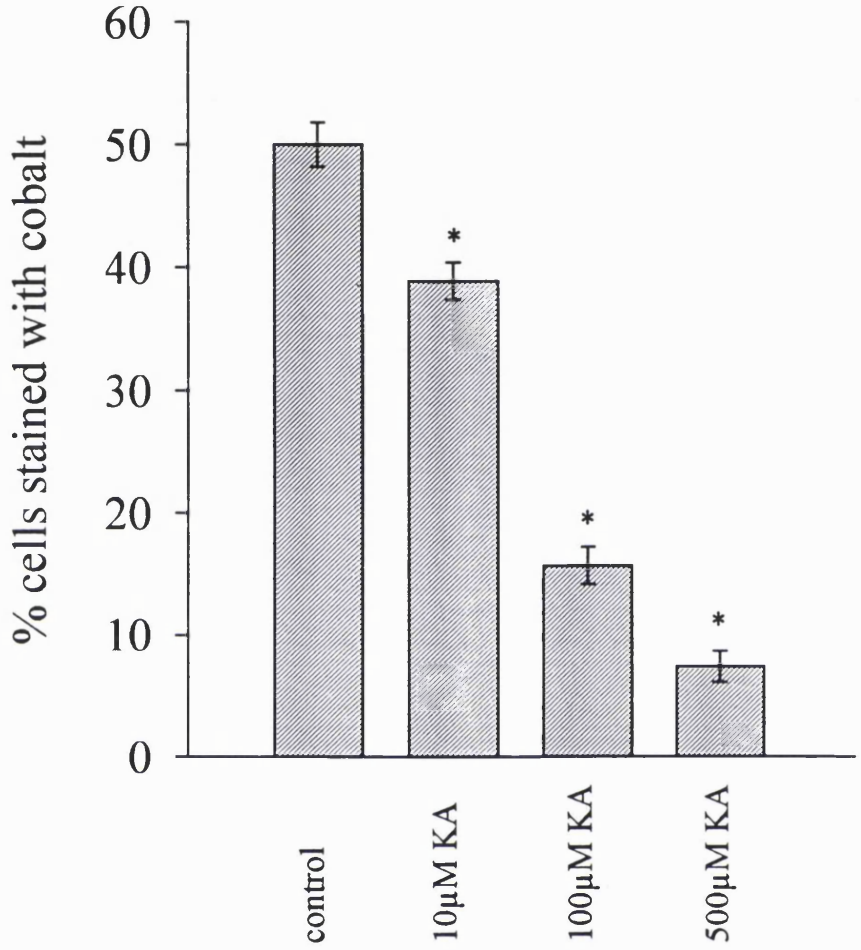

Figure 4.7

The effects of chronic exposure to kainate on Co^{2+}-staining in dissociated retinal cells.

Counts were made from 9 fields in 3 culture dishes with a mean of 372.3±36 cells per field. Chronic treatment (1 to 7 DIV) with 10, 100 and 500μM kainate all produced a significant reduction in the fraction of Co^{2+}-positive cells compared to controls (*, $p \leq 0.001$).

significant at the 0.1% level for all concentrations and was not accompanied by a reduction in overall cell number. These data suggest that activation of AMPA/kainate receptors early on in retinal development leads to a reduction in the Ca^{2+}-influx into cells expressing this receptor. This reduction in Ca^{2+}-entry is likely to be an important factor in determining the survival of cells maintained in kainate from early times.

4.3.8 The effects of prolonged AMPA/kainate receptor stimulation are blocked by CNQX

To investigate whether the initial actions of kainate were directly at the AMPA/kainate receptor, the non-NMDA receptor antagonist CNQX (20μM) (Tocris) was included in the culture medium with 10, 100 and 500μM kainate at 1 DIV and the cells grown in the presence of the two drugs for 6 days. CNQX was prepared in a stock solution containing DMSO so similar levels were added to all experimental and control dishes. Blocking AMPA/kainate receptors with CNQX prevented the reduction in Co^{2+}-staining observed after chronic kainate treatment (figure 4.8). These data suggest that kainate mediates its initial action on Ca^{2+}-influx directly via activation of AMPA/kainate receptors.

4.3.9 Excitotoxic death in kainate correlates with the presence of AMPA/kainate receptors the permit significant Ca^{2+}-entry into cells

In order to determine whether the presence of AMPA/kainate receptors which allow significant Ca^{2+}-influx correlates with susceptibility to excitotoxic death produced by activation of these receptors, cells were grown in the presence of kainate and CNQX as described in section 4.3.8. The culture medium containing kainate with CNQX was removed at 7 DIV and the

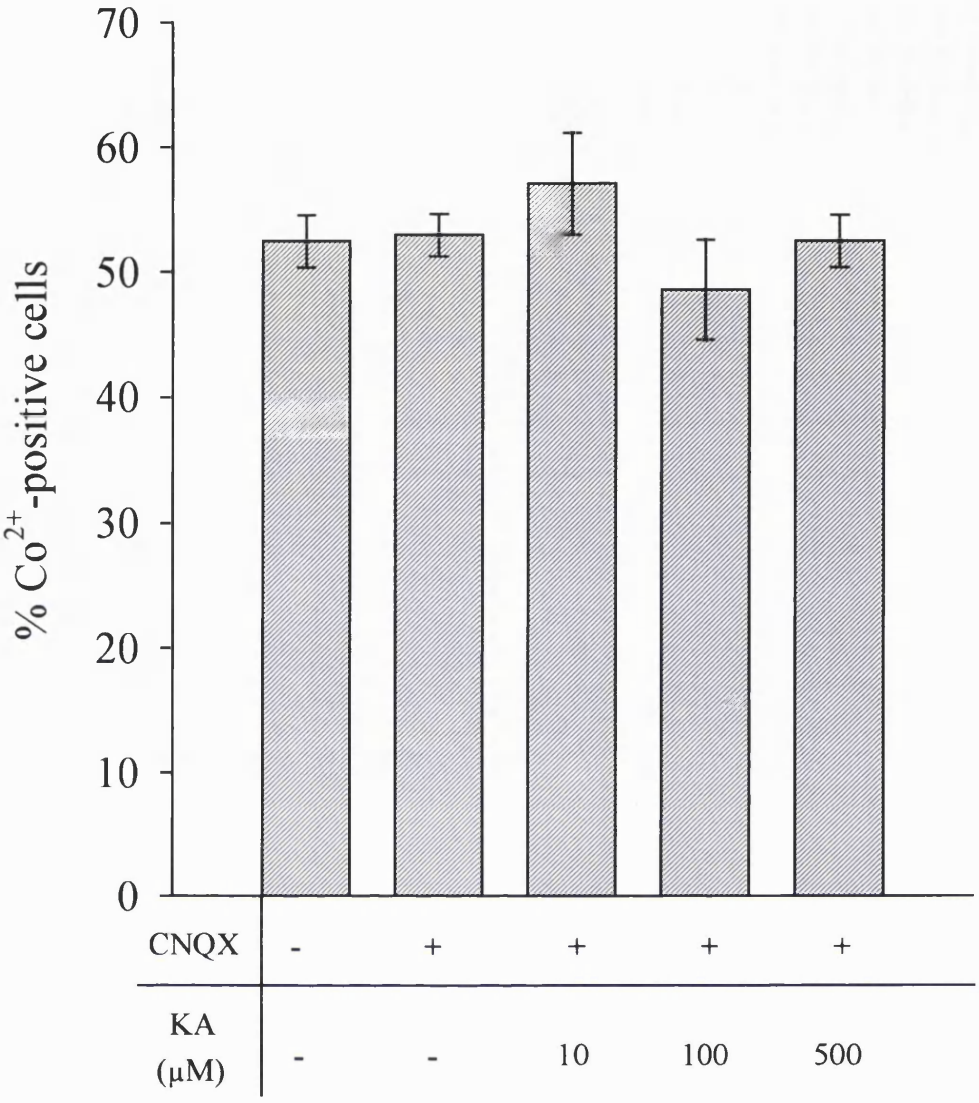

Figure 4.8

CNQX blocks the effects of kainate on the number of Co^{2+}-stained cells. Application of 20μM of the non-NMDA receptor antagonist CNQX prevented the reduction in Co^{2+}-staining produced by chronic exposure to kainate (1-7 DIV). CNQX blocked the effects of 10, 100 and 500μM kainate. Addition of CNQX in the absence of kainate had no effect on Co^{2+}-staining. Counts were made from 6 fields in 2 culture dishes for each experimental condition with a mean of 207.9±9.8 cells per field.

cultures then exposed to 100μM kainate alone for 15 hours. This treatment produced widespread cell death (data not shown) similar to that seen when kainate is applied to cells that have not previously seen the drug, late in their development. Data shown in section 4.3.8 shows the presence of a large fraction of cells that stain for Co^{2+} in cultures grown in the presence of CNQX and kainate, similar to the fraction of stained cells in control cultures. Together these data indicate that the presence of AMPA/kainate receptors with a high Ca^{2+}-permeability (shown by Co^{2+}-staining) leads to an increased susceptibility to excitotoxic death in the presence of kainate.

4.3.10 The pharmacology of the effects of chronic kainate treatment

The glutamate analogue kainate was used during most experiments in this chapter because its concentration can be controlled in culture since it is not taken up by glutamate uptake carriers present in the membrane of Müller cells (Brew and Attwell, 1987) (see chapter 3). However, the effects of kainate on reducing the number of Co^{2+}-stained cells could be mimicked by treatment with glutamate. Application of 100μM glutamate to the culture medium after 1 DIV reduced the number of cells that stain with Co^{2+} at 7 DIV compared to controls (figure 4.9) with no effect on cell number (228±10 cells/field in controls compared to 206±13 cells/field in glutamate treated cultures). The reduction in Co^{2+}-staining was significant at the 0.1% level. The effects of glutamate could be blocked by co-application of the non-NMDA receptor antagonist CNQX (20μM), but not by co-application of the NMDA receptor antagonist AP5 (20μM). These data suggest that chronic activation of AMPA/kainate receptors with glutamate early in development can lead to a reduction in the Ca^{2+}-influx through these channels and that glutamate may produce these effects through a direct action on the AMPA/kainate receptor itself.

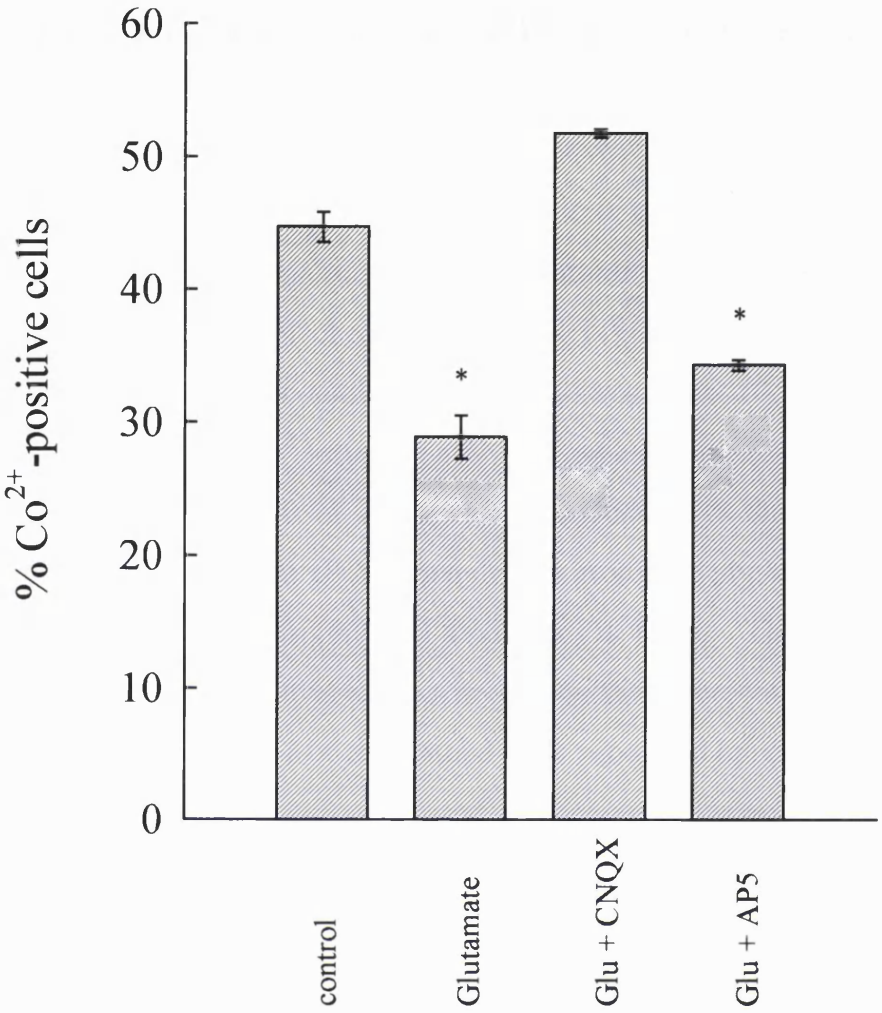

Figure 4.9

The effects of glutamate on Co^{2+}-staining.

Application of 100μM glutamate to the culture medium from 1 DIV leads to a significant reduction in the fraction of cells staining for Co^{2+} at 7 DIV compared to controls (*, $p \leq 0.001$). The effects of glutamate can be blocked by the non-NMDA receptor antagonist CNQX (20μM) but not by the NMDA receptor antagonist AP5 (20μM). Counts were made from 9 random fields in 3 dishes for each experimental condition with a mean of 247±7 cells per field.

Activation of AMPA/kainate receptors with kainate will lead to membrane depolarization. This may evoke glutamate release that can in turn activate other glutamate receptors. Although the effects of glutamate and kainate were blocked by CNQX (see above), the activation of NMDA receptors by glutamate released via kainate-evoked depolarization was investigated. This possibility seemed remote given that the actions of glutamate could not be blocked by AP5. The NMDA receptor antagonist AP5 (20μm) (Tocris) was co-applied to the cultures with 10, 100 and 500μM kainate from 1 DIV. Co^{2+}-staining at 7 DIV revealed that AP5 did not protect the cells from the effects of kainate and a reduction in the number of Co^{2+}-positive cells was seen at all 3 kainate concentrations employed (figure 4.10). These reductions were significant at the 0.1% level. The results of these experiments exclude the involvement of NMDA receptor activation in the reduction in the number of Co^{2+}-stained cells produced by kainate.

Glutamate release, secondary to kainate-evoked membrane depolarization, could act at metabotropic glutamate receptors. Moreover, it has been shown that high concentrations of kainate can directly activate metabotropic receptors (Shiells et al., 1981). To investigate whether activation of metabotropic receptors was involved in the effects of kainate on Co^{2+}-staining, the metabotropic glutamate receptor agonist *trans*-ACPD was added to the culture medium after 1 DIV. *Trans*-ACPD (150μM) had no effect on the percentage of Co^{2+}-positive cells at 7 DIV (figure 4.11) suggesting that the activation of metabotropic receptors is not involved in the actions of kainate.

Kainate-evoked membrane depolarization will also activate voltage-gated Ca^{2+} channels. To determine whether or not Ca^{2+}-influx through these channels was important for the effects produced by kainate, 20μM of each of

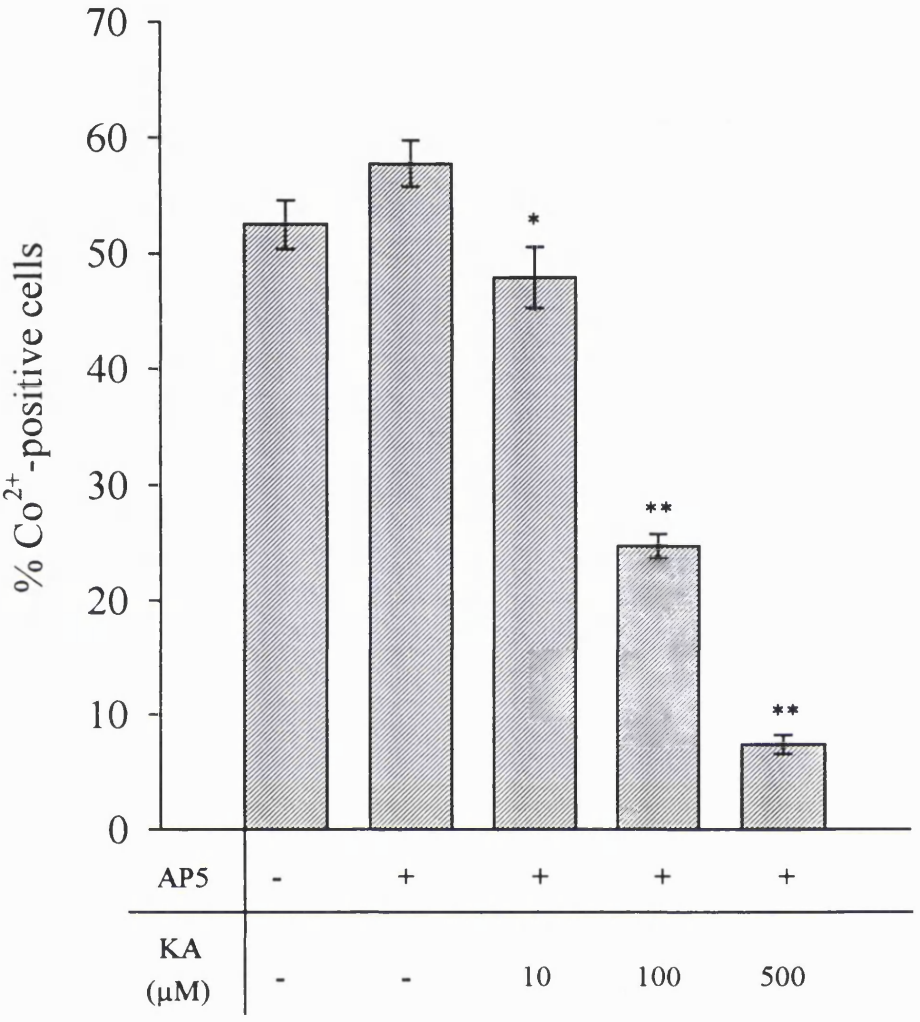

Figure 4.10

AP5 does not prevent the effects of kainate on Co^{2+}-staining.

Co-application of the NMDA receptor antagonist AP5 (20μM) with 10, 100 and 500μM kainate did not prevent the kainate-evoked reduction in the number of cells that stain with Co^{2+} (*, $p \leq 0.02$; **, $p \leq 0.001$). Counts were made from 5 fields in 2 dishes with a mean of 198.2±10 cells per field.

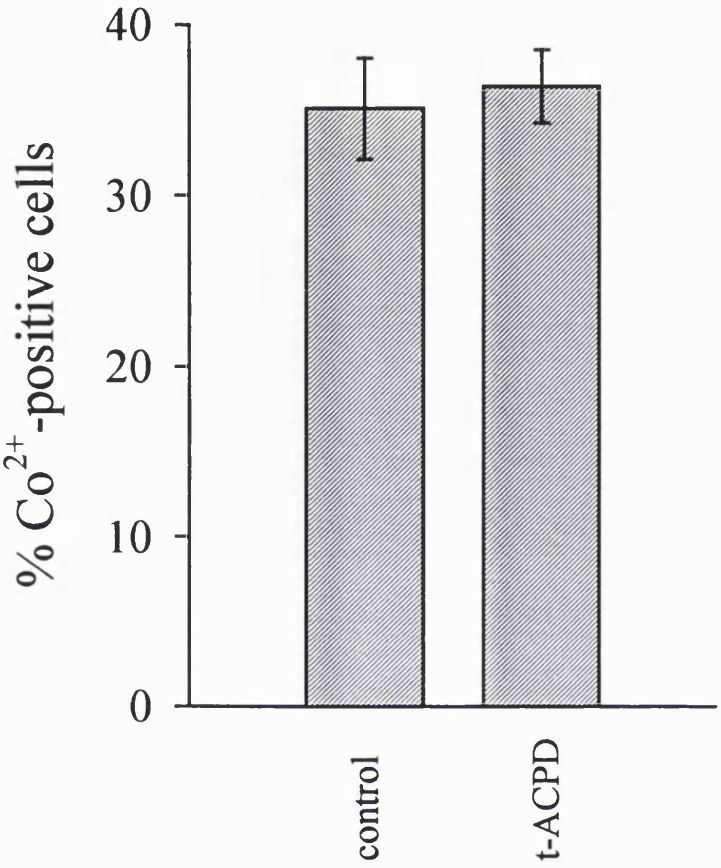

Figure 4.11

Trans-ACPD does not affect the number of Co^{2+}-stained retinal cells.
The metabotropic glutamate receptor agonist *trans*-ACPD (150μM) had no effect on the number of Co^{2+}-positive cells when it was applied to the cells from 1 to 7 DIV. Counts were made from 6 random fields in 2 dishes with a mean of 204±7 cells per field.

the L-type Ca^{2+} channels blockers nifedipine and diltiazem (both Sigma) were co-applied to the cells with 10, 100 and 500μM kainate at 1 DIV. These concentrations of the two drugs blocked about 90% of the L-type Ca^{2+} current in retinal cells during whole-cell patch clamp recordings (see chapter 3). Both diltiazem and nifedipine were prepared in DMSO so similar concentrations of this solvent were added to all control and experimental culture dishes. Co^{2+}-staining at 7 DIV showed that these blockers were ineffective at preventing the effects of kainate. Reductions in Co^{2+}-staining that were significant at the 0.1% level were seen at all concentrations of kainate employed (figure 4.12). These data indicate that the effects of prolonged AMPA/kainate receptor activation on Ca^{2+}-entry through the receptor does not involve the operation of voltage-gated Ca^{2+} channels.

The inhibitory neurotransmitter GABA is strongly depolarizing at early times in development of the retina (Yamashita and Fukada, 1993a, and see chapter 6). To confirm that the effects of kainate on Ca^{2+}-influx were not due to its depolarizing action, GABA was added to the culture medium for 6 days at a concentration of 100μM and the cells Co^{2+}-stained after 7 DIV. GABA had no effect on Ca^{2+}-influx and the percentage of Co^{2+}-positive cells was similar to controls (figure 4.13). This result shows that the down-regulation of Co^{2+}-staining is specific to the action of kainate at the AMPA/kainate receptor and is not due to secondary depolarization-evoked effects.

4.3.11 The time course of kainate's action

To determine the time course of the onset of the effects of kainate on the suppression of Co^{2+}-labelling, dissociated cultures were exposed to 500μM kainate after 4 DIV for periods between 15 and 60 minutes before they were Co^{2+}-stained. Exposure to kainate for 30 minutes slightly (though not

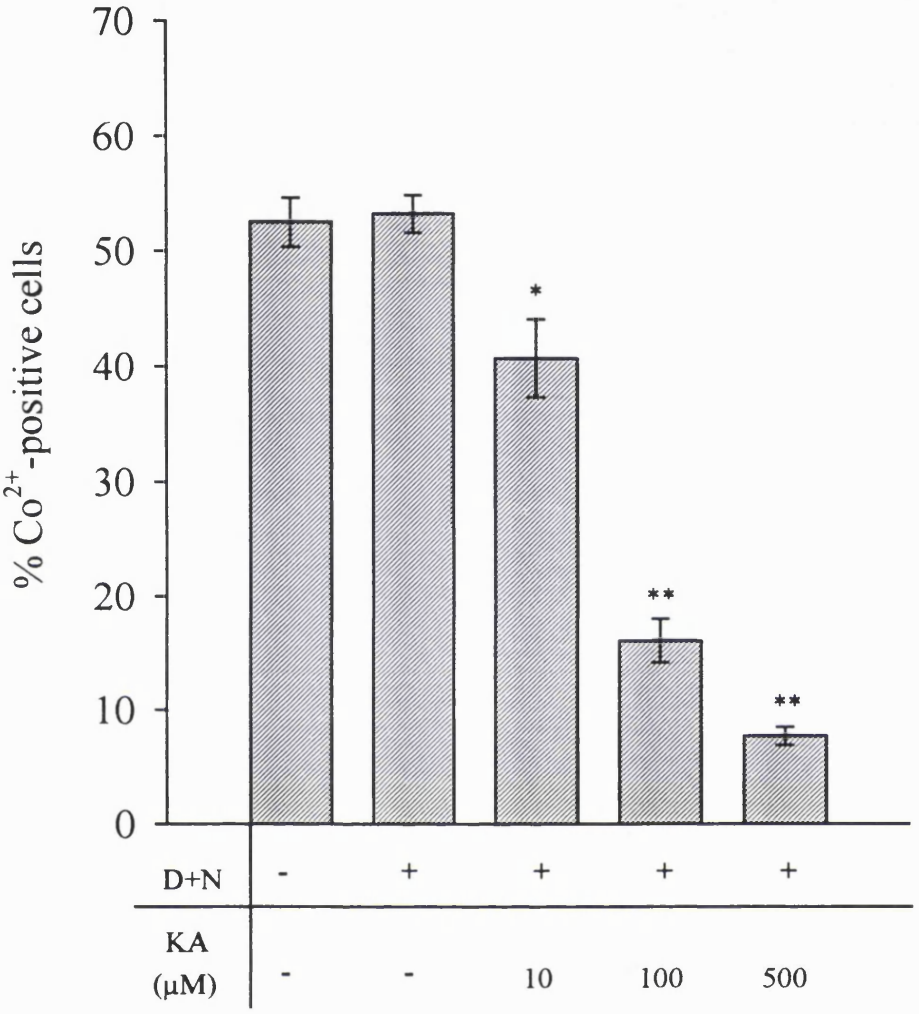

Figure 4.12

Blockers of voltage-gated Ca^{2+} channels do not protect retinal cells from the effects of kainate.

Co-application of diltiazem and nifedipine (20μM) with 10, 100 and 500μM kainate did not protect the cells from the reduction in Co^{2+}-staining which was significant at all 3 concentrations of kainate (*, $p \leq 0.02$; **, $p \leq 0.001$). Counts were made from 5 fields in 2 dishes with a mean of 180.8.2±10.4 cells per field.

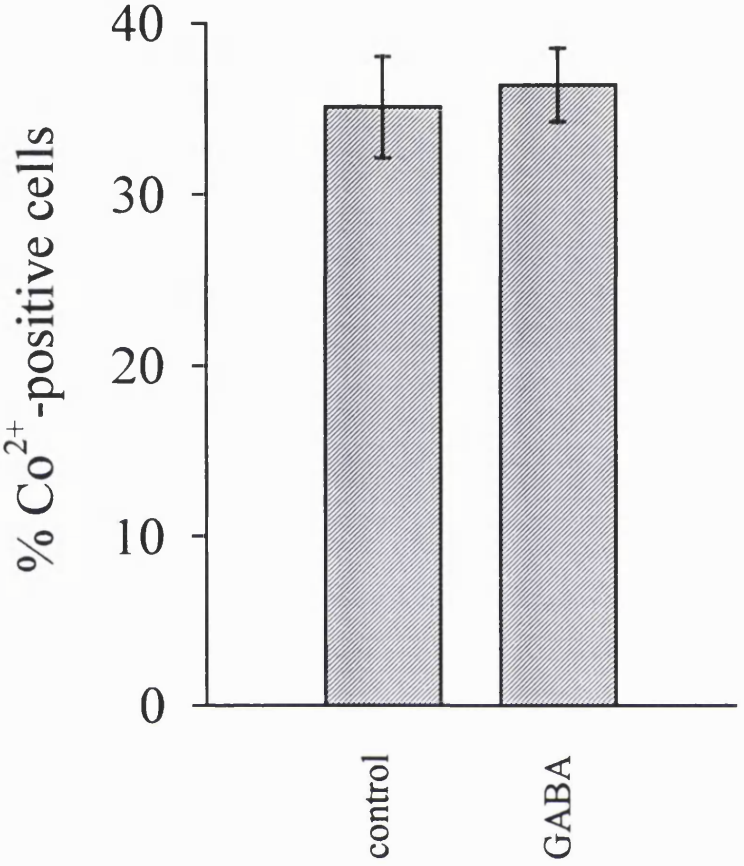

Figure 4.13

GABA does not affect the number of cells that stain with Co^{2+}.

GABA (100μM) was applied to the cells from 1 to 7 DIV. Counts were made from 6 random fields in 2 culture dishes with a mean of 305±12 cells per field.

significantly) reduced the fraction of Co^{2+}-stained cells from 29.7±2.4% to 26.7±1.6%. However, exposure to kainate for 60 minutes significantly reduced the number of stained cells by about 50% to 16.4±2.4% (significant at the 2% level) with no change in the total number of cells in the dishes (n=10). This suggests that kainate begins to exert its effects on Ca^{2+}-influx within an hour of exposure to the drug.

The suppression of Co^{2+}-staining by chronic activation of AMPA/kainate receptors was examined as a function of time in culture. Cells were exposed to 500μM kainate after 1 DIV and a sample was Co^{2+}-stained each day up until 9 DIV. In control dishes the percentage of cells stained by Co^{2+} rose with time reaching a peak at 5 DIV before falling at later times (figure 4.14). In cultures exposed to kainate early on the percentage of cells stained by Co^{2+} did not increase greatly with time (figure 4.14) and reductions in the number of cells stained compared to controls were apparent from the earliest times.

To determine whether or not the effects of kainate were reversible the drug was removed from the culture medium surrounding 7 day old cells that had been grown in 500μM kainate since 1 DIV. After removal of kainate from the dishes they were Co^{2+}-stained at intervals over a period of hours. The fraction of cells that stained rapidly increased until 6 hours when the percentage of Co^{2+}-positive cells reached control levels (figure 4.15). These data confirm that cells that normally express AMPA/kainate receptors with a significant Ca^{2+}-permeability are not killed by prolonged activation of these receptors at early times, rather long-term receptor activation produces a reduction in the Ca^{2+}-influx through the AMPA/kainate receptor that is restored on removal of the drug.

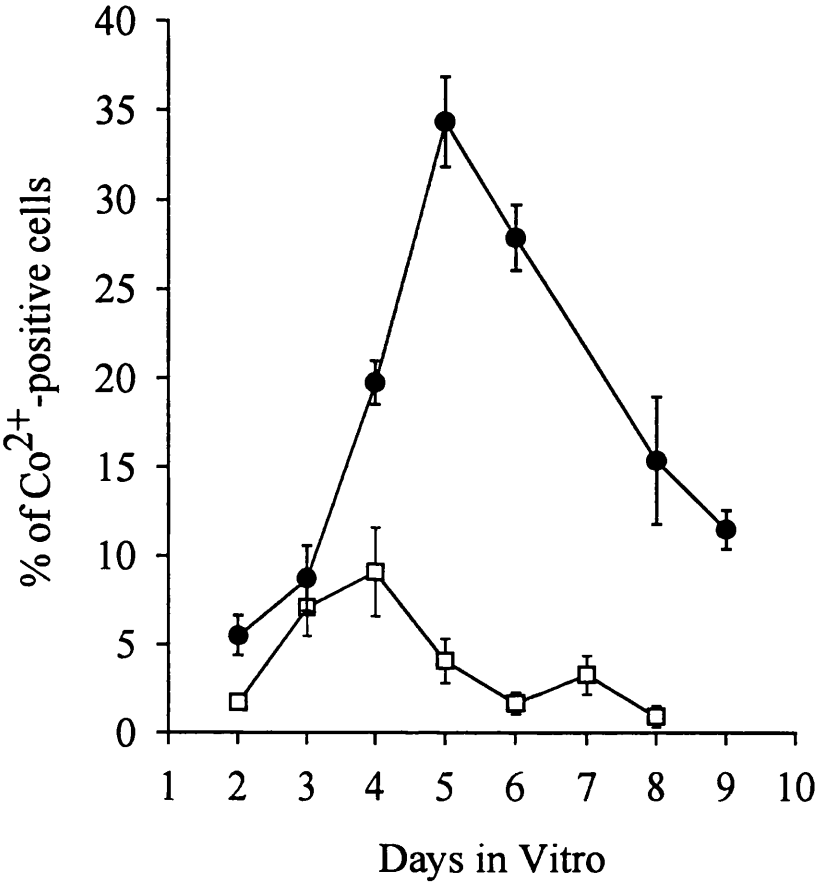

Figure 4.14

The fraction of Co^{2+}-positive cells as a function of time in culture.

Solid circles: Control cultures. Counts were made on each day in culture from 7 fields in 2 dishes with a mean of 319.5±24.6 cells per field. The number of Co^{2+}-positive cells rose over time reaching a peak at 5 DIV, followed by a fall at later times.

Hollow squares: Retinal cultures grown in 500μM kainate from 1 DIV. Counts were made from 9 fields in 3 dishes with a mean of 400±14.6 cells per field. The fraction of Co^{2+}-positive cells was reduced at all times compared to controls.

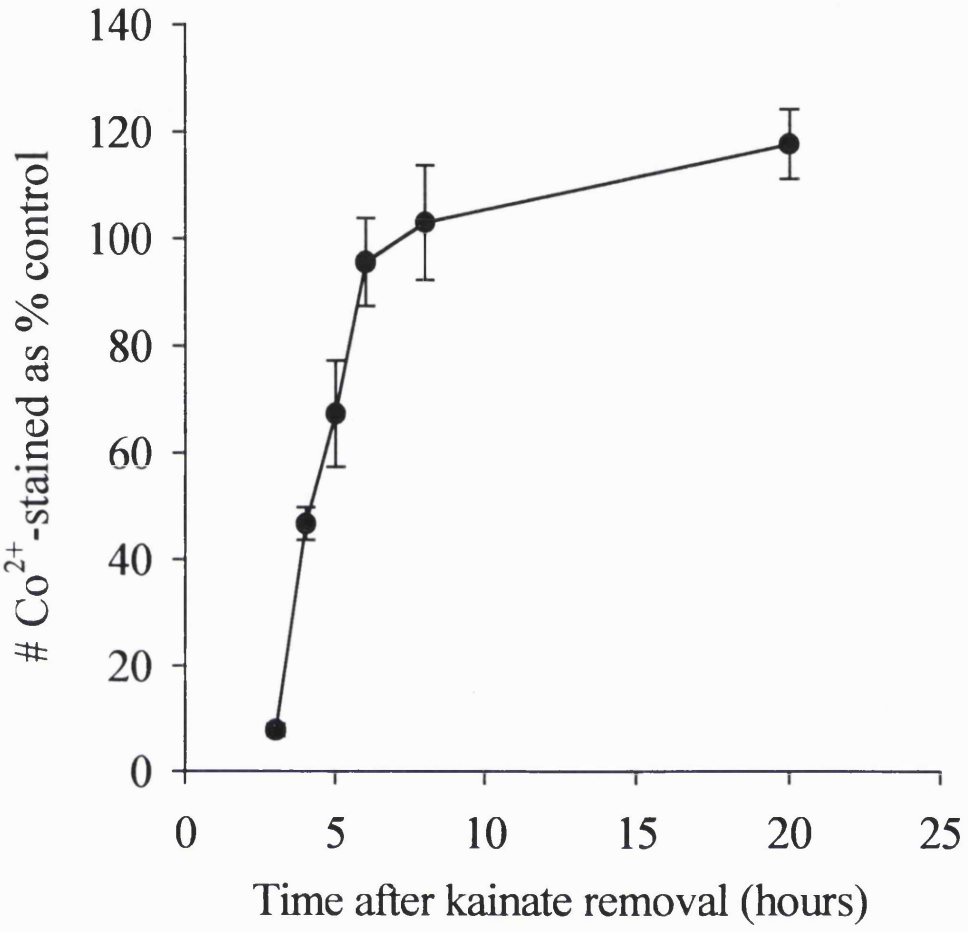

Figure 4.15

Time course of the reversal of the effects of exposure to kainate.

Kainate (500μM) was removed from the culture medium of dissociated retinal cells after 6 days exposure to the drug and within 6 hours the fraction of cells stained with Co^{2+} had increased to control levels. Counts were made from 6 fields in 2 dishes at each time point with a mean of 264.8±3.6 cells per field.

4.3.12 The effects of EGTA on the reduction in Ca^{2+}-influx produced by chronic activation of AMPA/kainate receptors

To investigate whether Ca^{2+}-entry was involved in triggering the reduction in Ca^{2+}-influx seen with chronic stimulation of AMPA/kainate receptors the following experiments were performed. Cells were grown in the presence of 500μM kainate from 1 DIV. After 6 DIV the kainate-containing culture medium was supplemented with the Ca^{2+} chelator EGTA (1mM) for a period of 8 hours before the cells were Co^{2+}-stained. Addition of EGTA to cells treated with kainate increased the fraction of cells that were Co^{2+}-positive when compared to cells grown in kainate that had not seen EGTA (significant at the 0.1% level) (figure 4.16). Control cultures were exposed to EGTA in the same way and this had no significant effects on the fraction of cells that stained with Co^{2+}. These data indicate that Ca^{2+}-influx may be involved in the mechanism by which chronic activation of AMPA/kainate receptors reduces Ca^{2+}-entry via these receptors in the long-term.

4.3.13 Whole-cell patch-clamp studies of kainate-evoked currents

Dissociated retinal cells were whole-cell patch-clamped as described in chapter 2. When 100μM kainate was bath applied to retinal cells it evoked membrane currents in all retinal neurons patched after 3 DIV (n=57) (17.9±4.3pA/pF in control cultures) (top trace figure 4.17). These figures exclude recordings from cones, glial cells and neurons prior to 3 DIV that were unresponsive to kainate.

It seemed possible that cell survival in kainate simply resulted from a reduction in the expression of the AMPA/kainate receptor or alternatively from receptor desensitization that reduced the current through the channel. To

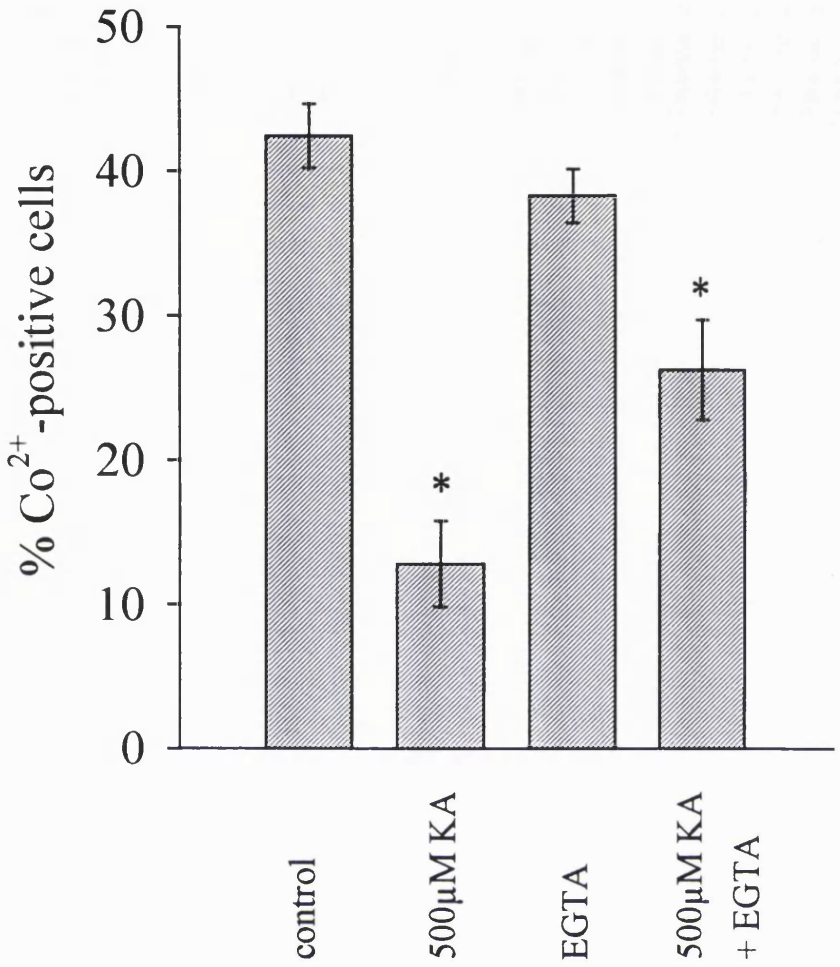

Figure 4.16

EGTA partially rescues retinal cells from the effects of chronic kainate treatment.

Cells were grown in the presence of 500µM kainate from 1 DIV. After 6 DIV the culture medium was further supplemented with 1mM EGTA for 8 hours before the cells were Co^{2+} stained. EGTA treatment increased the fraction of Co^{2+}-positive cells in these cultures compared to cultures that had been grown in kainate but had not been exposed to EGTA (*, $p \leq 0.001$). In control dishes exposed to 1mM EGTA for 8 hours the fraction of Co^{2+}-positive cells was not significantly different to controls that had not seen EGTA. Counts were made from 12 fields in 4 dishes with a mean of 291.6±10 cells per field

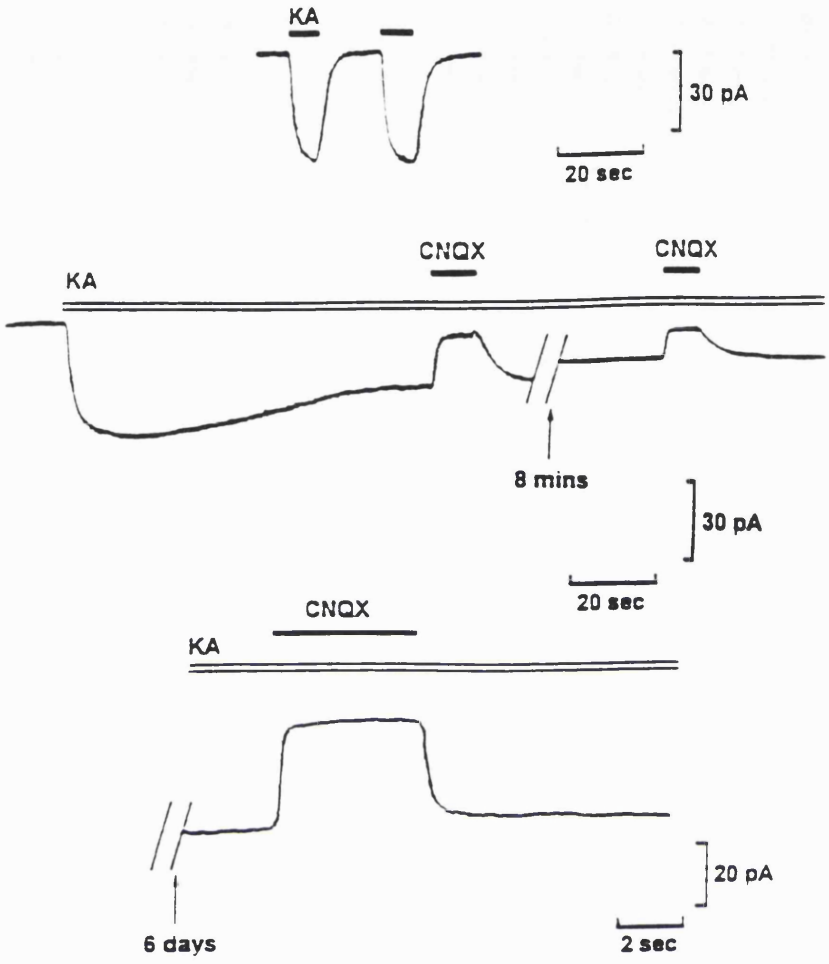

Figure 4.17

Whole-cell patch-clamp recordings from chick retinal cells.

Top trace: 100μM kainate evokes a current in chick retinal cells at 3 DIV (17.9±4.3pA/pF) (n=57). Middle trace: The current evoked by a long application of 100μM kainate in a control culture after 6 DIV from a holding potential of -60mV. The current is reduced to about 20% of its original size reaching steady-state in about 10 minutes (n=8). Bottom trace: Cells were maintained in the presence of 500μM kainate for 6 days and patch clamped in the same concentration of the drug. Cells continued to exhibit a current which was suppressed by application of 20μM CNQX. However, the current was reduced by about 78% by comparison to controls (4.01±1.03pA/pF) (n=10).

investigate this, cells that had been exposed to 500μM kainate since 1 DIV were whole-cell patch clamped after 6 days in the drug. The same concentration of kainate was added to all extracellular solutions, ensuring that cells were continually exposed to kainate after removal of the culture medium. Bath application of the non-NMDA receptor antagonist CNQX (20μM) during whole-cell recording suppressed an inward current with a mean magnitude of 4.01±1.03pA/pF (n=10) (bottom trace figure 4.17). Thus the cells continued to exhibit a current that could be suppressed by CNQX, however from a sample of 10 cells the current per pF was reduced by approximately 78% by comparison to controls (see above). This suggests that a significant fraction of the reduction in Co^{2+}-staining may be due to a reduction in the current evoked by the agonist. Long application of kainate to cells in control cultures (figure 4.17, middle trace) also showed a reduction in the kainate-evoked current which fell to about 20% of its original size over a period of 10 minutes, suggesting the reduction in current seen in cells grown in the presence of kainate may occur with a rapid time course. These results appear to suggest that kainate may exert its effects on Co^{2+}-staining through some form of long-term desensitization. The relationship between the current through the AMPA/kainate receptor and Co^{2+}-staining is considered in the discussion.

4.3.14 The involvement of phosphorylation in the effects of prolonged activation of AMPA/kainate receptors

It has been reported that phosphorylation involving protein kinase A (PKA) increases the open probability of the AMPA/kainate receptor channel which may lead to an increased Ca^{2+}-influx (Greengard et al., 1991, Keller et al., 1992). To investigate whether the decrease in Co^{2+}-staining produced by chronic activation of AMPA/kainate receptors was due to dephosphorylation of the receptor the following experiments were carried out. 8-bromo-cAMP

(100μM) was added to the culture medium of cells grown in the presence of 500μM kainate for 5 days. The cultures were Co^{2+}-stained after either 6 or 24 hours exposure to the drug. 8-Bromo-cAMP is a membrane permeant analogue of cAMP that activates PKA. Application of 8-bromo-cAMP to control retinal cultures after 6 DIV produced an increase in the fraction of cells that stained with Co^{2+} that was significant at the 0.1 and 2% level for the 6 and 24 hour treatment respectively (figure 4.18). In cultures grown in kainate from early times, 24 hour treatment with 8-bromo-cAMP increased the fraction of Co^{2+}-positive cells compared to controls (significant at the 0.2% level) whilst the 6 hour treatment had no significant effect (figure 4.18). Although exposure to 8-bromo-cAMP for 24 hours increased the number of cells stained by Co^{2+} in cultures that contained kainate, the number of stained cells remained significantly lower than in control cultures, suggesting that phosphorylation alone cannot explain the effects of kainate on Ca^{2+}-entry.

4.4 Discussion

4.4.1 Embryonic chick retinal cells express AMPA/kainate receptors that permit significant Ca^{2+}-entry

The Co^{2+}-staining technique developed by Pruss et al. (1991) was used to show that embryonic chick retinal cells, both in explant cultures and in dissociated cultures, express AMPA/kainate receptors that allow a significant Ca^{2+}-influx. Retinal explants taken from E6 chicks continue to develop under the culture conditions used and over a period of days differentiate to acquire a characteristic laminated morphology reminiscent of that seen *in vivo*. After 6 days in culture E6 retinal explants appear structurally similar to the E12 chick retina *in vivo* (Catsicas et al., 1995). The Co^{2+}-staining technique shows Ca^{2+}-permeable receptors to be present in large numbers in the inner part of the INL

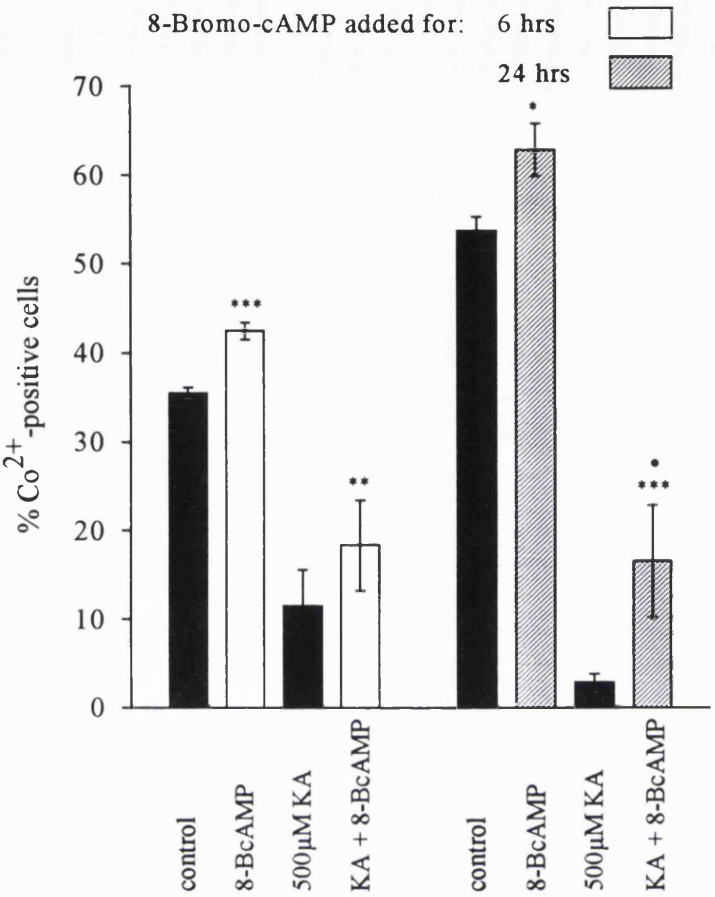

Figure 4.18

The effects of phosphorylation by PKA on Co^{2+}-staining in retinal cells. Application of 8-bromo-cAMP (100µM) to 6 day old cultures for 6 and 24 hours significantly increased the fraction of cells that stained with Co^{2+} compared to controls (***, $p<0.001$; *, $p<0.02$). Cells grown in 500µM kainate for 5 days were exposed to 8-bromo-cAMP for 6 or 24 hours. Kainate reduced the fraction of cells that stained with Co^{2+} and after treatment with 8-bromo-cAMP the reduction remained significant compared to control cultures (**, $p<0.01$; ***, $p\leq0.001$). The 24 hour treatment with 8-bromo-cAMP significantly increased the number of cells staining with Co^{2+} in comparison to kainate treated control cultures (•, $p<0.002$).

of the explants (section 4.3.1). The position and size of the Co^{2+}-stained cells in the INL suggests that the labelled population contains both amacrine and bipolar cells. The band of Co^{2+} -labelled cells found in the outer part of the INL in explants may represent horizontal cells. Occasional staining was seen in the GCL, however few cells survive in the GCL of retinal explants under the culture condition used.

Dissociated retinal cultures taken from day 8 embryos contained a large population of cells that stained with Co^{2+} with between 35-50% of cells expressing Ca^{2+}-permeable AMPA/kainate receptors by 5 DIV (section 4.3.4). The number of Co^{2+}-positive cells rose as a function of time in culture reaching a peak at 5 DIV before declining (section 4.3.11). The rise and fall in the number of stained cells is similar to that seen in the *in vivo* chick retina, where the number of Co^{2+}-positive cells peaks around E12 and declines by E19 (M. Catsicas, personal communication). During this period naturally-occurring cell death causes many cells in the chick retina to die (see section 1.6) and this may explain the reduction in stained cells.

Cells in dissociated cultures are mainly cone photoreceptors, Müller cells and amacrine cells (see chapter 3). Cone photoreceptors and Müller cells do not label with Co^{2+}, suggesting that these cells do not express Ca^{2+}-permeable AMPA/kainate receptors. Double-labelling with the Co^{2+}-staining technique and immunostaining with HPC-1 (an amacrine marker) revealed that over half of the amacrine population were also Co^{2+}-positive (section 4.3.5). This suggests that a large fraction of amacrine cells in culture express AMPA/kainate receptors that allow significant Ca^{2+}-entry. A population of cells that labelled with Co^{2+} did not label for HPC-1 and remain unidentified, however it is possible that these cells represent horizontal or bipolar cells.

In their original paper Pruss et al. (1991) do not establish the quantitative relationship between Co^{2+}-labelling and AMPA/kainate receptor expression. It is possible that a tiny amount of Co^{2+}-entry perhaps through a single receptor channel is sufficient for staining to occur, or alternatively a large quantity of Co^{2+} may have to enter through many hundreds of channels before labelling is seen. From the data shown in this chapter Co^{2+}-staining is clearly an all or none event and labelling never appears to be graded. This suggests that there is a threshold level of Co^{2+} which once exceeded leads to staining of the cells. Thus it seems an attractive hypothesis that the technique labels cells whose expression of Co^{2+}-permeable AMPA/kainate receptors lies above a certain minimum level, although it is possible that glutamate and its analogues have an all or none effect on the ability of Co^{2+} to enter cells.

The results of Ca^{2+} imaging studies (see chapter 6) confirm that Ca^{2+}-permeable AMPA/kainate receptors are present in embryonic chick retina from day 6. Electrophysiological studies have shown that these receptors are present in retinal ganglion cells in postnatal rats (Rorig and Grantyn, 1993) and horizontal cells in the catfish retina (O'Dell and Christensen, 1989). Unfortunately antibodies directed against AMPA/kainate receptor subunits that could identify the Ca^{2+}-permeable form of the receptor in the chick retina are not yet available. However *in situ* hybridization studies of the developing rat brain show a change in the ratio of GLUR1, 2 and 3 gene expression from the postnatal to adult animal (Pellegrini-Giampietro et al., 1992). They suggest that the increased labelling of GLUR2 mRNA, the subunit that confers low Ca^{2+}-permeability (Hollmann et al., 1991), later in development reflects a decrease in the Ca^{2+}-permeability of AMPA/kainate receptors in the adult rat brain. This indicates a specific role for the Ca^{2+}-permeable form of the receptor in development. Ca^{2+}-permeable AMPA/kainate receptors may have important influences on cytoplasmic Ca^{2+} during development, particularly

before the onset of the depolarizing electrical activity required to relieve the Mg^{2+} block of NMDA receptors that enables the passage of Ca^{2+} ions (Mayer et al., 1984).

4.4.2 Activation of non-NMDA receptors late in retinal development causes cell death

It is well established that excessive activation of excitatory amino acid receptors can initiate a cascade of intracellular biochemical events that ultimately leads to cell death (Olney et al., 1973, Choi, 1988). The non-NMDA receptor agonist kainate is reported to have neurotoxic properties in the adult and embryonic chick retina subsequent to E10 (Schwarcz and Coyle, 1977, Ehrlich and Morgan, 1980, Ingham and Morgan, 1983, Catsicas and Clarke, 1987). Consistent with this, when E6 retinal explants were exposed to 100μM kainate for 24 hours after 6 days in culture they showed extensive cell loss in the INL and GCL (section 4.3.2). The effects of kainate on cell survival were quantified in two ways using dissociated retinal cultures made from E8 chick retinae. Firstly, the total number of cells present in 6 day old cultures after acute AMPA/kainate receptor activation were counted (section 4.3.6). These experiments showed that the number of cells in the kainate-treated cultures were greatly reduced. It is possible that this reduction in number was due to a loss of adhesion, cells leaving the bottom of the dish to become suspended in the culture medium. However, careful inspection of the culture fluid failed to reveal any floating cells and experiments with propidium iodide, which gives a "snapshot" of cell death, showed that the kainate-treated cultures contained large numbers of cells that had lost their membrane integrity. It appears that dead cells in retinal cultures are rapidly phagocytosed, although it is also possible that some are washed from the culture dish during changes of the culture medium.

The cell death observed on acute exposure of 6 day old cultures to kainate is consistent with previous studies that report the neurotoxic effects of this glutamate analogue during late embryonic retinal development. The mechanism by which kainate leads to excitotoxic death in cultures of dissociated retinal neurons has not been investigated in this chapter. Kainate may exert its neurotoxic actions by depolarization-evoked opening of voltage-gated Ca^{2+} channels. However, blocking voltage-gated Ca^{2+} channels is usually insufficient to prevent cell death whether the NMDA or AMPA/kainate receptor is activated (Choi, 1987, Murphy and Miller, 1989, Brorson et al., 1994). Since both NMDA and non-NMDA receptors are present in many retinal cells, kainate could either exert its neurotoxic action directly (Seil et al., 1974, Bird and Gulley, 1979) or through the membrane depolarization-evoked release of glutamate that then acts at NMDA receptors (Balázs et al., 1990, Sucher et al., 1991). In cultures of rat retinal ganglion cells stimulation of AMPA/kainate receptors is only neurotoxic because it leads to the release of glutamate which activates NMDA receptors (Sucher et al., 1991). However studies of cerebellar Purkinje cells have shown that Ca^{2+}-entry through the AMPA/kainate receptor can cause excitotoxic cell death (Brorson et al., 1994), and in isolated chick retina excitotoxic neuronal death can be triggered by the activation of either NMDA or non-NMDA receptors (Romano et al., 1995). It has also been reported that kainate can interact directly with NMDA receptors to produce cell death. Michaels and Rothman (1990) demonstrate that cell death can be evoked in cultured hippocampal neurons by application of high concentrations of kainate (1mM) and that this effect could be blocked by the NMDA receptor antagonist MK-801. Cell death was not due to the release of endogenous glutamate because high concentrations of K^+ had no effect on cell survival. Thus kainate neurotoxicity in this system appears to be due to the non-specific activation of NMDA channels by kainate. This possibility is supported by single channel

recordings that show kainate can activate conductances similar to that of NMDA but with lower probability (Cull-Candy and Usowicz, 1987, Jahr and Stevens, 1987). However it seems unlikely that kainate produces cell death via NMDA receptor activation in dissociated retinal cultures because patch-clamp experiments (see section 4.3.13) show that the kainate-evoked currents in retinal cells are abolished by the non-NMDA receptor antagonist CNQX and because AP5 is ineffective in preventing cell death.

The neurotoxic effects of glutamate and its analogues are generally thought to involve an increase in $[Ca^{2+}]_i$ which then triggers cell death (Rothman, 1983, 1984). Tymianski et al. (1993) have shown that cell-permeant Ca^{2+}-chelators such as BAPTA-AM can reduce excitotoxic neuronal injury produced by over-activation of glutamate receptors. Cultures of dissociated retinal cells become susceptible to kainate neurotoxicity at a time when there is a high level of expression of Ca^{2+}-permeable non-NMDA receptors (section 4.3.11). It is likely that the influx of Ca^{2+} through the AMPA/kainate receptor contributes to, or is directly responsible for, triggering the neurotoxic effects of kainate in culture. This may explain the survival of retinal neurons in kainate early on when the level of expression of AMPA/kainate receptors with a high Ca^{2+}-permeability is low. Prolonged treatment with kainate in the presence of CNQX protects the cells from the reduction in Co^{2+}-staining seen in kainate (section 4.3.8). Subsequent treatment of these cultures with kainate alone produced widespread cell death similar to that seen in cultures late in development that had not previously been exposed to kainate (section 4.3.9). These data indicate that the presence of AMPA/kainate receptors that permit significant Ca^{2+}-influx correlates with susceptibility to excitotoxic cell death produced by AMPA/kainate receptor activation late in development. That Ca^{2+}-entry through the AMPA/kainate receptor can be responsible for the neurotoxic effects of glutamate and its

analogues is supported by recent studies on cultures of cortical neurons and Purkinje cells (Yin et al., 1994, Brorson et al., 1994).

4.4.3 Retinal cells survive activation of AMPA/kainate receptors early in development

Explants from E6 chick retina survived chronic activation of their AMPA/kainate receptors when they were grown in high concentrations of kainate from the time of explantation for up to 6 days in culture (section 4.3.2). The explants grown in kainate were structurally similar to controls and showed no signs of cell loss or damage. Indeed the subjective impression was that the structure of the explants cultured in kainate appeared nearer to that of the retina *in vivo*. Cell counts using dissociated cultures chronically treated with high concentrations of kainate showed no reduction in cell number compared to controls and staining with propidium iodide demonstrates that the cells retain their membrane integrity.

These data show that embryonic retinal cells can survive chronic activation of AMPA/kainate receptors early in development. In contrast cells drawn from the same retina are killed by acute activation of these receptors a few days later in development. Thus late in development a switch in the actions of glutamate and its analogue kainate occurs, and retinal neurons acquire an increased sensitivity to AMPA/kainate receptor activation that continues into adult life. A similar phenomenon is seen in the immature rat brain where there is a period of enhanced NMDA receptor sensitivity which peaks at postnatal day 7 (McDonald et al., 1988, Ikonomidou et al., 1989). At this developmental stage kainate produces little neurotoxicity (Campochiaro and Coyle, 1978), however in the adult rat brain kainate and AMPA are potent neurotoxins and sensitivity to NMDA is reduced (Olney, 1978). The

mechanisms underlying the developmental changes in NMDA toxicity are unclear. They are thought to result from a combination of changes in the expression of the receptor (Watanabe et al., 1992, Williams et al., 1993, Monyer et al., 1991), changes in the voltage-dependence of the Mg^{2+} block of the channel (Ben-Ari et al., 1988) or possibly the regulation of events occurring after NMDA receptor activation such as second messenger production and the activation of enzyme pathways.

Ca^{2+} imaging studies show changes in $[Ca^{2+}]_i$ in response to kainate in chick retina from E6 (see chapter 6). These experiments were carried out in the presence of blockers for NMDA receptors and voltage-gated Ca^{2+} channels and demonstrate the presence of Ca^{2+}-permeable AMPA/kainate receptors early in development. Thus the survival of retinal neurons exposed to kainate early on does not simply result from the absence of AMPA/kainate-gated receptors. Instead their survival may be explained by differences in the properties of the receptor at early times and/or because fewer receptors are present on the cell surface. Alternatively, the increased susceptibility to kainate late in development and in the adult retina may be due to a change in intracellular Ca^{2+}-buffering or other Ca^{2+}-mediated events downstream of Ca^{2+}-entry. Excess Ca^{2+}-influx can trigger a number of biochemical events that include the activation of several enzymes such as lipases, endonucleases, calpain 1, nitric oxide synthase and protein kinase C that can either damage cells directly or through the generation of free radicals (reviewed by Meldrum and Garthwaite, 1990). The survival of retinal cells in glutamate and kainate early on could reflect differences in one or several of these enzyme pathways, their absence, or differences in their sensitivity to Ca^{2+} early in development.

4.4.4 Cell survival during sustained AMPA/kainate receptor activation correlates with a reduction in Co^{2+}-staining

In both retinal explants and dissociated retinal cultures cell survival in glutamate and kainate correlated with a reduction in the fraction of cells stained with Co^{2+}. In retinal explants chronic activation of AMPA/kainate receptors at E6 completely abolished the Co^{2+}-staining usually seen after several days in culture, without any apparent alteration in overall cell number (section 4.3.3). In dissociated cultures of retinal cells stimulation of AMPA/kainate receptors with glutamate or kainate from 1 DIV reduced the fraction of Co^{2+}-positive cells seen later on (section 4.3.7). The reduction in Co^{2+}-staining produced by prolonged stimulation of AMPA/kainate receptors early in development reflects a reduction in the Ca^{2+}-influx into cells via these receptors. If Ca^{2+}-entry via AMPA/kainate receptors is the cause of excitotoxic death in retinal cells, it suggests that sustained activation of AMPA/kainate receptors early in development is neuroprotective because it reduces the Ca^{2+}-influx through them at later times thus sparing the cells.

The effects of kainate on Ca^{2+}-influx are rapid and reversible. Kainate begins to exert its effect on Ca^{2+}-influx within an hour of its application and the fraction of Co^{2+}-positive cells in cultures is subsequently reduced at all times compared to controls (section 4.3.11). The effects of kainate are reversible, the fraction that stain with Co^{2+} returning to control levels within hours of kainate's removal.

4.4.5 The effects of prolonged activation of AMPA/kainate receptors on Co^{2+}-staining are blocked by CNQX

The non-NMDA receptor antagonist CNQX blocked the effects of

chronic activation of AMPA/kainate receptors early in retinal development. This suggests that the initial effects of exposure to kainate on Ca^{2+}-influx are via an action at non-NMDA receptors. Kainate could either be acting at AMPA/kainate receptors or kainate-preferring receptors. However, studies on homomeric kainate receptors show that they have affinities for kainate in the nM to low μM range (Egeburg et al., 1991) whereas AMPA/kainate receptors have a much lower affinity (e.g. EC_{50} for kainate at GLUR1 is 35μM) (Hollmann et al., 1989). Since more than 10μM kainate is required to suppress Co^{2+}-staining this effect is likely to be due to an action at AMPA/kainate receptors rather than kainate-preferring receptors.

4.4.6 The pharmacology of the kainate-evoked reduction in Ca^{2+}-influx

The endogenous activator of AMPA/kainate receptors is glutamate. The effects of kainate on Ca^{2+}-influx through AMPA/kainate receptors was mimicked by prolonged exposure to glutamate (section 4.3.10). The reduction in Co^{2+}-staining was prevented by addition of the non-NMDA receptor antagonist CNQX but not the NMDA receptor antagonist AP5. This suggests glutamate mediates these effects via a non-NMDA receptor, as does kainate. These data indicate that endogenous glutamate may be able to alter the Ca^{2+}-permeability of AMPA/kainate receptors during early development of the retina and that exposure to glutamate early on is neuroprotective, sparing cells that see glutamate later on in development from excitotoxic death. Glutamate and AMPA, unlike kainate, usually evoke currents at AMPA/kainate receptors that rapidly desensitize leading to a reduction in current flow through the open channel (Hamill et al., 1981). However, patch-clamp studies of dissociated retinal neurons (chapter 3) show that glutamate and AMPA evoke large currents that persist in the presence of the agonist. The persistence of the current in glutamate may in part be due to activation of NMDA receptors at

which glutamate produces long-lasting currents (Lester et al., 1990, Lester and Jahr, 1992, Lester et al., 1993). That AMPA should produce persistent membrane currents is unexpected since in most CNS tissues it evokes currents that rapidly and completely desensitize (Trussell and Fischbach, 1989, Jonas and Sakmann, 1992, Colquhoun et al., 1992). This failure of the AMPA/kainate receptor in embryonic chick retina to desensitize may explain why it is that glutamate can mimic the effects of kainate in producing a reduction in Co^{2+}-staining.

Kainate was used in most of the experiments in this chapter because it is not taken up by the glutamate uptake carrier (Brew and Attwell, 1987) shown here to be present in chick retinal Müller cells, thus its concentration is more easily controlled than that of glutamate. However, the Müller cell glutamate uptake carrier is inhibited by kainate (Johnston et al., 1979, Robinson et al., 1991, 1993, Arriza, 1994) and this may in turn lead to an increase in the levels of glutamate in the cultures if it were released in response to the kainate-evoked depolarization. Thus it is possible that the effects of kainate may be enhanced through an increase in the concentration of glutamate in the culture medium that results from kainate application. This may in part explain why the reduction in Co^{2+}-staining produced by 100μM glutamate was not as great as the reduction seen in the same concentration of kainate.

4.4.7 Are the effects produced by AMPA/kainate receptor activation secondary to membrane depolarization?

Activation of AMPA/kainate receptors with kainate will lead to membrane depolarization, Ca^{2+}-influx via voltage-gated Ca^{2+} channels and the release of glutamate and other transmitters. While CNQX blocks the effects

of kainate (section 4.3.8) this does not prove that kainate produces its action directly, rather the effects on Co^{2+}-staining may be secondary to membrane depolarization. However, the NMDA receptor antagonist AP5 was unable to block the effects of kainate and the metabotropic glutamate receptor agonist *trans*-ACPD did not mimic the effects of kainate on Ca^{2+}-influx (section 4.3.10). This indicates that depolarization-evoked glutamate release and the subsequent activation of NMDA or metabotropic receptors are not involved in the actions of kainate.

Two lines of evidence suggest that the depolarization-evoked release of transmitters other than glutamate is not involved. Firstly, GABA cannot produce the effects of kainate and yet is known to depolarize retinal cells at this stage of development (Yamashita and Fukada, 1993a and see Chapter 6). Unfortunately attempts to examine the effects of membrane depolarization by growing cells in high $[K^+]_e$ were unsuccessful because the solutions employed killed the cells. Secondly, the effects of kainate persist in the presence of the Ca^{2+} channel blockers, diltiazem and nifedipine. In patch-clamp experiments these compounds blocked 90% of the Ca^{2+} current in retinal neurons (see chapter 3). The Ca^{2+}-evoked release of transmitters in cultures treated with these agents should be greatly decreased, however the fact that they have no effect on the kainate-evoked reduction in Co^{2+}-staining observed argues strongly against the effects being mediated via Ca^{2+}-dependent release of other transmitters. These experiments would also seem to rule out the possibility that the depolarization-evoked increase in $[Ca^{2+}]_i$ via voltage-gated Ca^{2+} channels is itself responsible for the reduction in Co^{2+} entry via the AMPA/kainate receptor. The most likely explanation for the effect would seem to involve Ca^{2+}-entry through the AMPA/kainate receptor itself.

4.4.8 $[Ca^{2+}]_i$ and other mechanisms for the down-regulation of Ca^{2+}-entry via AMPA/kainate receptors

$[Ca^{2+}]_i$ triggers many of the diverse effects of glutamate in different systems (Komuro and Rakic, 1993, Hartley et al., 1993, Rashid and Cambray-Deakin, 1992, Pearce et al., 1987). The initial Ca^{2+}-influx produced by AMPA/kainate receptor activation, either directly through the receptor itself or indirectly through voltage-gated Ca^{2+} channels, could be involved in triggering the long-term down-regulation of Ca^{2+}-entry through the receptor. However, Ca^{2+}-entry through voltage-gated Ca^{2+} channels does not seem to be required for the effects of kainate (see above).

There are two mechanisms by which kainate could bring about the reduction in the Ca^{2+}-entry into retinal cells monitored here using the Co^{2+}-staining technique. It could reduce the Ca^{2+}-permeability of individual receptors without affecting the total current through them, or it could reduce the total current through the receptor population without affecting their permeability. It is also possible that a reduction in current is accompanied by a reduction in the Ca^{2+}-permeability of the receptor. A reduction in current through the receptor could be brought about either by a change in the single channel current, receptor number or open probability. The experiments described in this thesis do not distinguish between these possibilities.

The patch-clamp experiments described in section 4.3.13 show that a CNQX-suppressible current is present in cells treated with kainate for 6 days. This current is considerably smaller than that evoked by kainate in cells in control cultures. However, the sample is small and the variation in the magnitude of the current is large. The current evoked in response to long-application of kainate to cells in control cultures also showed significant

reduction in magnitude with time. However, such reduction could result from a failure of the patch-pipette to control $[Na^+]_i$ and $[K^+]_i$ in the face of the flux produced by kainate. It is also possible that the run-down observed is pathological and results from the "wash-out" of some component of the intracellular milieu by the patch-pipette solution. The reduction in the kainate-evokable current is consistent with either a reduced receptor number or open time. Other studies that show that kainate produces a non-desensitizing current at AMPA/kainate receptors have involved only short (2-5 seconds) application of the agonist (Hamill et al., 1981, Keinänen et al., 1990). Experiments to determine whether the Ca^{2+}-permeability of individual receptors were changed by prolonged exposure to kainate were not carried out (see section 4.4.10).

Application of the Ca^{2+} chelator EGTA led to partial restoration of the normal level of Co^{2+}-staining when it was applied to cells grown in kainate for 6 days. This result suggests that the maintenance of the effects of kainate require a continued influx of Ca^{2+}, perhaps through the residual Ca^{2+}-permeability of the AMPA/kainate receptor or voltage-gated channels. Unfortunately it was not possible to examine the effects of concentrations of EGTA higher than 1mM in the culture medium because they led to failure of the cultures. Attempts were made to buffer $[Ca^{2+}]_i$ with BAPTA-AM from early times, however these too led to failure of the cultures or greatly retarded growth rates.

There is some evidence that the open probability of AMPA/kainate receptor channels can be modulated by phosphorylation (Knapp and Dowling, 1987, Linman et al., 1989, Greengard et al., 1991). The cAMP-dependent second messenger protein kinase A (PKA) is strongly implicated in these effects (Greengard et al., 1991, Keller et al., 1992). It is possible the

reduction in Ca^{2+}-influx that results from AMPA/kainate receptor activation may occur via a dephosphorylation that decreases channel open time, so reducing Ca^{2+}-influx. The PKA activator 8-bromo-cAMP significantly increased the number of cells stained with Co^{2+} both in control cultures and those that received chronic treatment with kainate. However, 8-bromo-cAMP did not return Co^{2+}-staining to control levels in the kainate treated cultures. The results obtained are consistent with phosphorylation producing an increase in the open probability of AMPA/kainate receptors.

Changes in receptor subunit composition could also be responsible for the reduction in Co^{2+}-staining produced by kainate. The activation of AMPA/kainate receptors early in development could either lead to a change in receptor subunit composition that alters the Ca^{2+}-permeability of the channel, or alternatively to an overall reduction in receptor expression. As discussed above, the patch-clamp experiments described in section 4.3.13 suggest that a reduction in AMPA/kainate receptor expression may occur in cells grown in kainate. However these experiments do not rule out a simultaneous reduction in the Ca^{2+}-permeability of the receptor. The Ca^{2+}-permeability of AMPA/kainate receptors depends on their subunit composition, GLUR1-4 (reviewed by Seeburg, 1993). GLUR1, 3 and 4 form Ca^{2+}-permeable receptor channels while GLUR2 alone or in combination with other subunits forms receptors with a much lower Ca^{2+}-permeability (Hollmann et al., 1991). Ca^{2+}-permeability is determined by a single amino acid residue at the Q/R site in TM II (Hume et al., 1991, Burnashev et al., 1992b). In GLUR2 an arginine (R) is present at this site, conferring low Ca^{2+}-permeability, while in GLUR1, 3 and 4 a glutamine (Q) is found at the Q/R site facilitating high Ca^{2+}-permeability. Interestingly, the GLUR2 gene does not carry the arginine codon at this site and it is only present after modification by RNA editing (Sommer et al., 1991). This means that inclusion of GLUR2 in the receptor

complex confers low Ca^{2+}-permeability if the Q/R site has undergone RNA editing. The fractional contribution of Ca^{2+} current through AMPA/kainate receptors has been estimated to be about 6 times greater through channels that are unedited at the Q/R site (Burnashev et al., 1995). It is possible that prolonged stimulation of AMPA/kainate receptors early in retinal development alters the subunit composition of the receptor, so reducing its Ca^{2+}-permeability. This may be achieved by a reduction in the expression of the edited form of GLUR2. However, in the absence of suitable oligonucleotide probes for glutamate receptor subunits in the chick retina this hypothesis cannot be investigated.

4.4.9 The functional implications of AMPA/kainate receptor activation during development

The results described in this chapter raise the possibility that exposure to glutamate early in development may alter the effects of exposure to this transmitter at later times. The extent to which glutamate is released by developing retinal neurons is unknown. However, a pool of glutamate is present within rabbit retinal neurons prior to synaptogenesis (Redburn et al., 1992) and within the optic and frontal lobes of the chick brain glutamate levels within the extracellular space are between 0.2-0.4μM throughout embryogenesis (Huether and Lajtha, 1991). As yet no-one has measured the concentration of transmitters in the extracellular space of the retina during development. Since the blood-brain-barrier in the chick does not develop until E12 (Kniesel and Wolburg, 1993) it is likely that the retina is exposed to the glutamate levels found in the plasma and it is possible that exocytosis from neurons or release by reversed uptake causes local increases in this concentration.

Acetylcholine (ACh) receptors are found at the motor end-plate prior to its innervation and nerves growing to the putative end-plate release ACh (Cohen et al., 1979, Frank and Fischbach, 1979, Young and Poo, 1983, Hume et al., 1983). This has led Haydon and Drapeau (1995) to propose a 'ready, set, go' model for synaptogenesis at the neuromuscular junction. The presence of ACh receptors and release machinery early on means that neurons are 'ready' to form connections and are 'set' to function when they come into contact with other neurons. Connection with other motoneurons causes a redistribution of postsynaptic ACh receptors so that they become positioned to optimally detect transmitter release in the synaptic cleft (reviewed by Hall and Sanes, 1993). Finally Haydon and Drapeau propose that neurons that release neurotransmitters before interaction with a target are those that form functional synapses, which are then modified by activity-dependent mechanisms.

It is possible that a similar model can be applied to development of glutamatergic synapses in the chick retina, with significant release of transmitter occurring prior to synapse formation. The down-regulation of Ca^{2+}-entry into immature neurons via AMPA/kainate receptors in response to this may play an important role in sparing cells from cell death during the pruning of cells that have failed to establish synaptic contacts that occurs later in development. Precocious release of transmitter may also be an important factor in determining the glutamate receptor subtypes that are expressed at mature synapses.

4.4.10 Suggestions for future experiments

Several important experiments remain to be carried out to clarify the nature of the changes brought about by extracellular glutamate during

development. Experiments to determine whether the Ca^{2+}-permeability of individual receptors is changed by prolonged exposure to glutamate and its analogues are necessary. Measurements of the changes in Ca^{2+}-permeability produced by these agents could be achieved by patch-clamping retinal cells grown in the presence or absence of kainate using bi-ionic conditions (Iino et al., 1990). In bi-ionic experiments the change in the reversal potential of the kainate-evoked current is measured when the external solution is changed from one containing only Na^{+} and an impermeant anion to one containing only Ca^{2+} and the same impermeant anion. This gives the Ca^{2+}- and Na^{+}-permeability relative to that of the Cs^{2+} ions used in the patch-pipette solution. It would be useful to determine the mechanism by which any change in Ca^{2+}-permeability revealed by such experiments is brought about. Experiments to investigate whether glutamate alters the subunit composition of AMPA/kainate receptors would be advantageous, however as yet there are no antibodies available that can distinguish between GLUR2 and GLUR3. Oligonucleotide probes are also unavailable.

It would be interesting to establish whether the cell death that normally occurs during late retinal development is in any way affected by glutamate receptor antagonists. CNQX could be injected into the eyes of chick embryo's prior to the period of naturally-occurring cell death and the effects of this on cell loss quantified. Similar experiments could be carried out to determine the effects of glutamate on the morphology of cells in the intact retina.

Chapter 5

The effects of glutamate analogues on neurite extension in embryonic chick retinal cells

5.1 Introduction

Neurotransmitters are known to act as regulatory signals in neuronal development, controlling processes such as neurite outgrowth (Pearce et al., 1987) and neurite extension (Brewer and Cotman, 1989). The excitatory neurotransmitter glutamate can affect neuronal outgrowth via its influence on $[Ca^{2+}]_i$. It can alter $[Ca^{2+}]_i$ via three routes. Firstly, it may change the membrane voltage and so influence Ca^{2+}-influx through voltage-gated channels. Secondly, glutamate may activate metabotropic receptors leading to the release of Ca^{2+} from internal stores. Finally some glutamate receptors themselves are permeable to Ca^{2+} such as the NMDA receptor (MacDermott et al., 1986, Ascher and Nowak, 1988) and the AMPA/kainate receptor (see Chapter 4 and Murphy and Miller, 1989, Gilbertson et al., 1991). This chapter examines the effects on neurite outgrowth of activating non-NMDA glutamate receptors in embryonic chick retinal cells during their early development. In the majority of these experiments the glutamate analogue kainate was employed in preference to glutamate because it is not taken up by the glutamate uptake carrier present in retinal Müller cells (Attwell et al., 1987) and it does not appear to be degraded under the circumstances used to culture retinal cells. The results presented in this chapter show:

1. Prolonged exposure to glutamate but not GABA leads to a reduction in neurite outgrowth.
2. The effects of glutamate may be mimicked by kainate and AMPA, but not

by the metabotropic receptor agonist *trans*-ACPD.

3. The effects of glutamate and its analogue kainate can be prevented by the non-NMDA receptor blocker CNQX, but not by the NMDA receptor blocker AP5.

4. Only part of the effects of kainate on neurite outgrowth are due to Ca^{2+}-influx through voltage-gated Ca^{2+} channels.

5.2 Methods

Primary cultures of embryonic chick retina were prepared as described in section 2.1. 24 hours after plating the culture medium was supplemented with the appropriate drug or combination of drugs. After 6 days *in vitro* (DIV) the number of primary neurites extended by the cells were counted using a hand-operated tally counter and the result expressed as the number of processes per 100 cells. In most experiments the processes from approximately 300 cells were counted from 5 fields in each of 3 replicate dishes. No attempt was made to distinguish between photoreceptors or retinal neurons. The counting process excluded the processes of retinal Müller cells because by the time the counts were made these glial cells had formed thin semi-confluent sheets on the bottom of the culture dish. The two-tailed version of the Student's T-test was used to determine the statistical significance of the data obtained (see section 2.3.6).

5.3 Results

5.3.1 The effects of glutamate and GABA on neurite outgrowth

The inhibitory neurotransmitter GABA was added to the culture medium at 1 DIV for 5 days at a concentration of 100μM and counts were

made as detailed in section 5.2. GABA had no effect on neurite outgrowth in dissociated retinal cultures (figure 5.1).

Application of the excitatory neurotransmitter glutamate (100μM) to the culture medium for 5 days reduced the number of processes extended by retinal cells (figure 5.2). The reduction was significant at the 0.1% level. The NMDA receptor antagonist D-AP5 (20μM) did not protect the cells from the effects of glutamate on neurite outgrowth when co-applied to the culture with glutamate in the medium (figure 5.2). However, the reduction in neurite extension produced by glutamate could be prevented by co-application of the non-NMDA receptor antagonist CNQX (20μM) and process outgrowth was restored to control levels (figure 5.2). These data suggest glutamate mediates its action on neurite outgrowth via a non-NMDA receptor.

5.3.2 The effects of glutamate analogues on neurite extension

Cultures were treated with 10, 100 or 500μM of the non-NMDA receptor agonist kainate for 5 days and the number of processes extended by cells counted as described in section 5.2. Kainate reduced process outgrowth compared to controls at all concentrations employed. Figure 5.3 shows an example of a 4 day old culture grown in 500μM kainate since 1 DIV. The cells appear healthy but the number of neurites extended is clearly reduced. The reduction seen in 10μM kainate was not significant at the 5% level, however the effects of 100 and 500μM kainate were both significant at the 0.1% level (Figure 5.4). Exposure to kainate did not affect the number of cells surviving in the cultures (see chapter 4).

The effects of kainate on neurite outgrowth may be mediated via an AMPA/kainate receptor or via a kainate-preferring receptor. To clarify

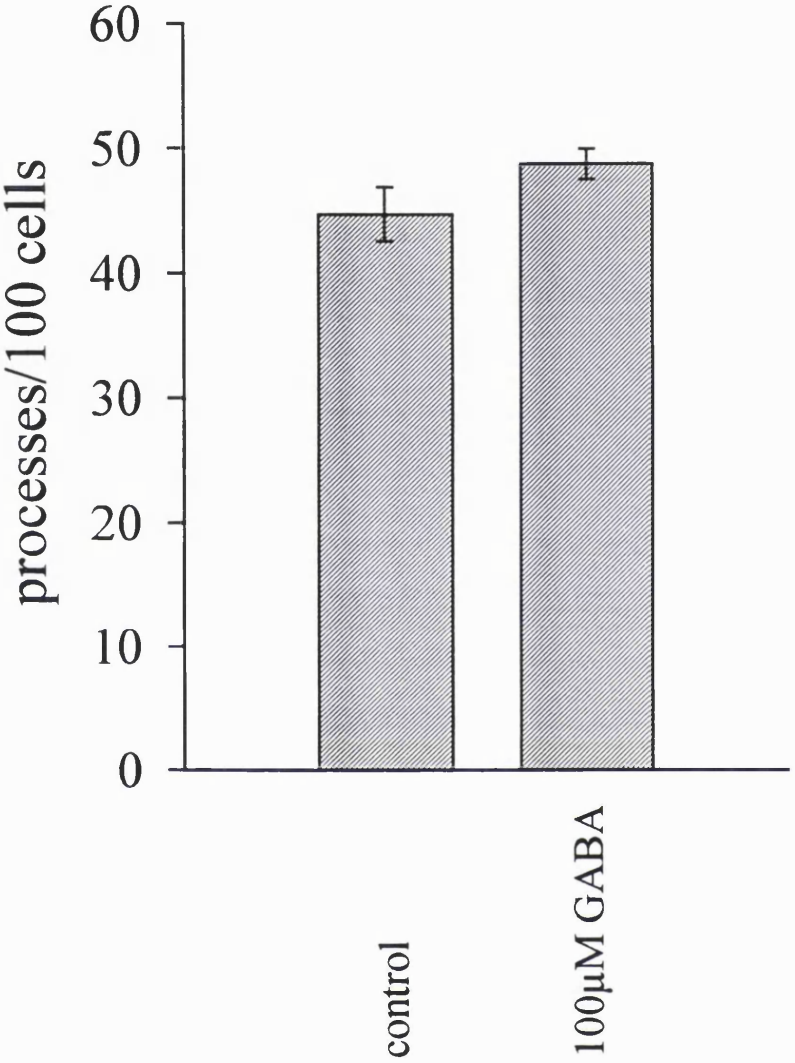

Figure 5.1

The inhibitory neurotransmitter GABA (100μM) does not affect process outgrowth. Counts were made from 5 fields with a mean of 360±31 cells per field.

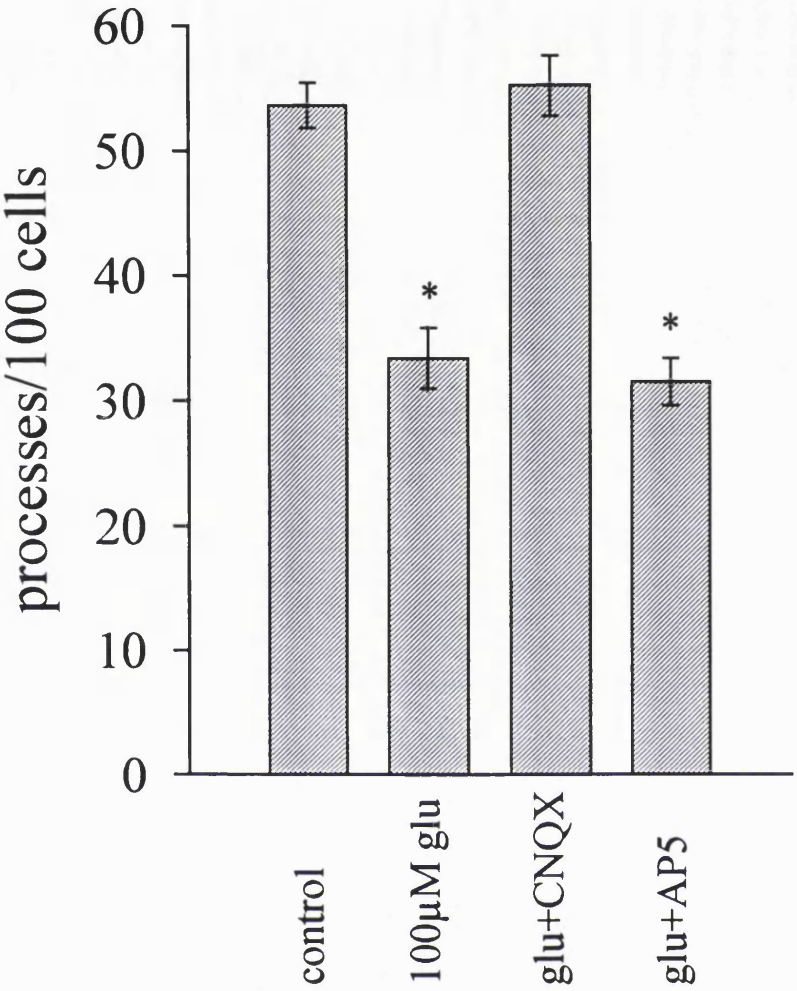

Figure 5.2

Glutamate (100μM glu) significantly reduces process outgrowth in retinal cells (*, $p<0.001$). Co-application of the non-NMDA receptor antagonist CNQX (20μM) blocked the effects of glutamate, while the NMDA receptor antagonist AP5 (20μM) did not and neurite outgrowth was significantly reduced in its presence ($p\leq 0.001$). Counts were made in 9 fields from 3 culture dishes with a mean of 525±11 cells per field.

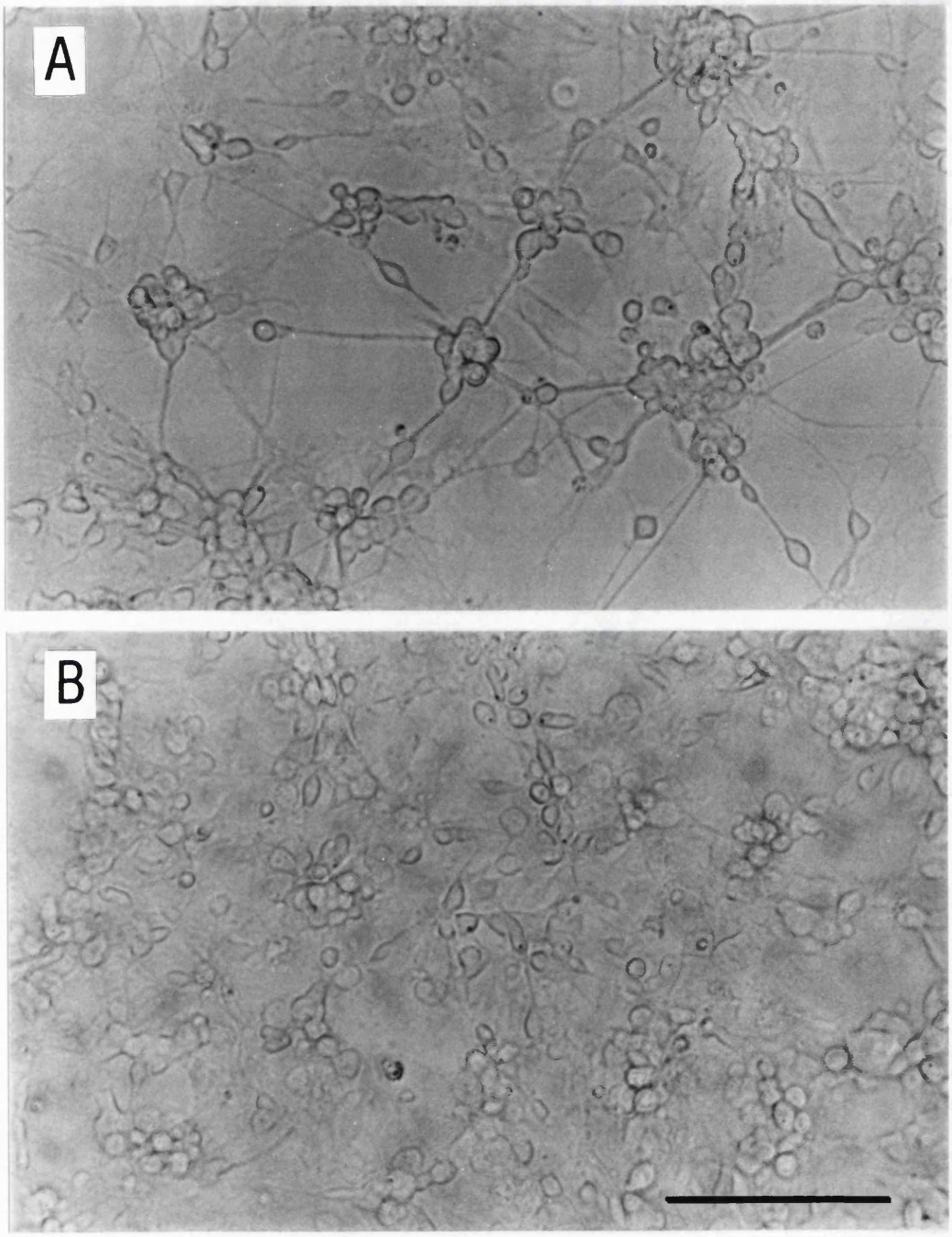

Figure 5.3

Kainate reduces neurite extension in cultured chick retinal cells.

A. Control retinal culture at 4 DIV. **B.** Retinal culture (4 DIV) after chronic exposure to 500μM kainate since 1 DIV. The cells appear healthy, however the cells extend fewer processes. Bar represents 100μm.

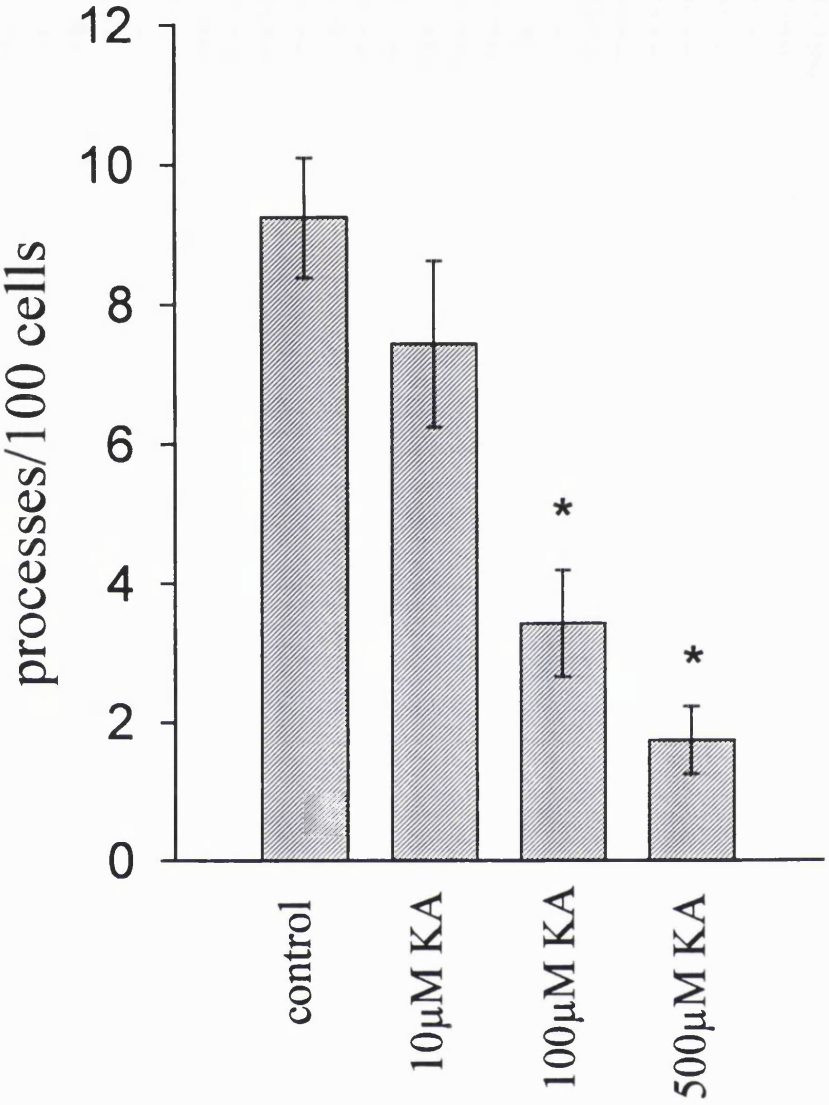

Figure 5.4

The effects of exposure to kainate on neurite outgrowth.

Counts were made from 3 culture dishes in 15 fields with a mean of 290±15 cells per field. Kainate (KA) reduced the number of processes extended by the cells at all concentrations. The effects of 10μM kainate were not significant, but 100 and 500μM kainate led to a significant reduction in process outgrowth (*, $p<0.001$ compared to controls).

whether the effects of kainate on neurite outgrowth could be mimicked by AMPA, the experiment described above was repeated using 10, 100 and 500μM AMPA. AMPA normally evokes rapidly desensitizing currents when it acts at AMPA/kainate receptors (Hamill et al., 1981, but see chapter 3), unlike kainate which generates currents that do not desensitize (Keinänen et al., 1990, Patneau and Mayer 1991). To prolong the effects of AMPA in culture, desensitization was inhibited by co-application of 500μM diazoxide. Diazoxide is also known to activate ATP-sensitive K^+ channels, so as a precaution glibenclimide (30μM) was applied to block these effects (Dunne et al., 1987). AMPA, in the presence of diazoxide and glibenclimide, caused a reduction in neurite outgrowth at all concentrations that was significant for 100 and 500μM at the 0.1% level, but not significant for 10μM AMPA at the 5% level (figure 5.5). Growing the cells in the presence of diazoxide and glibenclimide, in the absence of AMPA, also produced a small reduction in process extension that was significant at the 2% level.

Chronic exposure to 500μM AMPA in the absence of diazoxide also reduced neurite outgrowth in retinal cells (figure 5.6). The reduction was smaller than that seen in the same concentration of AMPA in the presence of diazoxide and was significant at the 0.2% level.

It is possible that the application of kainate to the cells in culture leads to membrane depolarization that in turn causes release of glutamate, which may then act at metabotropic glutamate receptors. It has also been reported that at high concentrations kainate may directly activate metabotropic receptors (Shiells et al., 1981). To investigate whether a metabotropic receptor plays a role in controlling neurite outgrowth, the metabotropic glutamate receptor agonist *trans*-ACPD was added to the culture medium at concentrations of 150 and 300μM for 5 days and counts were made as

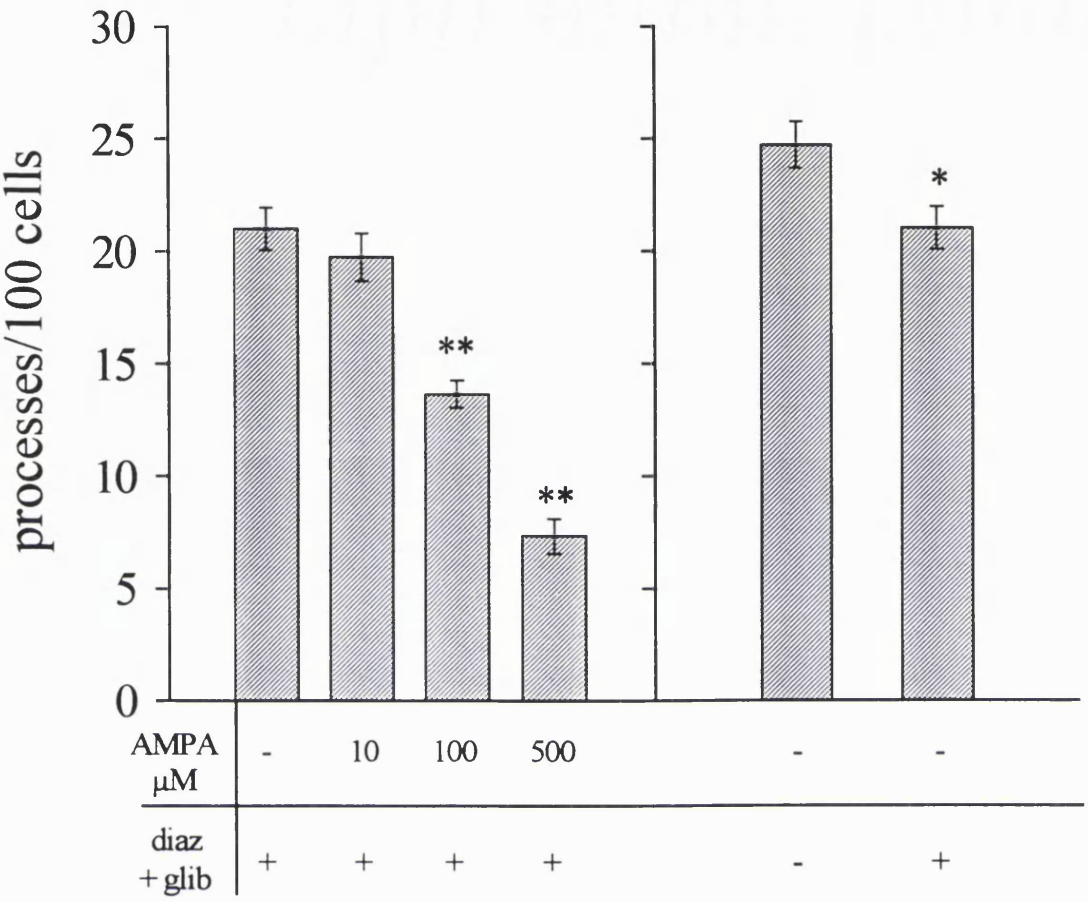

Figure 5.5

The effects of exposure to AMPA on neurite outgrowth.

Counts were made from 3 dishes in 15 fields with a mean of 507±18 cells per field. AMPA, in the presence of diazoxide and glibenclimide (diaz+glib), reduced the number of processes extended by the cells. The reduction was significant for 100 and 500μM, but not for 10μM AMPA (**,$p<0.001$). Diazoxide and glibenclimide, applied in the absence of AMPA, produced a small reduction in neurite outgrowth when compared to control (*, $p< 0.002$).

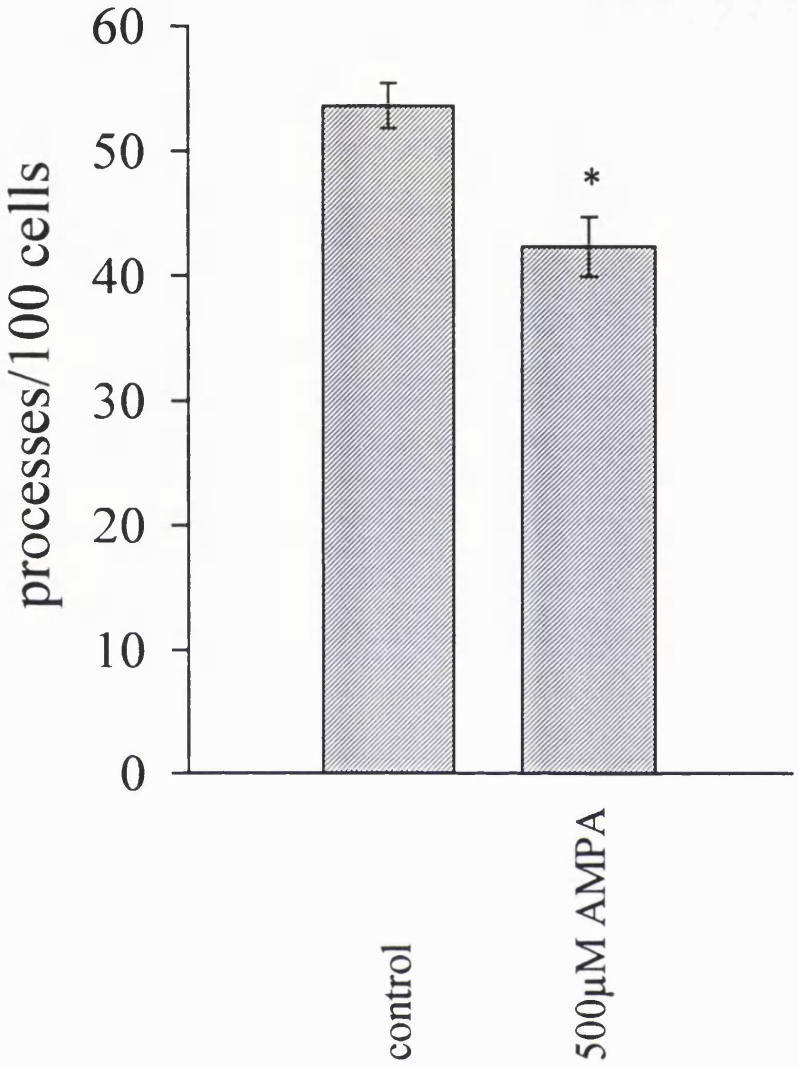

Figure 5.6

AMPA reduces neurite outgrowth in the absence of diazoxide.

500μM AMPA, in the absence of diazoxide to block desensitization, significantly reduced the number of processes extended by the cells compared to controls ($p \leq 0.002$). Counts were made from 9 fields in 3 dishes with a mean of 525±11 cells per field.

described in section 5.2. Both concentrations of *trans*-ACPD had no effect on neurite outgrowth and the number of processes extended by the cells remained at control levels (figure 5.7).

5.3.3 The pharmacology of the effects of kainate on neurite outgrowth

Although the effects of glutamate on neurite outgrowth were not blocked by AP5, the activation of NMDA receptors by glutamate released secondary to kainate-evoked membrane depolarization was investigated. The NMDA receptor antagonist D-AP5 (20μM, Tocris) was co-applied to the cultures with 10, 100 and 500μM kainate. AP5 did not protect the cells from the effects of kainate and reductions in process outgrowth were observed at all concentrations of kainate. 10, 100 and 500μM kainate produced reductions in outgrowth that were significant at the 2, 0.2 and 0.1% level respectively (figure 5.8). The application of AP5 alone did not significantly affect neurite outgrowth.

In contrast, addition of the non-NMDA receptor antagonist CNQX (20μM, Tocris) restored process outgrowth to control levels and above at all concentrations of kainate employed (figure 5.9). Culturing the cells in the presence of CNQX alone lead to a reduction in neurite outgrowth that was significant at the 0.1% level. CNQX was prepared in a stock solution containing DMSO, hence similar levels of DMSO were added to all control and experimental dishes. DMSO itself produced an increase in neurite outgrowth compared to controls that was significant at the 0.1% level.

5.3.4 The involvement of Ca^{2+}-influx via voltage-gated Ca^{2+} channels

In order to determine whether or not Ca^{2+}-influx through voltage-gated

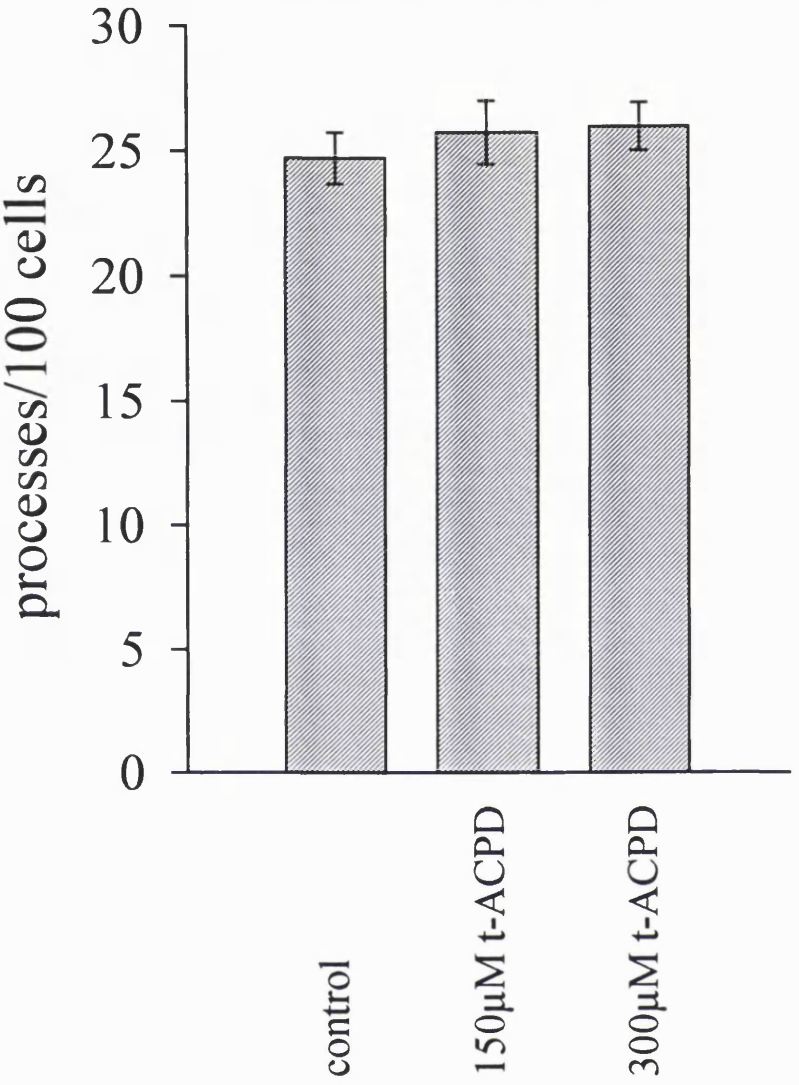

Figure 5.7

The effects of metabotropic receptor activation on process outgrowth. Counts were made from 3 culture dishes in 15 fields with a mean of 481±25 cells per field. Culturing retinal cells in the presence of 150 and 300μM *trans*-ACPD had no effect on neurite outgrowth.

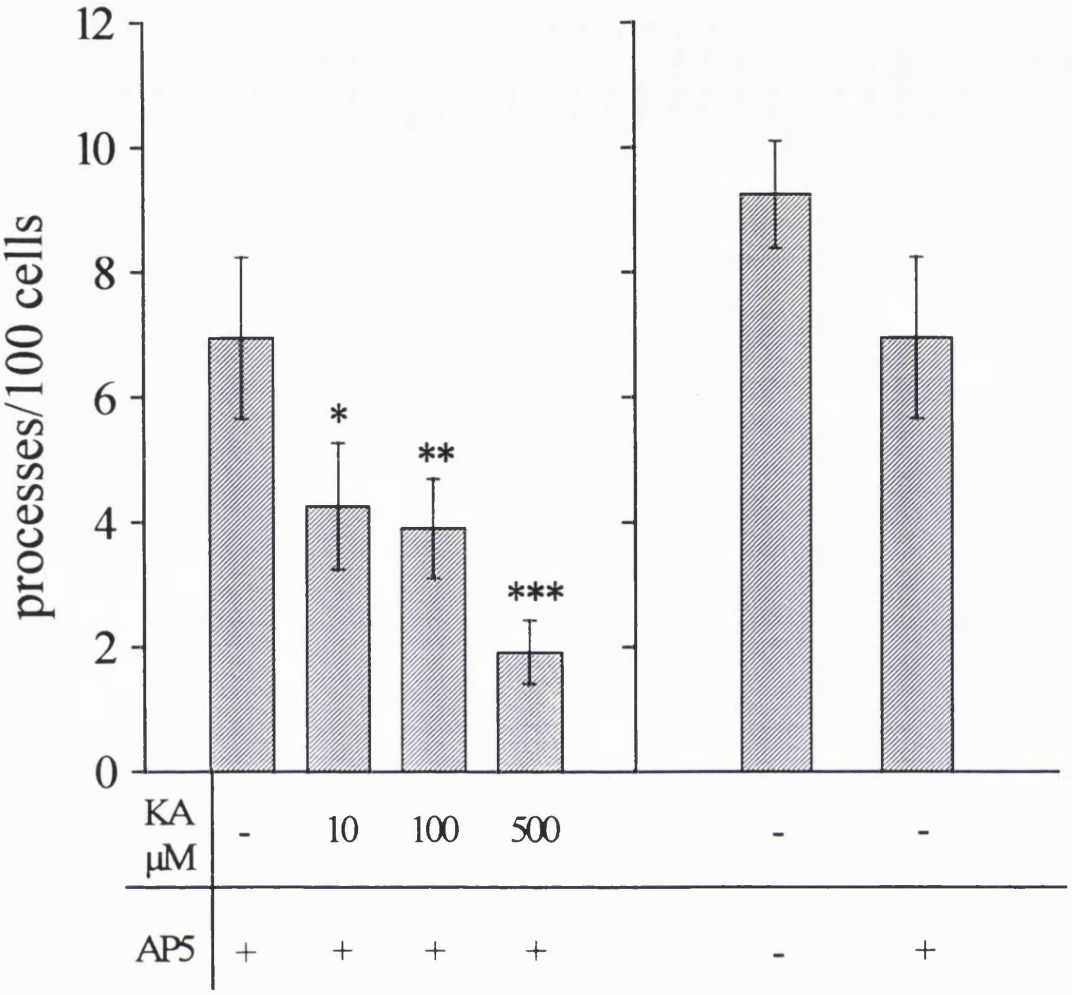

Figure 5.8

AP5 does not protect embryonic retinal cells from the effects of kainate on neurite outgrowth. Counts were made in 3 dishes from 15 fields of cells with a mean of 280±18 cells per field. In the presence of 20μM AP5 10, 100 and 500μM kainate produced a significant reduction in neurite outgrowth (*, $p<0.02$; **, $p<0.002$; ***, $p<0.001$ when compared to controls). Treatment with AP5 alone reduced process outgrowth but the reduction was not significant at the 5% level.

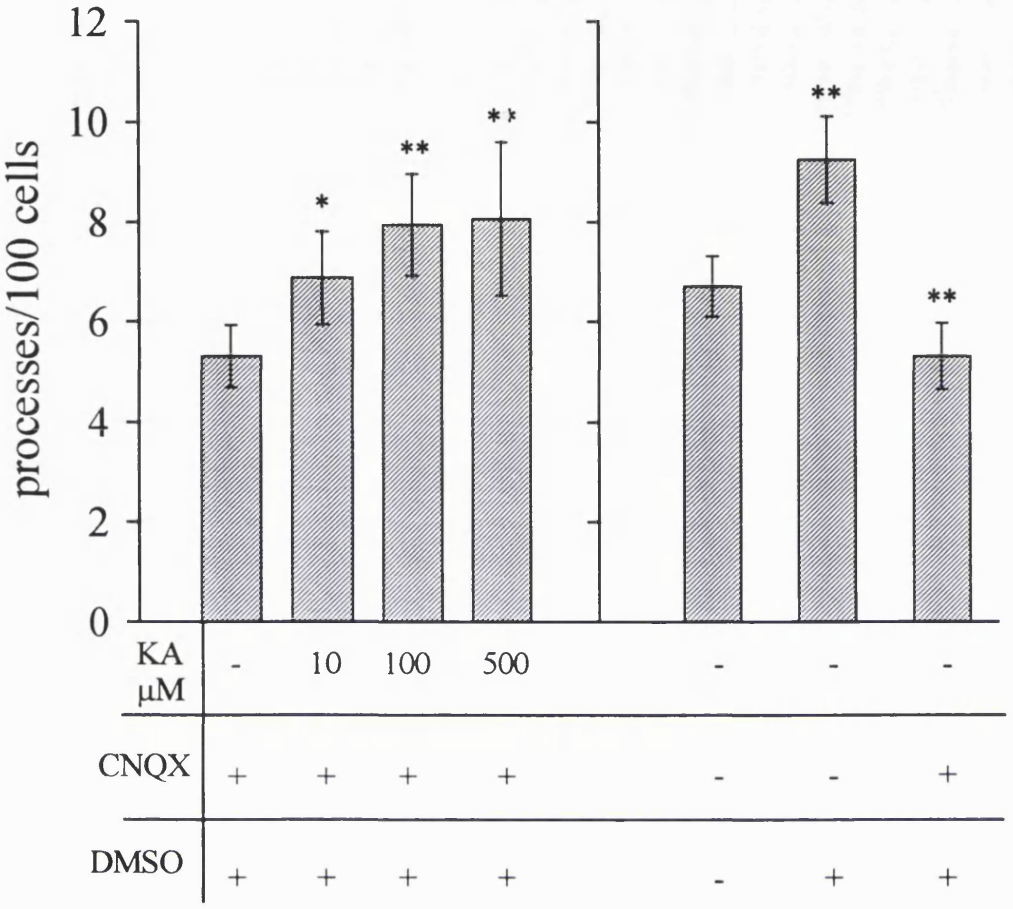

Figure 5.9

CNQX protects the cells from the reduction in neurite outgrowth produced by kainate (KA). Counts were made in 3 dishes from 15 fields of cells with a mean of 289±17 cells per field. In the presence of 20μM CNQX 10, 100 and 500μM kainate increased neurite outgrowth (*, $p>0.002$; **$p<0.001$ compared to the CNQX control). Cells cultured in the presence of CNQX and the absence of kainate showed a significant decrease in neurite outgrowth (**, $p<0.001$ when compared to DMSO control). Growing cells in DMSO alone lead to an increase in process extension (**, $p<0.001$ when compared to control).

channels was important for the effects produced by kainate, 20μM of each of the L-type Ca^{2+} channel blockers nifedipine and diltiazem (both Sigma) were co-applied to the cells with 10, 100 and 500μM kainate. In whole-cell patch-clamp experiments from embryonic retinal cells these concentrations of the blockers reduce the Ca^{2+} current by about 90% (see chapter 3). Both blockers were prepared as stock solutions in DMSO, so equal amounts of DMSO were added to control and experimental dishes. When cultured in the presence of the Ca^{2+} channel blockers, the cells were protected from the effects of 10 and 100μM kainate but 500μM kainate persisted in reducing neurite outgrowth (figure 5.10). This reduction was statistically significant at the 0.1% level. When the cells were grown in the presence of nifedipine and diltiazem alone, a reduction in process outgrowth was observed that was significant at the 0.1% level.

5.4 Discussion

$[Ca^{2+}]_i$ plays a pivotal role in the regulation of neurite outgrowth (Suarez-Isla et al., 1984, Mattson et al., 1988c). Kater et al. (1988) propose a model in which both low and high $[Ca^{2+}]_i$ levels inhibit neurite outgrowth while at moderate $[Ca^{2+}]_i$ process outgrowth is facilitated (figure 5.11). Thus neurite outgrowth shows a bell-shaped dependence on $[Ca^{2+}]_i$. Evidence to support this model comes from experiments in which $[Ca^{2+}]_e$ was varied and its effects on $[Ca^{2+}]_i$ and neurite outgrowth in rat sensory neurons was measured (Al-Mohanna et al., 1992). Neurite outgrowth showed the bell-shaped dependence on $[Ca^{2+}]_i$ suggested by Kater et al. (1988).

$[Ca^{2+}]_i$ can change in response to membrane depolarization or as a result of many other ligand/receptor mediated events. Several studies support the hypothesis that neurotransmitter levels in the developing CNS may

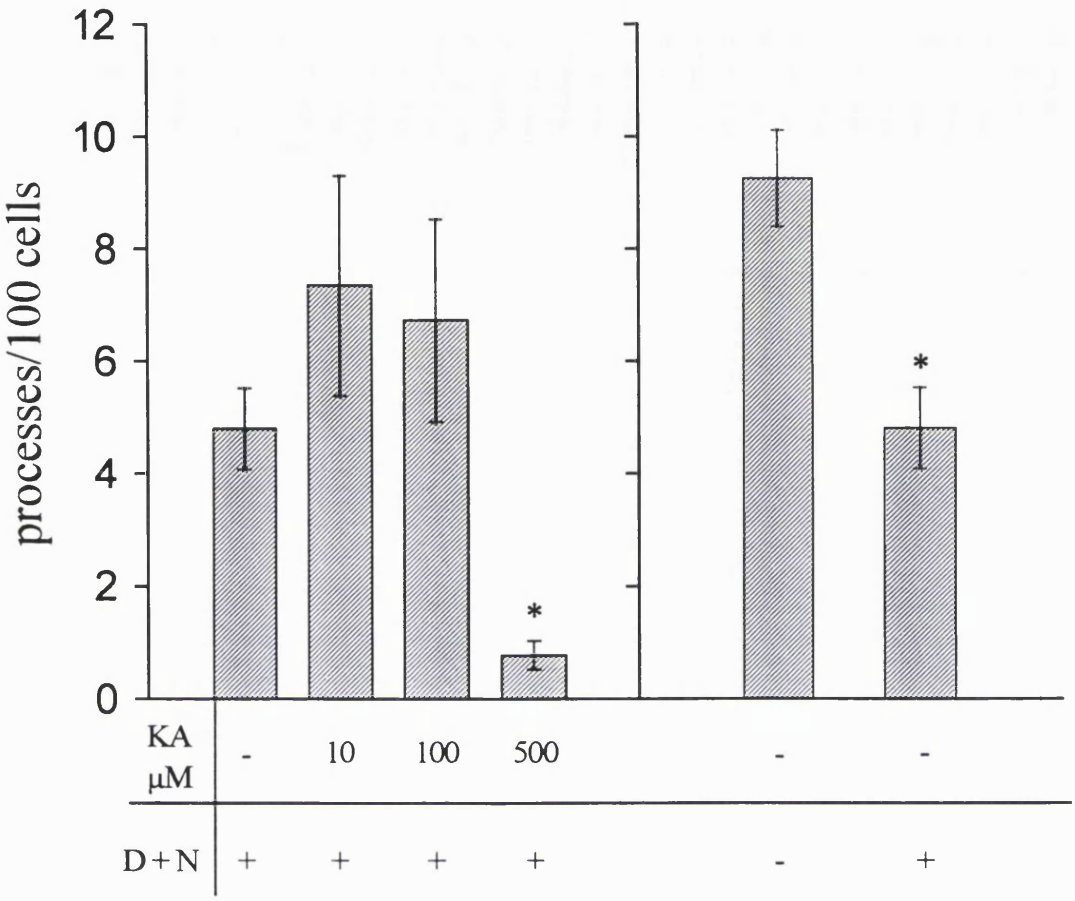

Figure 5.10

Ca^{2+} channel blockers only partially protect embryonic retinal cells from the effects of kainate on neurite outgrowth. Counts were made in 3 dishes from 15 fields of cells with a mean of 271±17 cells per field. In the presence of 20μM diltiazem and nifedipine (D+N) 10 and 100μM kainate (KA) had no significant effect on neurite outgrowth, whereas 500μM kainate produced a significant reduction in the number of processes extended by the cells. Treatment with diltiazem and nifedipine in the absence of kainate resulted in a significant decrease in process outgrowth. (*, $p<0.001$; when compared to controls).

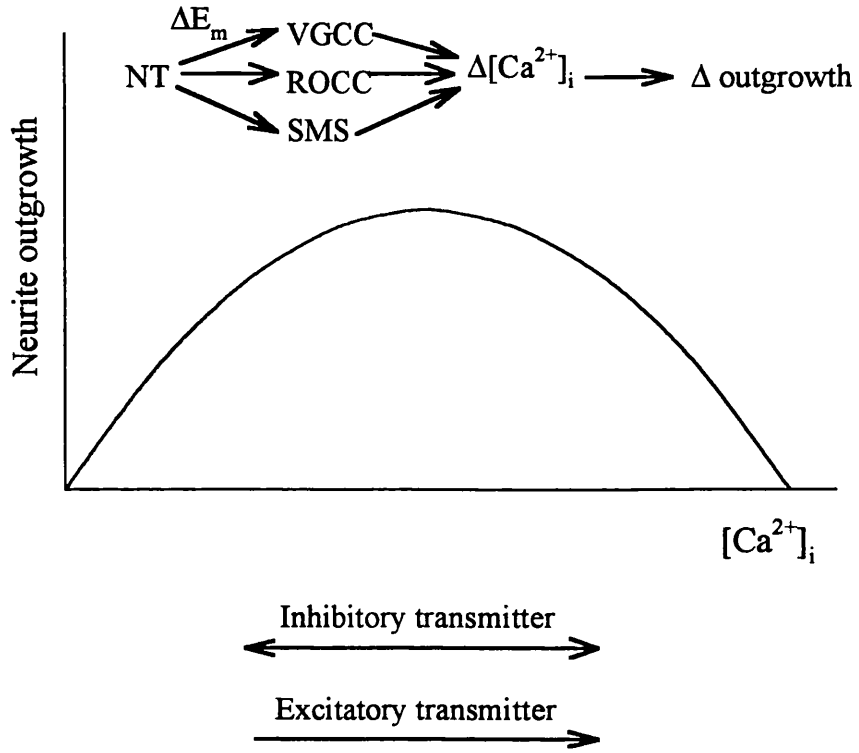

Figure 5.11

The relationship between Ca^{2+} and neurite outgrowth.

Diagram based upon the Lipton and Kater (1989) model. The equation above the diagram shows that neurotransmitters (NT) can alter $[Ca^{2+}]_i$ either by producing membrane depolarization that leads to the opening of voltage-gated Ca^{2+} channels (VGCC), by opening receptor-operated Ca^{2+} channels (ROCC) such as NMDA receptor channels or via receptors that activate second messenger systems (SMS) such as metabotropic receptors. The graph shows the bell-shaped dependence of neurite outgrowth on $[Ca^{2+}]_i$. Excitatory transmitters like glutamate increase $[Ca^{2+}]_i$ and inhibitory transmitters such as GABA can increase or decrease $[Ca^{2+}]_i$ depending on the stage of development (see section 5.4.1)

serve to maintain an optimal level of $[Ca^{2+}]_i$ and that deviations from these optimum concentrations can have profound effects on growth (reviewed by Kater et al., 1988, Mattson, 1988). It is not well understood how these optimum concentrations are established, maintained and modulated but in some cases the main mode of Ca^{2+}-entry appears to be through voltage-dependent Ca^{2+} channels activated by membrane depolarization (Robson and Burgoyne, 1989) or through channels operated by neurotransmitters such as the NMDA receptor (MacDermott et al., 1986). The excitatory neurotransmitter glutamate has the ability to alter $[Ca^{2+}]_i$ levels via several mechanisms and these are discussed below.

5.4.1 Glutamate and its analogues reduce neurite outgrowth in retinal neurons

GABA is usually considered as an inhibitory neurotransmitter and has been shown to produce significant effects on neurite outgrowth. Mattson and Kater (1989) showed that GABA reduced neurite outgrowth in cultured hippocampal neurons, whilst in the embryonic chick tectum GABA stimulates or inhibits neurite growth depending on the presence or absence of serum in the culture medium (Michler, 1990). GABA may act at $GABA_A$ or $GABA_B$ receptors that gate a Cl^- influx (Bormann, 1988, Qian and Dowling, 1993), or at $GABA_C$ receptors that initiate G-protein mediated events which can affect ion channels, including the closing of Ca^{2+} channels (reviewed by Bormann, 1988). The action of GABA at ionotropic receptors is usually to decrease excitability and thus reduce $[Ca^{2+}]_i$. However, it has also been shown that GABA can have a depolarizing action (Obata et al, 1978, reviewed by Cherubini et al, 1991), possibly because some cells maintain high $[Cl^-]_i$. The imaging studies in Chapter 6 show that application of GABA produces significant increases in $[Ca^{2+}]_i$ in the chick retina between E4 and E12. This

effect and the currents produced by GABA (see patch-clamp experiments in Chapter 3) can be blocked by bicuculline. These results show that GABA depolarizes retinal neurons at early times in development via an action at $GABA_A$ receptors. Despite this, prolonged exposure to GABA had no effect on neurite outgrowth in cultured embryonic retinal cells (section 5.3.1) and neurite extension remained similar to controls.

In contrast the excitatory neurotransmitter glutamate (100μM) reduced process outgrowth in retinal cells when applied to cultures over a period of days (section 5.3.1). The effects of glutamate were blocked by the non-NMDA receptor antagonist CNQX, but not by the NMDA receptor antagonist AP5, suggesting glutamate was acting via a non-NMDA receptor.

Prolonged activation of non-NMDA glutamate receptors with kainate caused a large reduction in the outgrowth of neurites from retinal neurons which increased with increasing kainate concentrations (10-500μM) (section 5.3.2). Kainate may be acting at AMPA/kainate receptors or at kainate-preferring receptors that are not activated by AMPA. Kainate-preferring receptors are formed from the glutamate receptor subunits GLUR5-7, KA1 and KA2 (for review see Feldmeyer and Cull-Candy, 1994). Electrophysiological studies on homomeric kainate receptors expressed in *Xenopus* oocytes show that these receptors have affinities for kainate in the nM to low μM range (Egebjerg et al., 1991). However the kainate concentration required to produce a half maximal effect at AMPA/kainate receptors is much greater (EC_{50} for kainate at GLUR1 is 35μM) (Hollmann et al., 1989). The high doses of kainate required to produce an action on neurite outgrowth makes it unlikely that kainate is acting via a kainate-preferring receptor. In chapter 4 patch-clamp studies showed that kainate evoked currents in cultured retinal cells that were long-lasting and that persisted in the

presence of kainate. Other studies have shown that when kainate is applied to AMPA/kainate receptors it activates a current with similar kinetics (Patneau and Mayer, 1991, Keinänen et al., 1990). In contrast kainate activates a transient response at kainate-preferring receptors followed by almost complete desensitization in the presence of the agonist (Herb et al. 1992), unlike those in cultured retinal cells. These data taken together suggest that kainate acts at AMPA/kainate receptors in the suppression of neurite outgrowth in cultured retinal cells.

Treatment of the cells with AMPA, a selective AMPA/kainate receptor agonist, also led to a reduction in outgrowth that was significant at concentrations of 100 and 500μM (section 5.3.2). AMPA was co-applied to the cells with diazoxide in all experiments. This served to block the fast desensitization typical of AMPA/kainate receptors when AMPA is used as the ligand (Yamada and Rothman, 1993). However AMPA (500μM) in the absence of diazoxide was also able to reduce neurite outgrowth in retinal cells. The patch-clamp experiments described in chapter 3 show that AMPA is able to evoke currents in cultured retinal cells that can be recorded after the time course expected for receptor desensitization. The failure of embryonic chick retinal AMPA/kainate receptors to desensitize may explain why AMPA and glutamate, which have similar fast kinetics at AMPA/kainate receptors elsewhere, were able to produce long term effects on neurite outgrowth in the absence of drugs which block receptor desensitization. The residual steady-state current through these receptors may be an important feature of embryonic AMPA/kainate channels that enables cells to sense the steady-state concentration of glutamate in the extracellular space.

5.4.2 The pharmacology of kainate's action on neurite production

The action of kainate at non-NMDA receptors will lead to a change in membrane voltage which can have one of several effects. Depolarization can evoke the release of endogenous glutamate which may act at NMDA receptors. NMDA receptors are permeable to Ca^{2+} and have been shown to play a key role in controlling neurite outgrowth in embryonic brain (Pearce et al., 1987, Brewer and Cotman, 1989). AP5, the NMDA receptor antagonist, was unable to block the reduction in process outgrowth caused by kainate, suggesting that kainate does not mediate this effect via the depolarization-evoked release of glutamate that then acts at the NMDA receptor (section 5.3.4). This was not unexpected since the effects of glutamate on neurite outgrowth were not prevented by AP5 (see section 5.4.1). In contrast, the non-NMDA receptor antagonist CNQX blocked the effects of kainate on neurite extension (section 5.3.3). These data imply that kainate exerts its action on neurite outgrowth directly via a non-NMDA receptor. Other studies have also shown that activation of non-NMDA receptors with kainate can affect process outgrowth. Mattson et al. (1988a) showed that glutamate could suppress neurite outgrowth in embryonic rat hippocampal pyramidal neurons and that these effects could not be blocked by AP5. The action of glutamate could be mimicked by kainate, but not by NMDA, suggesting non-NMDA receptors could regulate process outgrowth in these cells.

5.4.3 Routes for Ca^{2+}-influx in the presence of kainate

The most likely mechanism for the effects of glutamate and its analogues on neurite outgrowth involve an increase in $[Ca^{2+}]_i$. The routes for Ca^{2+}-entry into neurons in the presence of kainate have already been described in Chapter 4 and are treated here only briefly. Ca^{2+} will enter cells treated

with kainate as a consequence of the depolarization it evokes. Patch-clamp experiments described in chapter 3 show that embryonic chick retinal cells display Ca^{2+} currents that are largely blocked by the L-type channel antagonists diltiazem and nifedipine. Section 5.3.4 shows these compounds protect the cells from the effects on neurite outgrowth of 10 and 100μM, but not 500μM, kainate. This suggests that increasing $[Ca^{2+}]_i$ via entry through voltage-gated channels plays some part in the reduction in neurite extension produced by kainate. However the inability of the blockers to protect the cells from 500μM kainate implies that other mechanisms must exist whereby kainate can influence process outgrowth.

A second route for Ca^{2+}-entry is through the AMPA/kainate receptor itself. The Ca^{2+}-permeability of AMPA/kainate receptors depends on their subunit composition (see section 4.4.8 for discussion). Ca^{2+} imaging experiments in chapter 6 show Ca^{2+}-permeable AMPA/kainate receptors to be present in the embryonic chick retina from E6 onwards. These receptors may be important in determining $[Ca^{2+}]_i$ during development because they are not subject to a voltage-dependent block by Mg^{2+} and appear not to fully desensitize. Thus they may be activated by the glutamate in the extracellular space of the developing retina from early times, prior to the presence of spiking activity and synapse formation. It is possible that the initial Ca^{2+}-influx through these receptors is involved in the reduction of process extension produced by AMPA/kainate receptor activation (however, see section 5.4.4).

Some metabotropic glutamate receptors are linked via a G-protein to an intracellular signalling pathway that ultimately leads to the release of Ca^{2+} from internal stores (Nicoletti et al., 1986, Sladeczek et al., 1985). Activation of these receptors therefore provides a powerful mechanism whereby glutamate may alter $[Ca^{2+}]_i$ levels. Glutamate release, secondary to membrane

depolarization evoked by kainate, has the potential to activate these receptors. It has also been shown that at high concentrations kainate can act directly on metabotropic receptors (Shiells et al., 1981). However chronic application of the metabotropic agonist *trans*-ACPD (150 and 300μM) to the retinal cells had no effect on neurite outgrowth (section 5.3.2). *Trans*-ACPD is an agonist at all metabotropic receptors cloned to date (mGluR1-8), though its potency depends on subunit composition (for review see Nakanishi, 1994). That *trans*-ACPD is ineffective in affecting neurite outgrowth suggests that metabotropic receptors are not involved in the regulation of process outgrowth in chick retinal cells.

5.4.4 Decreases in intracellular Ca^{2+} may also reduce neurite outgrowth

In the preceding section the mechanisms discussed that can influence process outgrowth all involved an increase in $[Ca^{2+}]_i$. However from the model proposed by Kater et al. (1988) it might be expected that a decrease in $[Ca^{2+}]_i$ will have equally profound effects on neurite extension. Experiments in chapter 4 show that sustained activation of AMPA/kainate receptors in retinal neurons leads to a reduction in Ca^{2+}-entry through the receptor. Thus, it is possible that it is not the initial increase in Ca^{2+}-entry produced by kainate that reduces neurite outgrowth, but instead it may be the subsequent long-term decrease in Ca^{2+}-influx through the AMPA/kainate receptor that leads to this reduction in process extension. Application of the non-NMDA glutamate receptor antagonist CNQX (20μM), in the absence of kainate, produced a significant reduction in process outgrowth in retinal neurons (section 5.3.3). This may be due to the presence of basal levels of glutamate in the culture medium and fetal calf serum. It is possible that the retinal cells release glutamate into the medium which acts at non-NMDA receptors during the normal development of retinal cells. Addition of CNQX to the culture

medium will block receptor activation and so reduce Ca^{2+}-influx. As a result $[Ca^{2+}]_i$ will move away from its optimum for neurite outgrowth. Application of the Ca^{2+} channel blockers diltiazem and nifedipine also reduced neurite outgrowth in the absence of kainate (section 5.3.4). This too may be due to a decrease in $[Ca^{2+}]_i$ produced by a reduction in Ca^{2+}-influx through voltage-gated channels. Together these data suggest that neurite outgrowth is impaired if the $[Ca^{2+}]_i$ is shifted away from its optimum, either by an increase or decrease in cytoplasmic Ca^{2+} levels.

5.4.5 Ca^{2+}-dependent mechanisms that regulate neurite outgrowth

Ca^{2+}, other second messengers such as cAMP (Mattson et al., 1988c) and activation of PKC (Spinelli and Ishii, 1983) have been shown to affect neurite outgrowth, yet the mechanisms by which they execute their effects remain unclear. The events that underlie the changes in neurite extension initiated by Ca^{2+} are likely to involve cytoskeletal elements such as microtubules, microfilaments and associated proteins such as MAP2 and synapsin 1. There are suggestions that actin-based growth cone motility and microtubule-based neurite elongation are differentially regulated by Ca^{2+} (Mattson and Kater, 1987). Immunocytochemistry has shown that in leech neurons depolarization-evoked Ca^{2+}-entry leads to a loss of microfilaments in the tips of growing neurites and that this is associated with a cessation in neurite outgrowth (Neely and Gesemann, 1994). Several studies indicate that phosphorylation of cytoskeletal proteins can mediate cytoarchitectural responses to Ca^{2+}-influx including neurite outgrowth (Goldenring et al., 1986, Zor, 1983). It is thought that Ca^{2+} may act directly or through a kinase or calmodulin to regulate the cytoskeletal elements that underlie neurite outgrowth. In non-neuronal cells like fibroblasts and macrophages Ca^{2+}-binding proteins like calmodulin are important links between Ca^{2+} and the

cytoskeleton (Ramussen, 1981).

5.4.6 The functional implications of glutamate receptor activation during retinal development

Neurotransmitters, which mediate communication between nerve cells in the mature nervous system, are also known to be present during development prior to synaptogenesis. It has been shown that they are released by both target tissues and by developing axons and dendrites (collectively termed neurites) (Young, 1986, Lockerbie and Gordon-Weeks, 1986). Immunochemical studies of the developing rabbit retina show that pools of glutamate are present within retinal neurons prior to synaptogenesis (Redburn et al., 1992). Many *in vitro* investigations have been carried out on a variety of preparations to study the effects of neurotransmitter application on neurite morphology during development (see section 1.4). For example Mattson et al. (1988a) demonstrated that the neurotransmitter glutamate inhibits dendritic outgrowth in cultured hippocampal pyramidal neurons and Pearce et al. (1987) found that glutamate acting at NMDA receptors can stimulate the outgrowth of processes in cerebellar granule cells *in vitro*. The influence of glutamate on neurite outgrowth is often attributed to its action at NMDA receptors which are well-established as Ca^{2+}-permeable ion channels. The data shown in this chapter suggests that non-NMDA glutamate receptors also play an important role in the regulation of process outgrowth in the retina. With the recent discovery of non-NMDA receptor subunits that can assemble to form Ca^{2+}-permeable pores (Hollmann et al, 1991), it is not surprising that these receptors should also be involved in the regulation of developmental processes formerly thought to be controlled solely by NMDA receptors. The results obtained from Ca^{2+} imaging experiments described in the next chapter show that Ca^{2+}-permeable non-NMDA receptors are present during early retinal

development and that they appear before NMDA receptors. These studies are supported by ligand-binding experiments which show that AMPA/kainate receptors are expressed maximally in the chick retina at E7, whereas significant numbers of NMDA receptors do not appear until later (Somahono et al., 1988). Wong (1993) has used imaging techniques to demonstrate that non-NMDA receptors are able to elicit changes in $[Ca^{2+}]_i$ in embryonic rabbit retina throughout the period of dendritic and synaptic development, while NMDA does not produce rises in $[Ca^{2+}]_i$ until the second postnatal week. These reports together suggest that AMPA/kainate receptors may be of particular importance in early development, possibly because depolarizing electrical activity is absent during this period and the Mg^{2+} block of NMDA receptors would render them ineffective as sensors of extracellular glutamate.

Chapter 6

Imaging of Ca^{2+} signals evoked by neurotransmitters in the developing chick retina

6.1 Introduction

Ca^{2+} is known to produce many of the actions that result from transmitter receptor stimulation during development. Neurotransmitters can alter $[Ca^{2+}]_i$ via several mechanisms. Ca^{2+} may enter directly through the transmitter receptor channel itself, through voltage-gated Ca^{2+} channels or via activation of metabotropic receptors that lead to the release of Ca^{2+} from internal stores. Fluorescent dyes that monitor changes in $[Ca^{2+}]_i$ can be used to determine the presence of transmitter receptors that are able to produce such changes.

Ca^{2+} imaging techniques have several advantages over electrophysiological methods for studying developmental changes in the expression of transmitter receptors that can alter $[Ca^{2+}]_i$. Firstly, the use of fluorescent Ca^{2+} indicators allows changes in $[Ca^{2+}]_i$ to be monitored directly. Secondly, Ca^{2+} responses can be studied in the intact retina at early times when individual cells are small and patch-clamp recording would be difficult. Finally, imaging techniques allow the localization and identification of the population of responsive cells. Using the fluorescent Ca^{2+} indicator Calcium Green-1 the results in this chapter show that:

1. Muscarinic ACh receptors are present in chick retina at E4. Subsequent to E4 the increase in $[Ca^{2+}]_i$ produced by ACh application declines.
2. NMDA receptors are first detectable at E8. Increases in $[Ca^{2+}]_i$ in response

to NMDA increase with age and peak at E12.

3. Ca^{2+}-permeable non-NMDA receptors are present at E6 and subsequently increase in density. These receptors produce increases in $[Ca^{2+}]_i$ both when changes in membrane voltage are prevented and when voltage-gated Ca^{2+} channels are blocked.

4. $GABA_A$ receptors are present at E4 and their activation increases $[Ca^{2+}]_i$ at this time. By E14 application of GABA ceases to produce elevations of $[Ca^{2+}]_i$, possibly because it now shunts or hyperpolarizes retinal neurons as it does in the adult.

6.2 Methods

Experiments were performed either on whole or pieces of isolated embryonic chick retina, depending on the age of the embryo. Fluorescence imaging techniques were used to monitor changes in $[Ca^{2+}]_i$. Whole retinae were loaded with the cell permeant AM-ester of the Ca^{2+}-sensitive fluorescent dye Calcium Green-1 (see section 2.9.1). Calcium Green is a non-ratiometric dye that is slow to bleach and that increases its fluorescence 14 times on Ca^{2+} binding, so enabling the detection of small changes in $[Ca^{2+}]_i$. Once loaded, retinae were transferred to a Petri dish in which part of the bottom was replaced with a thin glass cover-slip. The retina was held down with a harp made from platinum wire with nylon strings. The change in the fluorescent intensity of the dye within the retina was recorded with a slow-scan cooled CCD camera (Digital Pixel model no. 2000) as described in section 2.9. Fluorescent images were usually recorded at 5 second intervals and the mean intensity within the central part of the image was calculated using Lucida 2.0 software (Kinetic Imaging, Liverpool). While Calcium Green is not a ratiometric dye estimates of $[Ca^{2+}]_i$ can be made using the single-wavelength equation (reviewed by Thomas and Delaville, 1991). However, in the

experiments described in this chapter Ca^{2+} concentrations were not calculated and changes in fluorescence were normalised with respect to the initial baseline fluorescence intensity. The changes in $[Ca^{2+}]_i$ were often small because only part of a large population of cells responded to the drug applied. In order to compare responses to a drug at different developmental stages, images were normalised to the mean of the largest fluorescence change they produced. Images were background subtracted by taking an image in a field of view that did not include retinal tissue and subtracting this from the images obtained during an experiment. The external solution was solution A (table 2.1) unless otherwise stated and all drugs were applied by superfusion. Confocal imaging techniques were used to produce images of embryonic chick retina in which the retinal layers responding to kainate could be identified.

6.3 Results

6.3.1 ACh responses are present in the retina from early times

Bath application of ACh produced increases in $[Ca^{2+}]_i$ when applied to E4 retinae at concentrations of 1μM or more. Figure 6.1 shows the elevation of $[Ca^{2+}]_i$ produced by application of 0.1, 1 and 10μM ACh. 0.1μM ACh was ineffective while 1 and 10μM ACh produced large responses.

6.3.2 ACh receptors in embryonic chick retina are muscarinic

ACh receptors fall into two main categories: nicotinic and muscarinic. Antagonists for both types of receptor were tested to determine the nature of the cholinergic response in embryonic chick retina. The muscarinic receptor antagonist atropine (1μM, Sigma) blocked the Ca^{2+} rise produced by 10μM ACh (n=12) as shown in figure 6.2. The effects of atropine were reversible,

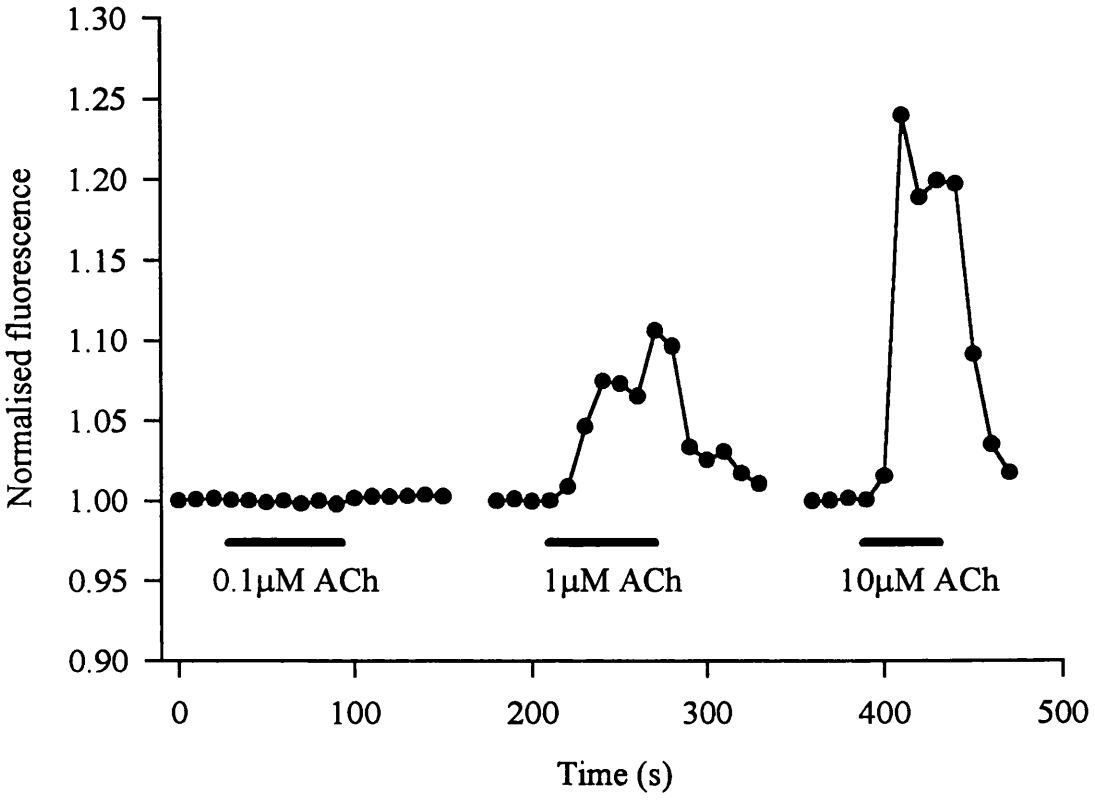

Figure 6.1

The dose-response relationship for ACh-evoked changes in fluorescence. ACh was bath applied to E4 chick retinae at a concentration of 0.1, 1 and 10μM. 0.1μM ACh did not produce any change in fluorescence. A small fluorescence increase was seen with 1μM ACh and a larger response was produced by 10μM ACh. The duration of the ACh application is indicated by a solid bar.

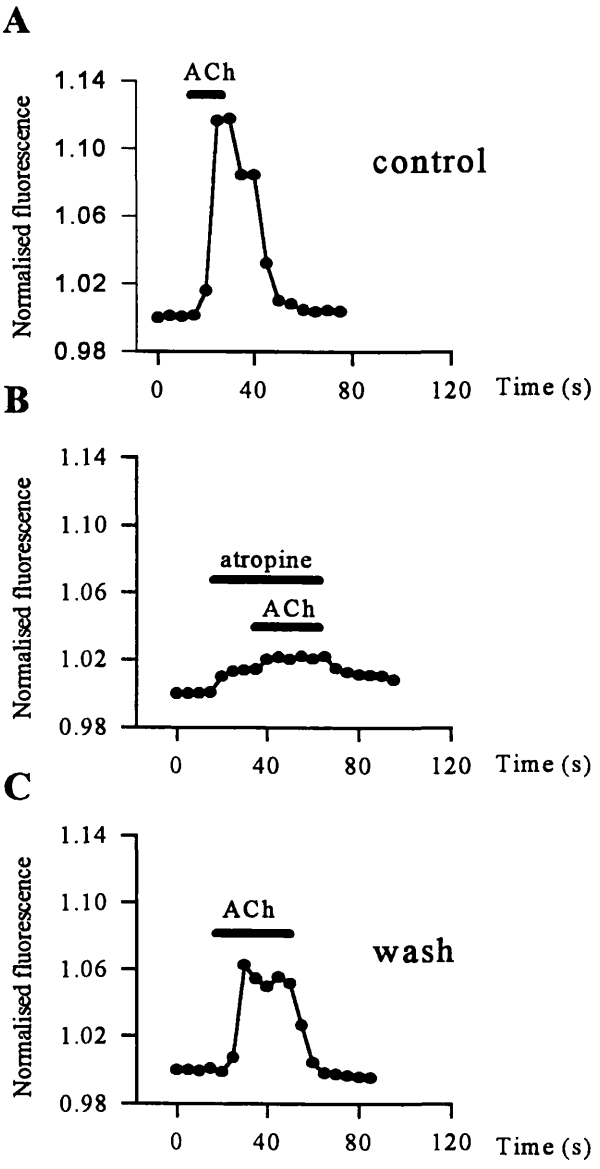

Figure 6.2

The ACh-evoked change in fluorescence in E4 retina is blocked by atropine. **A.** Application of 10μM ACh evokes an increase in fluorescence when applied to E4 chick retina. **B.** The effects of 10μM ACh are blocked by co-application of 1μM atropine. Atropine itself produced a small increase in fluorescence. **C.** The ACh-evoked response returns on reperfusion with Ringer's solution.

however, they required a long wash-out time (more than 30 minutes). Atropine itself usually produced a small response because it acts as a partial agonist at the muscarinic receptor. These data indicate that embryonic chick retinae express muscarinic ACh receptors during early development. The nicotinic receptor antagonists hexamethonium (200μM, Sigma) and tubocurarine (100μM, Sigma) applied together were unable to block the rise in $[Ca^{2+}]_i$ produced by 10μM ACh (n=9) (figure 6.3). However, the presence of these blockers prevented the initial transient seen in the response to ACh suggesting that this may arise from nicotinic receptors.

6.3.3 The change in the ACh-evoked Ca^{2+} response with embryonic age

All retinae tested from E4 onwards showed increases in $[Ca^{2+}]_i$ in response to 1, 10 and 100μM ACh (n=40). Retinae prior to E4 were not tested. In order to compare Ca^{2+} responses to ACh on different embryonic days the data were normalised to the mean of the responses obtained at E4, the time at which the largest changes in fluorescence evoked by 100μM ACh were obtained. The mean normalised fluorescence change to 100μM ACh fell from 100±5.9% (n=17) at E4 to 35.4±7.3% at E6 (n=5). The change in fluorescence continued to decline and by E8 the mean was 11±2.3% (n=4) of that at E4 (see figure 6.4). Retinae subsequent to E8 were not tested.

6.3.4 The Ca^{2+} signal produced by ACh is not solely due to activation of voltage-gated Ca^{2+} channels

The increase in $[Ca^{2+}]_i$ seen on ACh application may be due to Ca^{2+}-entry through voltage-gated Ca^{2+} channels or Ca^{2+} release from internal stores. To investigate whether the Ca^{2+} rise resulted from Ca^{2+}-entry through Ca^{2+}

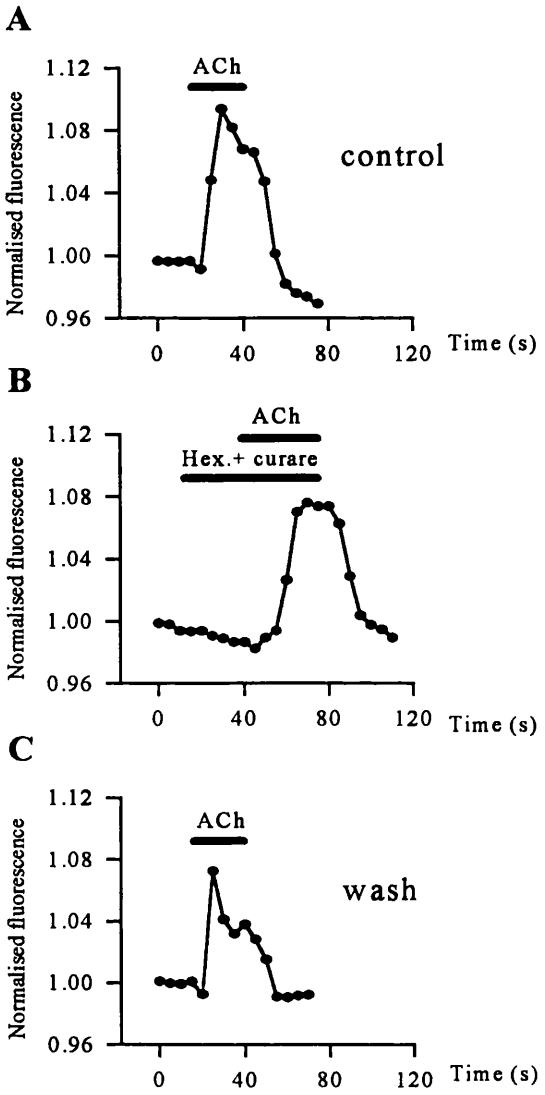

Figure 6.3

ACh-evoked Ca^{2+} responses at E4 are not blocked by hexamethonium and curare.

A. The increase in fluorescence produced by bath application of 10μM ACh. **B.** Hexamethonium (Hex.; 200μM) and tubocurarine (curare; 100μM) did not block the Ca^{2+} response evoked by 10μM ACh. However, the initial spike was absent. **C.** The ACh-evoked response after removal of hexamethonium and tubocurarine.

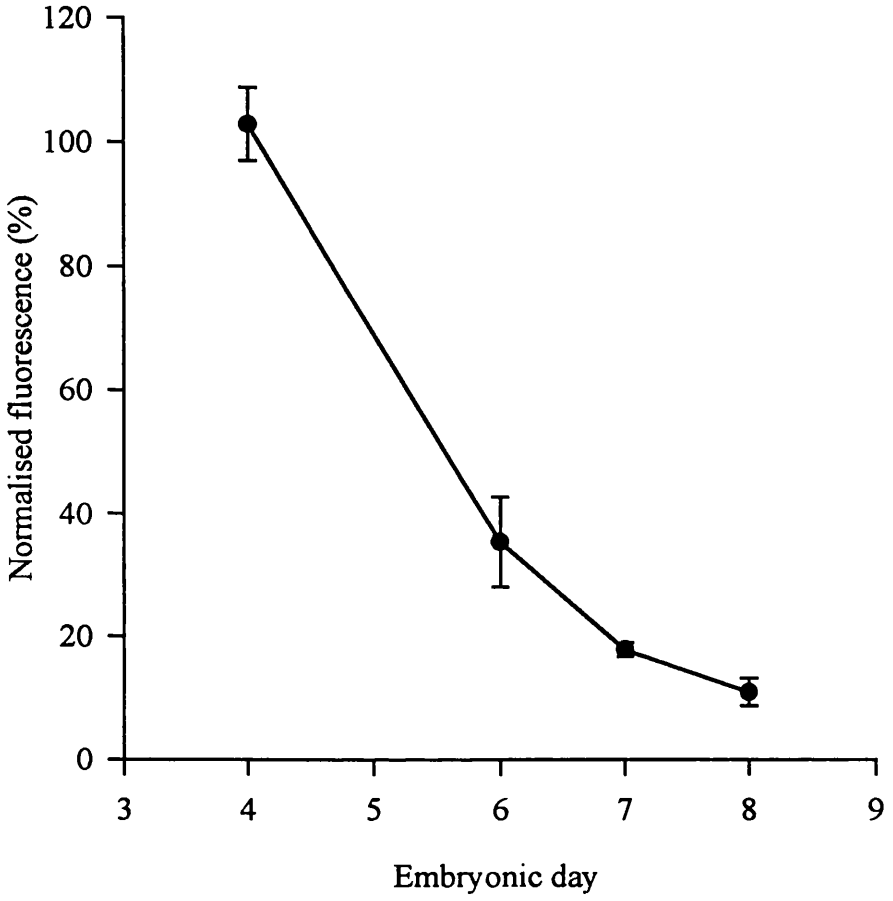

Figure 6.4

The developmental profile of the Ca^{2+} responses produced by 100μM ACh. The change in fluorescence (normalised to the mean of the responses at E4) produced by application of 100μM ACh as a function of embryonic day. Responses to ACh are maximal at E4, the earliest day tested, and subsequently decline.

channels, the L-type Ca^{2+} channel antagonists nifedipine and diltiazem (both 20μM) were co-applied with ACh (10μM). These concentrations of the drugs are effective blockers of the voltage-gated Ca^{2+} currents in chick retinal neurons (see chapter 3). Nifedipine and diltiazem did not block the rise in $[Ca^{2+}]_i$ produced by ACh, however the initial sharp peak seen on ACh application was absent and the steady-state response slightly reduced (n=3) (figure 6.5). These data suggest that while the rise in $[Ca^{2+}]_i$ produced by ACh is not due to the activation of voltage-gated Ca^{2+} channels, the Ca^{2+}-influx through them may contribute to the response.

6.3.5 NMDA receptor activation can elevate $[Ca^{2+}]_i$ from E8

The excitatory neurotransmitter glutamate has many well-established developmental effects through its influence on $[Ca^{2+}]_i$ (see chapters 4 and 5). NMDA receptors are associated with Ca^{2+}-permeable channels (MacDermott et al., 1986, Mayer and Westbrook, 1987, Ascher and Nowak, 1988) and thus can exert a direct effect on levels of cytoplasmic Ca^{2+}. In experiments where NMDA responses were studied Mg^{2+} was excluded from the external solution and 5μM glycine added to enhance the responses obtained (solution B, table 2.1). CNQX (20μM) was applied with NMDA to prevent secondary activation of non-NMDA receptors through depolarization-evoked glutamate release. Figure 6.6A shows the increase in fluorescence in E8 chick retina in response to application of 100μM NMDA in the presence of CNQX. No response was seen when NMDA was applied in the presence of AP5 (50μM) (figure 6.6B).

6.3.6 The change in the NMDA-evoked Ca^{2+} response with embryonic age

Bath application of 100μM NMDA produced increases in fluorescence

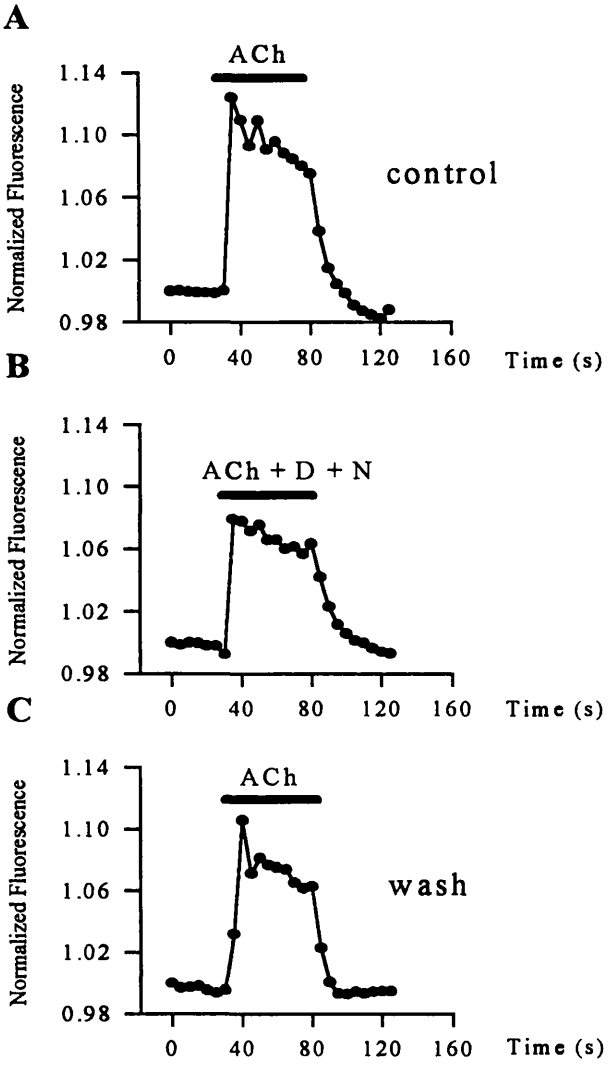

Figure 6.5

The role of voltage-gated Ca^{2+} channels in the generation of the ACh-evoked Ca^{2+} response.

A. The increase in fluorescence produced by bath application of 10μM ACh. **B.** Diltiazem and nifedipine (both 20μM) did not block the Ca^{2+} response evoked by 10μM ACh. However, the initial peak and steady-state response were slightly reduced. **C.** The initial peak of the ACh response returned after diltiazem and nifedipine were washed from the bath.

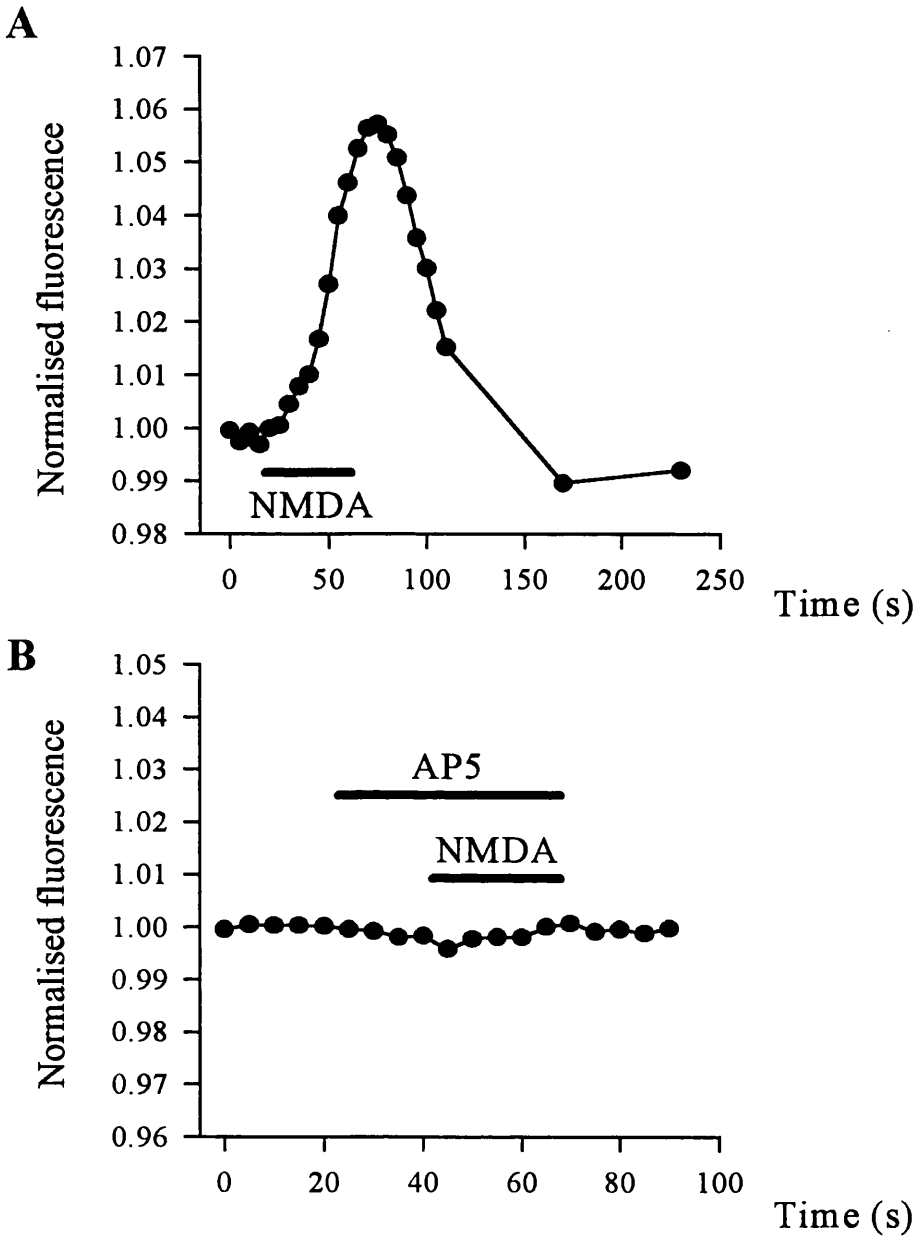

Figure 6.6

NMDA produces increases in $[Ca^{2+}]_i$ in E8 chick retina that are blocked by AP5.

A. 100μM NMDA evokes increases in $[Ca^{2+}]_i$ from E8 onwards. **B.** AP5 (50μM) blocks the response to NMDA (100μM). All experiments were performed in the presence of CNQX (20μM).

in chick retina tested from E8 onwards. Retinae tested prior to this time did not respond to NMDA (n=4). To compare Ca^{2+} responses to NMDA on different embryonic days the data was normalised to the mean of the responses obtained at E12, the day on which the largest changes in fluorescence were obtained. The normalised response to NMDA is shown plotted against embryonic day in figure 6.7. The mean fluorescence changes produced by 100μM NMDA increased from 23.1±2.2% of the maximum response at E8 (n=3) to 54.3±6.8% at E10 (n=4). The Ca^{2+} responses peaked at E12 (mean= 100±25%, n=3) and declined slightly at E13 (mean=83.1±22.7%, n=4). The decline was not significant at the 5% level. Retinae subsequent to E13 were not tested.

6.3.7 Ca^{2+}-permeable non-NMDA receptors are expressed in the embryonic chick retina from E6 onwards

Biochemical studies show that glutamate receptors are not present in the chick retina until E7 (Somahano et al., 1988). While, as shown above, Ca^{2+} elevations in response to NMDA were not apparent until after this day, the presence of Ca^{2+}-permeable AMPA/kainate receptors can be demonstrated in E6 chick retina using the Co^{2+}-staining technique (see chapter 5 and Catsicas et al., 1995). The action of the non-NMDA receptor agonist kainate on $[Ca^{2+}]_i$ was studied in early embryonic chick retina. All experiments were carried out with the NMDA receptor antagonist AP5 (20μM) and the Ca^{2+} channel blockers diltiazem and nifedipine (both 20μM) present in the external solution (solution A, table 2.1.). The composition of this solution was chosen to restrict the entry of Ca^{2+} to that through the non-NMDA receptor channel itself. Figure 6.8 shows the dose-response relationship for the Ca^{2+} responses produced by kainate in E9 retina. 1μM kainate produced a small change in

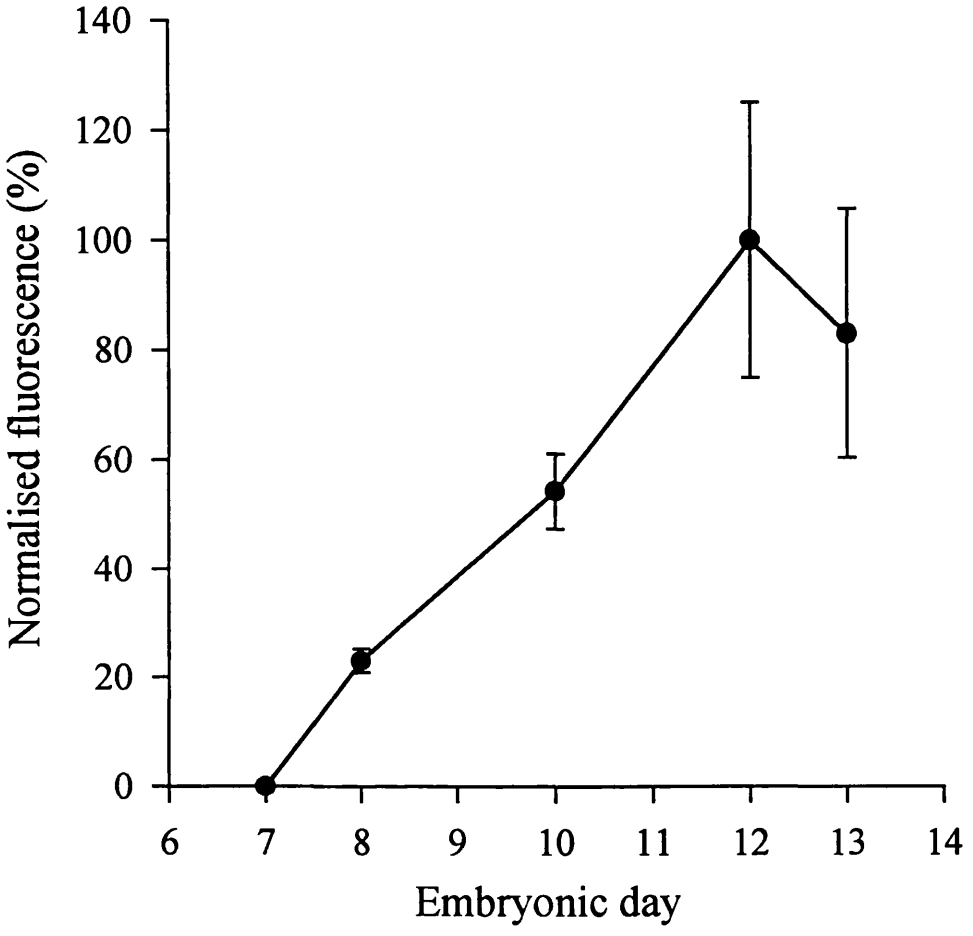

Figure 6.7

The developmental profile of the Ca^{2+} response produced by 100μM NMDA. The change in fluorescence (normalised to the mean of the response at E12) produced by application of 100μM NMDA as a function of embryonic day. Responses to NMDA were not apparent before E8 and peaked at E12.

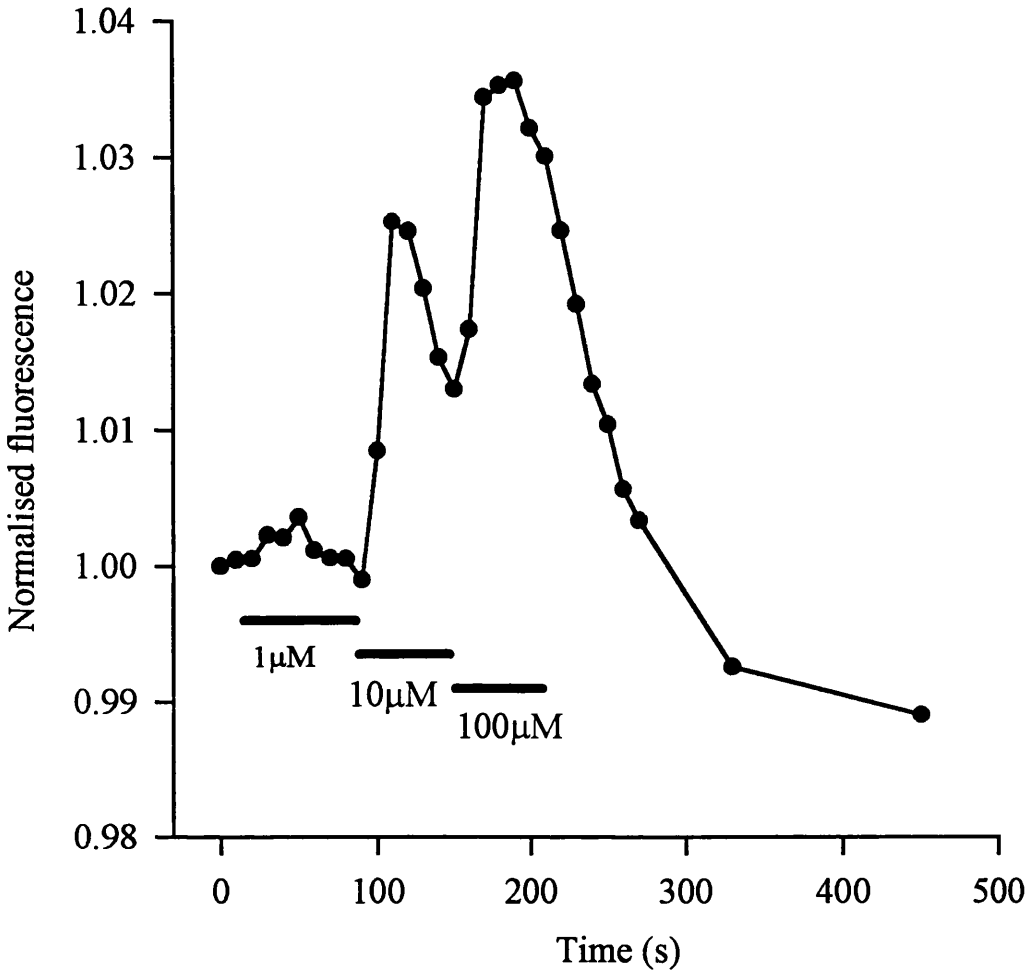

Figure 6.8

The dose-response relationship for the kainate-evoked changes in fluorescence in E9 retina.

Kainate was bath applied at concentrations of 1, 10 and 100μM. 1μM kainate produced only a small change in fluorescence. The fluorescence change increased with increasing concentrations of the drug. 100μM kainate was applied before the response to 10μM kainate had subsided. However, these data show that the top of the dose-response curve is higher than 10μM. The duration of the kainate application is indicated by a solid bar. The external solution contained AP5, diltiazem and nifedipine.

fluorescence intensity, while 10 and 100μM produced larger increases.

It was possible that some of the Ca^{2+}-influx produced by kainate resulted from the activation of voltage-gated Ca^{2+} channels that were not blocked by diltiazem and nifedipine, thus Na^+ in the external solution was replaced by choline. The object of this manoeuvre was to prevent the depolarization produced by Na^+ entry through non-NMDA receptors. In the absence of Na^+, K^+ efflux through the receptor should result in hyperpolarization. Kainate was able to evoke Ca^{2+} responses when Na^+ was replaced by choline in the Ringer's solution used (solution A, table 2.1 with NaCl replaced by choline chloride). The changes in $[Ca^{2+}]_i$ produced by kainate in choline Ringer's in E7 retina (n=3) are shown in figure 6.9. Raw fluorescence images taken before, during and after drug application are shown above a plot of the normalised fluorescence against time. These experiments were performed in the presence of AP5, diltiazem and nifedipine. The results suggest that effects secondary to kainate-evoked depolarization, such as activation of voltage-gated Ca^{2+} channels or release of glutamate that then acts at NMDA receptors, are not responsible for the increase in Ca^{2+} seen on application of kainate.

Subsequent to the kainate-evoked response the $[Ca^{2+}]_i$ often fell significantly below resting levels (as seen in figure 6.9). If Ca^{2+} is released from internal stores secondary to non-NMDA receptor activation regulatory mechanisms may pump Ca^{2+} out of the cytoplasm into internal Ca^{2+} stores to replenish them or into the external medium. This may temporarily reduce Ca^{2+} levels to below baseline if Ca^{2+} is removed from the cytoplasm at a higher rate than it is replaced. After application of high concentrations of kainate the retina often did not respond to further treatment with the drug. If Ca^{2+} release from internal stores contributes towards the kainate-evoked

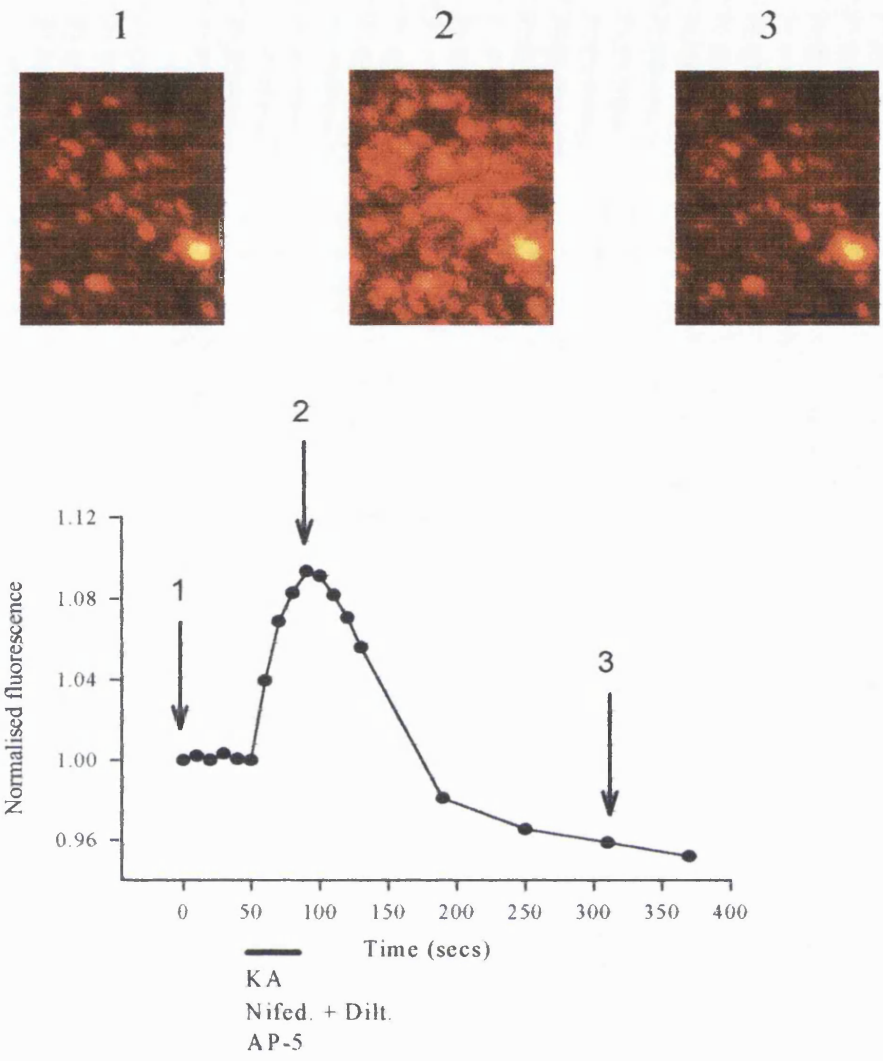

Figure 6.9

Increases in $[Ca^{2+}]_i$ in response to kainate in the absence of external Na^+. Background-subtracted fluorescence images corresponding to periods before (1), during (2) and after (3) application of 100μM kainate to E7 retina. Kainate evoked a fluorescence increase (2) when Na^+ was replaced with choline and AP5, diltiazem and nifedipine were co-applied. The solid black scale bar represents 100μm. The graph is a plot of the normalised fluorescence as a function of time. The period of kainate application is indicated by a solid bar. The fluorescent images shown above the graph are taken at the times indicated by the arrows marked 1, 2 and 3.

response then this failure of the response may be due to depletion of internal Ca^{2+} pools that then take a long time to refill.

6.3.8 Pharmacology of the kainate-evoked Ca^{2+} response

In order to determine whether or not kainate elevates $[Ca^{2+}]_i$ through activation of non-NMDA receptors, CNQX (50μM) was co-applied to cells along with kainate. Second responses to kainate were often difficult to obtain (see above) so kainate was applied with CNQX before it was applied alone. The Ca^{2+} response evoked by kainate in the presence of CNQX was greatly reduced in comparison to that produced by kainate alone (by between 50-75%, n=16). Figure 6.10 shows the increase in fluorescence in an E9 retina produced by application of 10μM kainate in the presence and absence of 50μM CNQX. In this example CNQX reduced the kainate-evoked response by about 75%.

Kainate may produce its effects on $[Ca^{2+}]_i$ through activation of AMPA/kainate receptors or kainate-preferring receptors. Application of the AMPA/kainate receptor agonist AMPA (100μM) evoked increases in $[Ca^{2+}]_i$ in embryonic chick retina (n=10). Figure 6.11 shows an example of the fluorescence increase produced by 100μM AMPA when applied to E8 retina. The AMPA-evoked response was blocked by addition of the AMPA/kainate receptor antagonist NBQX (10μM) (n=2). These experiments were carried out in the presence of AP5, diltiazem, nifedipine (all 20μM) and diazoxide (500μM). Diazoxide was employed in order to block the rapid desensitization characteristic of AMPA/kainate receptors (Yamada and Rothman, 1993, but see chapter 3). Responses to AMPA were obtained in the absence of diazoxide but the increases in fluorescence were small.

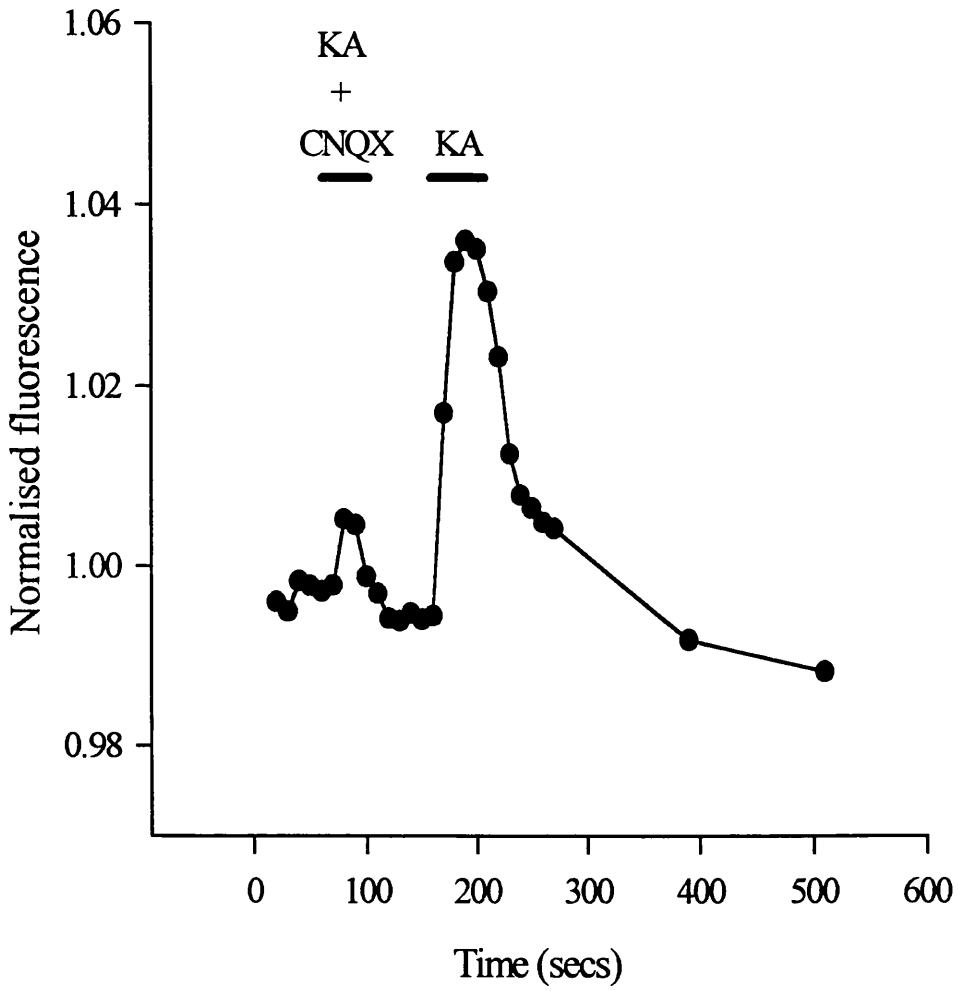

Figure 6.10

CNQX reduces the Ca^{2+} response to kainate.

Co-application of 10μM kainate with 50μM CNQX produced only a small increase in fluorescence in E9 retina. After CNQX was washed off kainate alone evoked a significantly larger increase.

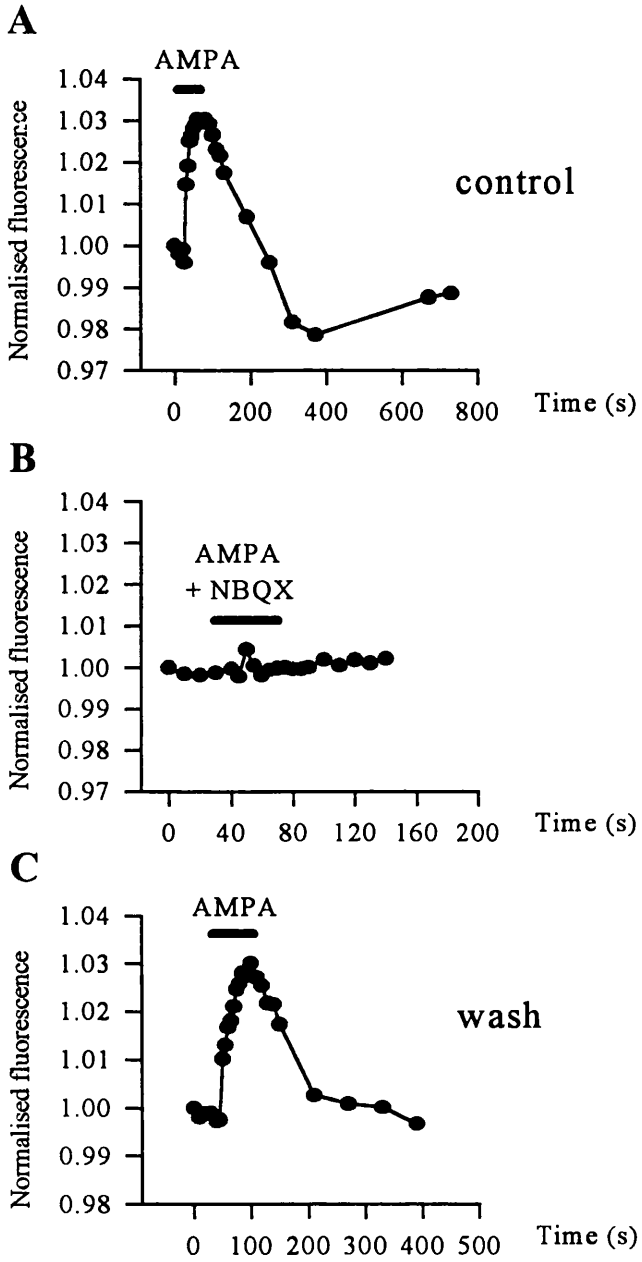

Figure 6.11

AMPA responses are blocked by NBQX.

A. 100μM AMPA evoked an increase in fluorescence in E8 retina in the presence of AP5, diltiazem, nifedipine and diazoxide. **B.** The AMPA-evoked Ca^{2+} response was blocked by 10μM NBQX. **C.** The recovery of the response to AMPA after washing NBQX from the external solution.

Significant increases in $[Ca^{2+}]_i$ result from application of kainate when voltage-gated Ca^{2+} channels are blocked with diltiazem and nifedipine and when depolarization is prevented by the use of choline Ringer's. AMPA also produced Ca^{2+} responses in the presence of diltiazem and nifedipine. These data are consistent with the presence of Ca^{2+}-permeable AMPA/kainate receptors in embryonic chick retina.

6.3.9 The change in the kainate-evoked Ca^{2+} response with embryonic age

To compare the Ca^{2+} responses produced by kainate on different embryonic days, the responses were normalised to the mean change in fluorescence evoked by 100μM kainate at E13 (the day when the largest responses to kainate were seen). Retinae subsequent to E13 were not tested. All experiments were carried out in the presence of AP5, diltiazem and nifedipine. At E4 responses to application of 100μM kainate were absent (n=4). Small increases in fluorescence were produced at E6 (mean=4.3±2%) (n=6), E7 (mean=11.4±0.9%) (n=3) and E8 (mean=16±3.7%) (n=7). By E9 the mean normalised fluorescence increase produced by kainate was 19.4±5.4% (n=7) of that obtained at E13 (100±16.2%, n=5) (figure 6.12).

6.3.10 Localization of Ca^{2+}-permeable non-NMDA receptors using confocal imaging

In order to determine which cells in the embryonic chick retina expressed Ca^{2+}-permeable non-NMDA receptors confocal imaging techniques were used. Kainate was applied to flat-mounted retinae and a confocal microscope used to produce sections in the ZX plane through the tissue before, during and after drug application. Dye loading varied between layers of the retina, with cells on the GCL side loading weakly and photoreceptors in

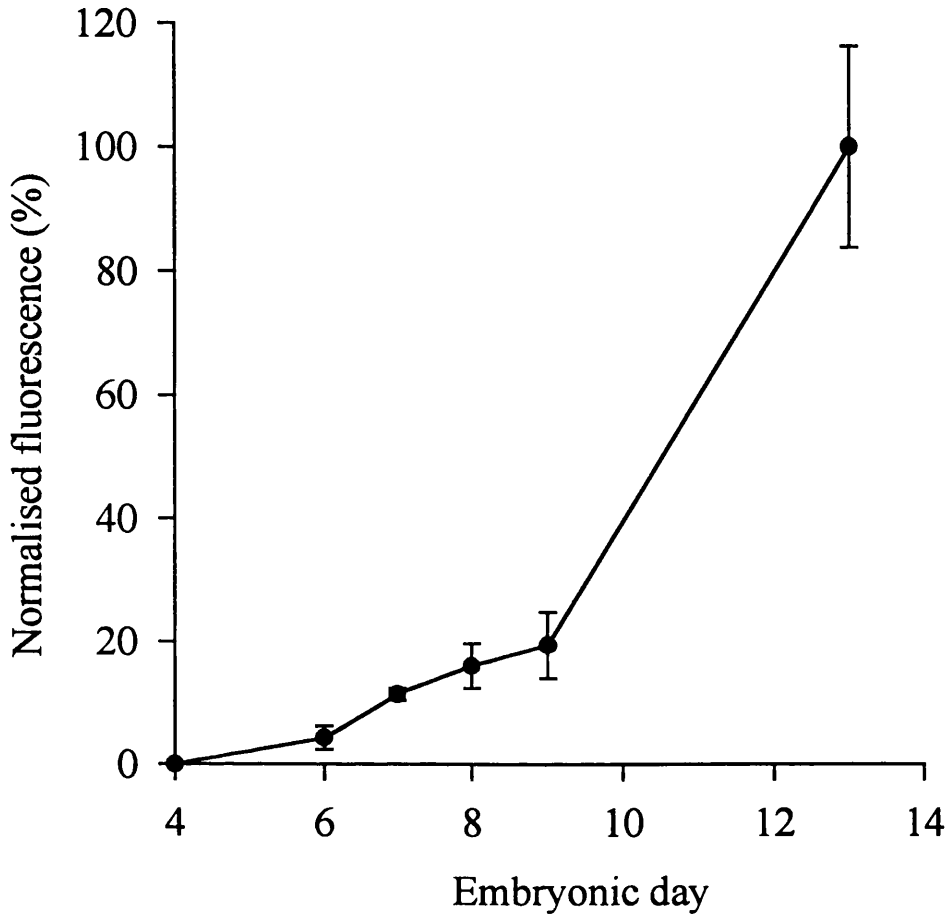

Figure 6.12

The effects of 100μM kainate on $[Ca^{2+}]_i$ plotted as a function of embryonic day.

The fluorescence signal normalised to the mean of the responses at E13 is shown against embryonic day. Responses to kainate were absent in E4 chick retina. Small fluorescence changes were apparent from E6 to E9 and by E13 kainate evoked large fluorescence increases.

the ONL loading very brightly. Bath application of 100μM kainate to a piece of E9 chick retina loaded with Calcium Green produced an increase in fluorescence in cells located in the GCL and INL (figure 6.13). Experiments were carried out in the presence of AP5, diltiazem and nifedipine as described in section 6.3.6. The results obtained here are consistent with those obtained in Co^{2+}-staining experiments (see section 4.3.1).

6.3.11 GABA elevates $[Ca^{2+}]_i$ in the retina at early times in development

GABA is a major inhibitory neurotransmitter in the adult retina, however, it has been reported to have a depolarizing action in the immature nervous system (Segal and Barker, 1984, Müeller et al., 1984, Cherubini et al., 1991 Wu et al., 1992, Yamashita and Fukuda, 1993a). Bath application of 100μM GABA caused a rise in $[Ca^{2+}]_i$ in embryonic chick retinae between E4 and E12 (n=29), suggesting that it depolarizes retinal neurons during this period. The effects of GABA could be blocked by the $GABA_A$ receptor antagonist bicuculline (n=6). Figure 6.14A shows the fluorescence increase evoked by application of 100μM GABA to E6 retina in solution A (table 2.1). When 50μM bicuculline was co-applied with GABA the increase in $[Ca^{2+}]_i$ seen in response to GABA alone was abolished (figure 6.14B). The block was reversible and the GABA-evoked response returned once bicuculline was removed from the external solution (figure 6.14C). These data indicate that embryonic chick retinae express $GABA_A$ receptors early in development and that at this time the action of GABA is to depolarize retinal cells.

In contrast to GABA the inhibitory neurotransmitter glycine failed to produce changes in $[Ca^{2+}]_i$ in 10 retinae tested between E6 to E14.

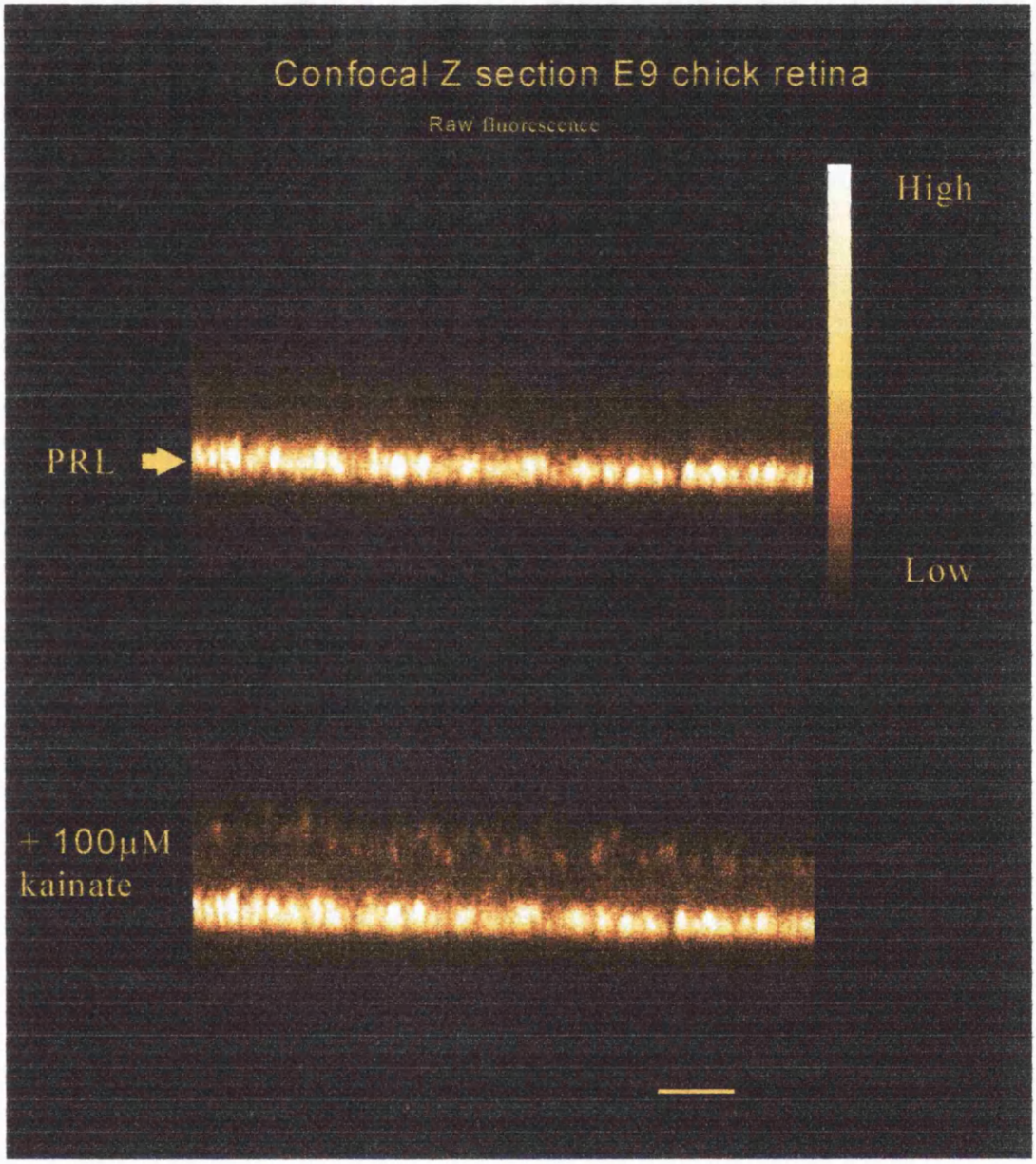

Figure 6.13

Localization of cells expressing Ca^{2+}-permeable non-NMDA receptors. Confocal Z sections taken before (top image) and during (bottom image) application of 100μM kainate to E9 chick retina. Kainate evoked an increase in fluorescence in cells located in the INL and GCL. The photoreceptor layer (PRL) is the most fluorescent layer. The yellow scale bar represents 50μm.

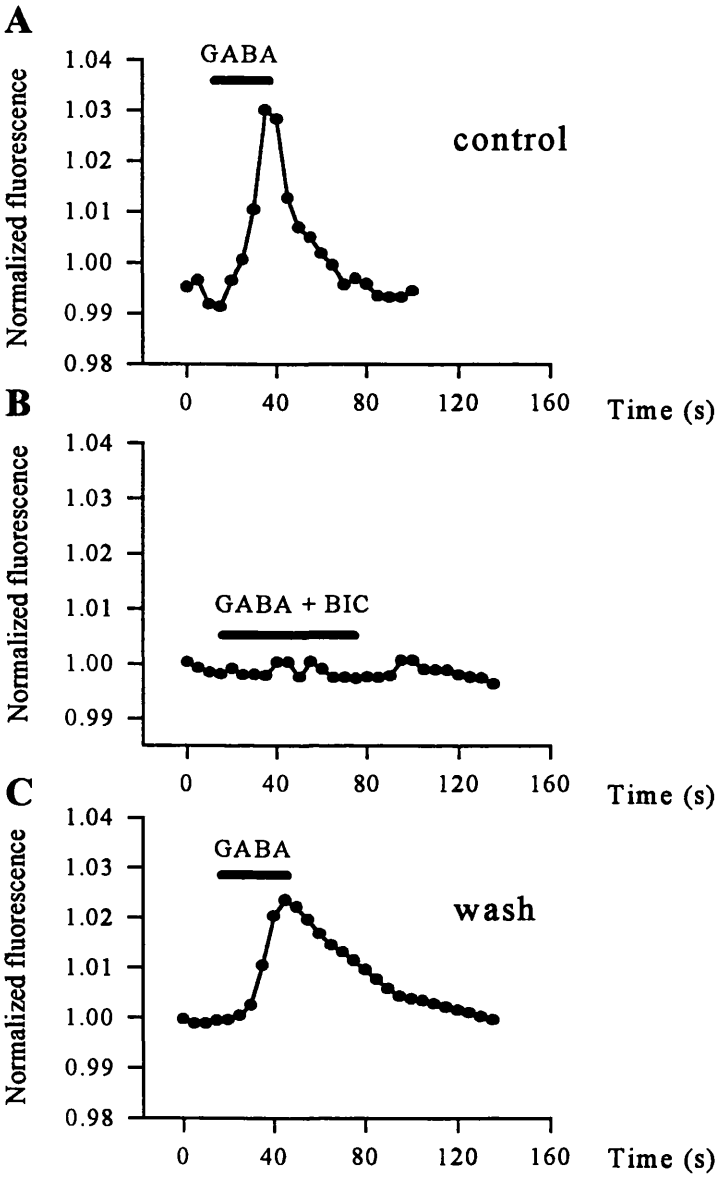

Figure 6.14

$GABA_A$ receptors are expressed in embryonic chick retina.

A. Bath application of 100μM GABA evoked an increase in fluorescence in E6 retina. **B.** The GABA-evoked response was blocked by co-application of the $GABA_A$ antagonist bicuculline (50μM). **C.** The GABA-evoked response returned after washing bicuculline from the external solution.

6.3.12 The change in the GABA-evoked Ca^{2+} response with embryonic age

Ca^{2+} responses to GABA were obtained as early as E4. Retinae prior to this age were not tested. At E4 83% of retinae responded to GABA (n=6), and on days subsequent to E4 and up until E12 GABA produced increases in $[Ca^{2+}]_i$ in all retinae tested (n=23). By E14 GABA-evoked changes in $[Ca^{2+}]_i$ were no longer apparent (n=3). Fluorescence changes evoked by 100μM GABA were normalised with respect to the mean of the data obtained at E8, the day when the largest responses to GABA were seen. The normalised data was then plotted as a function of embryonic age (figure 6.15). The mean change in fluorescence produced by GABA was 48±8.7% of the maximum response at E4 (n=5), 38.8±5.4% at E6 (n=8), 56±6.7% at E7 (n=5) and peaked at E8 (100±7.1%, n=4). The GABA-evoked Ca^{2+} responses declined by E12 (mean 70±8.2%, n=6) and were absent by E14 (n=3). Since GABA hyperpolarizes the membranes of nerve cells in the mature retina the absence of Ca^{2+} responses at late times in development may reflect a switch from its depolarizing action earlier on.

6.4 Discussion

The results described in this chapter show that embryonic chick retinal cells express neurotransmitter receptors of several different kinds early in development. The ability of these receptors to affect a change in $[Ca^{2+}]_i$ varies with time.

6.4.1 Muscarinic ACh responses in embryonic chick retina

ACh can produce increases in $[Ca^{2+}]_i$ from E4 to E8 (section 6.3.1 and

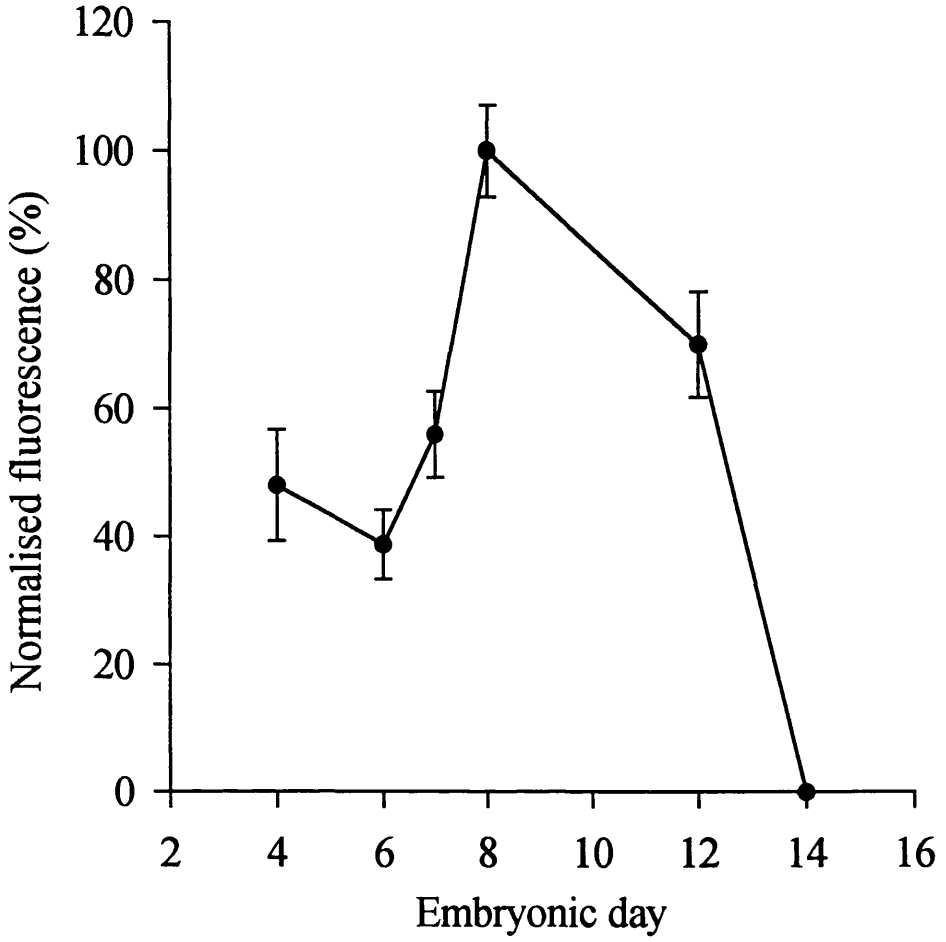

Figure 6.15

The effects of 100μM GABA on $[Ca^{2+}]_i$ plotted as a function of embryonic day.

Ca^{2+} responses to GABA were present at E4 and peaked at E8. By E14 GABA no longer evoked increases in $[Ca^{2+}]_i$.

6.3.2). The increases in $[Ca^{2+}]_i$ produced by ACh were largely blocked by the muscarinic antagonist atropine but only slightly reduced by the nicotinic antagonists hexamethonium and tubocurarine. Nicotinic ACh receptors can be detected biochemically in chick retina by E6 (Vogel and Nirenburg, 1976) and *in situ* hybridization studies have shown that the mRNAs for subunits of the nAChR are present in chick retina as early as E4.5 (Hamassaki-Britto et al., 1994b). However, the data obtained here suggests that muscarinic receptors exert a much more powerful influence on $[Ca^{2+}]_i$ than do nicotinic receptors early in chick retinal development. In the rabbit retina Wong (1995) has shown that muscarinic receptor activation produces Ca^{2+} increases between E20 and P5. She showed that muscarinic responses are confined to cells in the ventricular zone, while nicotinic responses first appear in early ganglion and amacrine cells.

Blocking voltage-gated Ca^{2+} channels with diltiazem and nifedipine produced a small reduction in both the ACh-evoked peak and the steady-state Ca^{2+} response. This reduction may reflect a contribution from voltage-gated channels that allows Ca^{2+} to enter secondary to ACh-evoked membrane depolarization. Yamashita et al. (1994b) have shown that nifedipine is ineffective in blocking the Ca^{2+} response produced by ACh in the embryonic chick retina and that removal of external Ca^{2+} causes only a minor reduction in the amplitude of the Ca^{2+} signal. They suggest that Ca^{2+} release from intracellular stores is responsible for the Ca^{2+} elevation produced by muscarinic receptor stimulation. This suggestion is supported by experiments using postnatal rabbit and rat retina and dissociated cells from whole E4 chick embryos where muscarinic receptor activation evokes Ca^{2+} release from IP_3-sensitive stores (Cutcliffe and Osbourne, 1987, Osbourne, 1988, Lohmann et al., 1991). In contrast the experiments of Wong (1995) show that muscarinic responses in the rabbit retina are completely abolished in the absence of

extracellular Ca^{2+} or in the presence of high concentrations of nickel, which blocks receptor-operated channels. She suggests that the muscarinic response is a result of Ca^{2+}-influx through receptor-operated channels rather than the release of Ca^{2+} from internal stores. This conclusion is supported by the observation that antagonists of voltage-gated Ca^{2+} channel do not affect the ACh-evoked response.

It is likely that the muscarinic ACh receptor plays an important role in the development of the retina since the $[Ca^{2+}]_i$ changes it produces are maximal at early times and subsequently decline. The ACh-evoked Ca^{2+} responses were greatest at E4 at a time when retinal cells are still undergoing mitosis (Kahn, 1974) and few cells have completed their differentiation (Nishimura, 1980). The response then declines reaching a plateau at E7-E8. In contrast, binding studies show that muscarinic binding sites are maximal at E13 in chick retina (Sugiyama et al., 1977). This makes it unlikely that the decline in the response to ACh is due to a decrease in receptor density. Yamashita et al. (1994b) suggest that the decrease in the retinal Ca^{2+} signal could be due to thickening of the retina as development progresses. However, the thickness of the retina only increases by 50% from E4 to E8 (Shen et al., 1956, Araki et al., 1982) and the fluorescence decrease in the ACh response during this period was 9 fold. A more likely explanation may be that the decline reflects a decrease in the ability of muscarinic receptor stimulation to mobilize Ca^{2+} from internal stores. Activation of some subtypes of muscarinic ACh receptors leads to IP_3 production (reviewed by Hulme et al., 1990) which then triggers Ca^{2+} release from internal stores (Berridge and Irvine, 1984). Osbourne et al. (1988) suggest that muscarinic receptors are more tightly coupled to phosphatidylinositol hydrolysis at early stages in chick retinal development. Thus the decline in the response to ACh may result from a decrease in IP_3 production and thus a reduction in Ca^{2+} release from internal

stores. Retinae subsequent to E8 were not tested with ACh, however it is likely that ACh evokes Ca^{2+} responses later in development due to an increase in the expression of nicotinic receptors (Vogel and Nirenburg, 1976, Hamassaki-Britto et al., 1994b).

6.4.2 NMDA responses in embryonic chick retina

NMDA produced increases in $[Ca^{2+}]_i$ in embryonic chick retina from E8 onwards which were blocked by application of the NMDA receptor antagonist AP5. The signals increased in amplitude with age and peaked at E12. NMDA receptors are well established as Ca^{2+}-permeable ligand-gated channels (MacDermott et al., 1986, Mayer and Westbrook, 1987, Ascher and Nowak, 1988) and exert a powerful influence on $[Ca^{2+}]_i$ in the adult nervous system. However, Ca^{2+} may only enter through the NMDA receptor once the Mg^{2+} block of the channel is relieved by membrane depolarization. Thus electrical activity is required before activation of NMDA receptors can affect $[Ca^{2+}]_i$. In the ferret and cat waves of electrical activity sweep across the retina at times just prior to the period of synapse formation (Meister et al., 1991, Wong et al., 1995). In the chick synapses first appear around E12 (Sheffield and Fischman, 1970, Hughes and LaVelle, 1974) and thus NMDA receptors are first expressed at a time when in other retinae spontaneous electrical activity begins (Meister et al., 1991).

6.4.3 Ca^{2+}-permeable non-NMDA receptors are expressed in embryonic chick retina

Kainate elevates $[Ca^{2+}]_i$ when applied to embryonic chick retina at concentrations of 1μM or more in the presence of AP5, diltiazem and nifedipine and in the absence of external Na^+. The effects of kainate are

reduced by the non-NMDA receptor antagonist CNQX. The AMPA/kainate receptor agonist AMPA also produces Ca^{2+} responses.

Activation of non-NMDA receptors with kainate will lead to membrane depolarization. This may open voltage-gated Ca^{2+} channels leading to the release of glutamate that may subsequently stimulate NMDA receptors. Both these secondary effects would be expected to produce Ca^{2+}-influx. It is also possible that depolarization could release ACh or some other transmitter that acts at a Ca^{2+}-permeable receptor or releases Ca^{2+} from intracellular stores. However, there are a number of reasons to believe that the Ca^{2+} signal produced by kainate results from a direct action at AMPA/kainate receptors. The involvement of NMDA receptors is unlikely because the response to kainate can occur at a time when NMDA fails to evoke a response (see above) and the response is not prevented by application of AP5. The responses are unlikely to result from the activation of voltage-gated Ca^{2+} channels because preventing the depolarization expected from the application of kainate with choline Ringer's and blocking the Ca^{2+} channels with diltiazem and nifedipine had no significant effect on the Ca^{2+} signal. These manoeuvres would also be expected to prevent any depolarization-evoked release of transmitter from retinal cells. Kainate can elevate $[Ca^{2+}]_i$ via a metabotropic receptor (Shiells et al., 1981), however, application of the metabotropic antagonist AP3 failed to prevent the rise in $[Ca^{2+}]_i$ (data not shown).

I did not investigate the role played by Ca^{2+}-induced Ca^{2+}-release (CICR) in the production of the kainate-evoked signal, however Kocsis et al. (1993) have shown that CICR plays an important role in the Ca^{2+} signals produced by cultured rat retinal cells in response to kainate. The involvement of CICR would explain some of the features of the response to kainate in the intact retina. The difficulty in obtaining responses to kainate following

application of high concentrations of the drug could result from the time taken to refill the intracellular Ca^{2+} store. The undershoot of $[Ca^{2+}]_i$ that follows stimulation of the AMPA/kainate receptor may result from the pumping of Ca^{2+} into the store and out of the cell at a rate greater than that of the steady-state Ca^{2+}-influx. CNQX was not effective at abolishing the rise in $[Ca^{2+}]_i$ as one would expect from its ability to block the kainate-evoked current in patch-clamp experiments (see chapter 4). This may in part be explained if kainate is linked to an increase in $[Ca^{2+}]_i$ by some mechanism that has a high gain such as CICR. Since CNQX is a competitive antagonist the small number of channels activated by kainate could then act to trigger CICR or some other mechanism releasing huge quantities of Ca^{2+} into the cytoplasm.

Responses to kainate were observed from E6 and increased with age to be 7 fold larger in amplitude by E14. The most likely explanation for the increase in the Ca^{2+} signal is an increase in either the density of Ca^{2+}-permeable non-NMDA receptors in the cell membrane or in the number of cells that carry the receptor. Results of confocal imaging (section 6.3.10) and Co^{2+}-staining experiments of retinal explants in chapter 4 suggest that many of the cells in the GCL and INL express Ca^{2+}-permeable non-NMDA receptors. However, since the number of Co^{2+}-stained cells decreases subsequent to E12, it is unlikely that the increase seen in the Ca^{2+} response to non-NMDA receptor stimulation simply results from increased cell number.

Ca^{2+}-permeable non-NMDA receptors appear in the embryonic chick retina before NMDA receptors (see above). Unlike NMDA receptors, non-NMDA receptors do not require membrane depolarization to enable Ca^{2+}-entry, and thus may exert an influence over $[Ca^{2+}]_i$ early in development prior to the onset of electrical activity.

6.4.4 GABA depolarizes retinal neurons early in chick retinal development

GABA usually acts as an inhibitory transmitter in the CNS. However, GABA produces increases in $[Ca^{2+}]_i$ early in embryonic chick retinal development which suggests that it depolarizes cells at that time. It is likely that the increase in Ca^{2+} is due to the opening of voltage-gated Ca^{2+} channels because it has been shown that it can be prevented by Ca^{2+} channel blockers (Yamashita and Fukuda, 1993a). GABA evoked Ca^{2+} responses at E4 but by E14 these responses were no longer apparent. This is probably because at later times GABA hyperpolarizes or shunts embryonic chick retinal cells as it does in the adult (Heidelberger and Matthews, 1991, Yamashita and Wässle, 1991). The effect of GABA on $[Ca^{2+}]_i$ was blocked by the $GABA_A$ antagonist bicuculline. $GABA_A$ receptors gate a Cl^--permeable channel and activation of these receptors normally allows an influx of Cl^- that leads to inhibition of neuronal excitability (Bormann, 1988, Feigenspan et al., 1993, Qain and Dowling, 1993). There are two possible explanations for the depolarizing actions of GABA in the embryonic retina. Firstly, cells may maintain an outward driving force for Cl^- by actively pumping Cl^- into the cell (Nishi et al., 1974, Gallagher et al., 1983, Misgeld et al., 1986, Reichling et al., 1994). Zhang et al. (1991) suggest that as development progresses the Cl^- extrusion system develops moving the Cl^- reversal potential more negative. Secondly, GABA could depolarize cells if its receptor was linked to a novel channel that was Na^+ and/or Ca^{2+}-permeable (Barker and Nicoll, 1973, Obata et al., 1978, Lambert et al., 1991). It remains to be discovered which of these mechanisms is responsible for the depolarizing action of GABA in the chick retina. GABA depolarizes retinal cells after the Ca^{2+} responses produced by ACh have declined and before the responses to kainate and NMDA have peaked. This suggests that GABA may have a developmental role specific to this period.

6.4.5 Functional implications of Ca^{2+} responses evoked by neurotransmitters early in retinal development

This chapter demonstrates that neurotransmitter receptors are expressed early in chick retinal development and that different receptors are present during different periods in development (see figure 6.16). Ca^{2+} responses to ACh and GABA are present by E4, several days before the appearance of glutamate responses. The Ca^{2+} response to ACh is greatest at E4 and the GABA response peaks at E8 when the ACh response has declined 9 fold. This suggests that these transmitters have specific roles early in development. Yamashita and Fukuda (1993b) showed in E3 chick embryo *in vitro* that muscarinic ACh Ca^{2+} responses initiated folding of the neural retina during optic cup formation. It is also possible that ACh is involved in the folding of the neural plate because increased acetlycholinesterase in amniotic fluid causes neural defects in chick (Pilowsky et al., 1982) and in humans (Smith et al., 1979). Early in development GABA may act as a trophic factor activating voltage-gated Ca^{2+} channels. For example in cultures of embryonic chick brain and retina GABA promotes neurite outgrowth (Sporerri, 1988, Michler, 1990, but see chapter 5) and in cultured cerebellar granule cells GABA induces synaptogenesis (Meier et al., 1984, Hansen et al., 1987).

Ca^{2+}-permeable non-NMDA receptors are not expressed until E6 in the chick retina. The effects of activation of these receptors during development are the subject of chapters 4 and 5 in this thesis. Prolonged activation or inhibition of AMPA/kainate receptors leads to a reduction in neurite outgrowth in cultured retinal cells (chapter 5) and the down-regulation of Ca^{2+}-entry into cells expressing these receptors (see chapter 4). This may protect neurons against cell death during pruning of cells that have failed to establish synaptic contacts later in development.

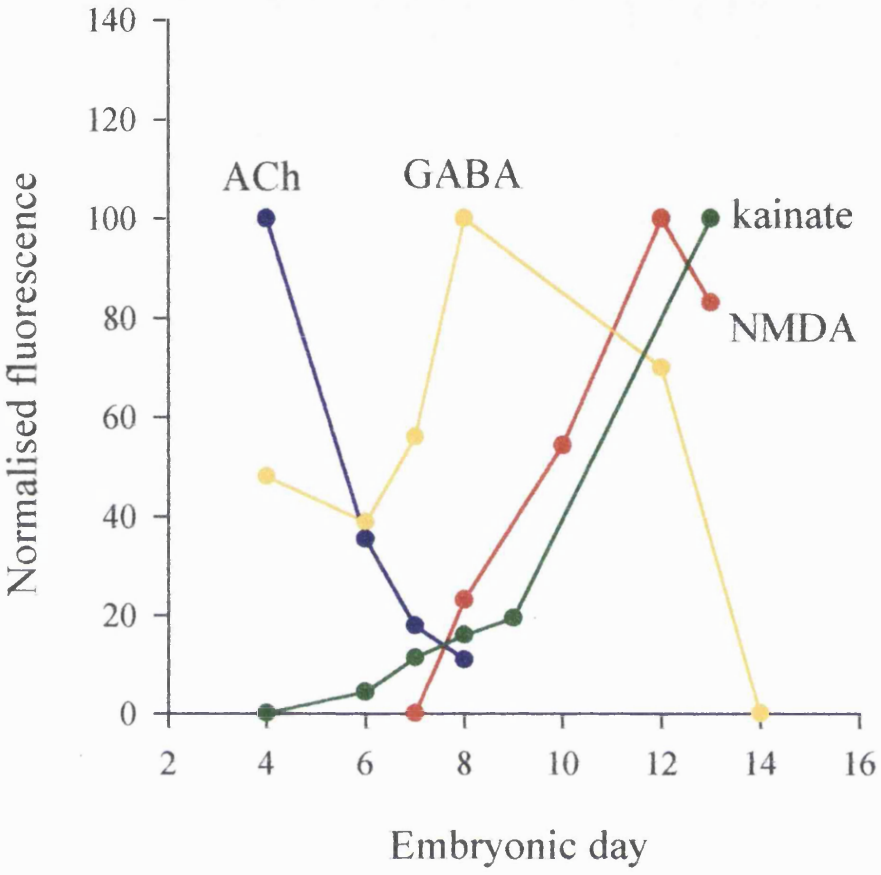

Figure 6.16

The developmental profile of the Ca^{2+} responses evoked by neurotransmitters in the developing chick retina.

Ca^{2+} responses produced by ACh are maximal at E4. At this time responses to GABA are small and responses to kainate and NMDA are absent. GABA-evoked Ca^{2+} signals become maximal at E8, when responses to ACh have declined 9 fold and when kainate and NMDA responses are small. GABA ceases to evoke Ca^{2+} signals by E14. Around this time Ca^{2+} signals evoked by NMDA and kainate are maximal.

NMDA responses do not appear until E8 in the chick retina, 2 days after Ca^{2+} responses to kainate were observed. If during early development electrical activity is absent then significant NMDA-evoked Ca^{2+} increases are unlikely to occur. At later times NMDA may have some influence over $[Ca^{2+}]_i$ since action potential activity involving ganglion and amacrine cells is known to occur. NMDA receptor activation affects neurite outgrowth (Brewer and Cotman, 1989), cell survival (Balázs, 1988) and cell migration (Kumoro and Rakic, 1993) and has been implicated in visual system development. For example in the frog NMDA antagonists disrupt the structure of retinal ganglion cell projections while NMDA increases the eye-specific segregation of their branches (Cline and Constantine-Paton, 1990, Cline et al., 1987).

6.4.6 Further studies

The experiments described in this chapter have shown that receptors for a number of transmitters exist at early times in development and the experiments described in chapters 4 and 5 show that their activation may have important effects. However, as yet there is little information concerning the release of transmitters in the embryonic retina. Two possible mechanisms exist for transmitter release; Ca^{2+}-dependent exocytosis and reversed uptake. It is important to determine whether and at what time in development these mechanisms become important. If significant depolarization-evoked transmitter release occurs at early times in the intact retina it opens the possibility of significant interaction between different neurotransmitters and their receptors. These interactions may be complex and have not been investigated here.

References

Abe, T. Sugihara, H., Nawa, H., Shigemoto, R., Mizuno, N. and Nakanishi, S. (1992) Molecular characterization of a novel metabotropic glutamate receptor mGLUR5 coupled to inositol phosphate/Ca^{2+} signal transduction. J. Biol. Chem. 267: 13361-13368.

Adam-Vizi, V. (1992) External Ca^{2+}-independent release of neurotransmitters. J. Neurochem. 58: 395-405.

Akazawa, C., Ohishi, H., Nakajima, Y., Okamoto, N., Shigemoto, R., Nakanishi, S. and Mizuno, N. (1994) Expression of mRNAs of L-AP4-sensitive metabotropic glutamate receptors (mGLUR4, mGLUR6, mGLUR7) in the rat retina. Neurosci. Lett. 171: 52-54.

Al-Mohanna, F.A., Cave, J. and Bolsover, S.R. (1992) A narrow window of intracellular calcium concentration is optimal for neurite outgrowth in rat sensory neurones. Dev. Brain Res. 70: 287-290.

Alder, R. (1986) The differentiation of retinal photoreceptors and neurons *in vitro*. Progress in Retinal Research, eds. Osbourne, N. and Chader, G. Peragmon Press, London 6: 1-27.

Alder, R. and Lindsey, J.D. (1985) Photoreceptor cells *in vivo* and monolayer culture: development of opsin-like immunoreactivity. Invest. Opthalmol. Vis. Sci. 26: 335.

Andine, P., Lehmann, A., Eilren, K., Wennberg, E., Kjeller, I., Nielsen, T. and Hagberg, H. (1988) The excitatory amino acid antagonist kynurenic acid

administered after hypoxic-ischemia in neonatal rats offers neuroprotection. Neurosci. Lett. 90: 208-212.

Araki, M. (1984) Immunochemical study on photoreceptor cell differentiation in the cultured retina of the chick. Dev. Biol. 103: 313-318.

Araki, M., Ide, C. and Saito, T. (1982) Ultrastructural localization of acetylcholinesterase activity in the developing chick retina. Acta Histochem. Cytochem. 15: 242-255.

Aramori, I. and Nakanishi, S. (1992) Signal transduction and pharmacological characteristics of a metabotropic glutamate receptor, mGLUR1, in transfected CHO cells. Neuron 8: 757-765.

Arriza, J.L., Fairman, W.A., Wadiche, J.I., Murdoch, G.H., Kavanaugh, M.P. and Amara, S.G. (1994) Functional comparisons of three glutamate transporter subtypes cloned from human motor cortex. J. Neurosci. 14: 5559-5569.

Aruffo, C., Ferszt, R., Hildebrandt, A.G. and Cervos-Navarro, J. (1987) Low doses of L-monosodium glutamate promote neuronal growth and differentiation *in vitro*. Dev. Neurosci. 9: 228-239.

Ascher, P. and Nowak, L. (1988) The role of divalent cations in N-methyl-D-aspartate responses of mouse central neurons in culture. J.Physiol. 399: 247-266

Attwell, D., Barbour, B. and Szatkowski, M. (1993) Nonvesicular release of neurotransmitter. Neuron 11: 401-407.

Balázs, R., Hack, H. and Jorgensen, O.S. (1990) Interactive effects involving different classes of excitatory amino acid receptors and the survival of cerebellar granule cells in culture. Int. J. Neurosci. 8: 347-359.

Balázs, R., Jorgensen, O.S. and Hack, N. (1988) N-methyl-D-aspartate promotes the survival of cerebellar granule cells in culture. Neurosci. 27: 437-451.

Barbour, B., Brew, H. and Attwell, D. (1988) Electrogenic glutamate uptake in glial cells is activated by extracellular potassium. Nature 335: 433-435.

Barbour, B., Brew, H. and Attwell, D. (1991) Electrogenic uptake of glutamate and aspartate into glial cells isolated from the salamander (*Ambystoma*) retina. J. Physiol. 436: 169-193.

Barker, J.L. and Nicoll, R.A. (1973) The pharmacology and ionic dependency of amino acid responses in the frog spinal cord. J. Physiol. 228: 259-277.

Barnstable, C.J. and Dräger, U.C. (1984) THY-1 antigen: a ganglion cell specific marker in rodent retina. Neurosci. 11: 847-855.

Barnstable, C.J., Hofstein, R. and Akagawa, K. (1985) A marker of early amacrine cell development in rat retina. Dev. Brain Res. 20: 286-290.

Ben-Ari, Y., Cherubini, E. and Krnjevic, K. (1988) Changes in voltage dependence of NMDA currents during development. Neurosci. Lett. 94: 88-92.

Benveniste, M., Clements, J., Vyklicky, L. and Mayer, M.L. (1990) A kinetic analysis of the modulation of N-methyl-D-aspartic acid receptors by glycine in mouse cultured hippocampal neurones. J. Physiol. 428: 333-357.

Bernard, V., Normand, E. and Bloch, B. (1992) Phenotypical characterization of the rat striatal neurons expressing muscarinic receptor genes. J. Neurosci. 12: 3591-3600.

Berridge, M.J. and Irvine, R.F. (1984) Inositol triphosphate, a novel second messenger in cellular signal transduction. Nature 312: 315-321.

Bettler, B., Boulter, J., Hermans-Borgmeyer, I., O'Shea-Greenfield, A., Deneris, E.S., Moll, C., Borgmeyer, U., Hollmann, M. and Heinemann, S. (1990) Cloning of a novel glutamate receptor subunit, GLUR5: expression in the nervous system during development. Neuron 5:583-595.

Bettler, B., Egebjerg, J., Sharma, G., Pecht, G., Hermans-Borgmeyer, I., Moll, C., Stevens, C. and Heinemann, S. (1992) Cloning of a putative glutamate receptor: a low affinity kainate-binding subunit. Neuron 8: 257-265.

Bird, S.J. and Gulley, R.L. (1979) Evidence against a presynaptic mechanism for kainate neurotoxicity in the cochlear nucleus. Neurosci. Lett. 15: 55-60.

Bonner, T.I., Buckley, N.J., Young, A.C. and Brann, M.R. (1987) Identification of a family of muscarinic receptor genes. Science 237: 527-532.

Bonner, T.I., Young, A.C., Brann, M.R. and Buckley, N.J. (1988) Cloning and expression of the human and rat m5 muscarinic acetylcholine receptor genes. Neuron 1: 403-410.

Bormann, J. (1988) Electrophysiology of $GABA_A$ and $GABA_B$ receptor subtypes. Trends Neurosci. 11: 112-116.

Bormann, J., Hamill, O.P. and Sakmann, B. (1987) Mechanism of anion permeation through channels gated by glycine and γ-aminobutyric acid in mouse cultures spinal neurones. J. Physiol. 385: 243-286.

Boulter, J., Hollmann, M., O'Shea-Greenfield, A., Hartley, M., Deneris, E., Maron, C. and Heinemann, S. (1990) Molecular cloning and functional expression of glutamate receptor subunit genes. Science 249: 1033-1037.

Brandstatter, J.H., Hartveit, E., Sassoe-Pognetto, M. and Wassle, H. (1994) Expression of NMDA and high affinity kainate receptor subunit mRNAs in the adult rat retina. Eur. J. Neurosci. 6: 1100-1112.

Brecha, N. (1983) Retinal neurotransmitters: histochemical and biochemical studies. Chemical Neuroanatomy, ed Emson, P.C., Raven, New York. 85-129.

Brecha, N.C. and Weigmann, C. (1994) Expression of GAT-1, a high affinity gamma-aminobutyric acid plasma membrane transporter in the rat retina. J. Comp. Neurol. 345: 602-611.

Brew, H. and Attwell, D. (1987) Electrogenic glutamate uptake is a major current carrier in the membrane of axolotl retinal glial cells. Nature 327: 707-709.

Brewer, G.J. and Cotman, C.W. (1989) NMDA receptor regulation of

neuronal morphology in cultured hippocampal neurons. Neurosci. Lett. 99: 268-273.

Bridges R.J., Stanley, M., Anderson, M. Cotman, C. and Chamberlin, R. (1991) Conformationally defined neurotransmitter analogues. Selective inhibition of glutamate uptake by one pyrrolidine-2, 4-dicarboxylate diasteromer. J. Med. Chem. 34: 717-725.

Brorson, J.R., Manzolillo, P.A. and Miller, R.J. (1994) Ca^{2+} entry via AMPA/KA receptors and excitotoxicity in cultured cerebellar Purkinje cells. J.Neurosci. 14: 187-197.

Burnashev, N., Monyer, H., Seeburg, P.H. and Sakmann, B. (1992a) Calcium-permeable AMPA/kainate receptors in fusiform cerebellar glial cells. Science 256: 1566-1570.

Burnashev, N., Monyer, H., Seeburg, P.H. and Sakmann, B. (1992b) Divalent ion permeability of AMPA receptor channels is dominated by the edited form of a single subunit. Neuron 8: 189-198.

Burnashev, N., Zhou, Z., Neher, E. and Sakmann, B. (1995) Fractional calcium currents through recombinant GLUR channels of the NMDA, AMPA and kainate receptor subtypes. J. Physiol. 4852: 403-418.

Burt, D.R. and Kamatchi, G.L. (1991) $GABA_A$ receptor subtypes: from pharmacology to molecular biology. FASEB J. 5: 2916-2923.

Campochiaro, P. and Coyle, J.T. (1978) Ontogenetic development of kainate

neurotoxicity: correlates with glutamatergic innervation. Proc. Natl. Acad. Sci. 75: 2025-2029.

Catsicas, M., Allcorn, S. and Mobbs, P. (1995) A developmental switch in the consequences of non-NMDA receptor activation in isolated chick retina. J. Physiol. 483.P: 60P.

Catsicas, M. and Mobbs, P. (1995) Waves are swell. Current Biol. 5: 977-979.

Catsicas, S. and Clarke, P.G.H. (1987) Spatiotemporal gradients of kainate sensitivity in the developing chick retina. J. Comp. Neurol. 262: 512-522.

Cauley, K., Agranoff, B.W. and Goldman, D. (1990) Multiple nicotinic acetylcholine receptor genes are expressed in goldfish retina and tectum. J. Neurosci. 10: 670-683.

Cherubini, E., Giairsa, J.L and Ben-Ari, Y. (1991) GABA: an excitatory transmitter in early postnatal life. Trends Neurosci. 14: 515-519.

Choi, D.W. (1985) Glutamate neurotoxicity in cortical cell culture is calcium dependent. Neurosci. Lett. 58: 293-297.

Choi, D.W. (1987) Ionic dependence of glutamate neurotoxicity. J. Neurosci. 7: 369-379.

Choi, D.W. (1988) Glutamate neurotoxicity and diseases of the nervous system. Neuron 1: 623-634.

Choi, D.W., Maulucci-Gedde, M.A. and Kriegstein, A.R. (1987) Glutamate neurotoxicity in cortical cell culture. J.Neurosci. 7: 357-368.

Clarke, P.B.S. (1992) The rise and fall of the α-bungarotoxin binding proteins. Trends Pharmacol. Sci. 13: 407-413.

Cline, H.T. and Constantine-Paton, M. (1990) NMDA receptor agonist and antagonists alter retinal ganglion cell arbor structure in the developing frog retinotectal projection. J. Neurosci. 10: 1197-1192.

Cline, H.T., Debski, E.A. and Constantine-Paton, M. (1987) N-methyl-D-aspartate receptor antagonist desegregates eye-specific stripes. Proc. Natl. Acad. Sci. USA. 84: 4342-4345.

Cohan, C.S., Connor, J.A. and Kater, S.B. (1987) Electrically and chemically mediated increases in intracellular calcium in neuronal growth cones. J. Neurosci. 7: 3588-3599.

Cohen, A.I. (1963) The fine structure of the visual receptors of the pigeon. Exp. Eye Res. 2: 88-97.

Cohen, J., Burne, J.F., McKinlay, C. and Winter, J. (1987) The role of laminin/fibronectin receptor complex in the outgrowth of retinal ganglion cell axons. Dev. Bio. 122: 407-418.

Cohen, M.J., Anderson, E., Zorychata, E. and Weldon, P.R. (1979) Acculmulation of acetylcholine receptors at nerve-muscle contacts in culture. Prog. Brain Res. 49: 335-349.

Collingridge, G.L. and Lester, R.A.J. (1989) Excitatory amino acid receptors in the vertebrate central nervous system. Pharmacol. Rev. 40: 143-210.

Collingridge, G.L. and Singer, W. (1990) Excitatory amino acid receptors and synaptic plasticity. Trends Pharmacol. Sci. 11: 290-296.

Colquhoun, D., Jonas, P. and Sakmann, B. (1992) Action of brief pulses of glutamate on AMPA/kainate receptors in patches from different neurones of rat hippocampal slices. J. Physiol. 458: 261-287.

Cull-Candy, S.G. and Usowicz, M.M. (1987) Multiple-conductance channels activated by excitatory amino acids in cerebellar neurons. Nature 325: 525-528.

Curtis, D.R. and Johnston, G.A.R. (1974) Amino acid transmitters in the mammalian central nervous system. Ergeb. Physiol. 69: 98-108.

Cutcliffe, N. and Osborne, N.N. (1987) Serotonergic and cholinergic stimulation of inositol phosphate formation in the rabbit retina. Brain Res. 421: 95-104.

Cutting, G.R., Curristin, S., Zoghbi, H., O'Hara, B.F., Seldin, M.F. and Uhl, G.R. (1992) Identification of a putative γ-aminobutyric acid (GABA) receptor subunit ρ2 cDNA and colocalization of the genes encoding ρ2 (GABAR2) and ρ1 (GABAR1) to human chromosome 6q14-q21 and mouse chromosome 4. Genomics 12: 801-806.

Cutting, G.R., Lu, L., O'Hara, B.F., Kasch, L.M., Montrose-Rafizadeh, C., Donovan, D.M., Shimada, S., Antonarakis, S.E., Guggino, W.B., Uhl, G.R.

and Kazazian, H.H. (1991) Cloning of the γ-aminobutyric acid (GABA) rho1 cDNA: A GABA receptor subunit highly expressed in the retina. Proc. Natl. Acad. Sci. USA 88: 2673-2677.

Desarmenjen, M.G. and Spitzer, N.C. (1991) Role of calcium and protein kinase C in development of the delayed rectifier potassium current in *Xenopus* spinal neurons. Neuron 7: 797-805.

Dineley-Miller, K. and Patrick, J. (1992) Gene transcripts for the nicotinic acetylcholine receptor subunit, β4, are distributed in multiple areas of the rat central nervous system. Mol. Brain. Res. 16: 339-344.

Dingledine, R., Hume, R.I. and Heinemann, F. (1992) Structural determinants of barium permeation and rectification in non-NMDA glutamate receptor channels. J. Neurosci. 12: 4080-4087.

Duke-Elder, S. (1963) Systems of opthalmology: Normal and abnormal development 3. London: Klimpton.

Dunne, M.J., Illot, M.C. and Peterson, O.H. (1987) Interaction of diazoxide, tolbutamide and ATP^4 on nucleotide dependent K^+ channels in an insulin secreting cell line. J.Mem.Bio. 99: 215-224.

Egebjerg, J., Bettler, B., Hermans-Borgmeyer, I. and Heinemann, S. (1991) Cloning of a cDNA for a glutamate receptor subunit activated by kainate but not AMPA. Nature 351: 745-748.

Ehinger, B. (1977) Glial and neuronal uptake of GABA, glutamic acid, glutamine and glutathione in the rabbit retina. Exp. Eye Res. 25: 221-234.

Ehrlich, D. and Morgan, I.G. (1980) Kainic acid destroys displaced amacrine cells in post-hatch chicken retina. Neurosci. Lett. 17: 43-48.

Ellis, R.E., Junying, Y. and Horvitz, R. (1991) Mechanisms and functions of cell death. Ann. Rev. Cell Biol. 7: 663-698.

Feigenspan, A., Wassle, H. and Bormann, J. (1993) Pharmacology of GABA receptor Cl^- channels in rat bipolar cells. Nature 361: 159-162.

Feldmeyer, D. and Cull-Candy, S. (1994) Elusive glutamate receptors. Current Biol. 4: 82-84.

Fenwick-EM; Marty-A; Neher-E. (1982) A patch-clamp study of bovine chromaffin cells and of their sensitivity to acetylcholine. J. Physiol. 331: 577-597.

Fonnum, F. (1984) Glutamate: a neurotransmitter in mammalian brain. J. Neurochem. 42: 1-11.

Frandsen, A. and Schousboe, A. (1993) Excitatory amino acid-mediated cytotoxicity and calcium homeostasis in cultured neurons. J. Neurochem. 60: 1202-1211.

Frank, E. and Fischbach, G.D. (1979) Early events in neuromuscular junction formation *in vitro* . J. Cell Biol. 83: 143-158.

Friedman, D.L. and Redburn, D.A. (1990) Evidence for functionally distinct subclasses of γ-aminobutyric acid receptors in rabbit retina. J. Neurochem. 55: 1189-1199.

Gallagher, J.P., Nakamura, J. and Shinnick-Gallagher, P. (1983) The effects of temperature, pH and Cl^- pump inhibitors on GABA responses recorded from cat dorsal root ganglia. Brain Res. 267: 249-259.

Gallo, V., Patneau, D.K., Mayer, M.L. and Vaccarino, F. (1994) Excitatory amino acid receptors in glial progenitor cells: molecular and functional properties. Glia 11: 94-101.

Gilbertson, T.A., Scobey, R. and Wilson ,M. (1991) Permeation of calcium ions through non-NMDA glutamate channels in retinal bipolar cells. Science 251: 1613-1615.

Gleason, E. and Wilson, M. (1989) Development of synapses between chick retinal neurons in dispersed culture. J. Comp. Neurol. 287: 213-224.

Gleason, E., Borges, S. and Wilson, M. (1993) Synaptic transmission between pairs of retinal amacrine cells in culture. J. Neurosci. 13: 2359-2370.

Glücksmann, A. (1951) Cell deaths in normal vertebrate ontogeny. Biol. Rev. 26: 59-86.

Goldberg, J.I. and Kater, S.B. (1989) Expression and function of the neurotransmitter serotonin during development of the *Helisoma* nervous system. Dev. Biol. 131: 483-495.

Goldenring, J.R., Vallano, M.L., Lasher, R.S., Ueda, T. and DeLorenzo, R.J. (1986) Association of calmodulin-dependent kinase II and its substrate proteins with neuronal cytoskeleton. Prog. Brain Res. 69: 341-354.

Goldman, Y.E. (1943) Potential, impedence and rectification in membranes. J. Gen. Physiol. 27: 37-60.

Greenagard, P., Jen, J., Naim, A.C. and Stevens, C.F. (1991) Enhancement of the glutamate response by cAMP dependent protein kinase in hippocampal neurons. Science 253: 1135-1138.

Greferath, U., Grunert, U., Muller, F. and Wassle, H. (1994) Localization of $GABA_A$ receptors in the rabbit retina. Cell Tissue Res. 276: 295-307.

Guastella, J., Nelson, N., Nelson, H., Czyzyk, L., Keynan, S., Miedel, M.C., Davidson, N., Lester, H.A. and Kanner, B.I. (1990) Cloning and expression of a rat brain GABA transporter. Science 249: 1303-1306.

Hall, Z.W. and Sanes, J.R. (1993) Synaptic structure and development: the neuromuscular junction. Neuron 10: 99-121.

Hamassaki-Britto, D.E., Brzozowska-Prechtl, A., Karten, H.J., Lindstrom, J.M. and Keyser, K.T. (1991) GABA-like immunoreactive cells containing nicotinic acetylcholine receptors in the chick retina. J. Comp. Neurol. 313: 394-408.

Hamassaki-Britto, D.E., Hermans-Borgmeyer, I., Heinemann, S. and Hughes, T.E. (1993) Expression of glutamate receptor genes in the mammalian retina: the localization of GLUR1 through GLUR7 mRNAs. J. Neurosci. 13: 1888-1898.

Hamassaki-Britto, D.E., Brzozowska-Prechtl, A., Karten, H.J., and Lindstrom, J.M. (1994a) Bipolar cells of the chick retina containing α-bungarotoxin-

sensitive nicotinic acetylcholine receptors. Vis. Neurosci. 11: 63-70.

Hamassaki-Britto, D.E., Gardino, P.F., Hokoc, J.N., Keyser, K.T., Karten, H.J., Linstrom, J.M., Britto, L.R. (1994b) Differential development of α-bungarotoxin-sensitive and α-bungarotoxin-insensitive nicotinic acetylcholine receptors in the chick retina. J. Comp. Neurol. 347: 161-170.

Hamill, O.P., Marty, A., Neher, M., Sakmann, B. and Sigworth, F.J. (1981) Improved patch-clamp techniques for high-resolution current recording from cells and cell-free membrane patches. Pflugers Archiv. 391: 85-100.

Hansen, G.H., Belhage, B., Schousboe, A. and Meier, E. (1987) Temporal development of GABA agonist induced alterations in ultrastructure and GABA receptor expression in cultured cerebellar granule cells. Int. J. Dev. Neurosci. 5: 263-269.

Hartley, D.M., Kurth, M.C., Bjerkness, L., Weiss, J.H. and Choi, D.W. (1993) Glutamate receptor-induced $^{45}Ca^{2+}$ accumulation in cortical cell culture correlates with subsequent neuronal degeneration. J.Neurosci. 13: 1993-2000.

Haydon, P.G. and Drapeau, P. (1995) From contact to connection: early events during synaptogenesis. Trends Neurosci. 18: 196-201.

Haydon, P.G., McCobb, D.P. and Kater, S.B. (1984) Serotonin selectively inhibits growth cone dynamics and synaptogenesis of specified idntified neurons. Science 226: 561-564.

Heidelberger, R. and Matthews, G. (1991) Inhibition of calcium influx and

calcium current by γ-aminobutyric acid in single synaptic terminals. Proc. Natl. Acad. Sci. USA 88: 7135-7139.

Heinemann, S., Boulter, J., Deneris, E., Conolly, J., Duvousin, R., Papke, R. and Patrick, J. (1990) The brain nicotinic acetylcholine receptor gene family. Prog. Brain. Res. 86: 195-203.

Herb, A., Burnashev, N., Werner, P., Sakmann, B., Wisden, W. and Seeburg, P.H. (1992) The KA-2 subunit of excitatory amino acid receptors shows widespread expression in brain and forms ion channels with distantly related subunits. Neuron 8: 775-785.

Hertz, L. (1979) Functional interactions between neurons and astrocytes Turnover and metabolism of putative amino acid transmitters. Progress in Neurobiol. 13: 277-323.

Hinkle, L., McCaig, D.D. and Robinson, K.R. (1981) The direction of growth of differentiating neurons and myoblasts from frog embryos in an applied electric field. J. Physiol. 314: 212-135.

Hodgkin, A.L. and Katz, B. (1949) The effect of sodium ions on the electrical activity of the giant axon of the squid. J. Physiol. 108: 37-77.

Hollmann, M. and Heinemann, S. (1994) Cloned glutamate receptor. Ann. Rev. Neurosci. 17: 31-108.

Hollmann, M., Hartley, M. and Heinemann, S. (1991) Ca^{2+}-permeability of KA-AMPA gated glutamate receptor channels depends on subunit composition. Science 252: 851-853.

Hollmann, M., O'Shea-Greenfield, A., Rogers, S.W. and Heinemann, S. (1989) Cloning by functional expression of a member of the glutamate receptor family. Nature 342: 643-648.

Honoré, T., Davies, S.N., Drejer, J., Fletcher, E.J., Jacobsen, P., Lodge, D. and Nielsen, F.E. (1988) Quinoxalinediones: potent competitive non-NMDA glutamate receptor antagonists. Science 241: 701-703.

Hoover, F. and Goldman, D. (1992) Temporally correlated expression of nAChR genes during development of the mammalian retina. Exp. Eye. Res. 54: 561-567.

Hosey, M.M. (1992) Diversity of structure, signaling and regulation within the family of muscarinic cholinergic receptors. FASEB J. 6: 845-852.

Huba, R. and Hofman, H.D. (1990) Identification of GABAergic amacrine-like neurons developing chick retinal monolayer cultures. Neurosci. Lett. 117: 37-42.

Huba, R. and Hofmann, H.D. (1991) Transmitter-gated currents of GABAergic amacrine-like cells in chick retinal cultures. J. Neurosci. 6: 303-314.

Huba, R., Schneider, H. and Hofmann, H.D. (1992) Voltage-gated currents of putative GABAergic amacrine cells in primary cultures and in retinal slice preparations. Brain Res. 577: 10-18.

Huether, G. and Lajtha, A. (1991) Changes in free amino acid concentrations

in serum, brain and CSF throughout embryogenesis. Neurochem. Res. 16: 145-150.

Huettner, J.E. (1990) Glutamate receptor channels in rat DRG neurons: activation by kainate and quisqualate and blockade of desensitization by Con A. Neuron 5: 255-266.

Hughes, W.F. and LaVelle, A. (1974) On the synaptogenic sequence in the chick retina. Anat. Rec. 179: 297-302.

Hughes, W.F. and McLoon, S.C. (1979) Ganglion cell death during normal retinal development in the chick: comparisons with cell death induced by early target field destruction. Exp. Neurol. 66: 587-560.

Hulme, E.C., Birdsall, N.J.M. and Buckley, N.J. (1990) Muscarinic receptor subtypes. Ann. Rev. Pharmacol. Toxicol. 30: 633-673.

Hume, R.I., Raymond, D. and Heinemann, S. (1991) Identification of a site in glutamate receptor subunits that controls calcium permeability. Science 253: 1028-1031.

Hume, R.I., Role, L.W. and Fischbach, G.D. (1983) Acetylcholine release from growth cones detected with patches of acetylcholine receptor-rich patches. Nature 305: 632-634.

Hutchins, J.B. (1994) Development of muscarinic acetylcholine receptors in the ferret retina. Dev. Brain Res. 82: 45-61.

Hutchins, J.B. and Hollyfield, J.G. (1985) Acetylcholine receptors in the

human retina. Invest. Opthal. Vis. Sci. 26: 1550-1557.

Hyndman, A.G. and Lemmon, V. (1987) Neurons and glia in purified retinal cultures identified by monoclonal antibodies to intermediate filaments. Neurosci. Lett. 75: 121-126.

Iino, M., Ozawa, S. and Tsuzuki, K. (1990) Permeation of calcium through excitatory amino acid receptor channels in cultured rat hippocampal neurons. J. Physiol. 424: 151-165.

Ikeda, K., Nagasawa, M., Mori, H., Araki, K., Sakimura, K., Watanabe, M., Inoue, Y., Mishina, M. (1992) Cloning and expression of the epsilon 4 subunit of the NMDA receptor channel. FEBS Lett. 313: 34-38.

Ikonomidou, C., Mosinger, J.L. and Olney, J.W. (1989) Hypothermia enhances protective effect of MK-801 against hypoxic/ischemic brain damage in infant rats. Brain Res. 487: 184-187.

Ingham, C.A. and Morgan, I.G. (1983) Dose-dependent effects of intra-vitreal kainic acid on specific cell types in chicken retina. Neurosci. 9: 165-181.

Ishii, T., Moriyoshi, K., Sugihara, H., Sakurada, K., Kadotani, H., Yokoi, M., Akazawa, C., Shigemoto, R., Mizuno, N., Masu, M et al. (1993) Molecular characterization of the family of the N-methyl-D-aspartate receptor subunits. J. Biol. Chem. 268: 2836-2843.

Jaffe, L.F. and Poo, M-M. (1979) Neurites grow faster towards the cathode than the anode in a steady field. J. Exp. Zool. 209: 115-128.

Jahr, C.E. and Stevens, C.F. (1987) Glutamate activates multiple single channel conductances in hippocampal neurons. Nature 325: 522-525.

Johnson, J.W. and Ascher, P. (1987) Glycine potentiates the NMDA response in cultured mouse brain neurons. Nature 325: 529-531.

Johnston, G.A.R. (1986) Multiplicity of GABA receptors, in Benzodiapine/ GABA receptors and Chloride channels. Olsen, R.W. and Ventor, J.C., eds., Alan R. Liss, Inc. NY 5: 57-71.

Johnston, G.A.R., Kennedy, S.M.E. and Twitchin, B. (1979) Action of the neurotoxin kainic acid on high affinity uptake of L-glutamic acid in rat brain slices. J. Neurochem. 32: 121-127.

Jonas, P. and Sakmann, B. (1992) Glutamate receptor channels in isolated patches from CA1 and CA3 pyramidal cells of rat hippocampal slices. J. Physiol. 455: 143-171.

Jones, P.G., Rosser, S.J. and Bulloch, A.G.M. (1986) Glutamate enhancement of neurite outgrowth in *Helisoma* neurons. Soc. Neurosci. Abstr. 12: 509.

Jursky, F., Tamura, S., Tamura, A., Mandiyan, S., Nelson, H. and Nelson, N. (1994) Structure, function and brain localization of neurotransmitter transporters. J. Exp. Biol. 196: 283-295.

Kahn, A.J. (1974) An autoradiographic analysis of the time of appearance of neurons in the developing chick neural retina. Dev. Bio. 38: 30-40.

Kanai, Y. and Hediger, M.A. (1992) Primary structure and functional characterization of a high-affinity glutamate transporter. Nature 360: 467-471.

Kater, S.B., Mattson, M., Cohan, C. and Conner, J. (1988) Calcium regulation of the neuronal growth cone. Trends Neurosci. 11: 315-321.

Keinänen, K., Wisden, W., Sommer, B., Werner, P., Herb, A., Verdoorn, TA., Sakmann, B. and Seeburg, P.H. (1990) A family of AMPA-selective glutamate receptors. Science 249: 556-560.

Keller, B.U., Hollmann, M., Heinemann, S. and Konnerth, A. (1992) Calcium influx through subunits GLUR1/GLUR3 of kainate/AMPA receptor channels is regulated by cAMP dependent protein kinase. EMBO J. 11: 891-896.

Kemp, J.A., Foster, A.C., Leeson, P.D., Priestley, T., Tridgett, R., Iversen, L.L. and Woodruff, G.N. (1988) 7-Chlorokynurenic acid is a selective antagonist at the glycine modulatory site of the N-methyl-D-aspartate receptor complex. Proc. Natl. Acad. Sci. USA 85: 6547-6550.

Keyser, K.T., Britto, L.R.G., Schoepfer, R., Whiting, P., Cooper, J., Conroy, W., Brozozowska-Prechtl, A., Karten, H.J. and Lindstrom, J. (1993) Three subtypes of α-bungarotoxin-sensitive nicotinic acetylcholine receptors are expressed in chick retina. J. Neurosci. 13: 442-453.

Keyser, K.T., Hughes, T.E., Whiting, P.J., Lindstrom, J.M. and Karten, H.J. (1988) Cholinoceptive neurons in the retina of the chick: An immunhistochemical study of the nicotinic acetylcholine receptors. Vis. Neurosci. 1: 349-366.

Kleckner, N.W. and Dingledine, R. (1988) Requirement for glycine in activation of NMDA receptors expressed in Xenopus oocytes. Science 238: 355-358.

Knapp, A.G. and Dowling, J.E. (1987) Dopamine enhances excitatory amino acid-gated conductances in cultured retinal horizontal cells. Nature 325: 437-439.

Kniesel, U. and Wolburg, H. (1993) Tight junction complexity in the retinal pigment epithelium of the chicken during development. Neurosci. Lett. 149: 71-74.

Kocsis, J.D., Rand, M.N., Chen, B., Waxman, S.G. and Pourcho, R. (1993) Kainate elicits elevated nuclear calcium signals in retinal neurons via calcium-induced calcium release. Brain Res. 616: 273-282.

Köhler, M., Burnashev, N., Sakmann, B. and Seeburg, P.H. (1993) Determinants of Ca^{2+} permeability in both TM1 and TM2 of high affinity kainate receptor channels: diversity by RNA editing. Neuron 10: 491-500.

Komuro, H. and Rakic, P. (1993) Modulation of neuronal migration by NMDA receptors. Science 260: 95-97.

Kress, M., Koltzenburg, M., Reeh, P.W. and Handwerker, H.O. (1992) Responsiveness and functional attributes of electrically localized terminals of cutaneous C-fibers *in vivo* and *in vitro* . J. Neurophysiol. 68: 581-595.

Krnjevic, K. and Schwartz, S. (1967) Some properties of unresponsive cells in the cerebral cortex. Exp. Brain Res. 3: 320-336.

Kutsuwada, T., Kashiwabuchi, N., Mori, H., Sakimura, K., Kushiya, E., Araki, K., Meguro, H., Masaki, H., Kumanishi, T., Arakawa, M. and Mishina, M. (1992) Molecular diversity of the NMDA receptor channel. Nature 358: 36-41.

Lambert, N.A., Borroni, A.M., Grover, L.M. and Teyler, T.J. (1991) Hyperpolarizing and depolarizing $GABA_A$ receptor-mediated dendritic inhibition in area CA1 of the rat hippocampus. J. Neurophysiol. 66: 1538-1548.

Lauder, J.M. (1993) Neurotransmitters as growth regulatory signals: role of receptors and second messengers. Trends Neurosci. 16: 233-239.

Leinders-Zufall, T., Rand, M.N. and Kocsis, J.D. (1994) Differential role of two Ca^{2+}-permeable non-NMDA glutamate channels in rat retinal ganglion cells: kainate-induced cytoplasmic and nuclear Ca^{2+} signals. J. Neurophysiol. 72: 2503-2516.

Lemmon, V. and Reiser, G. (1983) The developmental distribution of Vimentin in the chick retina. Dev. Brain Res. 11: 191-197.

Lester, R.A. and Jahr, C.E. (1992) NMDA channel behavior depends on agonist affinity. J. Neurosci. 12: 635-643.

Lester, R.A., Clements, J.D., Westbrook, G.L. and Jahr, C.E. (1990) Channel kinetics determine the time course of NMDA receptor-mediated synaptic currents. Nature 346: 565-567.

Lester, R.A., Tong, G. and Jahr, C.E. (1993) Interactions between the glycine

and glutamate binding sites of the NMDA receptor. J. Neurosci. 13: 1088-1089.

Levey, A.I., Edmunds, S.M., Koliatsos, V., Wiley, R.G. and Hellman, C.J. (1995) Expression of m1-m4 muscarinic acetylcholine receptor proteins in rat hippocampus and regulation by cholinergic innervation. J. Neurosci. 15: 4077-4092.

Lewis, G.P., Kaska, D.D., Vaughan, D.A. and Fischer, S.K. (1988) An immunochemical study of cat retinal Müller cells in culture. Exp. Eye Res. 47: 855-868.

Liao, C.F., Themmen, A.P.N., Joho, R. and Barberis, C. (1989) Molecular cloning and expression of a fifth muscarinic acetylcholine receptor. J. Biol. Chem. 264: 7328-7337.

Lin, Z.S. and Yazulla, S. (1994) Heterogeneity of $GABA_A$ receptor in goldfish retina. J. Comp. Neurol. 345: 429-439.

Linman, E.R., Knapp, A.G. and Dowling, J.E. (1989) Enhancement of kainate-gated currents in retinal horizontal cells by cyclic AMP-dependent protein kinase. Brain Res. 481: 399-402.

Linser, P. and Perkins, M. (1987) Regulatory aspects of the *in vitro* development of retinal Müller glial cells. Cell Differ. 20: 189-196.

Lipton, S.A. and Kater, S.B. (1989) Neurotransmitter regulation of neuronal outgrowth, plasticity and survival. Trends Neurosci. 12: 265-270.

Lipton, S.A., Frosch, M.P., Phillips, M.D., Tauck, D.L. and Aizenman, E. (1988) Nicotinic antagonists enhance process outgrowth by rat retinal ganglion cells *in vitro* . Science 239: 1293-1296.

Liu, Q.R., Lopez-Corcuera, B., Mandiyan, S., Nelson, H. and Nelson, N. (1993) Molecular characterization of four pharmacologically distinct gamma-aminobutyric acid transporters in mouse brain. J. Biol. Chem. 268: 2106-2112.

Lockerbie, R.O. and Gordon-Weeks, P.R. (1986) Further characterization of [^{3}H]gamma-aminobutyric acid release from isolated neuronal growth cones: role of intracellular calcium stores. Neurosci. 17: 1257-1266.

Lohmann, F., Drews, U., Donie, F. and Reiser, G. (1991) Chick embryo muscarinic and purinergic receptors activate cytosolic Ca^{2+} via phoshatidylinositol metabolism. Exp. Cell Res. 197: 326-329.

Lomelli, H., Wisden, W., Kohler, M., Keinanen, K., Sommer, B. and Seeburg, P.H. (1992) High-affinity kainate and domoate receptors in rat brain. FEBS Lett. 307: 139-143.

Lopez-Corcuera, B., Liu, Q.R., Mandiyan, S., Nelson, H. and Nelson, N. (1992) Expression of a mouse brain cDNA encoding novel γ-aminobutyric acid transporter. J. Biol. Chem. 267: 17491-17493.

Lucas, D.R. and Newhouse, J.P. (1957) The toxic effects of sodium L-glutamate on the inner layers of the retina. A.M.A. Arch. Opthalmol. 58: 193-201.

MacDermott, A.B., Westbrook, M.L., Smith, S.L. and Barker, J.L. (1986) NMDA receptor activation increases cytoplasmic calcium concentration in cultured spinal cord neurons. Nature 321: 519-522.

Mann, I.C. (1964) The development of the human eye. London: British Medical Association.

Marsh, G. and Beams, H.W. (1946) *In vitro* control of growing chick nerve fibers by applied electric currents. J. Cell Comp. Physiol. 27: 139-157.

Mattson, M.P. (1988) Neurotransmitters in the regulation of neuronal cytoarchitecture. Brain Res. Rev. 13: 179-212.

Mattson, M.P. and Kater, S.B. (1987) Calcium regulation of neurite elongaton and growth cone motility. J. Neurosci. 7: 4034-4043.

Mattson, M.P., Dou, P. and Kater, S.B. (1987) Pruning of hippocampal pyramidal neuron dendritic architecture *in vitro* by glutamate and a protective effect of GABA plus diazepam. Soc. Neurosci. Abstr. 13: 367.

Mattson, M.P., Dou, P. and Kater, S.B. (1988a) Outgrowth-regulating actions of glutamate in isolated hippocampal pyramidal neurons. J. Neurosci. 8: 2087-2100.

Mattson, M.P. and Kater, S.B. (1989) Excitatory and inhibitory neurotransmitters in the generation and degeneration of hippocampal neuroarchitecture. Brain Res. 478: 337-348.

Mattson, M.P., Lee, R.E., Adams, M.E., Guthrie, P.B. and Kater, S.B.

(1988b) Interactions between entorhinal axons and target hippocampal neurons: a role for glutamate in the development of hippocampal circuitry. Neuron 1: 865-876.

Mattson, M.P., Taylor-Hunter, A. and Kater, S.B. (1988c) Neurite outgrowth in individual neurons of a neuronal population is differentially regulated by calcium and cyclic AMP. J.Neurosci. 8: 1704-1711.

Mayer, M.L. and Westbrook, G.L. (1987) Permeation and block of N-methyl-D-aspartic acid receptor channels by divalent cations in mouse cultured central neurons. J.Physiol. 394: 501-527.

Mayer, M.L., Westbrook, G.L. and Guthrie, P.B. (1984) Voltage-dependent block by Mg^{2+} of NMDA responses in spinal cord neurons. Nature 309: 261-263.

McDonald, J.W. and Johnston, M.V. (1990) Physiological and pathophysiological roles of excitatory amino acids during central nervous system development. Brain Res. Rev. 15: 41-70.

McDonald, J.W., Silverstein, F.S. and Johnston, M.V. (1988) Neurotoxicity of N-methly-D-aspartate is markedly enhanced in developing rat central nervous system. Brain Res. 459: 200-203.

McGehee, D.S. and Role, L.W. (1995) Physiological diversity of nicotinic acetylcholine receptors expressed by vertebrate neurons. Ann. Rev. Physiol. 57: 521-546.

McLoon, S.C. and Lund, R.D. (1984) Loss of ganglion cells in fetal retina

transplanted to rat cortex. Brain Res. 314: 131-315.

Meguro, H., Mori, H., Araki, K., Kushiya, E., Kutsuwada, T., Yamazaki, M., Kumanishi, T., Arakawa, M., Sakimura, K.and Mishina, M. (1992) Functional characterization of a heteromeric NMDA receptor channel expressed from cloned cDNAs. Nature 357: 70-74.

Meier, E., Drejer, J. and Schousboe, A. (1984) GABA induces functionally active low-affinity GABA receptors on cultured cerebellar granule cells. J. Neurochem. 43: 1734-1744.

Meister, M., Wong, R.O., Baylor, D. A. and Shatz, C.J. (1991) Synchronous bursts of action potentials in ganglion cells of the developing mammalian retina. Science 252: 939-943.

Meldrum, B. and Garthwaite, J. (1990) Excitatory amino acid neurotoxicity and neurodegenerative disease. Trends Pharmacol. Sci. 11: 379-387.

Michaels, R.L. and Rothman, S.M. (1990) Glutamate neurotoxicity *in vitro* : antagonist pharmacology and intracellular calcium concentrations. J. Neurosci. 10: 283-292.

Michler, A. (1990) Involvement of GABA receptors in the regulation of neurite outgrowth in cultured embryonic chick tectum. Int. J. Dev. Neurosci. 8: 463-472.

Misgeld, U., Diesz, R.A., Dodt, H.U. and Luz, H.D. (1986) The role of chloride transport in postsynaptic inhibition of hippocampal neurons. Science 232: 1413-1415.

Mobbs, P., Brew, H. and Attwell, D. (1988) A quantitative analysis of glial cell coupling of the axolotl (*Ambystoma mexicanum*). Brain Res. 460: 235-245.

Monaghan, D.T., Bridges, R.J. and Cotman, C.W. (1989) The excitatory amino acid receptors: their classes, pharmacology, and distinct properties in the function of the central nervous system. Ann. Rev. Pharmacol. Toxicol. 29: 365-402.

Monyer, H., Seeburg, P.H. and Wisden, W. (1991) Glutmate-operated channels: developmentally early and mature forms arise by alternative splicing. Neuron 6: 799-810.

Monyer, H., Sprengel, R., Schoepfer, R., Herb, A., Higuchi, M., Lomeli, H., Burnashev, N., Sakmann, B. and Seeburg, P.H. (1992) Heteromeric NMDA receptors: molecular and functional distinction of subtypes. Science 256: 1217-1221.

Mori, H., Masaki, H., Yamakura, T. and Mishina, M. (1992) Identification by mutagenesis of a Mg^{2+}-block site of the NMDA receptor channel. Nature 358: 673-675.

Morita, T., Sakimura, K., Kushiya, E., Yamazaki, M., Meguro, H., Araki, K., Abe, T., Mori, K.J. and Mishina, M. (1992) Cloning and functional expression of a cDNA encoding the mouse β-subunit of the kainate-selective glutamate receptor channel. Mol. Brain Res. 14: 143-146.

Moriyoshi, K., Masu, M., Ishii, T., Shigemoto, R., Mizuno, N. and Nakanishi, S. (1991) Molecular cloning and characterization of the rat NMDA receptor.

Nature 354: 31-36.

Morris, B., Hicks, A., Wisden, W., Darlison, M., Hunt, S. and Barnard, E. (1990) Distinct regional expression of nicotinc acetylcholine receptor genes in chick brain. Mol. Brain Res. 7: 305-315.

Moyer, M., Bullrich, F. and Sheffield, J.B. (1990) Emergence of flat cells from glia in stationary cultures of embryonic chick neural retina. *In vitro* Cell Dev. Biol. 26: 1073-1078.

Müeller, A.L., Taube, J.S. and Schwartzkroin, P.A. (1984) Development of hyperpolarizing inhibitory postsynaptic potentials and hyperpolarizing response to γ-aminobutyric acid in rabbit hippocampus studied *in vitro* . J. Neurosci. 4: 860-867.

Murphy, S.N. and Miller, R.J. (1989) Regulation of Ca^{2+} influx into striatal neurons by kainic acid. J.Pharmacol.Exp.Ther. 249: 184-193.

Nakajima, Y., Iwakabe, H., Akazawa, C., Nawa, H., Shigemoto, R., Mizuno, N. and Nakanishi, S. (1993) Molecular characterization of a novel retinal metabotropic glutamate receptor mGLUR6 with a high agonist selectivity for l-2-amino-4-phosphonobutyrate. J. Biol. Chem. 268: 11868-11873.

Nakanishi, N., Shneider, N.A. and Axel, R. (1990) A family of glutamate receptor genes: evidence for the formation of heteromultimeric receptors with distinct channel properties. Neuron 5: 569-581.

Nakanishi, S. (1992) Molecular diversity and functions of glutamate receptors. Science 258: 597-603.

Nakanishi, S. (1994) Metabotropic glutamate receptors: syanaptic transmission, modulation, and plasticity. Neuron 13: 1031-1037.

Neely, M.D. and Gesemann, M. (1994) Disruption of microfilaments in growth cones following depolarization and calcium influx. J.Neurosci. 14: 7511-7520.

Newman, E.A. (1984) High potassium conductance in astrocyte end-feet. Science 233: 453-454.

Newman, E.A., Frambach, D.A. and Odette, L.L. (1984) Control of extracellular potassium levels by retinal glial cell potassium siphoning. Science 225: 1174-1175.

Nicholls, D.J. and Attwell, D. (1990) The release and uptake of amino acids. Trends Pharmacol. Sci. 11: 462-468.

Nicoletti, F., Wroblewski,J.T., Novelli, A., Alho, H., Guidotti, A. and Costa, E. (1986) The activation of inositol phosholipid metabolism as a signal-transducting system for excitatory amino acids in primary cultures of cerebellar granule cells. J.Neurosci. 6: 1905-1911.

Nicoll, R.A., Malenka, R.C. and Kauer, J.A. (1990) Functional comparison of neurotransmitter receptor subtypes in mammalian central nervous system. Physiol. Rev. 70: 513-565.

Nishi, S., Minota, S. and Karczmar, A.G. (1974) Primary afferent neurons: the ionic mechanism for GABA-mediated depolarization. Neuropharm. 13: 215-219.

Nishimura, Y. (1980) Determination of the developmental pattern of retinal ganglion cells in chick embryos by golgi impregnation and other methods. Anat. Embryol. 158: 329-347.

Novelli, A., Nicoletti, F., Wroblewski, J.T., Alho, H., Costa, E. and Guidotti, A. (1987) Excitatory amnio acid receptors coupled with guanylate cyclase in primary cultures of cerebellar granule cells. J. Neurosci. 7: 40-47.

Nowak, L., Bregestovski, P., Ascher, P., Herbet, A. and Prochiantz, A. (1984) Magnesium gates glutamate-activated channels in mouse central neurones. Nature 307: 462-465.

Nowycky, M.C., Fox, A.P. and Tsien, R.W. (1985) Three types of neuronal calcium channel with different calcium agoinst sensitivity. Nature 316: 440-443.

O'Dell, T.J. and Christensen, B.N. (1989) Horizontal cells isolated from catfish retina contain two types of excitatory amino acid receptors. J. Neurophysiol. 61: 1097-1109.

O'Hara, B.F., Andretic, R., Heller, H.C., Carter, D.B. and Kilduff, T.S. (1995) $GABA_A$, $GABA_C$ and NMDA receptor subunit expression in the suprachiasmatic nucleus and other brain regoins. Mol. Brain Res. 28: 239-250.

Obata, K., Oide, M. and Tanaka, H. (1978) Excitatory and inhibitory actions of GABA and glycine on embryonic chick spinal neurons in culutre. Brain Res. 144: 179-184.

Ohishi, H., Shigemoto, R., Nakanishi, S. and Mizuno, N. (1993a) Distribution ofthe mRNA for a metabotropic glutamate receptor (mGLUR3) in the rat brain: an *in situ* hybridization study. J. Comp. Neurol. 335: 252-266.

Ohishi, H., Shigemoto, R., Nakanishi, S. and Mizuno, N. (1993b) Distribution of the messenger RNA for a metabotropic glutamate receptor, mGLUR2, in the central nervous system of the rat. Neurosci. 53: 1009-1018.

Okamoto, N., Hori, S., Akazawa, C., Hayashi, Y., Shigemoto, R., Mizuno, N. and Nakanishi, S. (1994) Molecular characterization of a new metabotropic glutamate receptor mGLUR7 coupled to inhibitory cyclic AMP signal transduction. J. Biol. Chem. 269: 1231-1236.

Olney, J.W. (1969) Brain lesions, obesity and other disturbances in mice treated with monosodium glutamate. Science 164: 719-721.

Olney, J.W. (1978) Neurotoxicity of excitatory amino acids: Kainic acid as a tool in neurobiology, eds McGeer, E., Olney, J.W. and McGeer, P., NY: Raven.

Olney, J.W., Ho, O.L., Rhee, V. and De Gubareff, T. (1973) Neurotoxic effects of glutamate. New Engl. J. Med. 289: 1374-1375.

Oppenheim, R.W. (1991) Cell death during development of the nervous system. Ann. Rev. Neurosci. 14: 453-501.

Osborne, N.N. (1988) Muscarinic stimulation of inositol phosphate formation in rat retina: developmental changes. Vision Res. 28: 875-881.

Palmer, E., Monaghan, D.T. and Cotman, C.W. (1989) *Trans*-ACPD, a selective agonist of phosphoinositide-coupled excitatory amino acid receptor. Eur. J. Pharmacol. 166: 585-587.

Partin, K.M., Patneau, D.K., Winters, C.A., Mayer, M.L. and Buonanno, A. (1993) Selective modulation of desensitization at AMPA versus kainate receptors by cyclothiazide and concanavalin A. Neuron 11: 1069-1082.

Patneau, D.K. and Mayer, M.L. (1991) Kinetic analysis of interactions between kainate and AMPA: Evidence for activation of a single receptor in mouse hippocamapal neurons. Neuron 6: 785-798.

Pearce, I.A., Cambray-Deakin, M.A. and Burgoyne, R.D. (1987) Glutamate acting on NMDA receptors stimulates neurite outgrowth from cerebellar granule cells. FEBS Lett. 223: 143-147.

Pearson, H., Graham, M.E. and Burgoyne, R.D. (1992) Releationship between intracellular free calcium concentration and NMDA-induced cerebellar granule cell survival *in vitro* . Eur. J. Neurosci. 4: 1369-1375.

Pellegrini-Giampietro, D.E., Bennett, M.V.L. and Zukin, R.S. (1991) Differential expression of three glutamate receptor genes in developing brain: an *in situ* hybridization study. Proc. Natl. Acad. Sci. USA 88: 4157-4161.

Pellegrini-Giampietro, D.E., Bennett, M.V.L. and Zukin, R.S. (1992) Are Ca^{2+}-permeable kainate/AMPA receptors more abundant in immature brain? Neurosci. Lett. 144: 65-69.

Peralta, E.G., Ashkenazi, A., Winslow, J.W., Smith, D.H., Ramachandran, J.

and Capon, D.J. (1987) Distinct primary structures, ligand-binding properties and tissue-specific expression of four human muscarinic acetylcholine receptors. EMBO J. 6: 3923-3929.

Peters, S., Koh, J. and Choi, D.W. (1987) Zinc selectively blocks the action of N-methyl-D-aspartate on cortical neurons. Science 236: 589-593.

Pilowsky, P.M., Hodgson, A.J. and Chubb, I.W. (1982) Acetylcholinesterase in neural tube defects: a model using chick embryo amniotic fluid. Neurosci. 7: 1203-1214.

Pines, G., Danbolt, N.C., Bjoras, M., Zhang, Y., Bendahan, A., Eide, L., Koepsell, H., Storm-Mathisen, J., Seeberg, E. and Kanner, B.I. (1992) Cloning and expression of a rat brain L-glutamate transporter. Nature 360: 464-467.

Prada, C., Puga, J., Perez-Mendez, L., Lopez, R. and Ramirez, G. (1991) Spatial and temporal patterns of neurogenesis in the chick retina. Eur. J. Neurosci. 3: 559-569.

Pruss, R.M., Akeson, R.L., Racke, M.M. and Wilburn, J.L. (1991) Agonist-activated cobalt uptake identifies divalent cation-permeable kainate receptors on neurons and glial cells. Neuron 7: 509-518.

Qian, K. and Dowling, J.E. (1993) Novel GABA responses from rod-driven retinal horizontal cells. Nature 361: 162-164.

Rager, G.H. (1980) Development of the retinotectal projection in the chicken. Adv. Anat. Embryol. Cell. Biol. 63: 1-90.

Raju, T.R., Rao, M.S., Nagaraja, T.N., Meti, B.L. and Schulz, M. (1994) Retinal ganglion cell survival and neurite regeneration *in vitro* after cell death period are dependent upon target derived trophic factor and retinal glial factor(s). Brain Res. 664: 247-251.

Ramussen, H. (1981) Calcium and and cyclic AMP as synarchic messengers. Wiley Press, New York.

Ransom, R.W. and Stec, N.L. (1988) Cooperative modulation of [^{3}H]MK 801 binding to the N-methyl-D-aspartate receptor-ion channel complex by L-glutamate, glycine and polyamines. J. Neurochem. 51: 830-836.

Rashid, N.A. and Cambray-Deakin, M.A. (1992) N-methyl-D-aspartate effects on the growth, morphology and cytoskeleton of individual neurons *in vitro* . Dev. Brain Res. 67: 301-308

Redburn, D.A., Agarwal, S.H., Messersmith, E.K. and Mitchell, C.K. (1992) Development of the glutamate system in rabbit retina. Neurochem. Res. 17: 61-66.

Reh, T.A. and Constanine-Paton, M. (1985) Eye-specific segregation requires neural activity in 3-eyed Rana pipiens. J. Neurosci. 5: 1132-1143.

Reichling, D.B., Kyrozis, A., Wang, J. and MacDermott, A.B. (1994) Mechanisms of GABA and glycine depolarization-induced calcium transients in rat dorsal horn neurons. J. Physiol. 476: 411-421.

Robinson, M.B., Hunter-Ensor, M. and Sinor, J. (1991) Pharmacologically distinct sodium-dependent L-[^{3}H]glutamate transport processes in rat brain.

Brain Res. 544: 196-202.

Robinson, M.B., Sinor, J.D., Dowd, L.A. and Kerwin, J.F.J. (1993) Subtypes of sodium-dependent high affinity L-[^{3}H]glutamate transport activity: pharmacological specificity by sodium and potassium. J. Neurosci. 60: 167-179.

Robson, S.J. and Burgoyne, R.D. (1989) L-type calcium channels in the regulation of neurite outgrowth from rat dorsal root ganglion neurons in culture. Neurosci. Lett. 104: 110-114.

Rodriguez-Tebar, A., Jeffrey, P.L., Thoenen, H. and Barde, Y.A. (1989) The survival of chick retinal ganglion cells in response to brain-derived neurotrophic factor depends on their embryonic age. Dev. Bio. 136: 296-303.

Romano, C., Price, M.T. and Olney, J.W. (1995) Delayed excitotoxic neurodegeneration induced by excitatory amino acid agonists in isolated retina. J. Neurochem. 65: 59-67

Rorig, B. and Grantyn, R. (1993) Rat retinal ganglion cells express Ca^{2+}-permeable non-NMDA glutamate receptors during the period of histogenetic cell death. Neurosci. Lett. 153: 32-36.

Rothman, S.M. (1983) Synaptic activity mediates death of hypoxic neurons. Science 220: 536-537.

Rothman, S.M. (1984) Synaptic release of excitatory amino acid neurotransmitter mediates anoxic neuronal death. J. Neurosci. 4: 1884-1891.

Schnitzer, J. (1987) Retinal astrocytes: Their restriction to vascularized parts of the mammalian retina. Neurosci. Lett. 78: 29-34.

Schwarcz, R. and Coyle, J.T. (1977) Kainic acid: neurotoxic effects after intraocular infection. Invest. Ophthalmol. 16: 141-148.

Schwartz, E.A. (1987) Depolarization without calcium can release γ-aminobutyric acid from a retinal neuron. Science 238: 350-355.

Seeburg, P.H. (1993) The molecular biology of mammalian glutamate receptor channels. Trends Neurosci. 16: 359-365.

Segal, M. and Barker, J.L. (1984) Rat hippocampal neurons in culture: properties of GABA-activated Cl^- ion conductance. J. Neurophysiol. 51: 500-515.

Seil, F.J., Blank, N.K. and Leiman, A.L. (1974) Toxic effects of kainic acid on mouse cerebellum in tissue culture. Brain Res. 161: 253-265.

Shatz, C.J. and Stryker, M.P. (1988) Prenatal tetrodotoxin infusion blocks segregation of retinogeniculate afferents. Science 242: 87-89.

Sheffield, J.B. and Fischman, D.A. (1970) Intercellular junctions in the developing neural retina of the chick embryo. Z. Zellforsch. 104: 405-418.

Shen, S.C., Greenfield, P. and Boell, E.J. (1956) Localization of acetylcholinesterase in chick retina during histogenesis. J. Comp. Neurol. 106: 433-461.

vivo . Nature 282: 853-855.

Somahano, F., Roberts, P.J. and Lopez-Colome, A.M. (1988) Maturational changes in retinal excitatory amino acid receptors. Dev. Brain Res. 42: 59-67.

Sommer, B., Burnashev, N., Verdoorn, T.A., Keinanen, K., Sakmann, B. and Seeburg, P.H. (1992) A glutamate receptor channel with high affinity for domoate and kainate. EMBO J. 11: 1615-1656.

Sommer, B., Keinanen, K, Verdoorn, T.A., Wisden, W., Burnashev, N., Herb, A., Kohler, M., Takagi, T., Sakman, B. and Seeburg, P.H. (1990) Flip and Flop: A cell-specific functional switch in glutamate-operated channels of the CNS. Science 249 1580-1585.

Sommer, B., Sprengel, R. and Seeburg, P.H. (1991) RNA editing in brain controls a determinant of ion flow in glutamate-gated channels. Cell 67: 11-19.

Spinelli,W. and Ishii, D.N. (1984) Tumour promoter receptor regulation of neurite formation in cultured human neuroblastoma cells. Cancer Res. 43: 4119-4125.

Spira, A.W., Millar, T.J., Ishimoto, I., Epstein, M.L., Johnson, C.D., Dahl, J.L. and Morgan, I.G. (1987) Localization of choline acetyltransferase-like immunoreactivity in the embryonic chick retina. J. Comp. Neurol. 260: 526-538.

Spitzer, N.C. (1994) Spontaneous calcium spikes and waves in embryonic neurons: signalling systems for differentiation. Trends Neurosci. 17: 115-118.

Rothstein, J.D., Martin, L., Levey, A.I., Dykes-Hoberg, M., Jin, L., Wu, D., Nash, N. and Kuncl, R.W. (1994) Localization of neuronal and glial glutamate transporters. Neuron 13: 713-725.

Ruiz, M., Egal, H., Sarthy, V., Qian, X. and Sarker, H.K. (1994) Cloning, expression and localization of a mouse retinal gamma-aminobutyric acid transporter. Invest. Opthalmol. Vis. Sci. 35: 4039-4048.

Sakimura, K., Morita, T., Kushiya, E. and Mishina, M. (1992) Primary structure and expression of the γ2 subunit of the glutamate receptor channel selective for kainate. Neuron 8: 267-274.

Sakurada, K., Masu, M. and Nakanishi, S. (1993) Alteration of Ca^{2+} permeability and sensitivity to Mg^{2+} and channel blockers by a single amino acid substitution in the N-methyl-D-aspartate receptor. J. Biol. Chem. 268: 410-415.

Sarantis, M. and Attwell, D. (1990) Glutamate uptake in mammalian retinal glia is voltage- and potassium-dependent. Brain Res. 516: 322-325.

Saugstad, J.A., Kinkie, J.M., Mulvihill, E.R., Segerson, T.P. and Westbrook, G.L. (1994) Cloning and expression of a new member of the L-2-amino-4-phosphonobutyric acid-sensitive class of metabotropic glutamate receptors. Mol. Pharmacol. 45: 367-372.

Schneggenburger, R., Zhou, Z., Konnerth, A. and Neher, E. (1993) Fractional contribution of calcium to the cation current through glutamate receptor channels.
Neuron 11: 133-143.

Sheppard, A.M., Konopka, M., Robinson, S.R., Morgan, I.G. and Jeffrey, P.L. (1991) THY-1 antigen is specific to ganglion cells in chicks. Neurosci. Lett. 123: 87-90.

Shiells, R.A., Falk, G. and Naghshineh, S. (1981) Action of glutamate and aspartate analogs on rod horizontal and bipolar cells. Nature 294: 592-594.

Shimada, S., Cutting, G. and Uhl, G.R. (1992) γ-aminobutyric acid A or C receptor? γ-aminobutyric acid ρ1 receptor RNA induces bicuculline-, barbituate- and benzodiazipine-insensitive γ-aminobutyric responses in *Xenopus* oocytes. Mol. Pharmacol. 41: 683-687.

Sidman, R.L. (1961) Histogenesis of mouse retina studied with thymidine-H^3. Structure of the eye. Smelser, G.K., ed. Academic Press, New York. 487-506.

Silver, I.A. and Erecinska, M. (1990) Intracellular and extracellular changes of (Ca^{2+}) in hypoxia and ischemia in rat brain *in vivo* . J.Gen.Physiol. 95: 837-866.

Silvlotti, L. and Nistri, A. (1991) GABA receptor mechanisms in the central nervous system. Prog. Neurobiol. 36: 35-92.

Sladeczek, F., Pin, J.P., Recasens, M., Bockaert, J. and Weiss, S. (1985) Glutamate stimulates inositol phosphate formation in striatal neurones. Nature 317: 717-719.

Smith, J., Fauquet, M., Ziller, C. and Le Douarin, N.M. (1979) Acetylcholine synthesis by mesencephalic neural crest cells in the process of migration *in*

vivo . Nature 282: 853-855.

Somahano, F., Roberts, P.J. and Lopez-Colome, A.M. (1988) Maturational changes in retinal excitatory amino acid receptors. Dev. Brain Res. 42: 59-67.

Sommer, B., Burnashev, N., Verdoorn, T.A., Keinanen, K., Sakmann, B. and Seeburg, P.H. (1992) A glutamate receptor channel with high affinity for domoate and kainate. EMBO J. 11: 1615-1656.

Sommer, B., Keinanen, K, Verdoorn, T.A., Wisden, W., Burnashev, N., Herb, A., Kohler, M., Takagi, T., Sakman, B. and Seeburg, P.H. (1990) Flip and Flop: A cell-specific functional switch in glutamate-operated channels of the CNS. Science 249 1580-1585.

Sommer, B., Sprengel, R. and Seeburg, P.H. (1991) RNA editing in brain controls a determinant of ion flow in glutamate-gated channels. Cell 67: 11-19.

Spinelli,W. and Ishii, D.N. (1984) Tumour promoter receptor regulation of neurite formation in cultured human neuroblastoma cells. Cancer Res. 43: 4119-4125.

Spira, A.W., Millar, T.J., Ishimoto, I., Epstein, M.L., Johnson, C.D., Dahl, J.L. and Morgan, I.G. (1987) Localization of choline acetyltransferase-like immunoreactivity in the embryonic chick retina. J. Comp. Neurol. 260: 526-538.

Spitzer, N.C. (1994) Spontaneous calcium spikes and waves in embryonic neurons: signalling systems for differentiation. Trends Neurosci. 17: 115-118.

Spitzer, N.C., De Baca, R.C., Allen, K.A. and Holliday, J. (1993) Calcium dependence of differentiation of GABA immunoreactivity in spinal neurons. J. Comp. Neurol. 337: 168-175.

Spoerri, P.E. (1988) Neurotrophic effects of GABA in cultures of embryonic chick brain and retina. Synapse 2: 11-22.

Stern, P., Behe, P., Schoepfer, R. and Colquhoun, D. (1992a) Single-channel conductances of NMDA receptors expressed from cloned cDNAs: comparison with native receptors. Proc. R. Soc. Lond. B. Biol. Sci. 250: 271-277.

Stern, P., Edwards, F.A. and Sakmann, B. (1992b) Fast and slow components of unitary EPSCs on stellate cells elicited by focal stimulation in slices of rat visual cortex. J. Physiol. 449: 247-278.

Storck, T., Schulte, S., Hofmann, K. and Stoffel, W. (1992) Structure, expression, and functional analysis of a Na^+-dependent glutamate/aspartate transporter from rat brain. Proc. Natl. Acad. Sci. USA. 89: 10955-10959.

Suarez-Isla, B.A., Pelto, D.J., Thompson, J.M. and Rapoport, S.I. (1984) Blockers of calcium permeability inhibit neurite extension and formation of neuromuscular synapses in cell culture. Brain Res. 316: 263-270.

Sucher, N.J., Aizenman, E. and Lipton, S.A. (1991) N-methyl-D-aspartate antagonists prevent kainate neurotoxicity in rat ganglion cells *in vitro* . J. Neurosci. 11: 966-971.

Sugiyama, H., Daniels, M.P. and Nirenburg, M. (1977) Muscarinic

acetylcholine receptors of the developing retina. Proc. Natl. Acad. Sci. USA 74: 5524-5528.

Szatkowski, M. and Attwell, D. (1994) Triggering and execution of neuronal death in brain ischemia: two phases of glutamate release by different mechanisms. Trends Neurosci. 17: 359-365.

Tanabe, Y., Masu, M., Ishii, T., Shigemoto, R. and Nakanishi, S. (1992) A family of metabotropic receptors. Neuron 8: 169-179.

Tanabe, Y., Nomura, A., Masu, M., Shigemoto, R., Mizuno, N. and Nakanishi, S. (1993) Signal transduction, pharmacological properties and expression patterns of two rat metabotropic glutamate receptors, mGLUR3 and mGLUR4. J. Neurosci. 13: 1372-1378.

Thomas, A.P. and Delaville, F. (1991) Cellular calcium: A practical approach. IRL Press, eds McCormack, J.G. and Cobbold, P.H. Chapter 1: 1-54

Torp, R., Danbolt, N.C., Babaie, E., Bjoras, M., Seeberg, E., Storm-Mathisen, J. and Ottersom, O.P. (1994) Differential expression of two glial glutamate transporters in the rat brain: an *in situ* hybridization study. Eur. J. Neurosci. 6: 936-942.

Trussell, L.O. and Fischbach, G.D. (1989) Glutamate receptor desensitization and its role in synaptic transmission. Neuron 3: 209-218.

Tsien, R.W., Hess, P., McClesky E.W. and Rosenberg, R.L. (1987) Calcium channels: Mechanism of selectivity, permeation and block. Ann. Rev.

Biophys. Chem. 16: 265-290.

Tsien, R.Y. (1989) Fluorescent probes of cell signalling. Ann. Rev. Neurosci. 12: 227-253.

Turgeon, S.M. and Albin, R.L. (1993) Pharmacology, distribution, cellular localization and development of $GABA_B$ binding in rodent cerebellum. Neurosci. 55: 311-323.

Tymianski, M., Wallace, C.M., Spigelman, I., Uno, M., Carlen,P.L., Tator, C.H. and Charlton, M.P. (1993) Cell-permeant Ca^{2+} chelators reduce early excitotoxic and ischemic neuronal injury *in vitro* and *in vivo* . Neuron 11: 221-235.

Verdoorn, T.A., Burnashev, N., Monyer, H., Seeburg, P.H. and Sakman, B. (1991) Structural determinants of ion flow through recombinant glutamate receptor channels. Science 252: 1715-1718.

Vernino, S., Amador, M., Luetje, C.W., Patrick, J. and Dani, J.A. (1992) Calcium modulation and high calcium permeability of neuronal nicotinic acetylcholine receptors. Neuron 8: 127-134.

Vogel, Z. and Nirenberg, M. (1976) Localization of acetylcholine receptors during synaptogenesis in retina. Proc. Natl. Acad. Sci. USA 73: 1806-1810.

Wada, E., Wada, K., Boutler, J., Deneris, E., Heinemann, S., Patrick, J. and Swanson, L. (1989) The distribution of $\alpha 2$, $\alpha 3$ and $\beta 2$ neuronal nicotinic receptor subunit mRNAs in the central nervous system: a hybridization stydy histochemical study in the rat. J. Comp. Neurol. 284: 314-335.

Wang, Y., Gu, Q., Mao, F., Haugland, R.P. and Cynader, M.S. (1994) Activity-dependent expression and distribution of m1 muscarinic ACh receptors in visual cortex neuronal cultures. J. Neurosci. 14: 4147-4158.

Watanabe, M., Inoue, Y., Sakimura, K. and Mishina, M. (1992) Developmental changes in distribution of NMDA receptor channel subunit mRNAs. Neuroreport 3: 1138-1140.

Watkins, J.C. and Olverman, H.J. (1987) Agonists and antagonists for excitatory amino acid receptors. Trends Neurosci. 10: 265-272.

Webster, M.L. (1985) Cytogenesis, histogenesis and morphological differentiation of the retina. Ph.D. Thesis, University of New South Wales.

Werner, P., Voigt, M., Keinanen, K., Wisden, W. and Seeburg, P.H. (1991) Cloning of a putative high-affinity kainate receptor expressed predominantly in hippocampal CA3 neurons. Nature 351: 742-744.

Westbrook, G.L. and Mayer, M.L. (1987) Micromolar concentrations of Zn^{2+} antagonize NMDA and GABA responses of hippocampal neurons. Nature 328: 640-643.

White, R.D. and Neal, M.J. (1976) The uptake of L-glutamate by the retina. Brain Res. 111: 79-93.

Williams, K., Russel, S.L., Shen, Y.M. and Molinoff, P.B. (1993) Developmental switch in the expression of NMDA receptors occurs *in vivo* and *in vitro* . Neuron 10: 267-278.

Winegar, B.D., Kelly, R. and Lansman, J.B. (1991) Block of curent through single calcium channels by Fe, Co and Ni. Location of the transition metal binding site in the pore. J. Gen. Physiol. 97: 351-67.

Wisden, W. and Seeburg, P.H. (1993) A complex mosaic of high-affinity kainate receptors in rat brain. J. Neurosci. 13: 3582-3598.

Wong, O.L. and Mayer, M.L. (1993) Differential modulation of cyclothiazide and concanavalin A of desensitization at native AMPA and kainate-preferring receptors. Molec. Pharmacol. 44: 504-510.

Wong, R.O.L. (1993) Glutamate receptor subtypes in the developing rabbit retina. A.V.O Abstracts 4: 1221.

Wong, R.O.L. (1995) Cholinergic regulation of $[Ca^{2+}]_i$ during cell division and differentiation in the mammalian retina. J. Neurosci. 15: 2696-2706.

Wong, R.O.L., Chernjavsky, A., Smith, S.J. and Shatz, C.J. (1995) Early functional neural networks in the developing retina. Nature 374: 716-718.

Wu, W.L., Ziskind-Conhaim, L. and Sweet, M.A. (1992) Early development of glycine- and GABA-mediated synapses in rat spinal cord. J. Neuosci. 12: 3935-3945.

Yamada, K.A. and Rothman, S.M. (1992) Diazoxide blocks glutamate desensitization and prolongs excitatory postsynaptic currents in rat hippocampal neurons. J.Physiol. 458: 409-423.

Yamashita, M. and Fukuda, Y. (1993a) Calcium channels and GABA

receptors in the early embryonic chick retina. J. Neurobio. 24: 1600-1614.

Yamashita, M. and Fukuda, Y. (1993b) Incurvation of early embryonic neural retina by acetylcholine through muscarinic receptors. Neurosci. Lett. 163: 215-218.

Yamashita, M. and Wassle, H. (1991) Reversal potential of GABA-induced currents in rod bipolar cells of the rat retina. Vis. Neurosci. 6: 399-401.

Yamashita, M., Huba, R. and Hofmann, H.D. (1994a) Early *in vitro* development of voltage- and transmitter-gated currents in GABAergic amacrine cells. Dev. Brain Res. 82: 95-102.

Yamashita, M., Yoshimoto, Y. and Fukuda, Y. (1994b) Muscarinic acetylcholine responses in the early embryonic chick retina. J. Neurobiol. 25: 1144-1153.

Yin ,H., Turetsky, D., Choi, D.W. and Weiss, J.H. (1994) Cortical neurones with Ca^{2+} permeable AMPA/kainate channels display distinct receptor immunoreactivity and are GABAergic. Neurobiology of disease 1: 43-49.

Young, S.H. (1986) Spontaneous release of transmitter from the growth cones of Xenopus neurons *in vitro* . Dev. Biol. 113: 373-380.

Young, S.H. and Poo, M.M (1983) Spontaneous release of transmitter from growth cones of embryonic neurons. Nature 305: 634-637.

Zhang, L., Spigelman, I. and Carlen, P.L. (1991) Development of GABA-mediated, chloride-dependent inhibition in CA1 pyramidal neurons of

immature rat hippocamapl slices. J. Physiol. 444: 25-49.

Zheng, J.Q., Felder, M., Connor, J.A. and Poo, M-M. (1994) Turning of nerve growth cones induced by neurotransmitters. Nature 368: 140-144.

Zor, U. (1983) Role of cytoskeletal organization in the regulation of adenylate cyclase-cyclic adenosine monophosphate by hormones. Endocr. Rev. 4: 1-20.